Politechnika Wrocławska

DZIEDZINA: Dziedzina Nauk Ścisłych i Przyrodniczych
DYSCYPLINA: Nauki Chemiczne

ROZPRAWA DOKTORSKA

Nowe zastosowania zimnych plazm atmosferycznych generowanych w kontakcie z cieczą do poprawy charakterystyki analitycznej metody optycznej spektrometrii emisyjnej

Mgr inż. Monika Górska

Promotor:
Prof. dr hab. inż. Paweł Pohl

Słowa kluczowe: Zminiaturyzowane źródła wzbudzenia, Wyładowanie jarzeniowe pod ciśnieniem atmosferycznym, Ciekła anoda, Ciekła katoda, Optyczna spektrometria emisyjna, Analiza pierwiastkowa, Chemiczne generowanie par

WROCŁAW 2023

Chciałabym złożyć serdeczne podziękowania promotorowi mojej pracy doktorskiej prof. dr hab. **Pawłowi Pohlowi** za stworzenie warunków do realizacji badań i zdobywania nowych umiejętności, ogrom cierpliwości i gotowości do poświęcenia czasu oraz wsparcie i inspirację w trakcie mojej drogi do uzyskania tytułu doktora.

Chciałabym również podziękować dr **Krzysztofowi Grędzie** za poświęcony mi czas na naukę obsługi aparatury badawczej i konsultacje wyników badań, a także za cenne rady i wskazówki dotyczące różnych aspektów pracy naukowej.

SPIS TREŚCI

1. SPIS AKRONIMÓW

Akronim	Rozwinięcie	
	w języku angielskim	**w języku polskim**
AFS	Atomic Fluorescence Spectrometry	Atomowa spektrometria fluorescencyjna
APGD	Atmospheric Pressure Glow Discharge	Wyładowanie jarzeniowe generowane pod ciśnieniem atmosferycznym
ASA	Atomic Absorption Spectroscopy	Atomowa spektroskopia absorpcyjna
CDS	Cathode Dark Space	Ciemnia katodowa
CFA	Continuous Flow Analysis	Analiza w trybie ciągłym
CRM	Certified Reference Material	Certyfikowany materiał odniesienia
CVG	Cold Vapor Generation	Generowanie zimnych par
DBC	Dielectric Barrier Discharge	Wyładowanie barierowe
DL	Detection Limit	Granica wykrywalności
EIE	Easily Ionized Elements	Pierwiastki łatwo jonizujące
EJC GD	Electrolyte Jet Cathode Glow Discharge	Wyładowanie jarzeniowe generowane pomiędzy dwiema fazami ciekłymi
ELCAD	ELectrolyte CAthode Discharge	Wyładowanie jarzeniowe generowane w kontakcie z ciekłą katodą
FIA	Flow Injection Analysis	Wstrzykowa analiza przepływowa
FLA	Flowing Liquid Anode	Ciekła anoda
FLC	Flowing Liquid Cathode	Ciekła katoda
HDE	Hanging Drop Electrode	Wisząca kropla
HG	Hydride Generation	Generowanie wodorków
IC	Ion Chromatography	Chromatografia jonowa
ICP	Inductively Coupled Plasma	Plazma sona indukcyjnie
LEP	Liquid Electrode Plasma	Wyładowanie w cieczy
LS	Liquid Sampling	Ciekłe próbkowanie
MS	Mass Spectrometry	Spektrometria mass
OES	Optical Emission Spectroscopy	Optyczna spektroskopia emisyjna
PN	Pneumatic Nebulization	Nebulizacja pneumatyczna
QL	Quantification Limit	Granica oznaczalności
RSD	Relative Standard Deviation	Względne odchylenie standardowe
SAGD	Solution Anode Glow Discharge	Wyładowanie jarzeniowe generowane w kontakcie z ciekłą anodą
SBR	Signal-to-Background Ratio	Stosunek sygnału do tła
SCGD	Solution Cathode Glow Discharge	Wyładowanie jarzeniowe generowane w kontakcie z ciekłą katodą
TBC	Three-Body Collision	Zderzenie trzech ciał
US EPA	United States Environmental Protection Agency	Amerykańska agencja ochrony środowiska
XRF	X-Ray Fluorescence	Rentgenowska spektroskopia fluorescencyjna

2. SPIS PUBLIKACJI STANOWIĄCYCH PODSTAWĘ ROZPRAWY DOKTORSKIEJ

[D1] **M. Górska**, K. Gręda, P. Pohl, Determination of bismuth by optical emission spectrometry with liquid anode/cathode atmospheric pressure glow discharge. *Journal of Analytical Atomic Spectrometry 2021*, 36, 165-177.
DOI: 10.1039/D0JA00401D
IF (2021): 4.351 **MEiN: 100 pkt**

[D2] **M. Górska**, P. Pohl, Application of atmospheric pressure glow discharge generated in contact with liquids for determination of chloride and bromide in water and juice samples by optical emission spectrometry. *Talanta 2022*, 237, 1-11.
DOI: 10.1016/j.talanta.2021.122921
IF(2021): 6.556 **MEiN: 100 pkt**

[D3] **M. Górska**, P. Pohl, Coupling of chemical vapor generation with atmospheric pressure glow discharge optical emission spectrometry generated in contact with flowing liquid electrodes for determination of Br in water samples. *Microchemical Journal 2022*, 178, 1-9.
DOI: 10.1016/j.microc.2022.107391
IF (2021): 5.304 **MEiN: 70 pkt**

[D4] **M. Górska**, K. Gręda, P. Pohl, On the coupling of hydride generation (HG) with flowing liquid anode atmospheric pressure glow discharge (FLA-APGD) for determination of traces of As, Bi, Hg, Sb and Se by optical emission spectrometry (OES). *Talanta 2021*, 222, 1-10.
DOI: 10.1016/j.talanta.2020.121510
IF(2021): 6.556 **MEiN: 100 pkt**

[D5] **M. Górska**, P. Pohl, Simplified and rapid determination of Ca, K, Mg, and Na in fruit juices by flowing liquid cathode atmospheric glow discharge optical emission spectrometry. *Journal of Analytical Atomic Spectrometry 2021*, 36, 1455-1465.
DOI: 10.1039/D1JA00127B
IF (2021): 4.351 **MEiN: 100 pkt**

[D6] **M. Górska**, J. Weiss, P. Pohl, Fast and simple analysis of the content of Zn, Mg, Ca, Na, and K in selected beverages widely consumed by athletes by flowing liquid cathode atmospheric pressure glow discharge optical emission spectrometry. *Analytical Methods 2023*, 15, 1775-1789.
DOI: 10.1039/D3AY00092C
IF (2021): 4.351 **MEiN: 70 pkt**

3. STRESZCZENIE

Nieustannie postępująca urbanizacja i szybki rozwój przemysłu stawiają przed współczesną chemią analityczną wiele wyzwań dotyczących wiarygodnej analizy próbek środowiskowych, metalurgicznych i żywności. Oczekuje się, że stosowane metody pozwolą na wykonywanie dokładnych i precyzyjnych analiz przy jednoczesnej redukcji czasu i kosztów niezbędnych do jej przeprowadzenia. Obecnie stosowane wielkogabarytowe urządzenia pomiarowe do absorpcyjnej spektrometrii atomowej z atomizacją w piecu grafitowym (GF AAS) czy optycznej spektrometrii emisyjnej z plazmą sprzężoną indukcyjnie (ICP OES) pozwalają na wiarygodne oznaczanie wielu pierwiastków na poziomie śladowym i ultraśladowym, jednakże zastosowanie powyższych metod wiąże się z pewnymi niedogodnościami. Wśród nich za najważniejsze uważa się bardzo wysokie koszty zakupu oraz eksploatacji aparatury pomiarowej, co w sposób oczywisty przekłada się na koszt jednostkowy wykonania analizy. Dodatkowo, ze względu na swoje gabaryty, aparatura ta nie może być stosowana *in-situ*, a analiza próbek o złożonej matrycy wymaga wielogodzinnego ich przygotowania do pomiaru. Oba te czynniki znacząco wydłużają również czas wykonania samej analizy.

Z tego powodu, współczesny rozwój metod analizy pierwiastkowej próbek rzeczywistych skupiony jest wokół opracowywania alternatywnych źródeł wzbudzenia, od których oczekuje się zapewnienia przynajmniej tak samo dobrej charakterystyki analitycznej, przy jednoczesnym wpasowywaniu się w postępujący globalnie trend miniaturyzacji. Dąży się więc do opracowania konstrukcji urządzeń pomiarowych o rozmiarach na tyle niewielkich, żeby można było zastosować daną aparaturę w miejscu i czasie rzeczywistym, co pozwoliłoby wyeliminować lub ograniczyć do minimum etap pobierania i zabezpieczania (zwykle poprzez zakwaszanie) próbek oraz ich transportu do laboratorium. To w konsekwencji ma prowadzić do ograniczenia zużycia stężonych odczynników na etapie przygotowania próbek oraz skrócenia czasu trwania samej analizy. Jednocześnie nie pomija się aspektu związanego z kosztami wytworzenia oraz utrzymania wspomnianych źródeł wzbudzenia, dlatego proponowane konstrukcje opracowuje się z zastosowaniem stosunkowo tanich i łatwo dostępnych komponentów, co z kolei przekłada się na redukcję kosztów związanych z wykonywaniem pomiarów.

W związku z powyższym, celem niniejszej pracy doktorskiej było opracowanie konstrukcji oraz rozwój zminiaturyzowanych źródeł wzbudzenia, wykorzystujących wyładowanie jarzeniowe generowane pod ciśnieniem atmosferycznym w kontakcie z przypływającymi roztworami analitów. W początkowym etapie prac skonstruowano układ pomiarowy, w którym analizowany roztwór mógł pełnić rolę zarówno katody jak i anody. Taka konstrukcja pozwoliła stosować nowo opracowane źródło wzbudzenia jako dwa osobne układy – wyładowanie jarzeniowe generowane w kontakcie z ciekłą anodą (FLA APGD) oraz wyładowanie jarzeniowe generowane w kontakcie z ciekłą katodą (FLC APGD). Dzięki temu możliwe było zastosowanie obu wspomnianych układów do niektórych badań, porównanie podobieństw i różnic między nimi oraz określenie ich potencjału analitycznego. Dodatkowo drugą z elektrod mógł stanowić zarówno metalowy pręt jak i strumień gazu przepływającego przez rurkę wykonaną z odpowiedniego materiału. Takie rozwiązanie pozwalało w niektórych przypadkach całkowicie wyeliminować stosowanie gazu osłonowego, co przekładało się na niższe koszty związane z eksploatacją stosowanej aparatury pomiarowej. Po zakończeniu prac konstrukcyjnych, układy te zostały sprzęgnięte z optyczną spektrometrią emisyjną, służącą w niniejszych badaniach do detekcji promieniowania emitowanego przez badane źródła wzbudzenia. W toku prowadzonych badań opracowane konstrukcje były dodatkowo modyfikowane w celu poprawy wybranych parametrów analitycznych.

W kolejnych etapach, nowo opracowane układy pomiarowe zastosowano do analizy pierwiastkowej. Analizy te zostały zaplanowane w taki sposób, aby odnosiły się do możliwie najwięcej znanych wcześniej problemów związanych ze stosowaniem tego typu źródeł wzbudzenia. Dlatego prezentowane w niniejszej rozprawie doktorskiej badania skupiały się na poprawie granic wykrywalności trudno oznaczalnych pierwiastków, oznaczaniu nowych pierwiastków, modyfikacji składu analizowanego roztworu oraz opracowywaniu technik przygotowania próbek, pozwalających na znaczące skrócenie czasu trwania analizy.

4. SUMMARY

By reason of constantly growing urbanization and rapid industry development, modern analytical chemistry has to face challenges regarding reliable determination of environmental, metallurgical and food samples. It is expected that the applied techniques would allow for performing accurate and precise analyses, concurrently reducing the amount of time and costs that are essential to achieve this goal. Currently applied large-scale instrumentation such as graphite furnace atomic absorption spectrometry (GF AAS) or inductively coupled plasma optical emission spectroscopy (ICP OES) allow for reliable determination of many elements at trace and ultratrace levels, however, the application of the aforesaid techniques entails some inconveniences. The most important of such are high costs related to the purchase and utilization of the applied instrumentation, which in an obvious way translates to high unit cost of the analysis. Moreover, due to bulky nature of such devices, those techniques cannot be applied *in-situ* and the analysis of samples with complex matrix requires hours-long sample preparation. The both factors significantly prolong the time required for the analysis execution.

Accordingly, currently, the advance of measurement techniques applied for the elemental analysis is focused on developing new excitation sources that are expected to assure at least similar analytical performance while concurrently fitting into the miniaturization trend that is globally progressing. Therefore, the development of instrumentation that is low enough in size so it could be applied in the real time and place is pursued. This would allow to fully exclude or at least to confine to the bare minimum the steps of collecting and preserving (usually by acidification) samples as well as transporting them to the laboratory. This would consequently lead to limiting the usage of concentrated reagents at the sample preparation stage and reducing the time needed for performing the analysis itself. However, the factor of manufacturing and maintaining the mentioned systems is still important, that is why the proposed systems need to be developed using relatively cheap and easily accessible components, which further translates to the reduction of costs related to performing measurements.

To address the abovementioned issues, the aim of this doctoral thesis was to design and develop miniaturized excitation sources, relied on atmospheric pressure glow discharge generated in contact with overflowing analyzed solutions. At the very beginning, a system design that allowed for the analyzed solution being either a cathode or an anode was proposed. Such construction allowed to apply the newly developed excitation source as two separate systems – flowing liquid anode atmospheric pressure glow discharge (FLA APGD) and flowing liquid cathode atmospheric pressure glow discharge (FLC APGD). Due to this fact, it was possible to apply both mentioned systems for some studies as well as to compare similarities and differences between the two and to assess their potential in the analytical chemistry field. Moreover, the other electrode could be either a metal rod or a gas jet passing through an appropriate metal tube. Such a solution made it possible to fully exclude the application of shielding gas in some cases, which led to lower costs related to the exploitation of the used systems. After the constructing step, the developed systems were coupled to an optical emission spectrometer, acting as the radiation detector. During the research, the design of the developed systems was further modified to achieve the best possible effectiveness of their application.

In the next steps, newly developed systems were applied for elemental analysis. Those analyses were slated in such a way to address the most of the previously known issues related to the application of such excitation sources. That is why, the research, presented in this thesis focused on the improvement of the elements detection, with particular emphasis on elements that are usually hard to determine with fair detectability, the determination of elements that were not previously determined with the aid of such techniques, the modification of the analyzed solutions composition as well as the development of new samples preparation techniques that would allow for significantly reducing the time needed for performing the analysis.

5. PODSTAWY TEORETYCZNE

5.1. Wprowadzenie

Stale postępujący rozwój przemysłu stawia przed chemią analityczną coraz to nowe wyzwania dotyczące wiarygodnego oznaczania wybranych pierwiastków w próbkach środowiskowych, metalurgicznych i żywności na poziomie śladowym i ultraśladowym. W codziennej praktyce laboratoryjnej wykorzystuje się do tego celu głównie metody spektroskopowe, dla których komercyjnie dostępne są wielkogabarytowe urządzenia pomiarowe, tj.: atomową spektrometrię absorpcyjną (AAS), rentgenowską spektroskopię fluorescencyjną (XRF), atomową spektrometrię fluorescencyjną (AFS) czy też optyczną spektrometrię emisyjną (OES), w której źródłem wzbudzenia atomów analitów jest plazma sprzężona indukcyjnie (ICP), oraz spektrometrię mas (MS). Wśród wyżej wymienionych metod, największą popularnością cieszy się obecnie optyczna spektrometria emisyjna z plazmą sprzężoną indukcyjnie (ICP OES). Metoda ta zawdzięcza swoją popularność niskim granicom wykrywalności (ang. *detection limit*, DL), wysokiej dokładności (poprawności i precyzji) pomiarów oraz możliwości jednoczesnego oznaczania wielu pierwiastków o zróżnicowanym poziomie stężeń. Jednakże stosowanie zarówno ICP OES jak i pozostałych z wymienionych metod wiąże się z wysokimi kosztami zakupu aparatury pomiarowej oraz jej eksploatacji, co wynika ze złożoności stosowanych urządzeń oraz dużego zużycia energii elektrycznej i (w przypadku niektórych z ww. metod) gazu nośnego. To sprawia, że wiele laboratoriów nie jest w stanie pokryć kosztów zakupu i eksploatacji tychże urządzeń i zazwyczaj zleca wykonanie analiz zewnętrznym podmiotom. W celu ograniczenia kosztów związanych z użytkowaniem ICP OES, podejmowano w przeszłości próby miniaturyzacji tego układu pomiarowego, jednakże parametry spektroskopowe otrzymywane w toku tych badań znacząco odbiegały od tych oferowanych przez ich wielkogabarytowe odpowiedniki [1, 2].

Z tego powodu, w ostatnich latach uwaga badaczy skupiła się na poszukiwaniu zupełnie nowych, alternatywnych źródeł wzbudzenia w optycznej spektrometrii emisyjnej, które ze swej natury charakteryzują się niewielkimi rozmiarami, prostą konstrukcją oraz ograniczonym do niezbędnego minimum zużyciem energii elektrycznej i gazów, co w sposób naturalny przekłada się na redukcję kosztów związanych z użytkowaniem takich układów. Dużą grupę wspomnianych alternatywnych źródeł wzbudzenia stanowią wyładowania elektryczne generowane pod ciśnieniem atmosferycznym w kontakcie z analizowanymi roztworami, nazywane także mikroplazmowymi źródłami wzbudzenia. Wśród nich można wyróżnić: wyładowanie jarzeniowe generowane w kontakcie z ciekłą katodą (ang. *electrolyte cathode discharge*, ELCAD) [3], wyładowanie między dwiema elektrodami oddzielonymi membraną (ang. *discharge on boiling on a channel*, DBC) [4], wyładowanie jarzeniowe generowane pomiędzy dwiema fazami ciekłymi (ang. *electrolyte jet cathode glow discharge*, EJC GD) [5], wyładowanie w cieczy (ang. *liquid electrode plasma*, LEP) [6], wyładowania jarzeniowe generowane w kontakcie z ciekłą katodą [7–9], wyładowania jarzeniowe generowane w kontakcie z ciekłą anodą [10–12] oraz wyładowanie jarzeniowe generowane w kontakcie z wiszącą kroplą (ang. *hanging drop electrode-atmospheric pressure glow discharge*, HDE APGD) [13]. W przypadku wyładowań generowanych w kontakcie z ciekłą katodą lub anodą, badacze używają różnych nazw, w celu podkreślenia wprowadzonych przez siebie zmian konstrukcyjnych danego wyładowania. Wyładowanie jarzeniowe generowane w kontakcie z ciekłą katodą może być określane jako SCGD (ang. *solution cathode glow discharge*) [7], FLC APGD (ang. *flowing liquid cathode atmospheric pressure glow discharge*) [8] lub LS APGD (ang. *liquid sampling atmospheric pressure glow discharge*) [9], podczas gdy wyładowanie jarzeniowe generowane w kontakcie z ciekłą anodą oznacza się akronimami SAGD (ang. *solution anode glow discharge*) [10] lub FLA APGD (ang. *flowing liquid anode atmospheric pressure glow discharge*) [11]. W celu ujednolicenia nazewnictwa, w niniejszej pracy będą stosowane wyłącznie akronimy FLA APGD i FLC APGD. Spośród wszystkich ww. mikroplazmowych źródeł wzbudzenia, największym zainteresowaniem badaczy cieszą się metody FLA APGD OES i FLC APGD OES. Wynika to z faktu, że oferowane przez nie parametry spektroskopowe są zbliżone do tych, obserwowanych w przypadku ICP OES. W związku z tym, układy te pozwalają na prowadzenie analiz wielopierwiastkowych w szerokich zakresach stężeń, charakteryzują się stosunkowo niskimi wartościami DL oraz cechują się wysoką

poprawnością i precyzją wyników oznaczeń. Nie bez znaczenia jest również fakt, że konstrukcje te różnią się między sobą jedynie polaryzacją elektrod, co oznacza, że w toku trwania analizy można łatwo przełączać się pomiędzy tymi układami, bazując na tej samej konstrukcji. Niemniej jednak, z racji odmiennej polaryzacji elektrod, wyładowania te cechują się odmiennymi właściwościami, z których wynikają różnice np. w otrzymywanych wartościach DL lub ich podatności na efekty matrycowe. Dlatego w przypadku analiz wielopierwiastkowych, użyteczne może się okazać stosowanie obu tych układów jednocześnie poprzez dobranie odpowiedniej polaryzacji do każdego z pierwiastków/grupy pierwiastków [14].

5.2. Zasada działania układów FLA APGD i FLC APGD

Na rys. 1 przedstawiono ogólny schemat przykładowego układu APGD. Ze względu na fakt, że schemat ten może przedstawiać zarówno układ FLA jak i FLC, oznaczenie polaryzacji elektrod na rysunku zostało celowo pominięte.

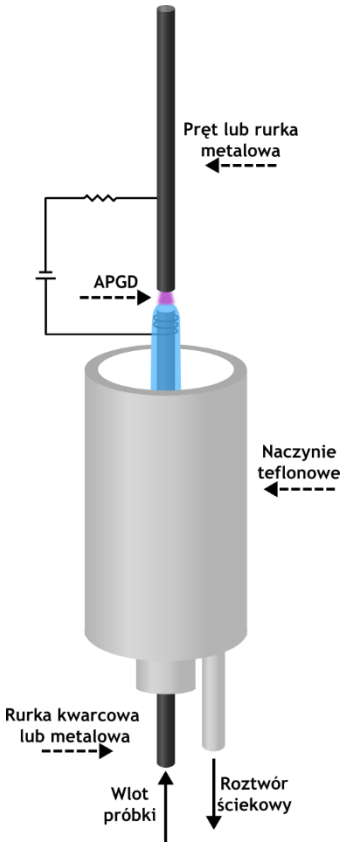

Rys. 1. Schemat przykładowego układu do generowania APGD w kontakcie z roztworem.

Przez pionowo ustawioną rurkę podawany jest analizowany roztwór, z użyciem pompy perystaltycznej. Rurka ta może być wykonana z różnych materiałów. W większości opisanych dotąd w literaturze konstrukcji wykorzystywano rurki szklane lub kwarcowe [15–17], zwykle z nałożonymi na nie rurkami grafitowymi, w celu zapewnienia kontaktu elektrycznego roztworowi będącemu bezpośrednio w kontakcie z plazmą [18–21]. Niemniej jednak, rurki ceramiczne [22] lub wolframowe [14] również były wykorzystywane. Roztwór ten następnie rozlewa się na górnym końcu rurki, tworząc powierzchnię tzw. ciekłej anody lub katody i spływa następnie do teflonowego zbiornika, z którego jest odpompowywany z użyciem tej samej pompy perystaltycznej. Prędkość przepływu analizowanego roztworu musi być dobrana w taki sposób, aby zapewnić nieprzerwany przepływ strugi, gdyż roztwór ten stanowi część obwodu elektrycznego. Drugą z elektrod jest albo metalowy pręt [10, 15, 16, 19] albo strumień gazu, przepływający przez metalową rurkę [23–26]. W przypadku tego drugiego rozwiązania, jako gaz nośny stosuje się Ar [26–28] lub He [18, 20, 25]. Stosowanie strumienia gazu jako drugą z elektrod ma szczególne znaczenie w przypadku techniki generowania wodorków (HG), ponieważ gaz ten pełni wówczas rolę zarówno gazu wyładowczego jak i gazu nośnego, transportującego lotne formy analitów do strefy wyładowania [24, 27–29]. Niemniej jednak, w przypadku układu FLA APGD, konieczne jest stosowanie mediów chłodzących ze względu na silne nagrzewanie się materiału katody, wynikające z energii przekazywanej przez strumień kationów uderzających w jej powierzchnię. W tym celu można zastosować ciągły strumień wody, opływający metalowy pręt [11], niemniej jednak, użycie gazu nośnego wydaje się spełniać to zadanie w sposób bardziej efektywny i w związku z tym rozwiązanie to jest częściej stosowane [20, 23, 30]. Materiał z jakiego wykonana jest druga z elektrod musi charakteryzować się odpowiednią przewodnością elektryczną oraz odpornością termiczną. Odporność termiczna jest szczególnie ważna w przypadku układu FLA APGD, dlatego w przeważającej większości opracowywanych metod stosuje się pręty/rurki wykonane z wolframu [**D4**, 20, 31, 32]. W przypadku układu FLC APGD, poza elektrodami wolframowymi [15, 16, 33–35], stosuje się również elektrody tytanowe [25, 27, 36], molibdenowe [37, 38], platynowe [21, 22, 39] oraz ze stali nierdzewnej [18, 40]. Odległość pomiędzy elektrodami zwykle mieści się w przedziale 1-5 mm [19, 21, 22, 41–43]. Wyładowanie jest generowane poprzez przyłożenie napięcia rzędu 1-2 kV do obu elektrod. W przypadku rurki doprowadzającej roztwór, napięcie to jest przykładane albo bezpośrednio do nałożonej na nią rurki grafitowej [39, 44, 45] albo za pomocą platynowej spirali oplatającej rurkę [20, 46]. W przypadku gdy źródło prądu charakteryzuje się jednocześnie wysoką

wydajnością prądową i niewielkim oporem wewnętrznym, możliwe jest powstanie łuku elektrycznego. Dlatego, w celu stabilizacji prądu, umieszcza się szeregowo w obwodzie elektrycznym opornik o rezystancji od kilkudziesięciu Ω do 10 kΩ [11, 17, 36, 45]. Do zasilania układu wyładowczego w przeważającej większości przypadków wykorzystuje się prąd stały, jednak znane są również prace, w których układ FLC APGD był zasilany prądem zmiennym [42, 47–49].

5.3. Transport analitów do plazmy

Jedną z niedogodności związanych z użyciem ICP jako źródła wzbudzenia w OES jest konieczność stosowania rozpylaczy i komór mgielnych do transportu roztworów wzorców i próbek do plazmy. Podejście to jest nisko-kosztowe i efektywne, niemniej wydajność rozpylania pneumatycznego roztworów wynosi zaledwie kilka procent [50]. To z kolei ogranicza maksymalną intensywność sygnałów analitów, co bezpośrednio przekłada się na otrzymywane wartości DL. Pewnym rozwiązaniem tego problemu jest sprzęgnięcie ICP z chemicznym generowaniem lotnych par (ang. *cold vapor generation*, CVG). Jednakże podejście to jest ograniczone jedynie do pierwiastków tworzących lotne formy (np. As, Bi, Ge, Hg, Pb, Sb, Se, Sn). Dodatkowo stosowanie tej techniki wiąże się z występowaniem interferencji matrycowych oraz nadmierną produkcją H_2, który może negatywnie wpływać na stabilność plazmy [46, 50–52].

W związku z powyższym, niewątpliwą zaletą układów wykorzystujących wyładowanie jarzeniowe generowane w kontakcie z analizowanymi roztworami jest samoistny transport analitów do plazmy. Pozwala to wyeliminować konieczność stosowania ww. rozpylaczy i komór mgielnych oraz zwiększa tym samym rejestrowane intensywności sygnałów analitów. Badacze udowodnili, że wydajność transportu analitów do plazmy w powyższych układach sięga nawet kilkudziesięciu procent [11, 20, 26, 46]. Pomimo intensywnego rozwoju wspomnianych układów w ciągu ostatnich lat, dokładny mechanizm atomizacji i wzbudzenia analitów nie został nigdy eksperymentalnie dowiedziony i pozostaje nadal przedmiotem debaty [36, 53]. Niemniej jednak, istnieje kilka teorii próbujących tłumaczyć zjawiska zachodzące w strefie wyładowczej.

W przypadku układu FLC APGD, proponowane mechanizmy obejmują rozpylanie katodowe [3, 54, 55], elektrorozpylanie [19, 56, 57] oraz kombinację kilku procesów [58, 59]. Rozpylanie katodowe opisywane jest trzema osobnymi modelami. Pierwszy z nich – rozpylanie jonowe w wyniku zderzeń jon-jon, zakłada, że obecne w plazmie jony o dużej energii uderzają w powierzchnię roztworu, powodując wybicie znajdujących się w nim jonów analitów. Niemniej jednak, jony te są zawracane w kierunku powierzchni roztworu w obszarze wyładowania zwanym ciemnią katodową (ang. *cathode dark space*, CDS), charakteryzującym się dużym natężeniem pola elektrycznego. Dlatego przyjmuje się, że aby wybite jony mogły zostać przetransportowane do wyższych sfer wyładowania, konieczna jest ich wcześniejsza rekombinacja z elektronami w wyniku zderzenia potrójnego (ang. *three-body collision*, TBC). W konsekwencji tego rodzaju zderzeń anality transportowane są do plazmy w postaci obojętnych atomów [3, 53, 55, 60, 61]. Kolejny model zakłada, że wspomniane obojętne atomy powstają jeszcze w roztworze analitu, ponieważ wskutek bombardowania powierzchni roztworu wysokoenergetycznymi jonami zachodzi jonizacja wody, w trakcie której powstają hydratowane elektrony, będące związkami o silnych właściwościach redukujących. W kolejnym etapie powstałe hydratowane elektrony powodują redukcję jonów analitów do obojętnych atomów, które następnie zostają przetransportowane do wyładowania w toku dalszych bombardowań powierzchni roztworu [53, 55, 62]. Ostatni model z kolei zakłada, że anality są rozpylane z powierzchni roztworu w postaci quasi-neutralnych większych klasterów, składających się z kationu metalu solwatowanego cząsteczkami wody. W dalszych etapach, wewnątrz takiego klastera następuje przeniesienie ładunku elektrycznego z metalu na cząsteczkę wody, co prowadzi do odczepienia się jonu hydroniowego, który w obszarze CDS jest zawracany do roztworu. Powstała natomiast elektrycznie obojętna cząsteczka jest w stanie dotrzeć do wyższych sfer wyładowania, aby tam ulec procesom desolwatacji i atomizacji [53, 55, 63].

W innych pracach dotyczących układów FLC APGD, badacze przypuszczają, że przynajmniej część analizowanego roztworu jest wprowadzana do wyładowania na drodze mechanizmu przypominającego elektrorozpylanie. Potwierdzają to obserwacje strefy wyładowczej z użyciem

technologii rozpraszania laserowego, ponieważ pod wpływem silnego pola elektrycznego następują chaotyczne fluktuacje powierzchni roztworu FLC oraz formowanie się aerozolu [19, 36, 56, 64–68]. Co ciekawe, zauważono, że wydajność powstawanie aerozolu zmniejsza się wraz ze spadkiem stężenia kwasu w roztworze FLC, służącego zwykle do zapewniania odpowiedniej jego przewodności. W związku z tym, gdyby procesy podobne do elektrorozpylania rzeczywiście zachodziły w układzie FLC APGD, ich mniejsza wydajność tłumaczyłaby obserwowany w tym układzie spadek intensywności sygnałów analitów wraz ze wzrostem pH roztworu [21, 36, 42, 44].
Pomijając opisane wyżej mechanizmy transportu analitów do plazmy w układzie FLC APGD, nie można wykluczyć istnienia również dodatkowych mechanizmów, które są za to odpowiedzialne, tj. termiczne odparowanie próbki, tworzenie kropel, chemiczne generowanie lotnych form analitów lub mechanizm jonizacji przypominający elektrorozpylanie [57, 58].
Z kolei w przypadku układu FLA APGD, mechanizm transportu analitów do plazmy wydaje się być zupełnie odmienny od tego, który zakładany jest dla układu FLC APGD. Wniosek taki można wysnuć chociażby na podstawie obserwowanych różnic w elektrycznych i optycznych właściwościach pomiędzy tymi dwoma układami [69–71]. Z racji odmiennej polaryzacji elektrod, powierzchnia roztworu FLA jest bombardowana strumieniem elektronów, które są zbyt lekkie żeby doprowadzić do rozpylania roztworu [11, 53, 72]. Dlatego obecnie uważa się, że w tym układzie anality są transportowane do plazmy w postaci jakiegoś rodzaju lotnych indywiduów, powstających na drodze reakcji elektrochemicznych pomiędzy jonami analitów a wspomnianymi wcześniej elektronami w fazie gazowej wyładowania lub roztworze [10, 11, 72]. Dowodem na słuszność tej teorii może być fakt, że na widmach FLA APGD obserwuje się jedynie sygnały pochodzące od pierwiastków, które są znane z tego, że tworzą lotne związki [11, 20, 53, 72]. Innym potwierdzeniem wspomnianego założenia może być opisana w literaturze reakcja przeniesienia elektronu, która jest odpowiedzialna za konwersję jonów H^+ do atomów H_2 lub redukcję jonów cyjanożelazianowych (III) do jonów cyjanożelazianowych (II) [73]. Możliwe jest również, że część elektronów docierających do roztworu FLA ulega solwatacji pod jego powierzchnią, ponieważ średnia głębokość penetracji elektronów w roztworze wynosi ok. 2,5±1,0 nm [74]. Niemniej jednak, pomimo kilku prób określenia natury wspomnianych lotnych związków [10, 26], dokładny mechanizm transportu analitów do plazmy w przypadku układu FLA APGD do dzisiaj nie został udowodniony i pozostaje przedmiotem dyskusji.

5.4. Morfologia widma

Na rys. 2 przedstawiono widma emisyjne tła układów FLA APGD i FLC APGD, zarejestrowane w zakresie 205-670 nm. Widma te nie różnią się od siebie pod względem jakościowym. W obu przypadkach, dominującym składnikiem widma jest pasmo cząsteczki OH, którego głowica znajduje się przy długości fali równej 306,4 nm, będące efektem struktury oscylacyjno-rotacyjnej dla przejścia $A^2\Sigma^+ \rightarrow X^2\Pi$ (0-0). Innymi głównymi pasmami obserwowanymi na widmie APGD są pasma cząsteczki N_2, związane ze strukturą oscylacyjno-rotacyjną dla przejścia $C^3\Pi_u \rightarrow B^3\Pi_g$, leżące w zakresie 280-450 nm oraz pasma NO, związane ze strukturą oscylacyjno-rotacyjną dla przejścia $A^2\Sigma^+ \rightarrow X^2\Pi$, obserwowane w zakresie 190-260 nm. Obecność pasma OH na widmie spowodowana jest generowaniem wyładowania w kontakcie z analizowanym roztworem – znajdujące się w roztworze cząsteczki wody ulegają rozkładowi, którego jednym z produktów jest rodnik OH. Natomiast występowanie pasm cząsteczki N_2 jest konsekwencją generowania wyładowania w układzie otwartym, w atmosferze otaczającego powietrza. Obecność pasm cząsteczek OH i N_2 na widmie jest konsekwencją ich wzbudzenia w warunkach wyładowania. Cząsteczki NO powstają jako produkt reakcji cząsteczek N_2 z O_2 obecnym w powietrzu, po czym również ulegają wzbudzeniu w wyładowaniu. Innymi wspólnymi składnikami widm obu układów wyładowczych są linie atomowe H i O, a konkretnie linie H I serii Balmera, (H_α z maksimum obserwowanym przy 656,3 nm oraz H_β, której maksimum intensywności obserwuje się przy 468,1 nm), linie atomowe O I znajdujące się przy długościach fali równych 777,2 i 844,6 nm oraz linie liczne jonowe O II obserwowane w zakresie 440-470 nm.

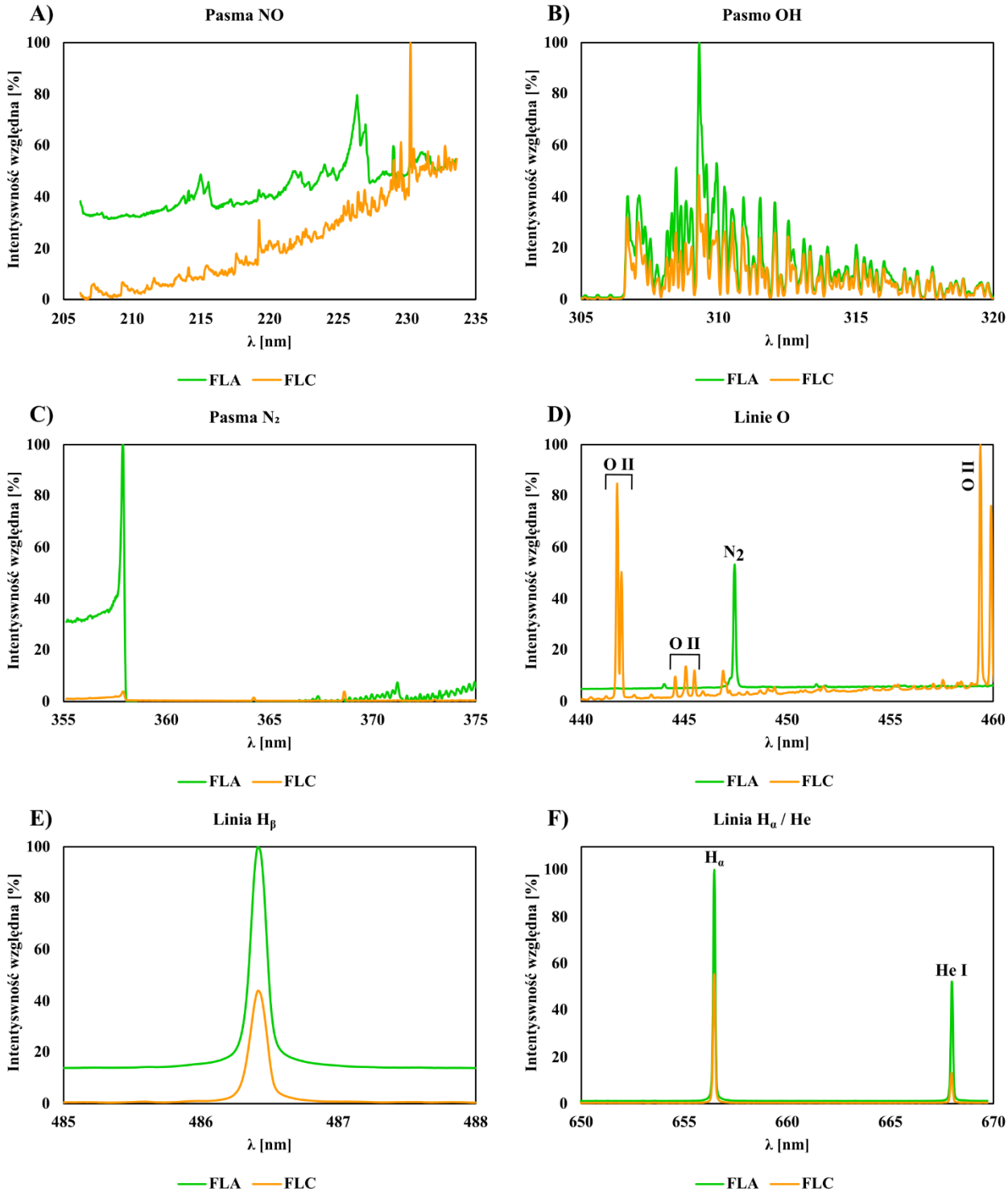

Rys. 2. Widma emisyjne tła zarejestrowane dla układów FLA APGD i FLC APGD w zakresie 355-670 nm, przedstawiające: pasma NO (A), pasmo OH (B), pasma N_2 (C) oraz linie O II, H_β, H_α i He I.

To co natomiast różni widma wspomnianych układów wyładowczych to intensywności obserwowanych pasm cząsteczek oraz linii atomowych i jonowych, będących składnikami tła. Intensywności pasm cząsteczek NO i N_2 są znacząco większe w przypadku układu FLA APGD, a jednocześnie intensywność pasma cząsteczki OH jest zauważalnie niższa w tym samym układzie. Zjawisko to można wytłumaczyć wynikami badań bilansu masy roztworu wprowadzanego do obu układów wyładowczych i odbieranego z nich po uprzednim kontakcie tych roztworów z wyładowaniem. Ubytek masy roztworu FLC po kontakcie z APGD, w głównej mierze związany z

odparowaniem wody, był ok. 3-krotnie większy w porównaniu do tego dla roztworu FLA. Dodatkowo temperatury roztworów, zmierzone bezpośrednio po ich kontakcie z wyładowaniem, wynosiły odpowiednio 39−42 °C oraz 30−32 °C dla roztworów FLC i FLA [11, 75]. Wyższa temperatura roztworu FLC wskazuje na większy strumień ciepła docierający z wyładowania do analizowanego roztworu, co jest najprawdopodobniej związane z wyższą energią jonów bombardujących jego powierzchnię (w porównaniu do energii elektronów uderzających w powierzchnię roztworu FLA). Mając na uwadze zarówno wyższą temperaturę roztworu FLC jak i wspomnianą w poprzednim rozdziale zdolność wysokoenergetycznych jonów do wybijania fragmentów analizowanego roztworu z jego powierzchni, należy spodziewać się większego odparowania wody w tym roztworze, co również zostało udowodnione we wspomnianych wyżej badaniach. To sprawia, że wyładowanie FLC APGD utrzymywane jest w atmosferze nasyconej parą wodą, która ogranicza dyfuzję cząsteczek N_2 do rdzenia wyładowania, skutkując większą intensywnością pasm OH i obniżoną intensywnością pasm NO i N_2.

W odróżnieniu od widma cząsteczkowego, widmo liniowe analitów jest dość ubogie. W przypadku obu omawianych w tej pracy układów obserwuje się średnio 2-4 linie atomowe, w tym głównie linie rezonansowe. Obecność linii jonowych na widmie układu FLC APGD jest rzadko spotykana [75], podczas gdy w przypadku FLA APGD nie została nigdy zaobserwowana. Dla porównania, przyjmuje się, że średnia liczba linii atomowych przypadających na jeden pierwiastek dla ICP OES wynosi 294 oraz obserwuje się liczne linie jonowe [76]. Tak znaczna różnica pomiędzy liczbą obserwowanych linii analitów wynika z różnic w temperaturach gazu dla obu plazm (ICP i APGD), wynoszących ok. 2000 K dla APGD i sięgających nawet 10 000 K w przypadku ICP [11, 43, 77]. Istotne różnice w morfologii widma dla układów FLA APGD i FLC APGD obserwuje się natomiast w przypadku liczby pierwiastków, których detekcja jest w ogóle możliwa. W przypadku układu FLC APGD, doniesienia literaturowe wskazują na możliwość oznaczania ok. 30 pierwiastków [65, 72], leżących w układzie okresowym w blokach s, p i d. Natomiast stosowanie układu FLA APGD pozwala oznaczyć zaledwie kilkanaście analitów [**D2**, 17, 20], przy czym część z nich jedynie w przypadku sprzęgnięcia układu FLA APGD z techniką HG [**D4**]. Wspólną cechą wszystkich pierwiastków, których detekcja jest możliwa w układzie FLA APGD jest to, że są one znane z tworzenia różnego rodzaju lotnych form, np. w reakcji z $NaBH_4$ [11]. W związku z tym, linie pierwiastków należących np. do bloku s nie są w tym układzie w ogóle obserwowane. Jednocześnie warto podkreślić, że intensywności linii emisyjnych pierwiastków, które można zaobserwować na widmach obu tych układów wyładowczych, są znacząco wyższe w przypadku stosowania układu FLA APGD.

W celu wyjaśnienia obserwowanych różnic jakościowych i ilościowych w morfologii widma liniowego analitów, wyznaczono wydajność transportu analitów do plazmy obu układów wyładowczych poprzez pomiar ich stężenia w roztworach FLA i FLC po uprzednim kontakcie z plazmą [11]. W cytowanej pracy ustalono, że wzrost intensywności sygnałów analitów w przypadku układu FLA APGD odpowiadał wzrostowi wydajności transportu w tym samym układzie. Obserwacje te można wytłumaczyć, bazując na omówionych w poprzednim rozdziale mechanizmach transportu analitów do plazmy. Mając na uwadze, że w układzie FLC APGD anality są transportowane do wnętrza wyładowania w wyniku rozpylania katodowego, można się spodziewać, że potencjalnie każdy pierwiastek znajdujący się w roztworze FLC może zostać przeniesiony do strefy wyładowczej. Z kolei w przypadku układu FLA APGD, powierzchnia roztworu bombardowana jest strumieniem elektronów, w związku z tym udział procesów rozpylania w transporcie analitów jest marginalny. Mając jednak na uwadze silnie redukujące właściwości wspomnianych elektronów z fazy gazowej lub hydratowanych oraz to, że obserwuje się wyłącznie linie emisyjne analitów tworzących lotne formy, uważa się, że w układzie tym anality są transportowane do wyładowania w postaci jakiegoś rodzaju lotnych form lub związków. Wspomniane lotne formy lub związki analitów powstają najprawdopodobniej w wyniku reakcji ich jonów z hydratowanymi elektronami i/lub rodnikami H na granicy faz roztwór-plazma [11, 20, 72]. Możliwość zastosowania układu FLA APGD jedynie do wąskiej grupy wybranych pierwiastków jest niewątpliwie jednym z jego ograniczeń. Warto mieć jednak na uwadze, że są to pierwiastki, których wartości DL zarówno dla układu FLC APGD jak i ICP są stosunkowo wysokie, co sprawia, że układy

te nie zawsze mogą znaleźć zastosowanie w monitorowaniu poziomu tychże analitów w próbkach rzeczywistych, w odniesieniu do obowiązujących norm. To sprawia, że stosowanie układu FLA APGD do ich oznaczania wydaje się być interesującą alternatywą, dzięki znacząco poprawionej wydajności ich transportu do wyładowania i – idącemu z tym w parze – wzrostowi intensywności ich linii emisyjnych.

5.5. Charakterystyka analityczna

W celu uzyskania wiarygodnych wyników pomiarów, stosowane konstrukcje pomiarowe powinny charakteryzować się przede wszystkim odpowiednio niskimi wartościami DL, ale także szerokim zakresem liniowości krzywych kalibracyjnych oraz wysoką precyzją pomiarów.

W tabeli 1 zestawiono wartości DL wszystkich pierwiastków, których detekcja jest możliwa z zastosowaniem układów FLA APGD i FLC APGD. W celu pokazania przydatności i potencjału detekcji wspomnianych układów, w tabel tej umieszczono wynikach badań opublikowanych w większości w ciągu ostatnich kilku lat.

Zestawiając wartości DL pierwiastków, których oznaczenie jest możliwe przy użyciu obu tych układów wyładowczych, można zauważyć, że wartości te są znacząco niższe w przypadku układu FLA APGD. Mimo że niektóre z pierwiastków wykazywały niewielkie różnice w przedstawionych zakresach granic wykrywalności pomiędzy tymi układami, warto zwrócić uwagę na różnice w sposobie prowadzenia pomiarów oraz wprowadzane modyfikacje składu analizowanego roztworu, co może wpłynąć na uzyskane wyniki. W większości z cytowanych prac, jako detektora używano OES [10, 15, 16, 20, 41, 78, 79], ale niektórzy badacze wykorzystywali detektor MS [19], co w sposób oczywisty przekłada się na otrzymywanie niższych wartości DL. Dodatkowo w niektórych pracach zastosowano technikę HG [11, 24, 43], co również zwiększa czułość rejestrowanych linii emisyjnych poprzez zwiększenie wydajności transportu analitów do plazmy.

Z tego powodu, w tabeli 1, poza zakresami granic wykrywalności oferowanych przez omawiane układy, zestawiono dodatkowo ich medianę. Porównanie wartości mediany DL dla pierwiastków, które były mierzone przy użyciu obu omawianych układów APGD wykazało, że w większości przypadków układ FLA APGD oferuje znacznie lepsze wartości DL. W tym przypadku wartość mediany wartości DL jest od 7 do ponad 500 razy niższa od tej dla układu FLC APGD.

Najmniejsze różnice w wartościach mediany obserwuje się dla Br i Cl, w przypadku których wynoszą one odpowiednio 7,7 i 12. Warto mieć jednak na uwadze, że pierwiastki te były oznaczane zaledwie w jednej (Cl) lub dwóch (Br) pracach tych samych autorów, w związku z czym uzyskane wartości mogą być niereprezentatywne. Z drugiej strony jednak, pierwiastki te oznaczano z zastosowaniem dokładnie tego samego układu, w którym zmieniano jedynie polaryzację elektrod, w związku z tym, można oczekiwać, że inne badania prowadziłyby do uzyskania podobnych rezultatów.

Pierwiastki As, Sb i Se, dla których wartości DL zestawiono w tabeli, były oznaczane wyłącznie przy użyciu techniki HG [11, 43]. Wartości DL otrzymane dla układu FLA APGD były albo zbliżone do tych oferowanych przez układ FLC APGD (As) albo znacząco gorsze (Sb, Se). Jedną z możliwych przyczyn takiego stanu rzeczy, mogą być różnice w warunkach prowadzenia tego procesu. Przykładowo, w obu pracach wykazano, że wydajność generowania wodorków zwiększa się wraz ze wzrostem stężenia kwasu (HCl) w roztworze analitów. Dlatego w pracy dotyczącej układu FLC APGD zakwaszano analizowany roztwór do stężenia HCl równego 20%. W przypadku układu FLA APGD, wyładowanie ulegało destabilizacji już przy stężeniu HCl wynoszącym 10%, dlatego pomiary prowadzono z zastosowaniem roztworów zakwaszonych do stężenie wynoszącego zaledwie 7,5%. Mogło to mieć wpływ na pogorszenie wydajności transportu analitów w układzie FLA APGD, a tym samym – na uzyskanie niższych wartości DL (w porównaniu do układu FLC APGD). Warto wziąć również pod uwagę intensywność tła w otoczeniu linii rezonansowych badanych analitów. W obu przytaczanych pracach [11, 43] badane linie emisyjne leżały w zakresie 200-235 nm, gdzie obserwuje się silną emisję pochodzącą od pasm cząsteczki NO, będącą znacząco większą w przypadku układu FLA APGD. Z tego powodu należy się spodziewać, że intensywność sygnałów analitów rejestrowana dla tego układu wyładowczego będzie niższa. Z drugiej strony jednak, w tym samym zakresie spektralnym obserwuje się m. in. linię Zn, której mediana otrzymywanych wartości DL,

przedstawiona w tabeli 1, jest ponad 500-krotnie niższa w przypadku układu FLA APGD. Inną prawdopodobną przyczyną obserwowanych różnic w wartościach DL dla As, Sb i Se, pomiędzy tymi układami wyładowczymi, są gorsze warunki wzbudzenia w przypadku układu FLA APGD, tj. gęstość elektronowa w tym układzie wyładowczym jest istotnie niższa w porównaniu do tej zmierzonej dla układu FLC APGD [11, 43], a jednocześnie pierwiastki te charakteryzują się wysoką energią wzbudzenia. Z tego powodu, można przypuszczać, że obserwowane różnice w wartościach DL dla tych pierwiastków są wypadkową wszystkich opisanych wyżej czynników.

Dla układu FLC APGD największą czułością charakteryzują się linie emisyjne litowców, co prowadzi do uzyskiwania najniższych wartości DL dla tych pierwiastków. Mediana wartości DL dla litowców wynosi poniżej 1 µg/l dla K, Li i Na oraz odpowiednio 7,6 i 2,0 dla Cs i Rb [15, 19, 23, 44, 85, 88]. Nieco wyższa mediana wartości DL dla Cs i Rb wynika z faktu, że linie rezonansowe tych pierwiastków leżą w zakresie bliskiej podczerwieni (780,0 i 852,1 nm), w którym większość stosowanych w badaniach detektorów charakteryzuje się stosunkowo niewielką czułością. Dość niskie wartości DL obserwuje się również dla linii Ag, Cd, In, Mg i Tl, których mediana granic wykrywalności wynosi odpowiednio 1,6, 15, 14,5, 21 i 6,4 µg/l [16, 19, 78, 83, 84, 89]. Pierwiastkami najtrudniej ulegającymi wzbudzeniu w układzie FLC APGD są Al, Br, Cl i Fe z medianą wartości DL wynoszącą odpowiednio 580, 1150, 18000 i 830 µg/l [23, 42, 78]. Z kolei w przypadku FLA APGD, najniższe wartości DL obserwuje się dla Ag, Cd i Tl (mediana w zakresie 0,03-0,05 µg/l) [11, 17, 20]. Stosunkowo wysoką czułość wykazują również linie In i Zn (mediana DL ok. 0,15 µg/l dla obu tych pierwiastków) [10, 20, 26, 31]. Najwyższe wartości DL obserwuje się dla Br, Cl i Pb (mediana odpowiednio 150, 1500 i 1,4 µg/l) [**D2**, **D3**, 11].

Warto w tym miejscu zauważyć, że wartości DL dla Br i Cl znacząco odbiegają od tych uzyskiwanych dla pozostałych pierwiastków, w obu układach, co częściowo zapewne jest spowodowane faktem, że linie rezonansowe Br i Cl również leżą w zakresie bliskiej podczerwieni (odpowiednio 827,2 i 837,6 nm). Niemniej jednak, głównym czynnikiem wydaje się być mechanizm transportu tych analitów do plazmy, ponieważ uważa się, że – w odróżnieniu od pozostałych analitów – w obu tych układach pierwiastki te są transportowane w postaci lotnych Br_2 i Cl_2 [**D2**, **D3**]. W badaniach dotyczących zastosowania układów APGD do oznaczania tych pierwiastków udowodniono, że w celu uzyskania wysokich sygnałów analitów potrzebne jest wysokie stężenie kwasu w roztworze, ale jednocześnie maksymalne stężenie kwasu jakie można było zastosować w cytowanych pracach było ograniczone przez stabilność układu wyładowczego. Dlatego, wydajność transportu analitów do plazmy była znacząco niższa w przypadku tych dwóch analitów, co – w połączeniu z niską czułością stosowanego detektora w badanym zakresie spektralnym – skutkowało uzyskaniem wysokich wartości DL.

Zakresy liniowości oferowane przez oba omawiane układy APGD nie różnią się istotnie pomiędzy nimi i obejmują 1-5 rzędów wielkości, przy czym węższe zakresy (1-2 rzędy wielkości) obserwuje się dla mniej czułych linii, np. As [28], Ca [79, 82, 93], Cu [42, 97], Fe [23, 42], Hg [32], Pb [30] lub Sr [44], a najszersze (4-5 rzędów wielkości) dla najbardziej czułych linii, np. Ag [13, 20], Cd [11, 16], Cs [19], K [80], Li [85], Na [80] lub Tl [17, 20].

Tabela 1. Wartości DL analitów w układach FLA APGD i FLC APGD.

Pierwiastek	**DL [µg/l]**					
	FLA APGD			**FLC APGD**		
	Zakres	**Mediana**	**Źródła**	**Zakres**	**Mediana**	**Źródła**
Ag	0,0015-1,0	0,03	[11, 17, 20, 43]	0,18-18	1,6	[13, 15, 16, 78]
Al	ND	ND	-	310-850	580	[78]
As*	1,7	1,7	[**D4**]	0,30-4,2	2,2	[28, 29]
Bi	0,34-2,0	0,85	[**D1**, **D4**, 17]	33-830	181	[41]
Br	150	150	[**D2**]	200-2100	1150	[**D1**, **D2**]
Ca	ND	ND	-	11-460	67,5	[18, 23, 78–86]
Cd	0,03-1,6	0,05	[10–12, 17, 20, 26, 43]	0,1-690	15	[13, 16, 19, 22, 42, 68, 78]
Cl	1500	1500	[**D2**]	18000	18000	[**D2**]
Co	ND	ND	-	80-290	100	[78, 87]
Cs	ND	ND	-	0,4-170	7,6	[15, 19, 23, 44, 85, 88]
Cu	ND	ND	-	4,0-110	48,5	[16, 19, 22, 42, 78]
Fe	ND	ND	-	200-1033	830	[23, 42, 78]
Ga	ND	ND	-	1,8-470	100	[89–91]
Ge*	ND	ND	-	0,50	0,5	[24]
Hg	0,03-2,4	0,43	[11, 17, 20, 32]	30-350	92	[16, 21]
In	0,03-5,5	0,15	[20, 31]	0,37-32	14,5	[18, 33, 78, 89, 90]
K	ND	ND	-	0,09-390	0,85	[15, 39, 78, 80, 83, 86, 88]
Li	ND	ND	-	0,08-8,0	0,53	[15, 18, 23, 84, 85, 88, 92]
Mg	ND	ND	-	0,63-340	21	[15, 81, 83, 85, 86, 93]
Mn	ND	ND	-	52-400	190	[18, 23, 78]
Na	ND	ND	-	0,02-48	0,22	[15, 80, 83, 84, 86, 93]
Ni	ND	ND	-	22-840	360	[16, 78, 87]
Pb	0.06-50	1,4	[11, 17, 20, 30, 43, 94]	0,01-970	29	[16, 23, 27, 42, 78, 95–97]
Rb	ND	ND	-	0,30-180	2,0	[15, 23, 44, 84, 85, 88]
Sb*	0,51	0,51	[**D4**]	0,36-1,2	0,36	[25, 29]
Se*	2,9	2,9	[**D4**]	0,20-3,1	0,2	[24, 29]
Sn*	ND	ND	-	0,80	0,8	[24]
Sr	ND	ND	-	13-2500	350	[18, 23, 44, 84, 85, 88, 92]
Tl	0,007-0,42	0,03	[11, 17, 20]	0,8-12	6,4	[19, 98]
Zn	0,018-1,9	0,14	[10, 11, 17, 20, 26, 94]	6,0-210	72	[13, 22, 23, 39, 78, 79]

ND – nie dotyczy

* – zastosowanie techniki HG

Precyzja pomiarów (wyrażana jako RSD) jest w dużej mierze uzależniona od stabilności przepływu roztworu ciekłej elektrody i dla obu układów wynosiła ona 0,2-7,2%, w pracach opublikowanych w ostatnich latach. Nieco gorsze wartości RSD obserwuje się ogólnie w przypadku układu FLA APGD [**D1**, **D4**, 10, 11]. Wynika to z faktu, że w trakcie pracy układu katoda bombardowana jest strumieniem wysokoenergetycznych jonów, co powoduje jej silne nagrzewanie się, a to w konsekwencji destabilizuje wyładowanie. Innym źródłem destabilizacji wyładowania mogą być fluktuacje powierzchni ciekłej elektrody, spowodowane stosowaniem pomp perystaltycznych do doprowadzania analizowanego roztworu do układu wyładowczego. Dlatego, w celu poprawy stabilności przepływu roztworu FLA i w konsekwencji – zwiększenia precyzji, część badaczy stosowała specjalne naczynia buforujące [21, 41, 44, 68, 90], tłumiki pulsacji umieszczone wewnątrz przewodu silikonowego [15, 78, 85, 86] lub specjalną rurkę antypulsacyjną [58]. Wyładowanie może być również stabilizowane poprzez chłodzenie stałej elektrody z zastosowaniem gazu osłonowego lub bloku chłodzącego z ciągłym przepływem wody [11, 20].

5.6. Efekty matrycowe

Kolejnym istotnym aspektem mającym wpływ na przydatność danej metody w analizie pierwiastkowej jest jej odporność na efekty matrycowe i interferencje spektralne. Jedną z istotnych niedogodności, związanych z praktycznym wykorzystywaniem metody ICP OES, jest mnogość linii emisyjnych obserwowanych dla każdego z pierwiastków, wynikająca z wysokiej temperatury plazmy. To powoduje, że występują tzw. interferencje spektralne, będące wynikiem nakładania się na siebie linii emisyjnych różnych pierwiastków leżących blisko siebie na widmie. Uniemożliwia to tym samym rejestrowanie intensywności danej linii i skutkuje koniecznością wyboru innej linii, o mniejszej czułości, co w oczywisty sposób powoduje pogorszenie wartości DL [76]. Z kolei w przypadku układów APGD tego rodzaju interferencje spektralne nie są zwykle obserwowane, z racji tego, że widma tych układów zawierają zaledwie kilka linii emisyjnych dla każdego z pierwiastków. Nieco inaczej ma się sytuacja w przypadku efektów matrycowych, wynikających z obecności innych składników próbki, mogących zakłócać pracę układu wyładowczego. Plazma typu ICP jest ogólnie odporna na efekty matrycowe, co związane jest bezpośrednio z jej wysoką temperaturą, która w większość przypadków pozwala na kompletną atomizację składników próbki [76]. Natomiast temperatura plazmy w układach APGD jest ok. 3 razy niższa, co zwiększa ich podatność na występowanie efektów matrycowych. Dla przykładu, w badaniach, w których wyznaczano czułość linii rezonansowej Hg (253,7 nm) dla układu FLC APGD, zaobserwowano najwyższą intensywność sygnałów w przypadku kiedy Hg była wprowadzana do plazmy w postaci prostych jonów, tj. Hg^{2+}. Natomiast gdy analizowany roztwór zawierał organiczne formy Hg, tj. metylortęć lub tiomersal, obserwowano ok. 2-4-krotny spadek intensywności tej samej linii atomowej [99]. W innych badaniach rejestrowano intensywność linii emisyjnej Ca I 422,7 nm dla roztworu FLC, który zawierał dodatek H_3PO_4 i porównywano tę intensywność do tej, zarejestrowanej dla roztworu bez dodatku tego kwasu. Zauważono wówczas, że dodatek H_3PO_4 do analizowanego roztworu skutkuje obniżeniem intensywności sygnału Ca o ok. 15-20%. Na pewną poprawę czułości linii Ca w obecności H_3PO_4 pozwoliło zwiększenie odległości międzyelektrodowej, skutkujące wzrostem temperatury plazmy, jednak rejestrowana intensywność linii Ca wciąż była o kilka procent niższa niż w przypadku gdy roztwór FLC nie zawierał H_3PO_4 [64]. Jeszcze innym przykładem mogą być badania, w których wyznaczano zawartość wybranych pierwiastków w próbkach miodu z użyciem układu FLC APGD, stosując jedynie rozcieńczenie i zakwaszenie jako metodę przygotowania próbek (nie zastosowano mineralizacji próbek). Ponieważ miody zawierają ok. 80% cukrów prostych, w pierwszej części tej pracy zbadano wpływ matrycy zawierającej glukozę i fruktozę w stężeniu równym 20 g/l na intensywności rejestrowanych sygnałów Ca, Cu, Fe, Li, Mg, Mn, Rb i Zn. Ustalono, że – w porównaniu do roztworu, który nie zawierał wspomnianych cukrów – intensywności sygnałów analitów były niższe o 15-50% [100]. W przypadku układu FLA APGD istnieje niewiele badań dotyczących wpływu dodatku wybranych związków na intensywności sygnałów analitów. Niemniej jednak, w jednej z prac badano wpływ dodatku CH_3OH oraz C_2H_5OH na intensywności rejestrowanych sygnałów Ag, Cd, Hg, In, Pb, Tl i Zn. Wyniki tych badań wykazały, że intensywność

sygnału In była ok. 35-krotnie większa w przypadku kiedy roztwór FLA zawierał dodatek wspomnianych związków, podczas gdy dla pozostałych pierwiastków ten sam dodatek badanych alkoholi nie wpływał znacząco na sygnały analitów (Cd, Hg, Tl, Zn) lub drastycznie je obniżał (Ag, Pb). Dodatkowo zaobserwowano destabilizację wyładowania dla stężenia wspomnianych alkoholi wynoszącego powyżej 3% [31]. Z kolei w innej pracy, badano wpływ wybranych soli, tj. $Fe(NO_3)_3$, NH_4NO_3, K_2SO_4, $MgSO_4$, KI, NH_4F, $KMnO_4$, $NaHCO_3$, KH_2PO_4, $K_2Cr_2O_7$, Na_2S, i $Ca(NO_3)_2$, w stężeniach wynoszących 2 i 20 g/l dla obu układów APGD na intensywności sygnałów Br i Cl. Zaobserwowano, że obecność wspomnianych soli w stężeniu 2 g/l nie miała istotnego wpływu na intensywności sygnałów analitów zarówno dla układu FLA APGD jak i układu FLC APGD. Z kolei w przypadku stężenia wynoszącego 20 g/l, obserwowano istotne spadki sygnałów obu analitów dla obu tych układach, przy czym układ FLA APGD okazał się być bardziej odporny na efekty matrycowe, niż FLC APGD [**D2**].

Nieco inaczej ma się kwestia wpływu obecności innych pierwiastków w badanej próbce na efekty matrycowe obserwowane w obu układach APGD. Wpływ pierwiastkowej matrycy na sygnały analitów jest o tyle istotny w praktycznym zastosowaniu danej metody, że nie każda próbka rzeczywista zawiera złożoną matrycę organiczną (np. próbki wód), natomiast w każdej z nich obecne są jony innych pierwiastków, nierzadko w dużych stężeniach. Można by się spodziewać, że układ FLC APGD będzie bardziej podatny na wspomniane efekty niż układ FLA APGD z racji bombardowania roztworu FLC wysokoenergetycznymi jonami, skutkującym rozpylaniem nie tylko jonów analitów ale także pozostałych pierwiastków, będących składnikami próbki. Stąd, wiedząc, że w układzie FLA APGD powierzchnia roztworu bombardowana jest strumieniem elektronów, które są zbyt lekkie by doprowadzić do rozpylania roztworu, można oczekiwać, że efekty matrycowe dla tego układu będą znikome. W rzeczywistości natomiast obserwuje się dokładnie odwrotne zachowanie obu tych układów. Okazuje się bowiem, że układ FLC APGD wykazuje się znikomą podatnością na wahania sygnałów analitów w obecności innych pierwiastków. Przykładowo, obecność jonów Ag^+, Al^{3+}, Ba^{2+}, Ca^{2+}, Cd^{2+}, Cr^{3+}, Cs^+, Ga^{3+}, K^+, Mg^{2+}, Mn^{2+}, Na^+, Sr^{2+} i Zn^{2+} (a także HPO_4^{2-}, $H_2PO_4^{2-}$, PO_4^{3-} i SO_4^{2-}) w stężeniu do 300 mg/l nie wpływa znacząco na sygnały Hg i Bi [21, 41]. Podobnie, nie obserwuje się istotnych wahań sygnału In w obecności jonów Cd^{2+}, Co^{2+}, Cu^{2+}, Mn^{2+}, Ni^{2+} i Pb^{2+} w stężeniach do 2 mg/l oraz Ca^{2+}, Cr^{3+}, Fe^{3+}, Ga^{3+}, K+, Mg^{2+}, Na^+ i Zn^{2+} w stężeniach do 20 mg/l [33, 90]. Innymi pierwiastkami odpornymi na obecność jonów współistniejących, w stosunkowo dużych stężeniach, są Ca, Cs, Ga, K, Mg, Na, Rb, Sr, Tl [72]. Mechanizm powstawania interferencji matrycowych dla układu FLC APGD nie został dotychczas odkryty, jednakże przyjmuje się, że może być on wynikiem wtórnych reakcji, które zachodzą w fazie wyładowania i prowadzą do powstania form analitów, które nie są atomizowane i wzbudzane, lub formy te wpływają negatywnie na warunki atomizacji i wzbudzenia w plazmie.

Natomiast układ FLA APGD okazuje się być wysoce podatny na efekty matrycowe związane z obecnością innych jonów w analizowanej próbce. Badane w tym układzie stężenia jonów współistniejących są zwykle stosunkowo niskie i wynoszą 1 lub 10 mg/l. W przypadku stężenia równego 1 mg/l efekty matrycowe nie są jeszcze zwykle obserwowane dla większości pierwiastków [20, 26], warto jednak podkreślić, że nawet tak niskie stężenie składników matrycy może powodować obniżenie sygnałów niektórych analitów, np. Bi w obecności Fe^{3+}, Mn^{2+}, Pb^{2+} i Sn^{2+} [**D1**] lub In w obecności Cu^{2+}, Fe^{3+} i Mn^{2+} [20]. Natomiast obecność interferentów w stężeniu 10 mg/l powoduje zauważalne obniżenie intensywności linii atomowych większości analitów, z czego najbardziej podatne na interferencje okazują się być Ag, Bi, In, Pb i Zn [11, 26, 31, 94, 101]. Warty uwagi jest również fakt, że najbardziej interferującymi składnikami matrycy są litowce i berylowce, a konkretnie Ca, K, Mg i Na [20, 94]. Z racji tego, że są to pierwiastki łatwo-jonizujące (ang. *easily ionized elements*, EIE), można przypuszczać, że przyczyną ich znaczącego wpływu na pogorszenie odpowiedzi analitów jest zaburzona równowaga jonowa plazmy, prowadząca do pogorszenia warunków wzbudzenia. Podobnie jak w przypadku układu FLC APGD, szczegółowy mechanizm odpowiadający za obserwowane efekty matrycowe w układzie FLA APGD nie został jeszcze poznany. Niemniej postuluje się, że – biorąc pod uwagę, że większość wspomnianych wyżej interferentów nie dostaje się do strefy wyładowania – procesy prowadzące do powstania efektów

matrycowych zachodzą jeszcze w roztworze i prawdopodobnie obejmują wtórne reakcje elektrochemiczne z solwatowanymi elektronami i/lub rodnikami H i OH, które są reakcjami konkurencyjnymi do procesu tworzenia lotnych form analitów [72]. Potwierdzeniem tego przypuszczenia mogą być obserwacje opisane w jednej z prac [94], w której udowodniono, że obecność jonów współistniejących negatywnie wpływa na wydajność transportu analitów do plazmy, a jednocześnie nie wpływa na wartości temperatury rotacyjnej (T_{rot}(OH)) i temperatury wzbudzenia (T_{wzb}(H)), co z dużym prawdopodobieństwem oznacza, że warunki wzbudzenia w wyładowaniu nie ulegają zmianie.

5.7. Zastosowanie w analizie pierwiastkowej

W większości z dotychczas opublikowanych prac prowadzenie analizy pierwiastkowej próbek rzeczywistych odbywa się poprzez sprzęgnięcie układów FLA APGD lub FLC APGD z detektorem OES. Wyładowania APGD pełnią w tych układach rolę atomizera i źródła wzbudzenia, co wyklucza konieczność stosowania dodatkowych źródeł wprowadzania próbek do plazmy, np. rozpylaczy pneumatycznych. Układy do generowania APGD zwykle pracują w trybie analizy o ciągłym przepływie (ang. *continuous flow analysis*, CFA), co pozwala na zastosowanie dłuższego czasu integracji widm, prowadząc tym samym do uzyskiwania stosunkowo niskich wartości DL [10, 13, 16, 20, 39, 49, 82, 88, 102]. W tym przypadku analizowane roztwory doprowadzane są do wyładowania z użyciem pomp perystaltycznych o natężeniu przepływu roztworu mieszczącym się zwykle w zakresie 2-5 ml/min. Z uwagi na ograniczoną dostępność niektórych próbek, dąży się do uzyskiwania możliwie najmniejszych natężeń przepływu roztworu, co ogranicza zużycie badanych preparatów. Jednym z zaproponowanych przez badaczy rozwiązań, nakierowanych na osiągnięcie tego celu, jest modyfikacja konstrukcji układu wyładowczego w taki sposób, żeby wyładowanie było generowane w kontakcie z wiszącą kroplą [13, 46, 103]. Tego typu układy wyładowcze nadal pracują w trybie analizy o ciągłym przepływie ale natężenie przepływu próbki jest tak zoptymalizowane, żeby kolejna porcja roztworu dopływała do końca rurki doprowadzającej dokładnie w momencie, w którym istniejąca już kropla, podtrzymująca wyładowanie, zostanie całkowicie odparowana. Podejście to zostało dotychczas zastosowane wyłącznie dla układu FLC APGD i pozwoliło zmniejszyć stosowane natężenia przepływu analizowanych roztworów do wartości 0,4-1,1 ml/min. Innym sposobem doprowadzania analitów do wyładowania, chętnie stosowanym przez niektóre grupy badawcze, jest działanie układów APGD w trybie analizy przepływowo-wstrzykowej (ang. *flow injection analysis*, FIA) [33, 34, 44, 80, 90, 95, 104, 105]. Objętość nastrzykiwanych próbek w trybie FIA mieści się w zakresie od 5 µl do 5 ml [16, 58, 90, 95, 104, 105]. Tryb analizy FIA również był dotychczas stosowany tylko dla układu FLC APGD. Ostatnim z często stosowanych metod wprowadzania analitów do plazmy jest wspomniana w poprzednich rozdziałach technika HG [24, 25, 27–29, 32]. W takich układach stała elektroda zostaje zastąpiona strumieniem gazu, który doprowadza anality do źródła wzbudzenia, a roztwory FLA/FLC zawierają jedynie wodny roztwór kwasu, pełniący rolę ciekłej elektrody i służący podtrzymaniu wyładowania. Do generowania wodorków stosuje się układy komercyjne, np. Hydride Generator 77 firmy Agilent [24, 25, 27, 28], lub samodzielnie skonstruowane układy **[D3**, **D4**, 29].

Omawiane układy APGD są stosowane do analizy pierwiastkowej różnego rodzaju próbek metalurgicznych, środowiskowych i żywności, które zostały zestawione w tabeli 2.

Tabela 2. Spis próbek analizowanych z zastosowaniem układów FLA APGD i FLC APGD.

Układ	**Próbka**	**Źródła**
FLA APGD	Gleba	[26, 32]
	Herbata	[11]
	Krew	[30]
	Liście herbaty	[11]
	Mleko	[106]
	Mosiądz	[11]
	Nerka świni	[12, 13]

	Osad ze strumienia	[26]
	Osady rzeczne	[30]
	Ryby	[32]
	Ryż	[26, 32]
	Soki	[**D2**]
	Wody syntetyczne	[10, 17, 26]
	Ścieki	[**D4**]
	Ścieki laboratoryjne	[17]
	Tłuszcz z homara	[11, 12]
	Wina	[14]
	Włosy	[30, 32]
	Woda gruntowa	[12]
	Woda kranowa	[**D1**, **D2**, **D4**, 13]
	Woda morska	[**D2**]
	Woda mineralna	[**D1**, **D2**, **D4**]
	Woda rzeczna	[**D1**, **D2**, **D4**]
	Woda źródlana	[13]
	Żeliwo	[94]
FLC APGD	Doustne roztwory glukonianów	[79]
	Hydrofity	[107]
	Koncentraty cynku	[68]
	Krew	[79]
	Lecznicze surowce roślinne	[82]
	Leki	[41]
	Mąka ryżowa	[28]
	Napary herbaty	[37]
	Osady rzeczne	[24, 95, 98, 108]
	Osad	[16]
	Ostrygi	[105]
	Pigmenty mineralne	[109]
	Płodowa surowica cielęca	[24]
	Popioły	[105, 110]
	Roztwór soli fizjologicznej	[88]
	Rudy	[96, 97]
	Ryby	[105, 107]
	Ryż	[28]
	Soki	[**D5**]
	Solanka	[80]
	Sole kopalniane	[83]
	Stopy cyrkonu	[67, 111]
	Szczepionki	[99]
	Ścieki	[21, 33, 39]
	Ścieki laboratoryjne	[95]
	Wina	[14]
	Włosy	[95, 108, 112]
	Woda jeziorna	[41, 81]
	Woda kranowa	[16, 21, 39]
	Woda morska	[**D2**, 16]
	Woda mineralna	[39, 86, 93]
	Woda rzeczna	[21, 39, 81]

Metoda przygotowania próbek do analizy zależy od matrycy badanej próbki. W przypadku próbek ciekłych, przygotowanie próbek do analizy zwykle ogranicza się do ich przesączenia przez filtry strzykawkowe [12, 13, 16, 17, 39, 44] oraz zakwaszenia z użyciem HNO_3 [13, 16, 17, 22, 81, 88, 93, 95], HCl [26, 27, 80] lub H_2SO_4 [**D2**, **D3**]. Jednakże w przypadku próbek stałych, proces przygotowania próbek do analizy wymaga zwykle większego nakładu pracy. Wyjątkiem są przypadki, w których stałe składniki próbki są rozpuszczalne w wodzie – wówczas preparatyka takich próbek może ograniczyć się do ich rozpuszczenia, odpowiedniego zakwaszenia oraz odwirowania (w celu usunięcia nierozpuszczonych cząstek stałych) [83]. W pozostałych przypadkach, konieczne jest przeprowadzenie mineralizacji na mokro, w celu pozbycia się stałej matrycy tych próbek i przeprowadzenia analitów do roztworu. Wspomnianą mineralizację zwykle prowadzi się z zastosowaniem stężonych kwasów, tj. HNO_3 [11, 24, 30, 32, 94] lub mieszaniny HNO_3 i HCl [68, 79, 82, 96], $HClO_4$ [95], HF [26], H_2O_2 [11–13, 24] lub mieszaniny HF i $HClO_4$ [30, 32] lub mieszaniny HF, $HClO_4$ oraz HNO_3 [16, 24, 95]. Mineralizację prowadzi się korzystając z pieców mikrofalowych, bloków grzewczych lub płyt elektrycznych, ogrzewanych do temperatury 100-280°C.

Biorąc pod uwagę, że w przypadku układu FLC APGD nie obserwuje się zwykle istotnych interferencji matrycowych, wynikających z obecności w roztworze jonów współistniejących, analizę próbek o nieskomplikowanej matrycy (np. wody) wykonuje się zwykle stosując do kalibracji metodę krzywej wzorcowej [16, 21, 22, 39, 44, 82–84]. Natomiast w przypadku próbek o bardziej złożonej matrycy, stosuje się metodę dodatku wzorca [96, 105, 111, 112] lub dopasowania matrycy [27, 88, 100]. Z kolei w przypadku układu FLA APGD obserwowane efekty matrycowe stanowią istotną przeszkodę w jego praktycznym wykorzystaniu do analizy pierwiastkowej metodą OES, dlatego metoda krzywej wzorcowej jest rzadko stosowana [10, 17]. Niemniej jednak, kalibracja z użyciem krzywej wzorcowej może być z powodzeniem stosowana w przypadku sprzężenia układu FLA APGD z techniką CVG. W tego typu układach sprzężonych, anality są oddzielane od innych składników matrycy i nie są wprowadzane do fazy wyładowania, dzięki czemu nie obserwuje się istotnych efektów matrycowych [30, 32].

Poprawność wyników analizy wykonanych metodą OES ze źródłami wzbudzeniem jakimi są układy FLC APGD i FLA APGD jest najczęściej weryfikowana poprzez porównanie wyników analizy wykonanej z zastosowaniem tych układów do wyników otrzymywanych z zastosowaniem metod odniesienia, takich jak ICP OES [11, 16, 39, 68, 79, 95, 96], ICP MS [17, 24, 25, 27, 82] lub chromatografii jonowej (ang. *ion chromatography*, IC) [83, 96]. Innym często stosowanym sposobem potwierdzania poprawności wyników wykonywanych metodami FLC APGD OES lub FLA APGD OES jest tzw. badanie odzysku w przypadku próbek, do których dodano określone ilości analitów [13, 17, 25, 27, 41, 94]. Ostatnim sposobem potwierdzenia poprawności wyników uzyskiwanych w toku analiz wspomnianymi powyżej metodami jest analiza certyfikowanych materiałów odniesienia (ang. *certified reference material*, CRM) [26–28, 32, 68, 95].

Pomimo tego, że większość badaczy stosuje omawiane układy APGD jako niezależne źródła wzbudzenia w OES lub MS, to warto w tym miejscu wspomnieć również o badaniach, w których stosowano wspomniane układy jako substytut klasycznych rozpylaczy pneumatycznych, mających za zadanie transportować anality do ICP. Tego typu badania były prowadzone zarówno dla układu FLA APGD [50, 113, 114] jak i FLC APGD [46]. W przypadku FLC APGD ICP OES, badano dużą liczbę pierwiastków (Ag, Al, As, Ba, Be, Bi, Ca, Cd, Co, Cr, Dy, Er, Eu, Fe, Ga, Ge, Hg, Ho, I, In, Ir, K, Li, Mg, Mn, Na, Nb, Ni, Os, Pb, Pr, Rb, Sb, Sc, Se, Sn, Sr, Tb, Tl, Y i Zn) i zaobserwowano średnio 2-krotny wzrost intensywności sygnałów analitów w porównaniu do tych mierzonych z zastosowaniem techniki nebulizacji pneumatycznej (ang. *pneumatic nebulization*, PN), chociaż w przypadku I i Y wzmocnienie to wynosiło nawet 6 razy [46]. Badacze zaobserwowali wysoką wydajność transportu analitów do ICP, wynoszącą w większości przypadków >80%, co niewątpliwie miało istotny wpływ na otrzymane przez nich wyniki [46]. Z kolei układ FLA APGD był stosowany jako technika wprowadzania roztworów próbek zarówno do ICP OES [113, 114] jak i ICP MS [50]. W przypadku ICP OES odnotowano poprawę wartości DL o ok. 2 razy dla Ag, Bi, Pb, Tl i Zn, 12 razy dla Cd, 90 razy dla Hg [114] oraz 140 razy dla Hg przy prowadzeniu analizy w trybie

przepływowo-wstrzykowym [50]. Z kolei zastąpienie techniki PN techniką CVG z zastosowaniem układu FLA APGD pozwoliło na uzyskanie wzmocnienia sygnałów Ag, Bi, Cd, Hg, Pb i Tl odpowiednio 8-, 4-, 13-, 13-, 9-, 10- i 7-krotnie w przypadku metody ICP MS [113]. Podobnie jak w przypadku układu FLC APGD, uważa się, że głównym czynnikiem wpływającym na obserwowane wzmocnienia sygnałów i obniżenie wartości DL jest większa ilość atomów analitów docierająca do ICP, będąca skutkiem zwiększonej wydajności generowania lotnych par analitów w układzie FLA APGD.

6. OPIS PUBLIKACJI NAUKOWYCH

6.1. Ogólny cel pracy

Celem niniejszej rozprawy doktorskiej była poprawa charakterystyki analitycznej metody OES poprzez zastąpienie typowego źródła wzbudzenia w postaci plazmy wielkogabarytowej, np. ICP, zminiaturyzowanymi źródłami wzbudzenia w postaci układów FLC APGD i FLA APGD oraz zastosowanie nowoopracowanych metod FLC APGD OES i FLA APGD OES do oznaczania wybranych pierwiastków w próbkach środowiskowych i żywności.

Mając na uwadze fakt, że wymienione układy wyładowcze są źródłem wielu reaktywnych form, np. rodników H, NO, OH i N_2, oraz elektronów, oczekiwano, że zastosowanie ich jako źródła wzbudzenia w OES wpłynie na poprawę charakterystyki analitycznej stosowanego detektora poprzez zwiększenie wydajności transportu analitów do rdzenia plazmy w wyniku rozpylania powierzchni strumienia cieczy i/lub kropel oraz tworzenia lotnych form wybranych pierwiastków w wyniku procesów i reakcji plazmochemicznych zachodzących na granicy faz plazma-ciecz. Dodatkowo, w przypadku wybranych pierwiastków tworzących lotne formy, oczekiwano dalszej poprawy charakterystyki analitycznej poprzez sprzęgnięcie badanych układów APGD z technikami HG/CVG.

Aby osiągnąć zamierzony cel, w pierwszej kolejności skonstruowano odpowiednie układy wyładowcze oraz sprzęgnięto je z detektorem. W celu poprawy charakterystyki analitycznej badanych metod oraz stabilności wyładowania, pierwotna konstrukcja była modyfikowana na dalszych etapach badań. W kolejnych etapach prac, zastosowano badane układy do:

- Oznaczania pierwiastków, które wcześniej nie były oznaczane z zastosowaniem tego typu układów, tj. Bi, Br i Cl, a także – w przypadku FLA APGD – As, Sb i Se;
- Poprawy granic wykrywalności wybranych pierwiastków (As, Bi, Br, Hg, Sb i Se) poprzez sprzęgnięcie badanych źródeł wzbudzenia z technikami HG/CVG;
- Zastosowanie badanych układów do analizy próbek napojów o złożonej matrycy z pominięciem etapu mineralizacji.

6.2. Zastosowanie układów FLA APGD i FLC APGD do oznaczania nowych pierwiastków [D1, D2]

W związku ze stale postępującą urbanizacją i szybkim rozwojem przemysłu, konieczne jest opracowanie wiarygodnych metod, pozwalających na szybkie, tanie, dokładne (prawdziwe i precyzyjne) oznaczanie pierwiastków w próbkach charakteryzujących się różnorodną matrycą.

W celu zapewnienia wiarygodności otrzymywanych wyników pomiarów, konieczne jest stosowanie aparatury charakteryzującej się odpowiednią czułością oraz niskimi granicami wykrywalności, przy jednoczesnym zapewnieniu wysokiej dokładności. Nie bez znaczenia są też szerokie zakresy liniowości, możliwość prowadzenia analiz wielopierwiastkowych oraz ograniczony do niezbędnego minimum proces przygotowania próbek, skracający tym samym czas wykonywanych analiz. Ponadto, oczekuje się, że współcześnie stosowane metody analityczne będą wykorzystywały zminiaturyzowane układy o prostej konstrukcji, pozwalające prowadzić analizy *in situ*, przy jednoczesnym obniżeniu kosztów związanych z zakupem i eksploatacją stosowanej aparatury pomiarowej.

Dlatego celem tego etapu prac było zwiększenie możliwości zastosowania układów FLA APGD i FLC APGD do oznaczania pierwiastków, które wcześniej nie były oznaczane z użyciem tego rodzaju źródeł wzbudzenia, tj. Bi, Br i Cl. Pierwiastki te mają istotny wpływ na środowisko naturalne, z racji ich szerokiego zastosowania w przemyśle. Przykładowo, Bi jest używany przy produkcji leków, kosmetyków, półprzewodników, stali i stopów, szkła i farb [115], a jego toksyczny wpływ na organizm ludzki został wielokrotnie udowodniony [115–117]. Z kolei Br i Cl wykorzystuje się w przemyśle chemicznym, głównie jako składniki środków dezynfekujących i pestycydów [118, 119]. Ich nadmiar może prowadzić do zanieczyszczenia wód gruntowych i powierzchniowych, co z kolei może wpłynąć na zdrowie ludzi i zwierząt, a także na rozwój ekosystemów wodnych. Z racji tego, że pierwiastki te – ze szczególnym naciskiem na Bi i Br – występują w próbkach naturalnych w stosunkowo niskich stężeniach, opracowanie wiarygodnej metody ich oznaczania jest sporym wyzwaniem [117]. W związku z tym, postanowiono zbadać możliwość użycia układów FLA APGD

i FLC APGD do oznaczania omawianych pierwiastków. Ponieważ układy te nigdy nie były wykorzystywane do oznaczania niemetali, dodatkowym celem oznaczania Br i Cl było porównanie ogólnej charakterystyki tychże układów pomiędzy oznaczaniem metali i niemetali.

6.2.1. Widma porównawcze

W pierwszym etapie badań zarejestrowano widma emisyjne układów FLA APGD i FLC APGD, w celu identyfikacji linii emisyjnych badanych pierwiastków. W przypadku oznaczania Bi [**D1**], analizowane roztwory zawierały 10 mg/l tego pierwiastka i były zakwaszone roztworem HNO_3 do stężenia 0,01 (FLA) lub 0,1 (FLC) mol/l. Badany zakres spektralny wynosił 200-280 nm. Zastosowano następujące parametry pomiarowe: natężenie prądu wyładowania równe 50 mA, natężenie przepływu roztworu próbki równe 3,5 ml/min oraz natężenie przepływu gazu równe 300 (FLA) lub 50 (FLC) ml/min. Z kolei w przypadku oznaczania Br i Cl [**D2**], przygotowano roztwory FLA i FLC zawierające mieszaninę obu tych pierwiastków, każde w stężeniu 1000 mg/l. Rejestrowano widma emisyjne w zakresie spektralnym 700-900 nm. Zastosowano następujące warunki pomiarowe: natężenie prądu wyładowania równe 40 mA, natężenie przepływu roztworu próbki równe 3,0 ml/min oraz natężenie przepływu gazu równe 150 ml/min. Zarejestrowane widma przedstawiono na rys. 2 i 3.

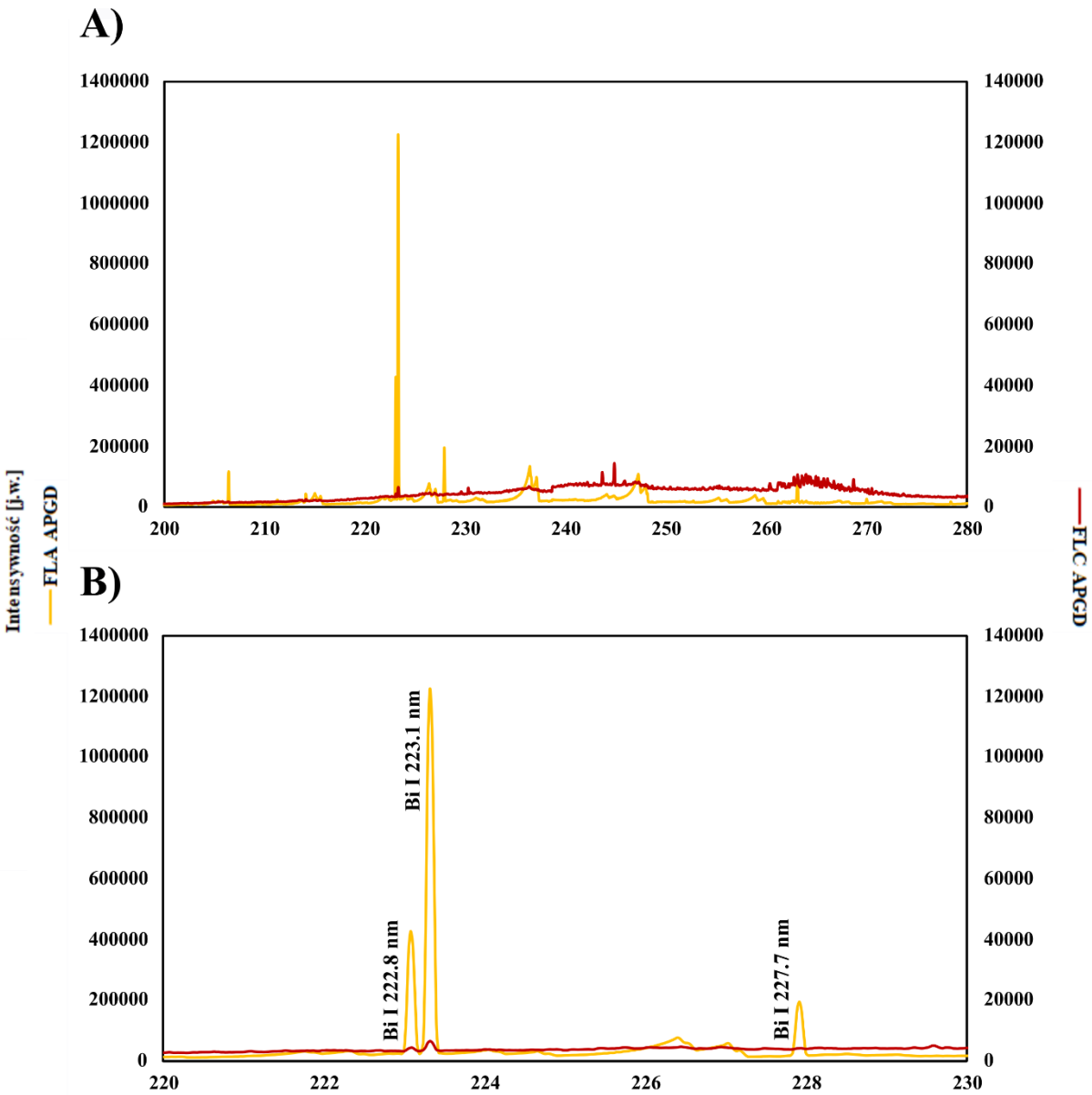

Rys. 3. Widmo układów FLA APGD i FLC APGD zarejestrowane w zakresie 200-280 nm (A) oraz jego zbliżenie w zakresie 220-230 nm (B) ze zidentyfikowanymi liniami atomowymi Bi.

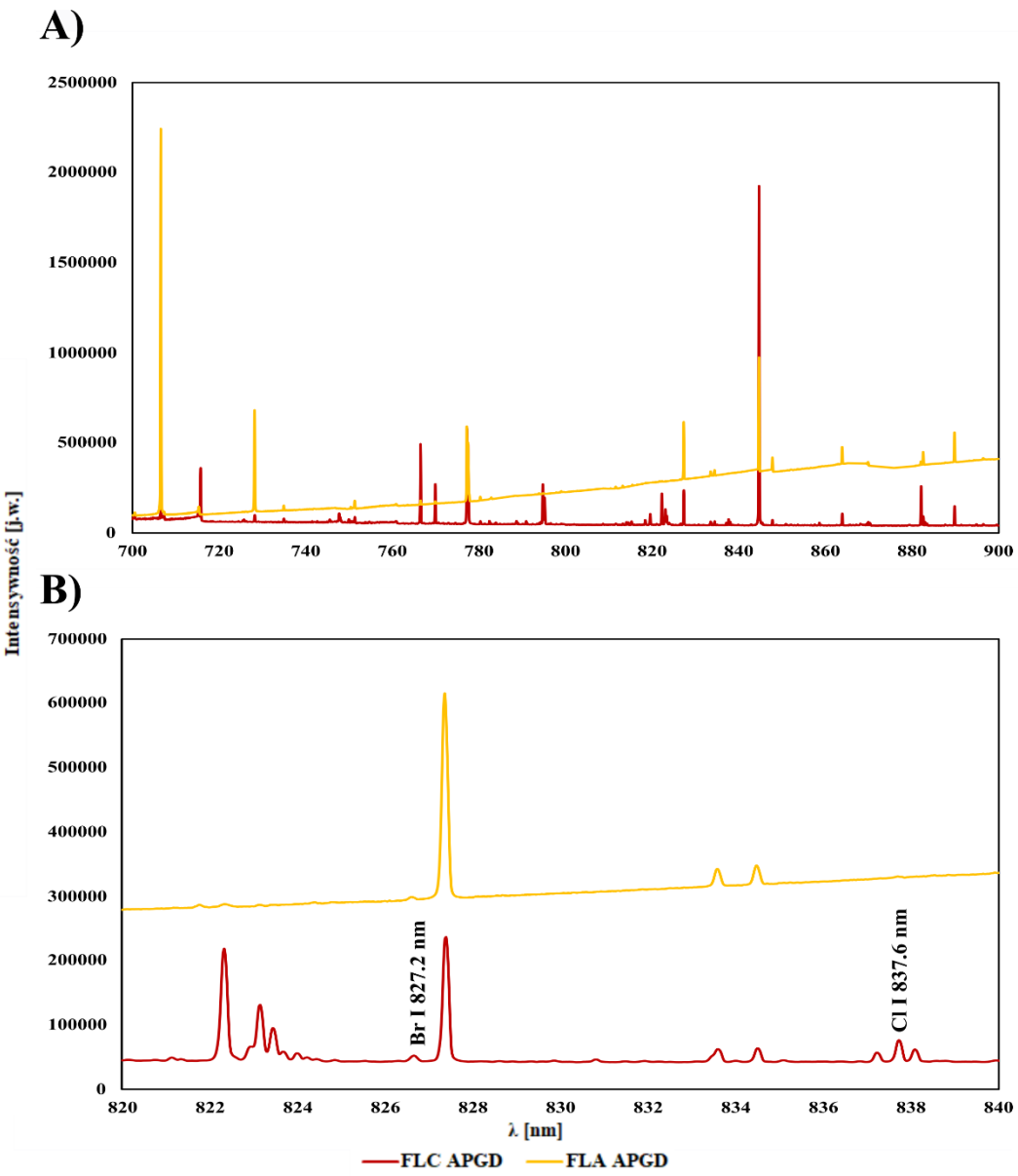

Rys. 4. Widmo układów FLA APGD i FLC APGD zarejestrowane w zakresie 700-900 nm (A) oraz jego zbliżenie w zakresie 820-840 nm (B) ze zidentyfikowanymi liniami atomowymi Br i Cl.

W przypadku Bi, odnotowano obecność 8 linii emisyjnych dla układu FLA APGD, z czego najbardziej czułą linią była linia rezonansowa przy 223,1 nm. Z kolei dla układu FLC APGD, oprócz niewielkiego sygnału od linii rezonansowej, dostrzeżono jeszcze obecność 3 innych linii (szczegóły w [**D1**]. Innymi składnikami widma były pasma cząsteczki NO, których intensywność była znacząco większa w przypadku układu FLA APGD. Różnica w intensywności pasm cząsteczki NO pomiędzy badanymi układami wynikała zapewne ze zwiększonego odparowania wody w przypadku układu FLC APGD, co ograniczało dyfuzję cząsteczek N_2 do wnętrza wyładowania (szczegóły w rozdziale 5.4). Pomimo wspomnianej wyżej zauważalnie większej intensywności tła, obserwowanej dla układu FLA APGD, wartość SBR (ang. *signal-to-background ratio*) linii rezonansowej Bi była ok. 50-krotnie wyższa w porównaniu do tej dla układu FLC APGD. Mając na uwadze, że Bi należy do grupy pierwiastków tworzących lotne formy [120], można domniemywać, że jego zwiększona emisja w przypadku układu FLA APGD była efektem opisanego w rozdziale 5.3 generowania jego lotnych indywiduów, prawdopodobnie w reakcji ze strumieniem elektronów, bombardujących powierzchnię ciekłej anody, i zwiększoną wydajnością transportu tego analitu do wnętrza wyładowania [11]. Innym czynnikiem, mogącym przyczyniać się do obserwowanych różnic w intensywności sygnału Bi może być wspomniane wyżej ograniczone odparowanie wody w przypadku FLA APGD, poprawiające warunki wzbudzenia w tym układzie.

Z kolei w przypadku Br i Cl, odnotowano obecność 14 linii Br dla obu badanych układów oraz 1 (FLA APGD) lub 12 (FLC APGD) linii Cl, przy czym największą czułością charakteryzowały się linie rezonansowe, tj. przy 827,2 nm (Br) i 837,6 (Cl) nm. Jedyną linią Cl, zarejestrowaną w przypadku układu FLA APGD, była linia rezonansowa, przy czym jej intensywność była o rząd wielkości niższa w porównaniu do tej zarejestrowanej dla układu FLC APGD. Z kolei intensywności linii rezonansowej Br były podobne pomiędzy badanymi układami wyładowczymi. Wartości SBR dla obu linii rezonansowych, pomimo zbliżonej wartości intensywności, były o 1 (Br) lub 2 (Cl) rzędy wielkości mniejsze w przypadku układu FLA APGD, co wynikało ze zwiększonej emisji tła w tym układzie. Tendencja ta jest zupełnie odmienna w przypadku intensywności sygnałów analitów obserwowanych dla tych układów dla pierwiastków obecnych w roztworze w postaci kationów, ponieważ intensywności linii emisyjnych analitów – a co za tym idzie, obserwowane wartości DL – są zwykle znacząco lepsze w przypadku układu FLA APGD [20]. Stąd, obserwowane w tej pracy różnice w intensywnościach można próbować tłumaczyć w oparciu o dyskutowany w rozdziale 5.3 mechanizm transportu analitów do plazmy. Uważa się bowiem, że według tego mechanizmu, w reakcjach redukcji kationów analitów z solwatowanymi elektronami i/lub rodnikami H powstają lotne formy tych analitów. W omawianej pracy anality były wprowadzane do układu w postaci anionów, dlatego reakcje redukcji nie mogły być odpowiedzialne za tworzenie ich lotnych form. Jednakże w fazie gazowej układów APGD oraz na granicy faz plazma-ciecz obecne są również rodniki OH [43], które mają potwierdzone właściwości utleniające. W związku z tym, można przypuszczać, że w przypadku tych dwóch pierwiastków, ich transport do wnętrza wyładowania odbywał się poprzez tworzenie lotnych cząsteczek Br_2 i Cl_2 w wyniku reakcji utleniania ich anionów ze wspomnianymi rodnikami OH [121, 122]. W związku z tym, warunki pomiarowe w jakich rejestrowano widma obu układów wyładowczych (w tym: stężenie kwasu) mogły nie być optymalne do efektywnego zajścia reakcji utleniania jonów Br^- i Cl^-, skutkując tym samym uzyskaniem niższych intensywności sygnałów analitów.

6.2.2. Optymalizacja warunków pracy układów

Z racji tego, że, w momencie prowadzenia omawianych badań, żaden z oznaczanych pierwiastków (Bi, Br, Cl) nie był wcześniej badany w stosowanych w tej pracy układach, można oczekiwać, że – poza wspomnianymi wyżej czynnikami – jedną z przyczyn obserwowanych różnic w intensywności sygnałów analitów były nieoptymalne warunki prowadzenia pomiarów. Dlatego, w celu wiarygodnego porównania możliwości analitycznych obu badanych układów, w kolejnym etapie badań przeprowadzono optymalizację ich kluczowych parametrów pracy. W tabeli 3 zestawiono parametry, które uznano za mające istotny wpływ na mierzone wartości sygnałów analitów, wraz z ich badanymi zakresami.

Tabela 3. Optymalizowane parametry pracy układów APGD do oznaczania Bi, Br i Cl, wraz z ich badanymi zakresami.

Parametr	**Wartości**		
	Bi		**Br i Cl**
	FLA APGD	**FLC APGD**	**FLA/FLC APGD**
Rodzaj kwasu	HCl / HNO_3		HNO_3 / H_2SO_4
Stężenie kwasu	0.001-0.01 mol/l	0.01-0.1 mol/l	0.01-2,00 mol/l
Natężenie prądu	30-70 mA		30-50 mA
Natężenie przepływu He	50-350 ml/min		150-350 ml/min
Natężenie przepływu próbki	1,0-4,5 ml/min		1,0-4,0 ml/min
Odległość międzyelektrodowa	1-5 mm		-

W przypadku oznaczania Bi z użyciem układu FLA APGD, stosowanie HCl do zakwaszania roztworu skutkowało uzyskaniem wartości SBR o ok. 35% niższych w porównaniu do tego, jakie otrzymano stosując zakwaszenie roztworem HNO_3. Prawdopodobną przyczyną obserwowanego zjawiska było tworzenie się nierozpuszczalnych cząsteczek BiOCl (szczegóły w [**D1**]). Z tego

powodu, w przypadku układu FLC APGD, pominięto etap badania wpływu rodzaju kwasu i zdecydowano o stosowaniu HNO_3 do zakwaszania wszystkich badanych roztworów dla obu układach. W przypadku Br i Cl, stosowanie zarówno HNO_3 jak i H_2SO_4 skutkowało otrzymaniem zbliżonych wartości SBR badanych pierwiastków dla obu układów. Jedynym wyjątkiem była wartość SBR dla Cl w przypadku układu FLA APGD, która okazała się być 2-krotnie wyższa w przypadku użycia H_2SO_4 do zakwaszania roztworu. W związku z powyższym, zdecydowano o kontynuowaniu badań z użyciem H_2SO_4, ze względu na wzmocnienie sygnału Cl dla układu FLA APGD oraz fakt, że H_2SO_4 jest zwykle stosowany do utleniania halogenów.
Wpływ pozostałych parametrów na intensywności sygnałów badanych analitów różnił się w zależności od analitu oraz rodzaju układu wyładowczego. W związku z tym, w tabeli 4 zamieszczono ogólne podsumowanie tych zależności, a szczegółowe dane dostępne są w [**D1**] i [**D2**].

Tabela 4. Wpływ rosnących wartości podanych parametrów pracy układów FLA APGD i FLC APGD na otrzymane wartości SBR badanych analitów dla tych układów.

Parametr	**FLA APGD**		**FLC APGD**	
	Bi	**Br i Cl**	**Bi**	**Br i Cl**
Stężenie kwasu	↓	↑	↑	↓
Natężenie prądu	↑	↓	↑	↑
Natężenie przepływu He	↑	*	↓	↓
Natężenie przepływu próbki	↑	*	↓	↑
Odległość międzyelektrodowa	↓	-	↓	-

* otrzymane wartości SBR różniły się dla poszczególnych pierwiastków oraz kombinacji tego parametru z innymi – szczegóły w [**D2**]

Zestawiając otrzymane w tej pracy wyniki z danymi literaturowymi, cytowanymi w części teoretycznej niniejszej pracy, można zauważyć, że tendencje w zmianach wartości SBR są zgodne z tymi, otrzymywanymi dla innych pierwiastków, badanych dla tych układów. Na tej podstawie, można przypuszczać, że mechanizm transportu Bi do wyładowania jest taki sam, jak dla innych pierwiastków. Podobnie wygląda sytuacja w przypadku oznaczania Br i Cl w przypadku układu FLC APGD. Aczkolwiek warto w tym miejscu podkreślić, że w przypadku optymalizacji stężenia kwasu, tendencje obserwowane dla Br i Cl były dokładnie odwrotne, niż dla innych pierwiastków. W celu wyjaśnienia tego zjawiska, należy rozpatrzyć wpływ stężenia kwasu na mechanizm transportu analitów do wyładowania. Obserwowana dla innych pierwiastków tendencja wzrostu wartości SBR sygnałów wraz ze zwiększaniem stężenia kwasu przypisywana jest odpowiadającemu mu spadkowi natężenia pola elektrycznego w obszarze CDS (powodującego zawracanie kationów analitów do roztworu), skutkującemu zwiększonym transportem analitów do wyższych sfer wyładowania. Ponieważ w niniejszej pracy anality były rozpylane z roztworu w postaci anionów, zwiększone natężenie pola elektrycznego w obszarze CDS wpływało raczej korzystnie na transport analitów w głąb wyładowania ze względu na ich przyśpieszanie w kierunku anody (szczegóły w [**D2**]). Z kolei zupełnie różne (w odniesieniu do danych publikowanych dla innych analitów) tendencje w zmienności wartości SBR zaobserwowano w przypadku oznaczania Br i Cl z użyciem układu FLA APGD. Jak można zauważyć analizując dane w tabeli 4, wpływ rosnących wartości stężenia kwasu i natężenia prądu wyładowania na sygnały analitów był dokładnie odwrotny niż w przypadku Bi (i tym samym – pozostałych analitów). Prawdopodobną przyczyną obserwowanych tendencji było – ponownie – występowanie analitów znajdujących się w roztworze w postaci anionów. Szczegółowy opis wpływu formy jonów na odpowiedź sygnałów analitów został przedstawiony w [**D2**]. Na tej podstawie można wysnuć konkluzję, że obserwowane tendencje w wartościach SBR dla tego układu, potwierdzają wcześniejsze przypuszczenie, że transport badanych analitów do plazmy odbywa się poprzez tworzenie lotnych Br_2 i Cl_2 w reakcji utleniania z rodnikami OH.

6.2.3. Charakterystyka analityczna

W optymalnych warunkach pracy obu układów wyładowczych wyznaczono ich charakterystykę analityczną poprzez wyznaczenie wartości DL, zakresu liniowości sygnałów, czułości linii emisyjnych i precyzji. W tabeli 5 zestawiono wartości DL otrzymane dla badanych analitów.

Tabela 5. Wartości DL Bi, Br i Cl otrzymane dla badanych układów APGD

Układ	**Analit**	**DL (mg/l)**
FLA APGD	Bi	0,00034
	Br	0,15
	Cl	1,5
FLC APGD	Bi	0,27 / 0,033*
	Br	2,1
	Cl	18

* - z dodatkiem 5% kwasu mrówkowego

Jak można zauważyć analizując dane w powyższej tabeli, wartości DL otrzymane dla układu FLA APGD były znacząco lepsze w porównaniu do tych, które otrzymano z użyciem układu FLC APGD, przy czym dysproporcja ta jest szczególnie dostrzegalna w przypadku Bi. Granica wykrywalności Bi dla układu FLA APGD była porównywalna z tymi, które otrzymano dla innych układów mikroplazmowych, w tym takich, w których stosowano technikę HG do wprowadzania próbki [17, 123, 124]. Ponadto, podobne wartości DL tego pierwiastka otrzymywano również w przypadku komercyjnie stosowanych wielkogabarytowych urządzeniach, np. ICP OES [125]. Z kolei wartości DL Br i Cl wahały się w zakresie 0,15-18 mg/l, będąc tym samym o kilka rzędów wyższe niż wartości DL otrzymywane dla innych pierwiastków dla odpowiadających im układów. Warto mieć jednak w tym miejscu na uwadze fakt, że – ze względu na ich powszechne zastosowanie w przemyśle – pierwiastki te (szczególnie Cl) są obecne w próbkach naturalnych w stosunkowo wysokich stężeniach. Dodatkowo wartości DL Cl (szczególnie dla układu FLA APGD) były wciąż lepsze niż ta, którą oferuje ICP OES.

6.2.4. Badanie efektów matrycowych

W kolejnym etapie zbadano wpływ efektów matrycowych na intensywności sygnałów analitów oraz przeprowadzono analizę próbek rzeczywistych. Badanie wpływu efektów matrycowych polegało na dodaniu do analizowanych roztworów jonów innych pierwiastków w stężeniach istotnie większych od stężenia analitów. Mierzone w tych warunkach sygnały porównano do sygnałów bazowych, tj. zmierzonych w warunkach bez dodatku badanych interferentów. W przypadku Bi, wpływ efektów matrycowych badano tylko dla układu FLA APGD, ponieważ czułość linii Bi była zbyt niska żeby móc uzyskać wiarygodne wyniki w przypadku układu FLC APGD. Uzyskane wyniki przedstawiono na rys. 4 i 5.

Jak można zwrócić uwagę analizując dane przedstawione na rys. 4, dodatek jonów pierwiastków interferujących w stężeniu 1 mg/l nie powodował występowania istotnych efektów matrycowych w oznaczeniach Bi z użyciem układu FLA APGD. Wyjątek stanowiły jony Fe, Mn i Sn, których obecność już w tak niewielkim stężeniu powodowała spadek intensywności sygnałów Bi do 26-61%.

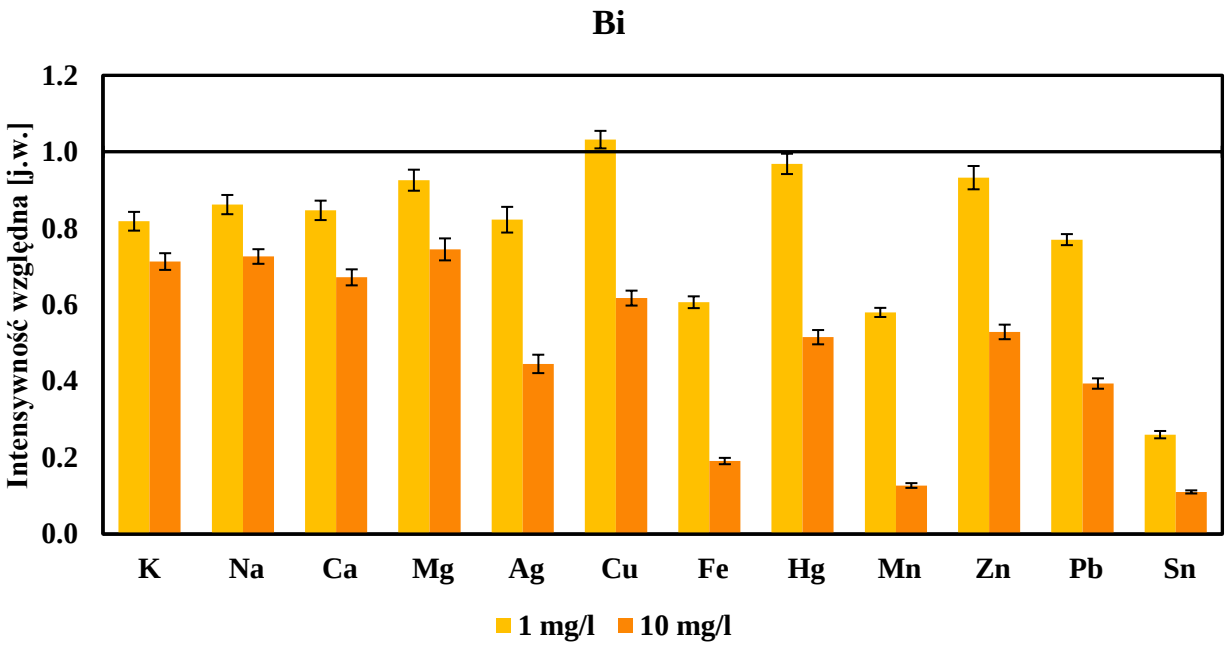

Rys. 5. Wpływ obecności pierwiastków interferujących w roztworze FLA na intensywność względną sygnału Bi (stężenie Bi równe 0,5 mg/l).

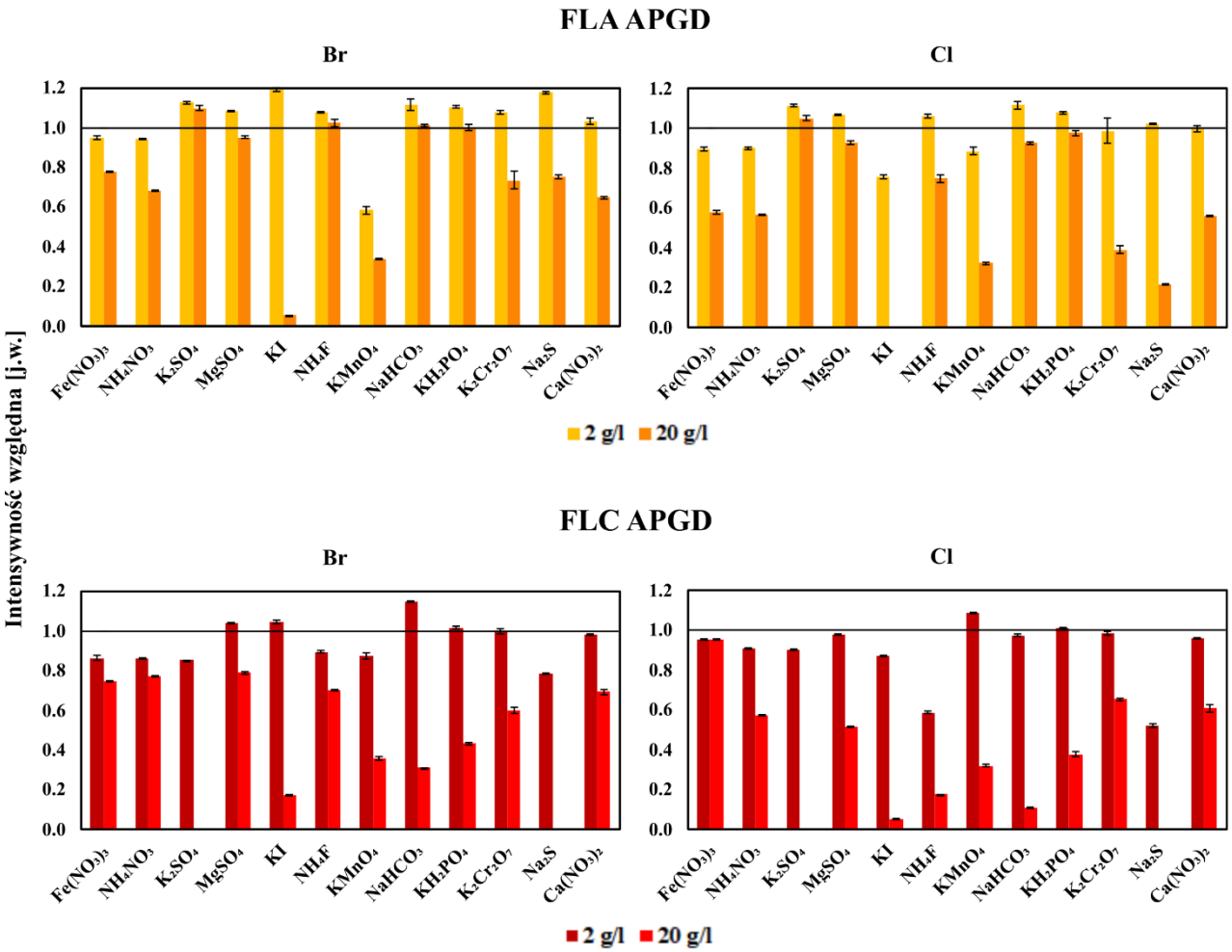

Rys. 6. Wpływ obecności pierwiastków interferujących w roztworach FLA i FLC na intensywność względną sygnałów Br i Cl (stężenie Br i Cl równe 100 i 1000 mg/l, odpowiednio dla FLA APGD i FLC APGD).

Niemniej jednak, warto mieć na uwadze, że stosunek stężenia analitu do interferenta wynosił w tym przypadku zaledwie 1/2. Natomiast obecność tych samych jonów w stężeniu 10 mg/l istotnie obniżała sygnały analitów do poziomu od ok. 70% dla litowców i berylowców do nawet 11% w przypadku Sn. Otrzymane w tej pracy wyniki są podobne do tych, które otrzymywano dla tego samego układu ale dla innych pierwiastków (szczegóły w rozdziale 5.6). Ponieważ próbki rzeczywiste zwykle stanowią mieszaninę różnych pierwiastków współistniejących, a różnica stężeń pomiędzy nimi i analitem jest znacznie większa niż badana tutaj tej pracy, można wysnuć konkluzję, że badany układ nie jest wolny od występowania efektów matrycowych, co jest jego poważnym ograniczeniem w przypadku analizy próbek rzeczywistych.
Nieco inaczej miała się sytuacja w przypadku wpływu obecności jonów współistniejących na sygnały Br i Cl. Ponieważ anality były wprowadzane do wyładowania w postaci anionów, postanowiono zbadać zarówno wpływ kationów jak i innych anionów na mierzone w tych warunkach sygnały Br i Cl. Do analizowanych roztworów dodawano osobno sole litowców i berylowców (wśród grupy kationów są to najpowszechniej występujące interferenty) o różnych resztach kwasowych. Uzyskane wyniki przedstawiono na rys. 5 i wskazują one na brak istotnych efektów matrycowych od badanych soli, znajdujących się w roztworach FLA i FLC w stężeniu 2 g/l, co było stężeniem 20 i 2 razy większym odpowiednio dla układu FLA APGD i FLC APGD. W przypadku układu FLA APGD, wyjątek stanowił jedynie roztwór FLA z dodatkiem $KMnO_4$, dla którego zaobserwowano spadek sygnału Br do poziomu ok. 60%. Natomiast w przypadku układu FLC APGD, zaobserwowano podobny spadek sygnału Cl, kiedy NH_4F i Na_2S stanowiły składnik matrycy próbki. Nieco gorsze wyniki uzyskano dla tych samych interferentów w stężeniu 20 g/l, szczególnie w przypadki KI, $KMnO_4$, $K_2Cr_2O_7$ i Na_2S, których obecność w roztworze powodowała spadek sygnałów analitów nawet poniżej 10% lub całkowicie destabilizowała wyładowanie. Warto mieć jednak na uwadze, że w próbkach rzeczywistych nie obserwuje się zwykle tak dużych stężeń jonów, szczególnie badanych anionów. Interesujące jest natomiast to, że obecność badanych soli w stężeniu 20 g/l wydawała się w większym stopniu pogarszać sygnały analitów w przypadku układu FLC APGD. Jest to tendencja, której nie obserwowano wcześniej w literaturze, ponieważ – jak wspomniano w rozdziale 5.6 – efekty matrycowe zwykle nie występują w przypadku tego układu. Obserwowane więc w tej pracy różnice wynikają zapewne z odmiennej natury badanych w tej pracy analitów. W przypadku kationów, uważa się, że obecność efektów matrycowych dla układu FLA APGD wynika z negatywnego wpływu interferentów na procesy redukcji analitów, prowadzące do utworzenia ich lotnych form. W tym przypadku aniony analitów nie ulegały procesom redukcji, można więc przyjąć, że wyniki obserwowane w tej pracy potwierdzają słuszność wspomnianej wyżej hipotezy odnoszącej się do mechanizmu pojawiania się efektów matrycowych w układzie FLA APGD.

6.2.5. Analiza próbek rzeczywistych

W celu zbadania przydatności stosowanych układów do analizy próbek rzeczywistych, oznaczono stężenie badanych analitów w próbkach wód (Bi, Br i Cl) oraz soków (Br i Cl). Oznaczenie Bi wykonano z zastosowaniem układu FLA APGD, podczas gdy do oznaczenia zawartości Br i Cl wykorzystano oba badane układy. Ze względu na obserwowane w poprzednim etapie badań silne efekty matrycowe w przypadku Bi, analizę prowadzono z zastosowaniem metody dodatku wzorca do kalibracji. Z kolei w przypadku Br i Cl, jako metodę kalibracji użyto zarówno metodę dodatku wzorca jak i krzywej wzorcowej. W przypadku Bi, metoda badania odzysku została zastosowana w celu potwierdzenia wiarygodności stosowanej metody analitycznej. Natomiast w przypadku Br i Cl, postanowiono sprawdzić poprawność otrzymanych wyników poprzez: test odzysku (Br), porównanie wyników otrzymanych pomiędzy dwoma układami oraz dla obu metod kalibracji (Br i Cl) oraz porównanie otrzymanych wyników z wynikami otrzymanymi metodą odniesienia, tj. ICP OES (Cl). W przypadku Bi i Br, z racji występowania tych pierwiastków w badanych próbkach na nieoznaczalnym poziomie, zastosowano dodatek tych analitów w stężeniach 100 mg/l dla Bi, oraz 50 mg/l (FLA APGD) lub 100 mg/l (FLC APGD) dla Br. Wyniki analiz zestawiono w tabeli 6 i 7.

Tabela 6. Wyniki oznaczania stężenia Bi w próbkach wód z zastosowaniem metody FLA APGD OES.

Próbka	**Dodano [µg/l]**	**Oznaczono [µg/l]**	**Odzysk [%]**
Woda mineralna		100,7±6,2	100,7
Woda rzeczna	100	86,5±8,3	86,5
Woda kranowa		90,3±7,0	90,3

Tabela 7. Wyniki oznaczania stężenia Br i Cl (w mg/l) w próbkach wód i soków z zastosowaniem metod FLA APGD OES i FLC APGD OES.

Analit	**Układ**	**Kalibracja**	**Próbka**					
			Woda lecznicza mineralna	**Woda rzeczna**	**Woda morska**	**Woda kranowa**	**Sok z buraka**	**Sok pomidorowy**
Br	FLA APGD	Krzywa wzorcowa	45,85±0,28	45,54±1,70	44,85±0,29	48,61±0,48	45,61±1,61	44,14±0,42
		Dodatek wzorca	48,43±0,26	49,23±3,21	46,34±1,78	46,10±0,15	48,50±1,58	54,89±2,98
	FLC APGD	Krzywa wzorcowa	103,9±4,4	134,1±5,6	114,9±2,4	115,6±2,1	140,8±2,8	135,0±3,5
		Dodatek wzorca	104,8±0,5	100,6±3,3	109,4±2,5	103,8±0,4	108,7±3,9	100,4±4,6
Cl	FLA APGD	Krzywa wzorcowa	1082±19	109,2±5,2	25300±851	39,64±0,36	3617±180	3583±223
		Dodatek wzorca	910,2±16,3	97,61±3,77	23410±930	34,14±0,76	3792±144	4462±116
	FLC APGD	Krzywa wzorcowa	972,3±32,2	144,1±11,2	25580±570	39,16±0,35	3453±148	4429±73
		Dodatek wzorca	1069±68	105,9±9,0	22080±900	37,44±2,18	3940±239	4708±11
	ICP OES	Krzywa wzorcowa	1010±7	< DL	24640±2009	< DL	-	-
		Dodatek wzorca	-	-	-	-	3522±198	4858±166

Wartości odzysków uzyskane dla Bi mieściły się w zakresie 86-101%, co potwierdza dobrą poprawność stosowanej metody pomiarowej. Niemniej jednak, warto mieć na uwadze, że wyniki te mogły być otrzymane wyłącznie z zastosowaniem metody dodatku wzorca jako metody kalibracji. Z kolei w przypadku oznaczania Br, wartości odzysków wynosiły od 88 do 110% (wyniki uzyskane na podstawie przeliczonych wartości z tabeli 7). Dodatkowo w większości przypadków wyniki uzyskane dla obu układów oraz obu sposobów kalibracji były ze sobą zbieżne. W przypadku Cl, wyniki te były również zgodne z danymi otrzymanymi metodą ICP OES. Na tej podstawie uznano, że oba badane układy wyładowcze i opracowane metody analityczne pozwalają na wiarygodne oznaczanie Br i Cl, zarówno z zastosowaniem metody dodatku wzorca jak i przy użyciu zewnętrznej krzywej wzorcowej. Wyniki te potwierdzają więc, że efekty matrycowe nie są poważnym ograniczeniem stosowanych metod w analizie badanych próbek na zawartość Br i Cl.

6.3. Sprzęgnięcie układów FLA i FLC APGD z techniką generowania lotnych par [D3, D4]

Techniki HG i CVG są powszechnie stosowane do wprowadzania próbek, zarówno w komercyjnie stosowanej aparaturze, jak np. ICP OES [126], jak również w układach mikroplazmowych [127]. Zawdzięczają one swoją popularność wysokiej wydajności transportu analitów do plazmy, skutkującej wzmocnieniem sygnałów analitów i obniżeniem otrzymywanych wartości DL, a także odseparowaniem analitów od nielotnych składników matrycy, co przyczynia się do obniżenia efektów matrycowych, poprawiając tym samym czułość sygnałów analitów mierzonych w trakcie analizy próbek rzeczywistych.

Jak wspomniano w rozdziale 5.4, możliwości układu FLA APGD ograniczają się do oznaczania jedynie kilku pierwiastków, o których wiadomo, że tworzą lotne formy. Na tej podstawie, przyjmuje się, że mechanizm transportu analitów do tego źródła wzbudzenia przebiega właśnie poprzez tworzenie jakiegoś rodzaju lotnych indywiduów, które następnie zostają samoistnie przetransportowane do plazmy. Dodatkowo istotnym ograniczeniem związanym z zastosowaniem tego układu wyładowczego w analizie próbek rzeczywistych jest negatywny wpływ składników matrycy na czułość sygnałów analitów. Z tego powodu, w tej części badań postanowiono sprzęgnąć układ FLA APGD z techniką HG/CVG w reakcji z tetrahydroboranem sodu (THB) do oznaczania As, Bi, Hg, Sb i Se. Oczekiwano, że zastąpienie wprowadzania analitów próbki do wyładowania bezpośrednio z roztworu FLA generowaniem lotnych wodorków tych analitów i wprowadzaniem ich do plazmy w strumieniu He pozwoli oznaczać te pierwiastki, których sygnały nie są normalnie rejestrowane dla tego układu wyładowczego (As, Sb i Se). Jednocześnie oczekiwano, że poprawi to wartości DL pozostałych pierwiastków (Bi, Hg). W przypadku wymienionych wyżej analitów, badania te ograniczono jedynie do układu FLA APGD, ponieważ podobne badania dla układu FLC APGD były już wcześniej prowadzone [29]. Dodatkowo postanowiono sprzęgnąć oba układy APGD z techniką CVG w reakcji z $KMnO_4$, w celu poprawy otrzymanych w poprzedniej pracy wartości DL Br. Badania te zostały ograniczone jedynie do oznaczania Br, ponieważ przeprowadzone badania wstępne wykazały, że uzyskanie odpowiednio dużych czułości dla Cl tą techniką wymagałoby zastosowania nieracjonalnie dużych stężeń H_2SO_4.

6.3.1. Widma porównawcze

Pierwszym etapem badań było porównanie intensywności sygnałów analitów i tła pomiędzy układami APGD z wprowadzaniem ich do wyładowania bezpośrednio z roztworu FLC lub FLA a układami APGD sprzęgniętymi z techniką HG/CVG. Stężenia As, Bi, Br, Hg, Sb i Se wynosiły odpowiednio 10, 10, 1000, 1, 10 i 10 mg/l. Do zakwaszenia roztworów FLA i FLC użyto H_2SO_4 (Br) lub HNO_3 (pozostałe anality) o stężeniach wynoszących: 1 mol/l (H_2SO_4/ FLA), 0,01 mol/l (H_2SO_4/ FLC) i 0,01 mol/l (HNO_3). Stężenia zarówno analitów jak i kwasu były takie same dla obu technik wprowadzania próbki, przy czym w przypadku technik HG/CVG, roztwory FLA i FLC służyły jedynie podtrzymaniu wyładowania. W celu zainicjowania reakcji tworzenia wodorków/lotnych par, przygotowano roztwory analitów w 1 mol/l H_2SO_4 (Br) lub 10% HCl (pozostałe anality) oraz roztwory utleniacza i reduktora, tj. 3% $KMnO_4$ (Br), 0,05% THB (Hg) i 0,3% THB (pozostałe

anality). Szczegółowe dane dotyczące warunków prowadzenia pomiarów zostały podane w [**D3**] i [**D4**]. Zarejestrowane widma przedstawiono na rys. 6 i 7.
Porównując widma otrzymane dla układów FLA APGD i HG FLA APGD (rys. 6), można zauważyć istotne różnice w ich morfologii, ponieważ generowanie wodorków powodowało obniżenie intensywności pasm cząsteczkowych NO do ok. 16 razy w porównaniu do intensywności tych pasm zmierzonych w przypadku wprowadzania analitów do wyładowania bezpośrednio z roztworu FLA. Prawdopodobną przyczyną obserwowanej odpowiedzi układu było wprowadzanie do wyładowania wraz z gazem nośnym H_2, który prawdopodobnie reagował z rodnikami NO, powodując obniżenie ich stężenia, a w konsekwencji obniżenie intensywności wspomnianych pasm cząsteczkowych. Pomimo dużego stężenia analitów, wysokie sygnały dla układu FLA APGD zaobserwowano jedynie dla Bi i Hg. Natomiast po sprzęgnięciu tego układu wyładowczego z techniką HG, zaobserwowano wysoką emisję linii Hg i Sb i nieco słabsze sygnały pochodzące od As, Bi i Se. Z kolei w przypadku Br, rejestrowano widma w zakresie, w którym nie obserwuje się występowania pasm cząsteczkowych. Niemniej jednak zauważono spadek intensywności tła na widmie układu CVG FLA APGD o ok. 20% i ok. 3-krotny wzrost intensywności tła widma układu CVG FLC APGD w porównaniu do odpowiadających im widm układów bez użycia techniki CVG. W konsekwencji, dla obu badanych układów, wzrost intensywności sygnału Br był nieco ponad 10-krotny w przypadku stosowania techniki CVG.

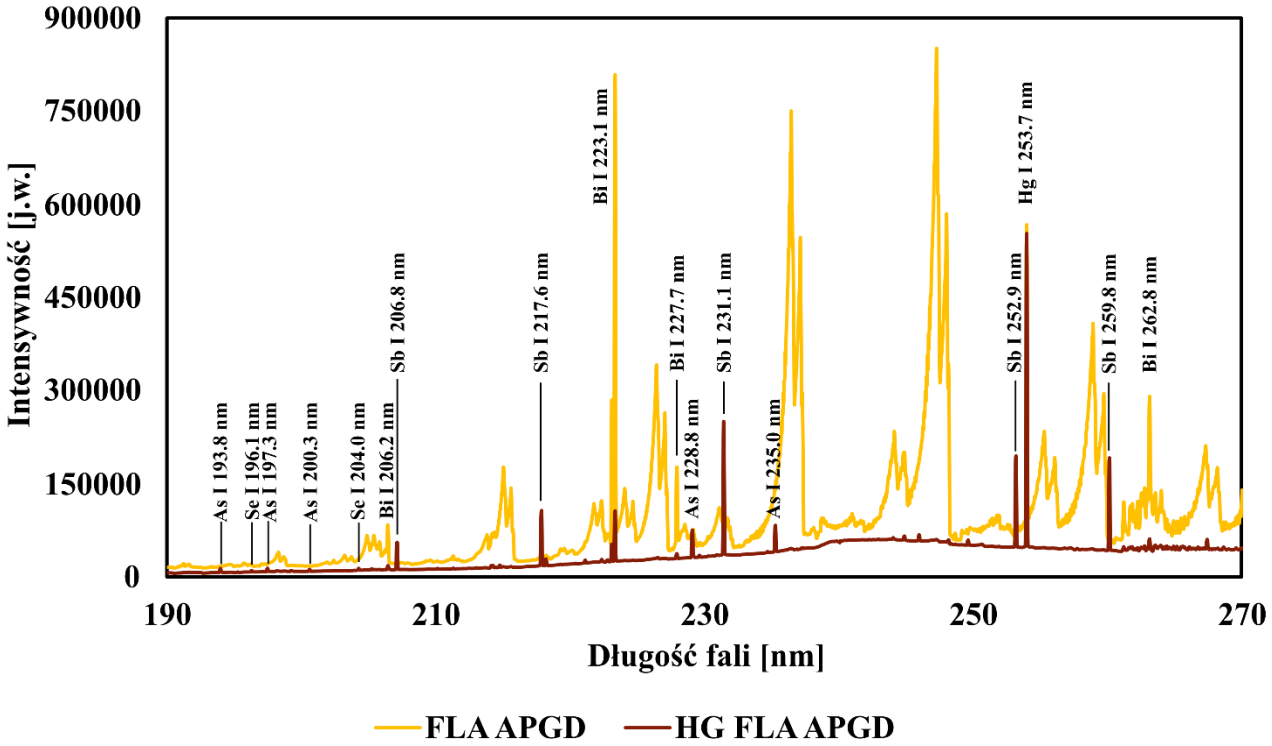

Rys. 7. Porównanie intensywności sygnałów As, Bi, Hg, Sb i Se na widmach układów FLA APGD z wprowadzaniem analitów do wyładowania bezpośrednio z roztworu FLA oraz z techniką HG.

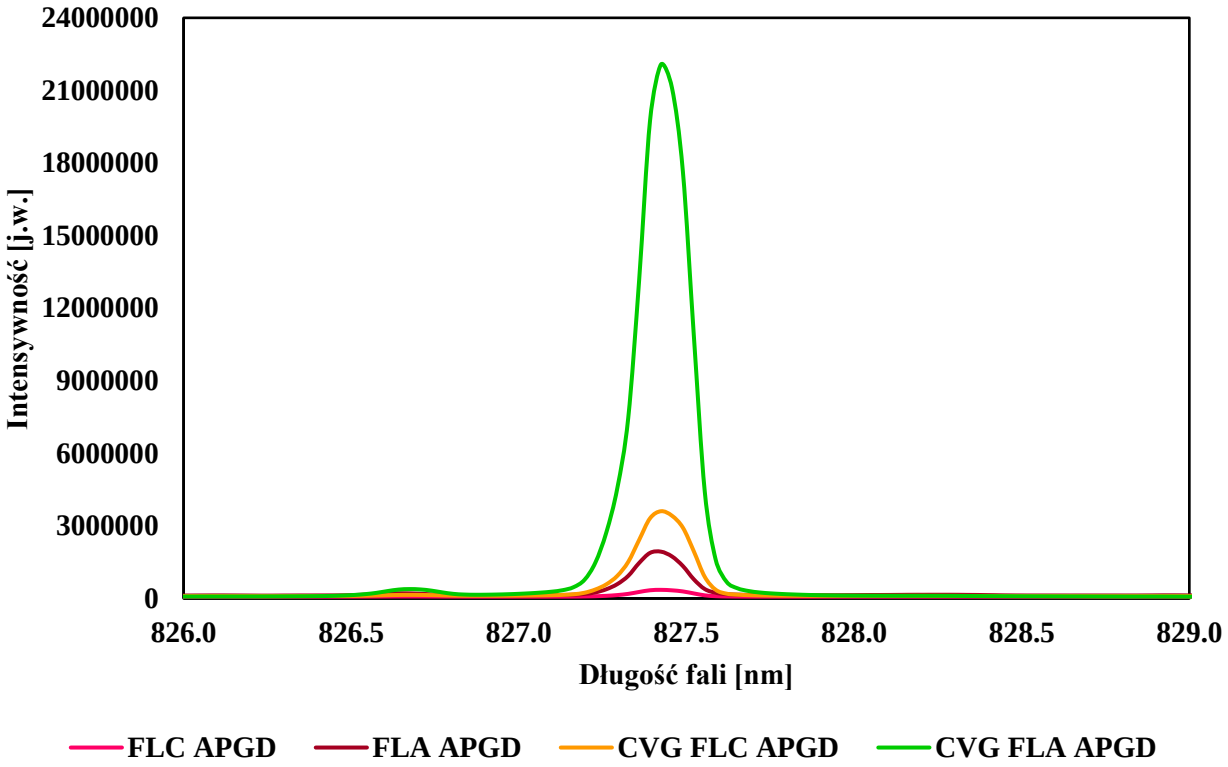

Rys. 8. Porównanie intensywności sygnału Br na widmie układów APGD z wprowadzaniem analitu do wyładowania bezpośrednio z roztworu FLA lub FLC oraz z techniką CVG.

6.3.2. Optymalizacja warunków pracy układu

W celu uzyskania możliwie najwyższych intensywności sygnałów, przekładających się na odpowiednio niskie wartości DL, kolejnym etapem badań było przeprowadzenie optymalizacji kluczowych parametrów pracy układu. W przypadku techniki HG badanymi parametrami były: natężenie prądu, natężenie przepływu He oraz stężenia HCl i THB. Z kolei w badaniach nad CVG optymalizowano jedynie stężenia $KMnO_4$ oraz H_2SO_4, zarówno w roztworach analitów jak i w roztworach FLA/FLC (szczegóły w [**D4**]). Stężenia analitów różniły się pomiędzy sobą ale były na tyle wysokie, żeby otrzymać mierzalną intensywność sygnału dla każdej badanej kombinacji parametrów. Podsumowanie uzyskanych wyników zamieszczono w tabeli 8.

Tabela 8. Wpływ rosnących wartości podanych parametrów na otrzymane wartości SBR badanych analitów dla układów FLA APGD i FLC APGD.

Parametr	**FLA APGD**						**FLC APGD**
	As	**Bi**	**Br**	**Hg**	**Sb**	**Se**	**Br**
Natężenie prądu	↑	↑	-	*[a]	↑	↑	-
Natężenie przepływu He	↑	↑	-	↑	↑	↑	-
Stężenie HCl	**[b]	↓	-	**	↓	**	-
Stężenie H_2SO_4[c]	-	-	↑ / ↑	-	-	-	↑ / *
Stężenie THB	↓[d]	↓[d]	-	↓[d]	↓[d]	↓[d]	-
Stężenie $KMnO_4$	-	-	↑	-	-	-	↑

[a] nieliniowa odpowiedź sygnału analitu (szczegóły w [**D4**])
[b] brak istotnej różnicy
[c] odpowiednio dla roztworu FLA i FLC
[d] maksimum wartości SBR dla C_{THB} równego 0,005% (Hg), 0,01% (Sb), 0,05% (Bi) i 0,1% (As i Se)

Analizując dane w powyższej tabeli, można zauważyć, że w przypadku pierwiastków, dla których stosowano technikę HG, sygnały analitów rosły wraz ze wzrostem natężenia prądu (z wyjątkiem Hg) i natężenia przepływu He. Obserwowany wzrost sygnałów wraz z rosnącymi wartościami natężenia prądu wynika najprawdopodobniej z poprawy warunków wzbudzenia w wyładowaniu. Natomiast wyższe natężenia przepływu gazu powodują zwiększenie wydajności wprowadzania lotnych form analitów do wyładowania w jednostce czasu, skutkując tym samym większą ilością atomów analitów w plazmie. Wzrost stężenia HCl nie wpływał istotnie na otrzymywane wartości SBR dla większości badanych pierwiastków. Wyjątek stanowiły jedynie Bi i Sb, dla których zaobserwowano spadek intensywności linii emisyjnych analitów wraz ze wzrostem stężenia kwasu. Z kolei wzrost stężenia THB skutkował początkowym wzrostem wartości SBR dla analitów, osiągających swoje maksimum dla stężenia THB równego 0,005% (Hg), 0,01% (Sb), 0,05% (Bi) i 0,1% (As i Se) oraz następującym po nim liniowym spadkiem aż do końca badanego zakresu stężenia kwasu. W związku z tym, można uznać, że ogólnie wzrost stężenia zarówno HCl jak i THB wpływał niekorzystnie na intensywności sygnałów analitów. Możliwą przyczyną takiego stanu rzeczy mogło być wprowadzanie wraz z lotnymi formami analitów aerozolu zawierającego cząsteczki HCl i THB do wyładowania i/lub zwiększonej ilości H_2, skutkujące pogorszeniem warunków wzbudzenia. Z kolei w przypadku Br, w większości przypadków zaobserwowano wzrost intensywności jego sygnału wraz ze wzrostem wszystkich badanych stężeń reagentów dla obu układów. Jedynym wyjątkiem była zmiana wartości SBR w przypadku rosnących stężeń H_2SO_4 w roztworze FLC, ponieważ maksimum intensywności sygnału zaobserwowano dla stężenia H_2SO_4 równego 0,1 mol/l, co przypadało mniej więcej na połowę badanego zakresu. W przypadku rosnących stężeń reagentów, podobne zależności intensywności sygnałów od stężenia H_2SO_4 i $KMnO_4$ obserwowano wcześniej w literaturze [128, 129]. Ponieważ obserwowana odpowiedź sygnałów analitów nie zależała od rodzaju układu (polaryzacji elektrod), można przypuszczać, że obserwowany wzrost intensywności sygnałów wraz ze zwiększaniem stężenia omawianych reagentów wynikał ze zwiększonej wydajności generowania lotnego Br_2. Wpływ stężenia H_2SO_4 w roztworach FLA/FLC na otrzymywane wartości SBR analitów jest nieco trudniejszy do wytłumaczenia. W przypadku wprowadzania analitów bezpośrednio z roztworu FLA (dla układu FLA APGD) obserwuje się zwykle spadek intensywności sygnałów analitów wraz ze wzrostem stężenia kwasu, który tłumaczy się zmniejszaniem ilości solwatowanych elektronów w wyniku rekombinacji z jonami H_3O^+, których stężenie rośnie wraz ze wzrostem stężenia kwasu. Niemniej jednak, efekt ten nie mógł być istotną przeszkodą w tym przypadku, ponieważ anality nie były wprowadzane do wyładowania z roztworu FLA. Dlatego można przypuszczać, że zwiększona ilość jonów H_3O^+ powodowała wzrost stężenia reaktywnych rodników H i OH, poprawiając tym samym warunki wzbudzenia w wyładowaniu. Dodatkowo wraz ze wzrostem stężenia kwasu maleje odparowywanie wody do wyładowania, co również mogło przyczynić się do poprawy warunków wzbudzenia. Z kolei dla układu FLC APGD, optymalne stężenie kwasu w roztworze FLC było takie samo jak w przypadku wprowadzania analitów do plazmy bezpośrednio z roztworu, jednakże przyczyna takiego stanu rzeczy była najprawdopodobniej inna. W przypadku wprowadzania analitów do plazmy, uważa się, że obserwowany wzrost sygnałów wraz ze wzrostem stężenia kwasu wynika z malejącego spadku napięcia katodowego i odpowiadającemu mu obniżeniu natężenia pola elektrycznego w strefie CDS. Skutkowało to ułatwionym transportem analitów do wyższych sfer wyładowania. Niemniej jednak, ponownie w tym przypadku obserwowany efekt nie mógł wpływać na intensywności linii emisyjnych, ze względu na odmienny mechanizm transportu analitów do plazmy. Dlatego uznano, że początkowy wzrost intensywności sygnałów, obserwowany w tej pracy, wynikał ze wspomnianego wcześniej zmniejszonego odparowania wody do wyładowania, a następujący po nim spadek intensywności linii emisyjnych mógł być spowodowany nadmierną produkcją rodników H, pogorszającą warunki wzbudzenia w tym układzie.

6.3.3. Charakterystyka analityczna i analiza próbek rzeczywistych

W optymalnych warunkach pracy układów (zestawionych w [**D3**] i [**D4**]), wyznaczono ich charakterystykę analityczną. Szczegółowe dane przedstawione są w powyższych pracach, natomiast w tabeli 9 zestawiono otrzymane wartości DL.

Tabela 9. Wartości DL badanych pierwiastków uzyskane dla układów FLA APGD i FLC APGD z zastosowaniem technik HG/CVG.

Pierwiastek	**Układ**	**DL [µg/l]**
As	HG FLA APGD	1,7
Bi	HG FLA APGD	0,85
Br	CVG FLA APGD	50
	CVG FLC APGD	200
Hg	HG FLA APGD	0,04
Sb	HG FLA APGD	0,51
Se	HG FLA APGD	2,9

W przypadku pierwiastków, dla których zastosowano technikę HG, uzyskane wartości DL nie różniły się znacząco od tych, otrzymywanych dla innych układów, w których stosowano tą samą metodę wprowadzania analitów do plazmy (szczegóły w [**D4**]), włączając w to układ HG FLC APGD. Na tej podstawie można wysnuć przypuszczenie, że to wydajność generowania wodorków miała decydujący wpływ na otrzymywane intensywności sygnałów, a nie rodzaj układu. Natomiast, w przypadku Br, uzyskane wartości DL były ok. 3 razy lepsze od tych otrzymanych w poprzedniej pracy ([**D2**]), w porównaniu z odpowiadającymi układami bez techniki CVG. Różnica ta wynika zapewne z faktu, że zastosowanie techniki CVG jako metody wprowadzania próbki poprawiało wydajność generowania lotnych indywiduów Br.

W celu potwierdzenia przydatności opracowanych metod z CVG FLA/FLC APGD w analizie próbek rzeczywistych z detekcją OES, wykonano oznaczenie badanych pierwiastków w próbkach wód. Wszystkie badane pierwiastki były oznaczane w wodzie rzecznej i kranowej. Dodatkowo oznaczano Br w wodzie z zalewu oraz pozostałe pierwiastki w wodzie mineralnej. Ponadto przeprowadzono analizę certyfikowanego materiału odniesienia ścieków na zawartość Hg. Dla wszystkich prowadzonych analiz zastosowano metodę zewnętrznej krzywej wzorcowej do kalibracji, jednakże w przypadku oznaczania Br, wykorzystano dodatkowo metodę dodatku wzorca. Ponieważ badania wstępne potwierdziły, że badane próbki nie zawierały oznaczalnych zawartości analizowanych pierwiastków (nie licząc Hg w próbce CRM-u), dla wszystkich próbek zastosowano dodatek analitów w stężeniach nieprzekraczających zaleceń Amerykańskiej Agencji Ochrony Środowiska (ang. *United States Environmental Protection Agency*, US EPA), jeżeli takie regulacje istniały, lub w odpowiednio niskich stężeniach w innym przypadku (szczegóły w [**D3**] i [**D4**]). Otrzymane wyniki odzysku (względem dodanych lub certyfikowanych stężeń) przedstawiono w tabeli 10. Dla uproszczenia, we wspomnianej tabeli zestawiono jedynie wyniki uzyskane dla krzywej wzorcowej (pominięto metodę dodatku wzorca w przypadku Br). Szczegółowe wyniki dotyczące wspomnianej metody dodatku wzorca znajdują się w [**D3**].

Tabela 10. Wyniki oznaczania stężenia badanych pierwiastków (wyrażone jako odzysk, w %) w próbkach wód z zastosowaniem metod FLA APGD OES i FLC APGD OES.

Pierwiastek	Układ	Odzysk [%]				
		Woda rzeczna	Woda mineralna	Woda kranowa	Woda z zalewu	Ścieki (CRM)
As	HG FLA APGD	89,8 ± 4,9	96,6 ± 9,8	81,3 ± 5,0	-	-
Bi	HG FLA APGD	102 ± 6	102 ± 5	85,0 ± 6,3	-	-
Br	CVG FLA APGD	109±2	-	103±5	97,0±4,0	-
	CVG FLC APGD	104±3	-	101±6	110±3	-
Hg	HG FLA APGD	104 ± 4	91,5 ± 4,9	92,5 ± 5,8	-	95,7±5,8
Sb	HG FLA APGD	102 ± 3	100 ± 2	101 ± 2	-	-
Se	HG FLA APGD	NZ	NZ	NZ	-	-

NZ – nie zarejestrowano sygnału

Otrzymane wartości odzysków mieściły się w zakresie 81-110%, co potwierdzało dobrą poprawność opracowanych metod, a także wskazywało na brak efektów matrycowych (ponieważ wyniki te uzyskano stosując do kalibracji krzywe wzorcowe). Jednakże zastosowanie metody HG FLA APGD OES nie pozwoliło na oznaczenie Se w badanych próbkach. Wynikało to z faktu, że oznaczenie Bi i Se nie mogło być prowadzone razem z pozostałymi analitami, ponieważ dodatek mieszaniny mocznika z kwasem askorbinowym (w celu uzyskania zredukowanych form As i Sb w roztworze) powodował spadek intensywności sygnałów Bi i Se. W związku z tym, próbki do oznaczeń tych dwóch pierwiastków zostały przygotowane osobno, przeprowadzając uprzednio proces mineralizacji, co w konsekwencji spowodowało ponad 5-krotne rozcieńczenie badanych próbek. To z kolei oznacza, że ostateczne stężenie Se w tych próbkach było nieco poniżej granicy oznaczalności (ang. *quantification limit*, QL). Niemniej jednak, sygnał linii rezonansowej Se był obecny na rejestrowanych widmach, natomiast jego intensywność była zbyt niska żeby otrzymać wiarygodne wyniki analizy.

6.4. Zastosowanie układu FLC APGD do oznaczania próbek rzeczywistych z wykorzystaniem uproszczonej metody przygotowania próbek [D5, D6]

Analiza próbek rzeczywistych o złożonej matrycy (w tym matrycy organicznej) z zastosowaniem metod spektrometrycznych zwykle wymaga przeprowadzenia procesu mineralizacji na etapie przygotowania próbek. Jedną z przyczyn przeprowadzania mineralizacji jest to, że obecność składników matrycy organicznej w badanej próbce może powodować zmiany intensywności sygnałów, co oznaczałoby konieczność stosowania metody dodatku wzorca jako metody kalibracji. Kolejną z nich jest to, że analizowane roztwory są często wprowadzane do źródła wzbudzenia za pomocą cienkich kapilar, które mogą zostać zatkane, jeżeli roztwór ma dużą lepkość i gęstość, i/lub zawiera cząstki stałe. Jednakże przeprowadzenie mineralizacji wiąże się z wieloma niedogodnościami, wśród których wyróżnić można długi czas przygotowania próbki (ok. 5-10 godzin), konieczność stosowania stężonych odczynników (zwykle kwasów utleniających) i poddania próbki działaniu wysokiej temperatury. W tych warunkach istnieje ryzyko zanieczyszczenia próbki i/lub straty analitów.

Dlatego, w tej części badań postanowiono opracować metodę oznaczania próbek o wysokiej zawartości matrycy organicznej, w której etap przygotowania próbek do analizy ograniczałby się jedynie do rozcieńczenia i zakwaszenia (z całkowitym pominięciem procesu mineralizacji). Badanymi próbkami były soki oraz grupa napojów spożywana przez sportowców, takich jak odżywki białkowe, pre-workout, napoje energetyzujące, i inne tego rodzaju. Z racji tego, że analiza dotyczyła próbek żywności, oznaczano wyłącznie zawartości składników mineralnych. Do osiągnięcia tego celu wykorzystano układ FLC APGD, ponieważ (jak wspomniano w rozdziale 5.4 i 5.6) po pierwsze, charakteryzuje się stosunkowo dużą odpornością na efekty matrycowe, a po drugie – w odróżnieniu od układu FLA APGD – pozwala na oznaczanie np. litowców, berylowców czy pierwiastków bloku d.

By osiągnąć założony cel, w pierwszym etapie badań przeprowadzono optymalizację kluczowych parametrów pracy układu FLC APGD. Następnie, w optymalnych warunkach wyznaczono wartości DL badanych analitów. W kolejnym kroku zbadano wpływ różnych rozcieńczeń badanych próbek na intensywności sygnałów analitów i na tej podstawie wybrano optymalne rozcieńczenia stosowane do analiz. Ostatnim etapem prowadzonych badań było przeprowadzenie analiz próbek rzeczywistych na zawartość wybranych pierwiastków i porównanie otrzymanych wyników z wynikami uzyskanymi metodą odniesienia, którą stanowiła metoda ICP OES.

6.4.1. Optymalizacja warunków pracy układu

W pierwszej kolejności przeprowadzono badania wstępne w celu ustalenia, które pierwiastki znajdują się w badanych próbkach. Badane próbki zostały rozcieńczone ok. 10-100 razy, po czym przeprowadzono ich analizę jakościową i półilościową metodą FLC APGD OES, rejestrując widma emisyjne w zakresie 200-900 nm. Na widmach wszystkich badanych próbek zidentyfikowano mierzalne sygnały pochodzące od Ca, Mg, Na i K. Dodatkowo dla jednej z próbek (napój wielowitaminowy z dodatkiem Zn), zidentyfikowano również sygnał pochodzący od Zn o dużej intensywności. W związku z tym, wszystkie dalsze etapy badań dotyczyły wyżej wymienionych pierwiastków.

W celu uzyskania możliwie najwyższych intensywności sygnałów analitów, pozwalających na zastosowanie dużych rozcieńczeń próbek, przeprowadzono optymalizację kluczowych parametrów pracy układu. Badanymi parametrami były natężenie prądu oraz natężenie przepływu próbki, w przypadku wszystkich analizowanych próbek, a także stężenie kwasu oraz natężenie przepływu gazu, dla napojów spożywanych przez sportowców. Optymalizację dla wszystkich badanych próbek, prowadzono w roztworach bez matrycy, natomiast w przypadku próbek napojów, optymalizowano dodatkowo wspomniane parametry, stosując próbki rzeczywiste i porównując otrzymane wyniki z tymi, uzyskanymi dla próbek bez matrycy. Uzyskane wyniki przedstawiono w tabeli 11 (badania dotyczące soków, roztwory bezmatrycowe) i rys. 8 i 9 (badania dotyczące napoi, odpowiednio roztwór bezmatrycowy i wybrana próbka rzeczywista). W tabeli 11, dla uproszczenia zestawiono jedynie wyniki uzyskane dla Na, ponieważ ogólne tendencje zmiany SBR w zależności od różnych wartości badanych parametrów nie różniły się dla poszczególnych analitów. Jednocześnie linia Na charakteryzowała się największą czułością, w związku z tym zmiany wartości SBR były najbardziej zauważalne w przypadku tego pierwiastka. Z kolei na rys. 9 przedstawiono wpływ badanych parametrów na wartości SBR analitów dla przykładowej próbki (mleko migdałowe bez dodatku cukru), ponieważ nie odnotowano znaczących różnic w odpowiedzi analitów pomiędzy próbkami.

Tabela 11. Wpływ natężenia prądu i przepływu próbki na wartości SBR Na – wyniki otrzymane z użyciem roztworów bez matrycy.

Prąd	Przepływ próbki [ml/min]						
[mA]	1,0	1,5	2,0	2,5	3,0	3,5	4,0
30	16,79	14,85	13,09	11,49	10,00	8,80	7,85
40	*	23,03	20,02	17,89	16,11	14,49	12,96
50	*	*	26,55	24,24	22,02	19,88	18,37
60	*	*	*	*	*	26,10	24,44

* – niestabilne wyładowanie w danych warunkach

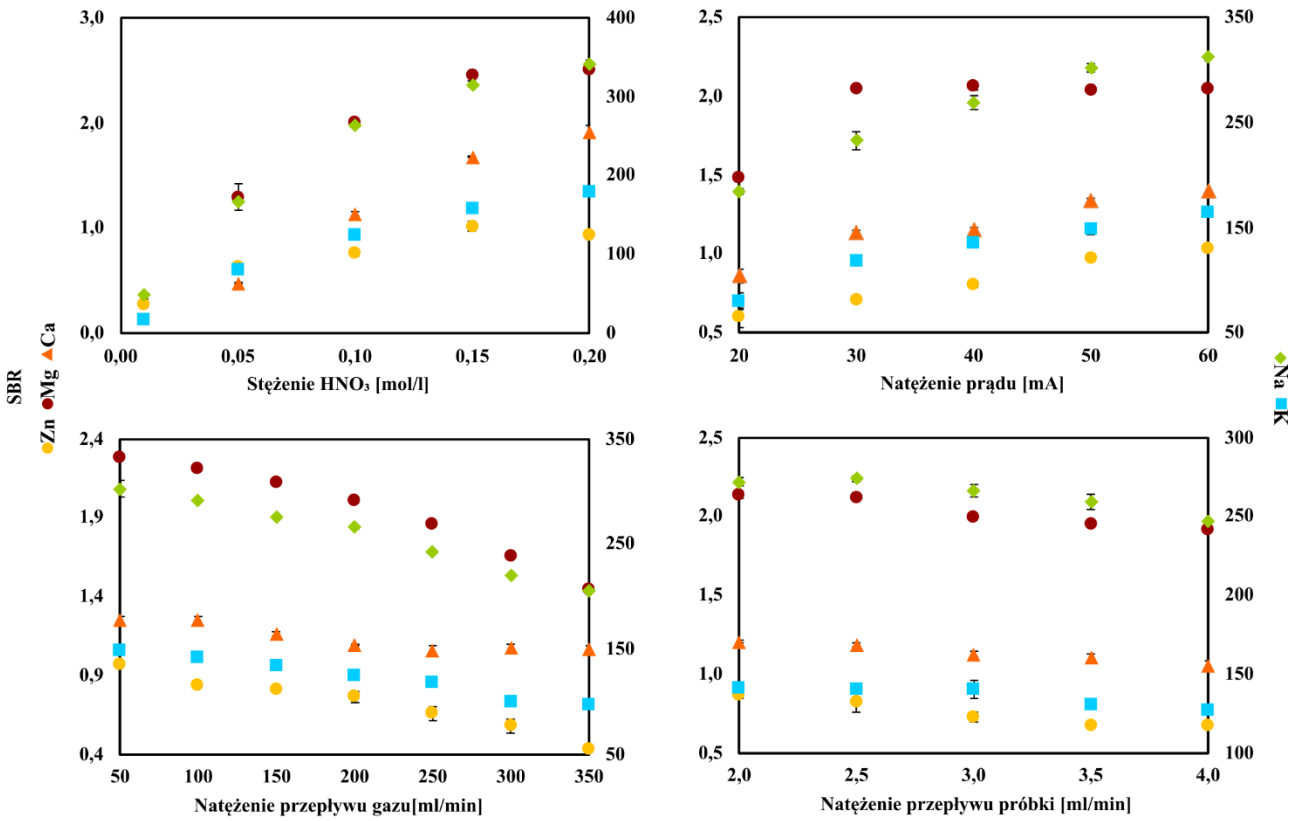

Rys. 9. Wpływ stężenia kwasu oraz natężenia: prądu, przepływu gazu i przepływu próbki na wartości SBR badanych analitów – wyniki otrzymane z użyciem roztworów bez matrycy.

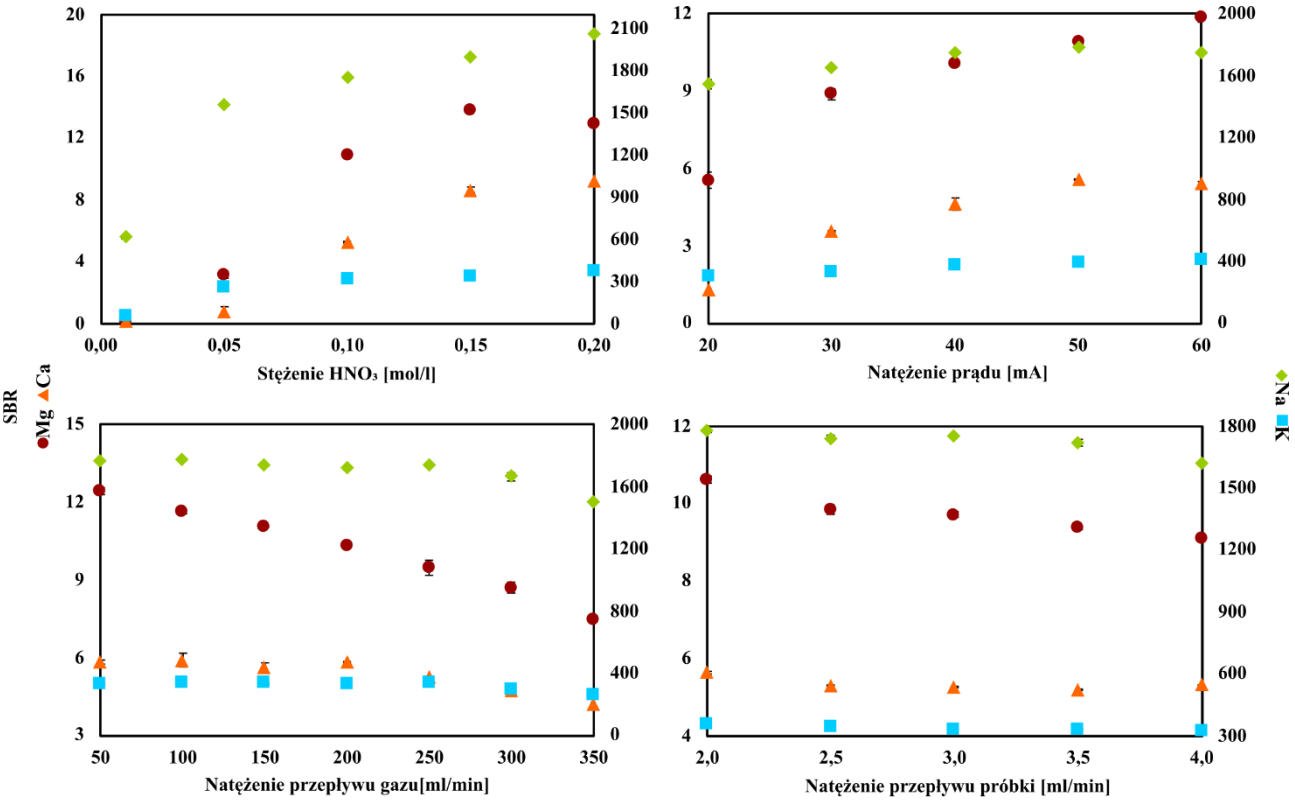

Rys. 10. Wpływ stężenia kwasu oraz natężenia: prądu, przepływu gazu i przepływu próbki na wartości SBR badanych analitów – wyniki otrzymane z użyciem roztworu mleka migdałowego bez dodatku cukru.

Analizując dane przedstawione w tabeli 11 i na rys. 8, można zauważyć, że wartości SBR wszystkich badanych analitów rosły wraz ze wzrostem stężenia kwasu i natężenia prądu oraz malały wraz ze wzrostem natężenia przepływów gazu i próbki. Niemniej jednak należy w tym miejscu podkreślić, że zaobserwowano problemy z utrzymaniem stabilnej pracy wyładowania dla niektórych skrajnych wartości, np. natężenia prądu równego 60 mA czy natężeń przepływu próbki i gazu równych odpowiednio 2,0 i 50 ml/min. Dodatkowo warto również wspomnieć, że w przypadku badania napojów spożywanych przez sportowców zmieniono nieco konstrukcję układu wyładowczego, poprzez zwiększenie średnicy rurki doprowadzającej roztwór, co pozwoliło na zwiększenie badanego zakresu stężeń HNO_3 z poziomu 0,1 mol/l w przypadku soków do poziomu 0,2 mol/l, co przełożyło się na uzyskanie wyższych wartości SBR.
Z kolei porównując wyniki przedstawione na rys. 8 i 9 (wpływ badanych parametrów na wartości SBR analitów w odpowiednio roztworze bezmatrycowym i roztworze mleka migdałowego bez dodatku cukru), można zauważyć, że odpowiedzi sygnałów analitów nie różniły się od siebie znacząco, a ogólne tendencje (spadku/wzrostu wartości SBR) były takie same. Obserwacje te sugerowały, że odpowiedzi analitów zależały w tym przypadku raczej od warunków wzbudzenia w wyładowaniu niż od składu matrycowego próbek, co z kolei sugerowało brak występowania efektów matrycowych (szczegóły w [**D6**]). Niemniej jednak w przypadku niektórych próbek rzeczywistych zaobserwowano pogorszoną stabilność pracy układu wyładowczego, co oznaczało, że rozcieńczenia próbek wybrane na etapie optymalizacji były najprawdopodobniej zbyt niskie i powinny zostać zwiększone w celu prowadzenia faktycznych analiz.

6.4.2. Charakterystyka analityczna i optymalizacja rozcieńczeń próbek

W celu wybrania optymalnego rozcieńczenia próbek do analiz, kilka czynników musiało zostać wziętych pod uwagę. Pierwszym z nich były wartości DL badanych analitów. W związku z tym, wyznaczono charakterystykę analityczną metody FLC APGD OES (szczegóły w [**D5**] i [**D6**]) i ustalono, że wartości DL oznaczanych pierwiastków wahały się w granicach 0,02-21 µg/l, w zależności od konstrukcji układu wyładowczego, warunków pomiarów oraz rodzaju pierwiastka. Na tej podstawie uznano, że uzyskane wartości DL pozwalają na stosowanie stosunkowo dużych rozcieńczeń, ponieważ oczekiwano występowania badanych analitów na poziomie stężeń rzędu od kilku mg/l do nawet kilku g/l. Kolejnym czynnikiem była odporność układu wyładowczego na efekty matrycowe. Ponieważ badane próbki nie zawierały złożonej matrycy nieorganicznej, a jednocześnie – jak wspomniano w rozdziale 5.6 – układ FLC APGD charakteryzuje stosunkowo dużą odpornością na obecność jonów współistniejących w roztworze FLC, uznano, że matryca nieorganiczna nie powinna stanowić problemu w analizie próbek rzeczywistych. Spodziewano się jednak, że złożona matryca organiczna – obecna w większości badanych próbek – może mieć negatywny wpływ na czułość sygnałów analitów. Ostatnim aspektem, który musiał być wzięty pod uwagę była stabilność wyładowania. W tym przypadku spodziewano się, że złożona matryca organiczna może negatywnie wpływać na stabilność wyładowania, jak to miało miejsce np. w [**D4**], pomimo tego, że próbki badane w tamtej pracy zawierały o wiele prostszą matrycę. Mając więc na uwadze dwa ostatnie aspekty, celem tej części badań było zarówno ustalenie najniższych możliwych rozcieńczeń, przy których można jeszcze przeprowadzić wiarygodną analizę jak i zbadanie dla jakich najwyższych rozcieńczeń można nadal uzyskać sygnały analitów o odpowiednio dużej intensywności.
W związku z tym, w przypadku soków, przygotowano każdą z badanych próbek w 5 rozcieńczeniach, których krotność zmieniała się w zakresie 10-1000. Z kolei próbki napojów były rozcieńczane w zakresach 10-100, 10-1000 lub 100-10000, w zależności od czułości sygnałów obserwowanych w poprzednim etapie badań. Szczegółowe wyniki zostały przedstawione w [**D5**] i [**D6**]. Sygnał Mg zmieniał się liniowo w całym zakresie badanych rozcieńczeń dla wszystkich próbek. Podobnie zachowywał się sygnał Ca, chociaż w przypadku próbek soku z cytryny, z limonki, z granatu, z pigwy i pomidorowego, maksymalne rozcieńczenie, dla którego nadal obserwowano liniową odpowiedź sygnału, wynosiło 50. Z kolei w przypadku K i Na obserwowano odchylenia od liniowości dla mniejszych rozcieńczeń dla większości badanych próbek, przy czym maksymalna wartość rozcieńczenia, dla której liniowość sygnału była zachowana różniła się pomiędzy poszczególnymi

próbkami. Działo się tak dlatego, że stężenie tych analitów w badanych próbkach było na tyle duże, że dla niższych rozcieńczeń górny zakres liniowości został przekroczony. W związku z powyższym, można przypuszczać, że wpływ matrycy próbek na intensywności sygnałów analitów był znikomy i wszelkie odchylenia od liniowości, obserwowane dla niższych rozcieńczeń, wynikały z ograniczonego zakresu liniowości sygnałów analitów. Dlatego uznano, że, chociaż Ca i Mg mogłyby być oznaczane nawet w zakresie rozcieńczeń 10-50, bardziej optymalne byłoby zastosowanie większego rozcieńczenia próbek, tak aby wszystkie anality mogły być oznaczane w tak samo rozcieńczonej próbce. Dodatkowo wybranie większego rozcieńczenia do analizy poprawiłoby stabilność wyładowania oraz ograniczyłoby ewentualny wpływ matrycy na odpowiedź analitów. Z drugiej strony jednak należało wziąć pod uwagę, że anality charakteryzujące się najmniejszą czułością (Ca i Mg) występowały w większości badanych próbek na stosunkowo niewielkich poziomach stężeń. Dlatego też zastosowane rozcieńczenie nie mogło być jednocześnie zbyt wysokie. Bazując więc na wynikach uzyskanych na tym etapie badań, uznano, że optymalnymi rozcieńczeniami do analizy będą: 1000-krotne w przypadku wszystkich próbek soków oraz 50-5000-krotne dla pozostałych próbek (szczegóły w [**D6**]).

6.4.3. Analiza próbek rzeczywistych

W celu ustalenia przydatności badanych metod do analizy próbek rzeczywistych, oznaczono zawartość Ca, K, Mg, Na i Zn w badanych próbkach i porównano otrzymane wyniki z metodą odniesienia, tj. ICP OES. Przygotowanie próbek do analizy polegało jedynie na ich rozcieńczeniu do wartości wspomnianych w poprzednim rozdziale oraz zakwaszeniu za pomocą HNO_3 do stężenia końcowego równego 0,1 mol/l w przypadku próbek soków i 0,2 mol/l dla pozostałych próbek. Natomiast w przypadku próbek mleka migdałowego, konieczne było zastosowanie dodatkowo sączenia z użyciem filtrów membranowych (0,45 μm), ponieważ dodatek kwasu do analizowanego roztworu powodował wytrącenie się osadu białka. To samo zjawisko występowało w przypadku próbek odżywki białkowej, ale ze względu na duże rozcieńczenie tych próbek, uznano, że sączenie może zostać w tym przypadku pominięte. Z kolei przygotowanie próbek do pomiarów metodą ICP OES wymagało przeprowadzenia mineralizacji, która została szczegółowo opisana w [**D5**] i [**D6**]. Do kalibracji użyto zewnętrznej krzywej wzorcowej, zarówno w przypadku metody FLC APGD OES jak i metody ICP OES. Otrzymane wyniki, wyrażone jako procent odzysku w odniesieniu do metody referencyjnej, przedstawiono w tabeli 12. Kolorem żółtym zaznaczono wyniki, które istotnie odbiegały od wartości odniesienia.

Na podstawie danych przedstawionych w powyższe tabeli, można zauważyć, że w przypadku oznaczania K i Na otrzymane wyniki były w dobrej zgodności z wynikami uzyskanymi metodą ICP OES. Potwierdza to dobrą poprawność opracowanej metody FLC APGD OES. Natomiast w przypadku oznaczania Ca, w niektórych próbkach soków uzyskane wyniki istotnie odbiegały od wartości odniesienia wyznaczonych za pomocą metody ICP OES. Z kolei stężenia uzyskane dla Mg we wszystkich próbkach soków były o ok. połowę niższe od wartości odniesienia. Dodatkowo niskie wartości odzysków Mg zaobserwowano również w przypadku jednej z próbek energy drink-a oraz obu próbek mleka migdałowego. Wyniki te były nieco zaskakujące, biorąc pod uwagę to, że na poprzednich etapach badań nie odnotowano występowania jakichkolwiek efektów matrycowych. Jednakże wspomniane rozbieżności pomiędzy wartościami stężeń otrzymanymi z zastosowaniem obu metod, tj. FLC APGD OES i ICP OES, można wytłumaczyć występowaniem związków organicznych, np. kwasów karboksylowych w przypadku próbek soków, w matrycy analizowanych próbek. Związki te są zdolne do tworzenia kompleksów i/lub osadów z jonami Ca i Mg. Zakładając, że stosunek stężeń wspomnianych związków do stężeń analitów jest większy od 1, liniowość odpowiedzi analitów wraz ze zmianą rozcieńczenia próbki zostałaby zachowana, co najprawdopodobniej miało miejsce w tym przypadku.

Tabela 12. Wartości odzysków Ca, K, Mg, Na i Zn dla próbek analizowanych metodą FLC APGD OES w odniesieniu do zawartości zmierzonych metodą odniesienia (ICP OES).

Próbka	**Odzysk [%]**				
	Ca	K	Mg	Na	Zn
Sok jabłkowy	109	109	53.2	103	-
Sok z banana	157	108	53.8	107	-
Sok z czarnej porzeczki	97.5	102	54.9	111	-
Sok z cytryny	104	108	48.8	107	-
Sok z limonki	79.4	107	56.8	106	-
Sok z granatu	73.2	104	54.5	96.9	-
Sok z pigwy	91.0	107	50.6	103	-
Sok pomidorowy	72.4	103	52.0	101	-
Coca-cola zero	95.3	101	104	91.3	-
Coca-Cola original	98.8	111	99.0	91.6	-
Energy drink z dodatkiem Mg	93.3	101	57.7	103	-
Energy drink z dodatkiem Zn	112	98.9	103	99.5	93.8
Black bez cukru	93.7	100	88.6	94.5	-
Black	98.2	107	91.7	93.9	-
Pre-workout	96.3	106	98.0	99.4	-
BCAA (smak cytrynowy)	106	95.5	99.1	91.2	-
BCAA (smak pomarańczowy)	95.1	96.5	88.6	108	-
Mleko migdałowe bez cukru	106	107	65.9	99.6	-
Mleko migdałowe	95.1	108	75.5	89.9	-
Odżywka białkowa (smak czekoladowy)	111	91.2	93.8	90.1	-
Odżywka białkowa (smak truskawkowy)	110	93.0	92.4	99.3	-

W związku z niezadawalającymi wynikami oznaczania Ca i Mg w niektórych próbkach, powtórzono analizę wszystkich próbek soków oraz wspomnianych wyżej 3 próbek napojów, tym razem z zastosowaniem metody dodatku wzorca. Szczegółowe wyniki tych analiz zostały przedstawione w [**D5**] i [**D6**]. Uzyskane wartości odzysków mieściły się w zakresie 91–109%.
Na podstawie uzyskanych wyników, można więc uznać, że opracowana metoda FLC APGD OES daje wiarygodne wyniki analizy próbek o złożonej matrycy z zastosowaniem jedynie rozcieńczenia i zakwaszenia na etapie przygotowania próbek. Mimo że w niektórych przypadkach oznaczenie Mg i Ca wiąże się z koniecznością zastosowania metody dodatku wzorca do kalibracji, warto mieć na uwadze, że wykorzystanie metody dodatku wzorca jest nadal mniej praco- i czasochłonne niż rozkład mokry próbek.

7. PODSUMOWANIE I WNIOSKI

W ramach niniejszej rozprawy doktorskiej przeprowadzono szereg badań z zastosowaniem układów FLA APGD i FLC APGD, co miało na celu poszerzenie istniejącej dotychczas wiedzy na temat mechanizmu procesów i reakcji w nich zachodzących oraz poprawę charakterystyki analitycznej metody OES z wykorzystaniem obu wspomnianych źródeł wzbudzenia. Prowadzone badania zostały podzielone na 3 grupy i obejmowały:

- Wykorzystanie wyładowań APGD do oznaczania nowych (niebadanych wcześniej) analitów,
- Sprzęgnięcie badanych układów z technikami HG/CVG,
- Zastosowanie układu FLC APGD do oznaczania próbek o złożonej matrycy z wykorzystaniem uproszczonej procedury przygotowania próbek do analizy.

W badaniach nad zastosowaniem wyładowań APGD do oznaczania Bi, Br i Cl ustalono, że oba układy APGD pozwalają na oznaczanie wyżej wymienionych pierwiastków, przy czym wartości DL uzyskane dla Bi są zbliżone do tych, otrzymywanych dla innych analitów z użyciem tych samych

układów. Z kolei wartości DL Br i Cl okazały się być znacząco wyższe, wyższe też jednak były stężenia tych analitów (szczególnie Cl) w analizowanych próbkach rzeczywistych. Ostatecznie udowodniono, że metoda FLA APGD OES pozwala na bardziej wiarygodne (niż ICP OES) oznaczanie Br i Cl w próbkach rzeczywistych. Dodatkowo poszczególne etapy prowadzonych badań (porównanie widm w szerokim zakresie, optymalizacja warunków pomiarowych czy badanie wpływu jonów interferujących na sygnały analitów) wskazały na istotne różnice w charakterystyce pracy obu układów pomiędzy oznaczaniem metali/półmetali a niemetali, wynikającej głównie z różnych mechanizmów wprowadzania oznaczanych pierwiastków (w formie anionów lub kationów) do źródła wyładowania.

Sprzęgnięcie badanych układów APGD z technikami HG/CVG umożliwiło z kolei:

- Oznaczanie pierwiastków trudnowzbudzalnych (As, Sb i Se), których oznaczenie z zastosowaniem wprowadzania analitów do wyładowania bezpośrednio z roztworu FLA/FLC jest niemożliwa;
- Poprawę granic wykrywalności innych pierwiastków (Br, Hg);
- Redukcję efektów matrycowych (ze szczególnym uwzględnieniem układu FLA APGD), będącą efektem odseparowania lotnych form analitów od matrycy próbki.

Prowadzone badania wskazały również na pewne ograniczenia zastosowania technik HG/CVG. Jednym z nich były, zaobserwowane w trakcie badań dotyczących generowania wodorków, silne efekty pamięci, związane z osadzaniem się śladowych ilości analitów (głównie Hg) na elementach konstrukcyjnych układu, wynikające z dużej czułości odpowiadających im sygnałów. Natomiast w przypadku Cl, okazało się, że generowanie lotnego Cl_2 w reakcji ze związkiem utleniającym nie jest możliwe bez zastosowania bardzo dużych stężeń H_2SO_4.

Zastosowanie układu FLC APGD pozwoliło na analizę próbek rzeczywistych o złożonej matrycy z wykorzystaniem uproszczonej metody przygotowania próbek, sprowadzającej się do ich rozcieńczenia i zakwaszenia. Ze względu na niskie wartości DL oznaczanych pierwiastków (Ca, K, Mg, Na i Zn), w badanym układzie możliwe było zastosowanie dużych rozcieńczeń próbek, co z kolei pozwala ograniczyć wpływ efektów matrycowych od niektórych współistniejących składników próbki, jak również ogranicza zużycie próbki. W większości przypadków analiza mogła z powodzeniem zostać przeprowadzona z wykorzystaniem zewnętrznej krzywej wzorcowej do kalibracji. Jednakże w przypadku oznaczania Mg i Ca w niektórych próbkach konieczne było zastosowanie metody dodatku wzorca.

Mając na uwadze wyniki badań prowadzonych w ramach niniejszej rozprawy doktorskiej, uznano, że metody FLA APGD OES i FLC APGD OES mogą być interesującą alternatywą dla metod z dostępną komercyjnie wielkogabarytową aparaturą pomiarową. Przemawiają za tym liczne korzyści, związane z zastosowaniem układów wykorzystujących wyładowania APGD jako źródła wzbudzenia w OES, tj.:

- Samoistny transport analitów do źródła wzbudzenia, eliminujący konieczność stosowania wyspecjalizowanych układów wprowadzania próbki, przy jednoczesnym zwiększeniu wydajności transportu analitów do plazmy, skutkującym istotnym obniżeniem uzyskiwanych wartości DL;
- Zminiaturyzowana i uproszczona konstrukcja układów wyładowczych, pozwalająca na obniżenie kosztów związanych zarówno z zakupem jak i eksploatacją stosowanych urządzeń pomiarowych, w tym – kosztów związanych ze zużyciem gazu i energii elektrycznej;
- Charakterystyka analityczna – w tym szczególnie granice wykrywalności – będąca zbliżona (lub nawet lepsza) do tej, oferowanej przez niektóre urządzenia wielkogabarytowe, jak np. do FAAS czy ICP OES;
- Możliwość wykonywania analiz próbek o złożonej matrycy bez konieczności ich rozkładu mokrego, co znacząco upraszcza analizę i skraca czas jej trwania, a dodatkowo minimalizuje ryzyko związane ze stratami analitów i zanieczyszczeniem analizowanych próbek.

8. BIBLIOGRAFIA

[D1] M. Gorska, K. Greda, P. Pohl, *Determination of bismuth by optical emission spectrometry with liquid anode/cathode atmospheric pressure glow discharge*. J. Anal. At. Spectrom. 2021, 36, 165-177.
DOI: 10.1039/D0JA00401D
[D2] M. Gorska, P. Pohl, *Application of atmospheric pressure glow discharge generated in contact with liquids for determination of chloride and bromide in water and juice samples by optical emission spectrometry*. Talanta 2022, 237, 1-11.
DOI: 10.1016/j.talanta.2021.122921
[D3] M. Gorska, P. Pohl, *Coupling of chemical vapor generation with atmospheric pressure glow discharge optical emission spectrometry generated in contact with flowing liquid electrodes for determination of Br in water samples*. Microchem. J. 2022, 178, 1-9.
DOI: 10.1016/j.microc.2022.107391
[D4] M. Gorska, K. Greda, P. Pohl, *On the coupling of hydride generation (HG) with flowing liquid anode atmospheric pressure glow discharge (FLA-APGD) for determination of traces of As, Bi, Hg, Sb and Se by optical emission spectrometry (OES)*. Talanta 2021, 222, 1-10.
DOI: 10.1016/j.talanta.2020.121510
[D5] M. Gorska, P. Pohl, *Simplified and rapid determination of Ca, K, Mg, and Na in fruit juices by flowing liquid cathode atmospheric glow discharge optical emission spectrometry*. J. Anal. At. Spectrom. 2021, 36, 1455-1465.
DOI: 10.1039/D1JA00127B
[D6] M. Gorska, J. Weiss, P. Pohl, *Fast and simple analysis of the content of Zn, Mg, Ca, Na, and K in selected beverages widely consumed by athletes by flowing liquid cathode atmospheric pressure glow discharge optical emission spectrometry*. Anal. Methods 2023, 15, 1775-1789.
DOI: 10.1039/D3AY00092C
[1] Y. Yin, J. Messier, J. A. Hopwood. *Miniaturization of inductively coupled plasma sources*. IEEE Trans. Plasma Sci. 1999, 27, 1516–1524.
DOI: 10.1109/27.799834
[2] O. B. Minayeva, J. A. Hopwood. *Microfabricated inductively coupled plasma-on-a-chip for molecular SO2 detection: a comparison between global model and optical emission spectrometry*. J. Anal. At. Spectrom. 2003, 18, 856–863.
DOI: 10.1039/B303821A
[3] T. Cserfalvi, P. Mezei, P. Apai. *Emission studies on a glow discharge in atmospheric pressure air using water as a cathode*. J. Phys. D: Appl. Phys. 1993, 26, 2184–2188.
DOI: 10.1088/0022-3727/26/12/015
[4] B. K. Zuev, V. V. Yagov, M. L. Getsina, B. A. Rudenko. *Discharge on Boiling in a Channel as a New Atomization and Excitation Source for the Flow Determination of Metals by Atomic Emission Spectrometry*. J. Anal. Chem. 2002, 57, 907–911.
DOI: 10.1023/A:1020475025336
[5] V. V. Yagov, M. L. Getsina, B. K. Zuev. *Use of Electrolyte Jet Cathode Glow Discharges as Sources of Emission Spectra for Atomic Emission Detectors in Flow-Injection Analysis*. J. Anal. Chem. 2004, 59, 1037–1041.
DOI: 10.1023/B:JANC.0000047005.47648.f0
[6] A. Kitano, A. Iiduka, T. Yamamoto, Y. Ukita, E. Tamiya, Y. Takamura. *Highly sensitive elemental analysis for Cd and Pb by liquid electrode plasma atomic emission spectrometry with quartz glass chip and sample flow*. Anal. Chem. 2011, 83, 9424–9430.
DOI: 10.1021/ac2020646
[7] M. R. Webb, F. J. Andrade, G. Gamez, R. McCrindle, G. M. Hieftje. *Spectroscopic and electrical studies of a solution-cathode glow discharge*. J. Anal. At. Spectrom. 2005, 20, 1218–1225.
DOI: 10.1039/B503961D

[8] P. Jamroz, W. Zyrnicki. *Spectroscopic Characterization of Miniaturized Atmospheric-Pressure dc Glow Discharge Generated in Contact with Flowing Small Size Liquid Cathode*. Plasma Chem. Plasma Process. 2011, 31, 681–696.
DOI: 10.1007/s11090-011-9307-2
[9] H. W. Paing, K. A. Hall, R. Kenneth Marcus. *Sheathing of the liquid sampling – Atmospheric pressure glow discharge microplasma from ambient atmosphere and its implications for optical emission spectroscopy*. Spectrochim. Acta B 2019, 155, 99–106.
DOI: 10.1016/j.sab.2019.03.002
[10] X. Liu, Z. Zhu, D. He, H. Zheng, Y. Gan, N. Stanley Belshaw, S. Hu, Y. Wang. *Highly sensitive elemental analysis of Cd and Zn by solution anode glow discharge atomic emission spectrometry*. J. Anal. At. Spectrom. 2016, 31, 1089–1096.
DOI: 10.1039/C6JA00017G
[11] K. Greda, K. Swiderski, P. Jamroz, P. Pohl. *Flowing Liquid Anode Atmospheric Pressure Glow Discharge as an Excitation Source for Optical Emission Spectrometry with the Improved Detectability of Ag, Cd, Hg, Pb, Tl, and Zn*. Anal. Chem. 2016, 88, 8812–8820.
DOI: 10.1021/acs.analchem.6b02250
[12] P. Jamroz, K. Greda, A. Dzimitrowicz, K. Swiderski, P. Pohl. *Sensitive Determination of Cd in Small-Volume Samples by Miniaturized Liquid Drop Anode Atmospheric Pressure Glow Discharge Optical Emission Spectrometry*. Anal. Chem. 2017, 89, 5729–5733.
DOI: 10.1021/acs.analchem.7b01198
[13] K. Swiderski, P. Pohl, P. Jamroz. *A miniaturized atmospheric pressure glow microdischarge system generated in contact with a hanging drop electrode – a new approach to spectrochemical analysis of liquid microsamples*. J. Anal. At. Spectrom. 2019, 34, 1287–1293.
DOI: 10.1039/C9JA00038K
[14] K. Greda, P. Pohl. *Direct analysis of wines from the province of Lower Silesia (Poland) by microplasma source optical emission spectrometry*. Food Chem. 2022, 371, 131178.
DOI: 10.1016/j.foodchem.2021.131178
[15] J. Wang, P. Tang, P. Zheng, X. Zhai. *Analysis of metal elements by solution cathode glow discharge-atomic emission spectrometry with a modified pulsation damper*. J. Anal. At. Spectrom. 2017, 32, 1925–1931.
DOI: 10.1039/C7JA00212B
[16] X. Peng, X. Guo, F. Ge, Z. Wang. *Battery-operated portable high-throughput solution cathode glow discharge optical emission spectrometry for environmental metal detection*. J. Anal. At. Spectrom. 2019, 34, 394–400.
DOI: 10.1039/C8JA00369F
[17] M. Yuan, X. Peng, F. Ge, Q. Li, K. Wang, D.-G. Yu, Z. Wang. *Simplified design for solution anode glow discharge atomic emission spectrometry device for highly sensitive detection of Ag, Bi, Cd, Hg, Pb, Tl, and Zn*. Microchem. J. 2020, 155, 104785.
DOI: 10.1016/j.microc.2020.104785
[18] K. Greda, P. Jamroz, P. Pohl. *Ultrasonic nebulization atmospheric pressure glow discharge — Preliminary study*. Spectrochim. Acta B 2016, 121, 22–27.
DOI: 10.1016/j.sab.2016.04.008
[19] A. J. Schwartz, K. L. Williams, G. M. Hieftje, J. T. Shelley. *Atmospheric-pressure solution-cathode glow discharge: A versatile ion source for atomic and molecular mass spectrometry*. Anal. Chim. Acta 2017, 950, 119–128.
DOI: 10.1016/j.aca.2016.10.045
[20] K. Greda, M. Gorska, M. Welna, P. Jamroz, P. Pohl. *In-situ generation of Ag, Cd, Hg, In, Pb, Tl and Zn volatile species by flowing liquid anode atmospheric pressure glow discharge operated in gaseous jet mode - Evaluation of excitation processes and analytical performance*. Talanta 2019, 199, 107–115.
DOI: 10.1016/j.talanta.2019.02.058

[21] J. Yu, L. Yin, Q. Lu, F. Feng, Y. Kang, H. Luo. *Highly sensitive determination of mercury by improved liquid cathode glow discharge with the addition of chemical modifiers*. Anal. Chim. Acta 2020, 1131, 25–34.
DOI: 10.1016/j.aca.2020.07.050
[22] Y.-J. Zhou, J. Ma, F. Li, T. Xian, Q.-H. Yuan, Q.-F. Lu. *Sensitivity improvement of solution cathode glow discharge-optical emission spectrometry by external magnetic field for optical determination of elements*. Microchem. J. 2020, 158, 105224.
DOI: 10.1016/j.microc.2020.105224
[23] P. Zheng, W. Li, J. Wang, N. Wang, C. Zhong, Y. Luo, X. Wang, X. Mao, C. Lai. *Analytical Performance of Hollow Anode-Solution Cathode Glow Discharge-Atomic Emission Spectrometry*. Anal. Lett. 2020, 53, 693–704.
DOI: 10.1080/00032719.2019.1668007
[24] C. Huang, Q. Li, J. Mo, Z. Wang. *Ultratrace Determination of Tin, Germanium, and Selenium by Hydride Generation Coupled with a Novel Solution-Cathode Glow Discharge-Atomic Emission Spectrometry Method*. Anal. Chem. 2016, 88, 11559–11567.
DOI: 10.1021/acs.analchem.6b02807
[25] M. Zhao, X. Peng, B. Yang, Z. Wang. *Ultra-sensitive determination of antimony valence by solution cathode glow discharge optical emission spectrometry coupled with hydride generation*. J. Anal. At. Spectrom. 2020, 35, 1148–1155.
DOI: 10.1039/D0JA00009D
[26] X. Liu, Z. Liu, Z. Zhu, D. He, S. Yao, H. Zheng, S. Hu. *Generation of Volatile Cadmium and Zinc Species Based on Solution Anode Glow Discharge Induced Plasma Electrochemical Processes*. Anal. Chem. 2017, 89, 3739–3746.
DOI: 10.1021/acs.analchem.7b00126
[27] J. Cheng, Q. Li, M. Zhao, Z. Wang. *Ultratrace Pb determination in seawater by solution-cathode glow discharge-atomic emission spectrometry coupled with hydride generation*. Anal. Chim. Acta 2019, 1077, 107–115.
DOI: 10.1016/j.aca.2019.06.003
[28] X. Guo, X. Peng, Q. Li, J. Mo, Y. Du, Z. Wang. *Ultra-sensitive determination of inorganic arsenic valence by solution cathode glow discharge-atomic emission spectrometry coupled with hydride generation*. J. Anal. At. Spectrom. 2017, 32, 2416–2422.
DOI: 10.1039/C7JA00228A
[29] K. Greda, P. Jamroz, D. Jedryczko, P. Pohl. *On the coupling of hydride generation with atmospheric pressure glow discharge in contact with the flowing liquid cathode for the determination of arsenic, antimony and selenium with optical emission spectrometry*. Talanta 2015, 137, 11–17.
DOI: 10.1016/j.talanta.2014.11.073
[30] X. Peng, M. Zhao, M. Yuan, Z. Wang. *Solution anode glow discharge optical emission spectrometry: Volatile hydride introduction from the gas jet nozzle cathode for ultrasensitive determination of lead*. Talanta 2021, 225, 121995.
DOI: 10.1016/j.talanta.2020.121995
[31] K. Greda, S. Burhenn, P. Pohl, J. Franzke. *Enhancement of emission from indium in flowing liquid anode atmospheric pressure glow discharge using organic media*. Talanta 2019, 204, 304–309.
DOI: 10.1016/j.talanta.2019.06.015
[32] M. Yuan, X. Peng, F. Ge, M. Zhao, Q. Li, Z. Wang. *Ultrasensitive determination of mercury by solution anode glow discharge atomic emission spectrometry coupled with hydride generation*. Chin. Chem. Lett. 2020, 31, 2814–2818.
DOI: 10.1016/j.cclet.2020.03.055
[33] W. Zu, Y. Yang, Y. Wang, X. Yang, C. Liu, M. Ren. *Rapid determination of indium in water samples using a portable solution cathode glow discharge-atomic emission spectrometer*. Microchem. J. 2018, 137, 266–271.
DOI: 10.1016/j.microc.2017.11.001

[34] T. A. Doroski, M. R. Webb. *Signal enhancement in solution-cathode glow discharge — optical emission spectrometry via low molecular weight organic compounds*. Spectrochim. Acta B 2013, 88, 40–45.
DOI: 10.1016/j.sab.2013.07.014
[35] J. Ma, Z. Wang, Q. Li, R. Gai, X. Li. *On-line separation and preconcentration of hexavalent chromium on a novel mesoporous silica adsorbent with determination by solution-cathode glow discharge-atomic emission spectrometry*. J. Anal. At. Spectrom. 2014, 29, 2315–2322.
DOI: 10.1039/C4JA00273C
[36] A. J. Schwartz, S. J. Ray, E. Elish, A. P. Storey, A. A. Rubinshtein, G. C-Y Chan, K. P. Pfeuffer, G. M. Hieftje. *Visual observations of an atmospheric-pressure solution-cathode glow discharge*. Talanta 2012, 102, 26–33.
DOI: 10.1016/j.talanta.2012.07.096
[37] P. Jamroz, P. Pohl, W. Zyrnicki. *An analytical performance of atmospheric pressure glow discharge generated in contact with flowing small size liquid cathode*. J. Anal. At. Spectrom. 2012, 27, 1032–1037.
DOI: 10.1039/C2JA30017F
[38] K. Greda, P. Jamroz, P. Pohl. *Effect of the addition of non-ionic surfactants on the emission characteristic of direct current atmospheric pressure glow discharge generated in contact with a flowing liquid cathode*. J. Anal. At. Spectrom. 2012, 28, 134–141.
DOI: 10.1039/C2JA30275F
[39] J. Yu, S. Yang, D. Sun, Q. Lu, J. Zheng, X. Zhang, X. Wang. *Simultaneously determination of multi metal elements in water samples by liquid cathode glow discharge-atomic emission spectrometry*. Microchem. J. 2016, 128, 325–330.
DOI: 10.1016/j.microc.2016.05.019
[40] K. Greda, P. Jamroz, P. Pohl. *Comparison of the performance of direct current atmospheric pressure glow microdischarges operated between a small sized flowing liquid cathode and miniature argon or helium flow microjets*. J. Anal. At. Spectrom. 2013, 28, 1233.
DOI: 10.1039/C3JA50062D
[41] J. Yu, Y. Kang, Q. Lu, H. Luo, Z. Lu, L. Cui, J. Li. *Improvement of analytical performance of liquid cathode glow discharge for the determination of bismuth using formic acid as a matrix modifier*. Microchem. J. 2020, 159, 105507.
DOI: 10.1016/j.microc.2020.105507
[42] H. Yuan, D.-Z. Yang, X. Li, L. Zhang, X.-F. Zhou, W.-C. Wang, Y. Xu. *A pulsed electrolyte cathode discharge used for metal element analysis by atomic emission spectrometry*. Phys. Plasmas 2019, 26, 53505.
DOI: 10.1063/1.5088547
[43] K. Swiderski, A. Dzimitrowicz, P. Jamroz, P. Pohl. *Influence of pH and low-molecular weight organic compounds in solution on selected spectroscopic and analytical parameters of flowing liquid anode atmospheric pressure glow discharge (FLA-APGD) for the optical emission spectrometric (OES) determination of Ag, Cd, and Pb*. J. Anal. At. Spectrom. 2018, 33, 437–451.
DOI: 10.1039/C7JA00374A
[44] Q. Lu, H. Luo, J. Yu, Y. Kang, Z. Lu, J. Li, W. Yang. *Evaluation of a sampling system coupled to liquid cathode glow discharge for the determination of rubidium, cesium and strontium in water samples*. Microchem. J. 2020, 158, 105246.
DOI: 10.1016/j.microc.2020.105246
[45] J. Wang, S. Li, P. Zheng, K. Liu, P. Tang. *Time-resolved emission spectroscopy and plasma characteristics of a pulsed electrolyte cathode atmospheric pressure discharge system*. J. Anal. At. Spectrom. 2018, 33, 1014–1020.
DOI: 10.1039/C8JA00041G
[46] K. Swiderski, M. Welna, K. Greda, P. Pohl, P. Jamroz. *Hanging drop cathode-atmospheric pressure glow discharge as a new method of sample introduction for inductively coupled plasma-optical emission spectrometry*. Anal. Bioanal. Chem. 2020, 412, 4211–4219.

DOI: 10.1007/s00216-020-02685-7
[47] X. Lu, M. Laroussi. *Ignition phase and steady-state structures of a non-thermal air plasma*. J. Phys. D: Appl. Phys. 2003, 36, 661–665.
DOI: 10.1088/0022-3727/36/6/308
[48] Q. Xiao, Z. Zhu, H. Zheng, H. He, C. Huang, S. Hu. *Significant sensitivity improvement of alternating current driven-liquid discharge by using formic acid medium for optical determination of elements*. Talanta 2013, 106, 144–149.
DOI: 10.1016/j.talanta.2012.12.013
[49] J. Wang, M. He, P. Zheng, Y. Chen, X. Mao. *Comparison of the Plasma Temperature and Electron Number Density of the Pulsed Electrolyte Cathode Atmospheric Pressure Discharge and the Direct Current Solution Cathode Glow Discharge*. Anal. Lett. 2019, 52, 697–712.
DOI: 10.1080/00032719.2018.1487449
[50] K. Greda, M. Welna, A. Szymczycha-Madeja, P. Pohl. *Flow injection gas analysis (FIGA) for more sensitive determination of Hg by inductively coupled plasma optical emission spectrometry*. Talanta 2023, 253, 124072.
DOI: 10.1016/j.talanta.2022.124072
[51] A. Ramesh Kumar, P. Riyazuddin. *Chemical interferences in hydride-generation atomic spectrometry*. Trends Anal. Chem. 2010, 29, 166–176.
DOI: 10.1016/j.trac.2009.12.002
[52] P. Pohl, P. Jamroz, M. Welna, A. Szymczycha-Madeja, K. Greda. *Chemical-vapor generation of transition metals through the reaction with tetrahydroborate in recent achievements in analytical atomic spectrometry*. Trends Anal. Chem. 2014, 59, 144–155.
DOI: 10.1016/j.trac.2014.04.010
[53] X. Peng, Z. Wang. *Systematic evaluation of advance in application and discharge mechanism of solution electrode glow discharge*. Chin. Chem. Lett. 2022, 33, 61–70.
DOI: 10.1016/j.cclet.2021.06.017
[54] P. Mezei, T. Cserfalvi, M. Jánossy. *Pressure Dependence of the Atmospheric Electrolyte Cathode Glow Discharge Spectrum*. J. Anal. At. Spectrom. 1997, 12, 1203–1208.
DOI: 10.1039/A608528H
[55] T. Cserfalvi, P. Mezei. *Investigations on the element dependency of sputtering process in the electrolyte cathode atmospheric discharge*. J. Anal. At. Spectrom. 2005, 20, 939–944.
DOI: 10.1039/B504610F
[56] M. R. Webb, F. J. Andrade, G. M. Hieftje. *Compact glow discharge for the elemental analysis of aqueous samples*. Anal. Chem. 2007, 79, 7899–7905.
DOI: 10.1021/ac070789x
[57] A. J. Schwartz, J. T. Shelley, C. L. Walton, K. L. Williams, G. M. Hieftje. *Atmospheric-pressure ionization and fragmentation of peptides by solution-cathode glow discharge*. Chem. Sci. 2016, 7, 6440–6449.
DOI: 10.1039/C6SC02032A
[58] C. G. Decker, M. R. Webb. *Measurement of sample and plasma properties in solution-cathode glow discharge and effects of organic additives on these properties*. J. Anal. At. Spectrom. 2016, 31, 311–318.
DOI: 10.1039/C5JA00243E
[59] P. Jamroz, K. Greda, P. Pohl, W. Zyrnicki. *Atmospheric Pressure Glow Discharges Generated in Contact with Flowing Liquid Cathode: Production of Active Species and Application in Wastewater Purification Processes*. Plasma Chem. Plasma Process. 2014, 34, 25–37.
DOI: 10.1007/s11090-013-9503-3
[60] Y. S. Park, S. H. Ku, S. H. Hong, H. J. Kim, E. H. Piepmeier. *Fundamental studies of electrolyte-as-cathode glow discharge-atomic emission spectrometry for the determination of trace metals in flowing water*. Spectrochim. Acta B 1998, 53, 1167–1179.
DOI: 10.1016/S0584-8547(98)00154-2

[61] P. Mezei, T. Cserfalvi, H. J. Kim, M. A. Mottaleb. *The influence of chlorine on the intensity of metal atomic lines emitted by an electrolyte cathode atmospheric glow discharge*. Analyst 2001, 126, 712–714.
DOI: 10.1039/B010057I
[62] Q. He, Z. Zhu, S. Hu, L. Jin. *Solution cathode glow discharge induced vapor generation of mercury and its application to mercury speciation by high performance liquid chromatography-atomic fluorescence spectrometry*. J. Chromatogr. A 2011, 1218, 4462–4467.
DOI: 10.1016/j.chroma.2011.05.034
[63] A. I. Maximov, A. V. Khlustova. *The influence of solution component transfer to the plasma on gas discharge properties*. High Temp. Mater. Process. 2007, 11, 527–535.
DOI: 10.1615/HighTempMatProc.v11.i4.50
[64] M. R. Webb, F. J. Andrade, G. M. Hieftje. *Use of electrolyte cathode glow discharge (ELCAD) for the analysis of complex mixtures*. J. Anal. At. Spectrom. 2007, 22, 766–774.
DOI: 10.1039/B616989A
[65] P. Pohl, P. Jamroz, K. Swiderski, A. Dzimitrowicz, A. Lesniewicz. *Critical evaluation of recent achievements in low power glow discharge generated at atmospheric pressure between a flowing liquid cathode and a metallic anode for element analysis by optical emission spectrometry*. TrAC, Trends Anal. Chem. 2017, 88, 119–133.
DOI: 10.1016/j.trac.2017.01.002
[66] D. E. Moon, M. R. Webb. *Imaging studies of emission and laser scattering from a solution-cathode glow discharge*. J. Anal. At. Spectrom. 2020, 35, 1859–1867.
DOI: 10.1039/D0JA00134A
[67] R. Manjusha, M. A. Reddy, R. Shekhar, S. Jai Kumar. *Determination of cadmium in Zircaloys by electrolyte cathode discharge atomic emission spectrometry (ELCAD-AES)*. Anal. Methods 2014, 6, 9850–9856.
DOI: 10.1039/C4AY01242A
[68] Q. Lu, F. Feng, J. Yu, L. Yin, Y. Kang, H. Luo, D. Sun, W. Yang. *Determination of trace cadmium in zinc concentrate by liquid cathode glow discharge with a modified sampling system and addition of chemical modifiers for improved sensitivity*. Microchem. J. 2020, 152, 104308.
DOI: 10.1016/j.microc.2019.104308
[69] P. Bruggeman, J. Liu, J. Degroote, M. G. Kong, J. Vierendeels, C. Leys. *Dc excited glow discharges in atmospheric pressure air in pin-to-water electrode systems*. J. Phys. D: Appl. Phys. 2008, 41, 215201.
DOI: 10.1088/0022-3727/41/21/215201
[70] Q. Xiong, Z. Yang, P. J. Bruggeman. *Absolute OH density measurements in an atmospheric pressure dc glow discharge in air with water electrode by broadband UV absorption spectroscopy*. J. Phys. D: Appl. Phys. 2015, 48, 424008.
DOI: 10.1088/0022-3727/48/42/424008
[71] P. Bruggeman, P. Guns, J. Degroote, J. Vierendeels, C. Leys. *Influence of the water surface on the glow-to-spark transition in a metal-pin-to-water electrode system*. Plasma Sources Sci. Technol. 2008, 17, 45014.
DOI: 10.1088/0963-0252/17/4/045014
[72] P. Pohl, P. Jamroz, K. Greda, M. Gorska, A. Dzimitrowicz, M. Welna, A. Szymczycha-Madeja. *Five years of innovations in development of glow discharges generated in contact with liquids for spectrochemical elemental analysis by optical emission spectrometry*. Anal. Chim. Acta 2021, 1169, 338399.
DOI: 10.1016/j.aca.2021.338399
[73] C. Richmonds, M. Witzke, B. Bartling, S. Whan Lee, J. Wainright, C.-C. Liu, R. Mohan Sankaran. *Electron-transfer reactions at the plasma-liquid interface*. J. Am. Chem. Soc. 2011, 133, 17582–17585.
DOI: 10.1021/ja207547b

[74] P. Rumbach, D. M. Bartels, R. Mohan Sankaran, D. B. Go. *The solvation of electrons by an atmospheric-pressure plasma*. Nat. Commun. 2015, 6, 7248–7254.
DOI: 10.1038/ncomms8248
[75] P. Mezei, T. Cserfalvi. *Electrolyte Cathode Atmospheric Glow Discharges for Direct Solution Analysis*. Appl. Spectrosc. Rev. 2007, 42, 573–604.
DOI: 10.1080/05704920701624451
[76] J. W. Olesik. *Elemental Analysis Using ICP-OES and ICP/MS*. Anal. Chem. 1991, 63, 12A-21A.
DOI: 10.1021/ac00001a711
[77] B. M. Fontoura, F. Cora Jofre, T. Williams, M. Savio, G. L. Donati, J. A. Nobrega. *Is MIP-OES a suitable alternative to ICP-OES for trace element analysis?* J. Anal. At. Spectrom. 2022, 37, 966–984.
DOI: 10.1039/D1JA00375E
[78] A. J. Schwartz, S. J. Ray, G. C.-Y. Chan, G. M. Hieftje. *Spatially resolved measurements to improve analytical performance of solution-cathode glow discharge optical-emission spectrometry*. Spectrochim. Acta B 2016, 125, 168–176.
DOI: 10.1016/j.sab.2016.10.004
[79] J. Yu, X. Zhang, Q. Lu, X. Wang, D. Sun, Y. Wang, W. Yang. *Determination of calcium and zinc in gluconates oral solution and blood samples by liquid cathode glow discharge-atomic emission spectrometry*. Talanta 2017, 175, 150–157.
DOI: 10.1016/j.talanta.2017.07.040
[80] C. Yang, L. Wang, Z. Zhu, L. Jin, H. Zheng, N. Stanley Belshaw, S. Hu. *Evaluation of flow injection-solution cathode glow discharge-atomic emission spectrometry for the determination of major elements in brines*. Talanta 2016, 155, 314–320.
DOI: 10.1016/j.talanta.2016.04.060
[81] J. Yu, X. Zhang, Q. Lu, L. Yin, F. Feng, H. Luo, Y. Kang. *Liquid Cathode Glow Discharge as an Excitation Source for the Analysis of Complex Water Samples with Atomic Emission Spectrometry*. ACS omega 2020, 5, 19541–19547.
DOI: 10.1021/acsomega.0c01906
[82] Y. Wang, M. Su, D. Sun, C. Wu, X. Zhang, Q. Lu, C. Dong. *Comparative study of magnesium and calcium in Codonopsis pilosula samples detected by CF-LIBS and LCGD-AES*. Microchem. J. 2018, 137, 318–323.
DOI: 10.1016/j.microc.2017.11.011
[83] J. Yu, Z. Zhang, Q. Lu, D. Sun, S. Zhu, X. Zhang, X. Wang, W. Yang. *High-Sensitivity Determination of K, Ca, Na, and Mg in Salt Mines Samples by Atomic Emission Spectrometry with a Miniaturized Liquid Cathode Glow Discharge*. J. Anal. Methods. Chem. 2017, 2017, 7105831.
DOI: 10.1155/2017/7105831
[84] P. Zheng, W. Li, J. Wang, X. Zhai, X. Mao, X. Wang, C. Lai. *Spatially Resolved Characteristics of Solution Cathode Glow Discharge Source Coupled with an Interference Filter Wheel as Spectral Discrimination Device*. Anal. Lett. 2020, 53, 31–39.
DOI: 10.1080/00032719.2019.1636060
[85] A. J. Schwartz, S. J. Ray, G. M. Hieftje. *Evaluation of interference filters for spectral discrimination in solution-cathode glow discharge optical emission spectrometry*. J. Anal. At. Spectrom. 2016, 31, 1278–1286.
DOI: 10.1039/C6JA00127K
[86] P. Zheng, N. Wang, J. Wang, X. Mao, C. Lai, C. Zhong, W. Li, Y. Luo. *Classification of bottled mineral waters using solution cathode glow discharge optical emission spectroscopy and chemometrics methods*. Microchem. J. 2019, 151, 104216.
DOI: 10.1016/j.microc.2019.104216
[87] J. Yu, X. Zhang, Q. Lu, D. Sun, X. Wang, S. Zhu, Z. Zhang, W. Yang. *Evaluation of analytical performance for the simultaneous detection of trace Cu, Co and Ni by using liquid cathode glow discharge-atomic emission spectrometry*. Spectrochim. Acta B 2018, 145, 64–70.
DOI: 10.1016/j.sab.2018.04.011

[88] P. Zheng, X. Zhai, J. Wang, P. Tang. *Analytical Characterization of a Solution Cathode Glow Discharge with an Interference Filter Wheel for Spectral Discrimination*. Anal. Lett. 2018, 51, 2304–2315.
DOI: 10.1080/00032719.2017.1421213
[89] M. Gorska, P. Pohl. *Comparison of the performance of atmospheric pressure glow discharges operated between a flowing liquid cathode and either a pin-type anode or a helium jet anode for the Ga and In determination by the optical emission spectrometry*. Talanta 2021, 226, 122155.
DOI: 10.1016/j.talanta.2021.122155
[90] J. Yu, Y. Kang, Q. Lu, H. Luo, L. Cui, Z. Lu, J. Li. *Determination of gallium and indium by solution cathode glow discharge as an excitation source for atomic emission spectrometry*. Spectrochim. Acta B 2020, 172, 105968.
DOI: 10.1016/j.sab.2020.105968
[91] H. Li, W. Zu, F. Liu, Y. Wang, Y. Yang, X. Yang, C. Liu. *Determination of gallium in water samples by atomic emission spectrometry based on solution cathode glow discharge*. Spectrochim. Acta B 2019, 152, 25–29.
DOI: 10.1016/j.sab.2018.12.004
[92] P. Zheng, Y. Chen, J. Wang, S. Xue. *A pulsed atmospheric-pressure discharge generated in contact with flowing electrolyte solutions for metal element analysis by optical emission spectrometry*. J. Anal. At. Spectrom. 2016, 31, 2037–2044.
DOI: 10.1039/C6JA00213G
[93] P. Zheng, Y. Gong, J. Wang, X. Zeng. *Elemental Analysis of Mineral Water by Solution-Cathode Glow Discharge–Atomic Emission Spectrometry*. Anal. Lett. 2017, 50, 1512–1520.
DOI: 10.1080/00032719.2016.1233243
[94] K. Greda, A. Szymczycha-Madeja, P. Pohl. *Study and reduction of matrix effects in flowing liquid anode - Atmospheric pressure glow discharge - Optical emission spectrometry*. Anal. Chim. Acta 2020, 1123, 81–90.
DOI: 10.1016/j.aca.2020.05.026
[95] J. Mo, L. Zhou, X. Li, Q. Li, L. Wang, Z. Wang. *On-line separation and pre-concentration on a mesoporous silica-grafted graphene oxide adsorbent coupled with solution cathode glow discharge-atomic emission spectrometry for the determination of lead*. Microchem. J. 2017, 130, 353–359.
DOI: 10.1016/j.microc.2016.10.008
[96] J. Yu, S. Zhu, Q. Lu, Z. Zhang, D. Sun, X. Zhang, X. Wang, W. Yang. *Liquid Cathode Glow Discharge as a Microplasma Excitation Source for Atomic Emission Spectrometry for the Determination of Trace Heavy Metals in Ore Samples*. Anal. Lett. 2018, 51, 2128–2140.
DOI: 10.1080/00032719.2017.1406492
[97] J. Yu, S. Yang, Q. Lu, D. Sun, J. Zheng, X. Zhang, X. Wang, W. Yang. *Evaluation of liquid cathode glow discharge-atomic emission spectrometry for determination of copper and lead in ores samples*. Talanta 2017, 164, 216–221.
DOI: 10.1016/j.talanta.2016.11.015
[98] W. Zu, Y. Wang, X. Yang, C. Liu. *A portable solution cathode glow discharge-atomic emission spectrometer for the rapid determination of thallium in water samples*. Talanta 2017, 173, 88–93.
DOI: 10.1016/j.talanta.2017.05.073
[99] R. Shekhar, D. Karunasagar, K. Dash, M. Ranjit. *Determination of mercury in hepatitis-B vaccine by electrolyte cathode glow discharge atomic emission spectrometry (ELCAD-AES)*. J. Anal. At. Spectrom. 2010, 25, 875–879.
DOI: 10.1039/B927010H
[100] K. Greda, P. Jamroz, A. Dzimitrowicz, P. Pohl. *Direct elemental analysis of honeys by atmospheric pressure glow discharge generated in contact with a flowing liquid cathode*. J. Anal. At. Spectrom. 2015, 30, 154–161.
DOI: 10.1039/C4JA00261J

[101] M. Gorska, P. Pohl, K. Greda. *The application of antioxidant compounds to minimize matrix effects in flowing liquid anode atmospheric pressure glow discharge optical emission spectrometry*. Microchem. J. 2021, 164, 105975.
DOI: 10.1016/j.microc.2021.105975
[102] M. R. Webb, F. J. Andrade, G. M. Hieftje. *High-throughput elemental analysis of small aqueous samples by emission spectrometry with a compact, atmospheric-pressure solution-cathode glow discharge*. Anal. Chem. 2007, 79, 7807–7812.
DOI: 10.1021/ac0707885
[103] K. Swiderski, K. Greda, P. Pohl, P. Jamroz. *The sensitive determination of Ag, Pb and Tl as well as reduction of spectral interferences in a hanging drop cathode atmospheric pressure glow discharge excitation microsource equipped with a Dove prism system*. J. Anal. At. Spectrom. 2022, 37, 517–527.
DOI: 10.1039/D1JA00433F
[104] W. Clay Davis, R. Kenneth Marcus. *An atmospheric pressure glow discharge optical emission source for the direct sampling of liquid media*. J. Anal. At. Spectrom. 2001, 16, 931–937.
DOI: 10.1039/B103437P
[105] R. Shekhar, D. Karunasagar, M. Ranjit, J. Arunachalam. *Determination of elemental constituents in different matrix materials and flow injection studies by the electrolyte cathode glow discharge technique with a new design*. Anal. Chem. 2009, 81, 8157–8166.
DOI: 10.1021/ac901380v
[106] M. A. Mottaleb, Y.-A. Woo, H.-J. Kim. *Evaluation of open-air type electrolyte-as-cathode glow discharge-atomic emission spectrometry for determination of trace heavy metals in liquid samples*. Microchem. J. 2001, 69, 219–230.
DOI: 10.1016/S0026-265X(01)00087-X
[107] R. Shekhar. *Improvement of sensitivity of electrolyte cathode discharge atomic emission spectrometry (ELCAD-AES) for mercury using acetic acid medium*. Talanta 2012, 93, 32–36.
DOI: 10.1016/j.talanta.2012.02.004
[108] Q. Li, Z. Zhang, Z. Wang. *Determination of Hg2+ by on-line separation and pre-concentration with atmospheric-pressure solution-cathode glow discharge atomic emission spectrometry*. Anal. Chim. Acta 2014, 845, 7–14.
DOI: 10.1016/j.aca.2014.08.008
[109] Z. Wang, R. Gai, L. Zhou, Z. Zhang. *Design modification of a solution-cathode glow discharge-atomic emission spectrometer for the determination of trace metals in titanium dioxide*. J. Anal. At. Spectrom. 2014, 29, 2042–2049.
DOI: 10.1039/C4JA00173G
[110] R. Shekhar, K. Madhavi, N. N. Meeravali, S. Jai Kumar. *Determination of thallium at trace levels by electrolyte cathode discharge atomic emission spectrometry with improved sensitivity*. Anal. Methods 2014, 6, 732–740.
DOI: 10.1039/C3AY40390D
[111] R. Manjusha, M. A. Reddy, R. Shekhar, S. Jaikumar. *Determination of major to trace level elements in Zircaloys by electrolyte cathode discharge atomic emission spectrometry using formic acid*. J. Anal. At. Spectrom. 2013, 28, 1932–1939.
DOI: 10.1039/C3JA50202C
[112] Z. Zhang, Z. Wang, Q. Li, H. Zou, Y. Shi. *Determination of trace heavy metals in environmental and biological samples by solution cathode glow discharge-atomic emission spectrometry and addition of ionic surfactants for improved sensitivity*. Talanta 2014, 119, 613–619.
DOI: 10.1016/j.talanta.2013.11.010
[113] K. Greda, M. Welna, P. Pohl. *Determination of Ag, Bi, Cd, Hg, Pb, Tl, and Zn by inductively coupled plasma mass spectrometry combined with vapor generation assisted by solution anode glow discharge - A preliminary study*. Talanta 2022, 246, 123500.
DOI: 10.1016/j.talanta.2022.123500

[114] Z. Cai, Z. Wang. *Evaluation of solution anode glow discharge as a vapor generator in ICP-OES procedures: Application to highly sensitive determination of Cd and Hg*. Anal. Chim. Acta 2022, 1203, 339724.
DOI: 10.1016/j.aca.2022.339724
[115] P. C.A. Jeronimo, A. N. Araujo, M. B.S.M. Montenegro, D. Satinsky, P. Solich. *Colorimetric bismuth determination in pharmaceuticals using a xylenol orange sol–gel sensor coupled to a multicommutated flow system*. Anal. Chim. Acta 2004, 504, 235–241.
DOI: 10.1016/j.aca.2003.10.049
[116] A. Slikkerveer, F. A. de Wolff. *Pharmacokinetics and toxicity of bismuth compounds*. Med. Toxicol. Adverse Drug Exp. 1989, 4, 303–323.
DOI: 10.1007/BF03259915
[117] H. Ashkenani, M. Ali Taher. *Application of a new ion-imprinted polymer for solid-phase extraction of bismuth from various samples and its determination by ETAAS*. Int. J. Environ. Anal. Chem. 2013, 93, 1132–1145.
DOI: 10.1080/03067319.2012.708746
[118] Y.-L. Yu, Y. Cai, M.-L. Chen, J.-H. Wang. *Development of a miniature dielectric barrier discharge-optical emission spectrometric system for bromide and bromate screening in environmental water samples*. Anal. Chim. Acta 2014, 809, 30–36.
DOI: 10.1016/j.aca.2013.11.054
[119] A. Takeda, S. Yamasaki, H. Tsukada, Y. Takaku, S. Hisamatsu, N. Tsuchiya. *Determination of total contents of bromine, iodine and several trace elements in soil by polarizing energy-dispersive X-ray fluorescence spectrometry*. J. Soil Sci. Plant Nutr. 2011, 57, 19–28.
DOI: 10.1080/00380768.2010.548313
[120] W. Nei Lopes dos Santos, A. de Freitas Santos Junior, L. Oliveira Bastos Silva, B. Rosa Da Silva Santos, D. Levi Franca Da Silva. *Multivariate optimization of a digestion procedure for bismuth determination in urine using continuous flow hydride generation and atomic fluorescence spectrometry*. Microchem. J. 2017, 130, 147–152.
DOI: 10.1016/j.microc.2016.07.023
[121] D. Zehavi, J. Rabani. *Oxidation of aqueous bromide ions by hydroxyl radicals. Pulse radiolytic investigation*. J. Phys. Chem. 1972, 76, 312–319.
DOI: 10.1021/j100647a006
[122] M. Saran, I. Beck-Speier, B. Fellerhoff, G. Bauer. *Phagocytic killing of microorganisms by radical processes: consequences of the reaction of hydroxyl radicals with chloride yielding chlorine atoms*. Free Radic. Biol. Med. 1999, 26, 482–490.
DOI: 10.1016/S0891-5849(98)00187-7
[123] J. Kratzer, J. Bousek, R. E. Sturgeon, Z. Mester, J. Dedina. *Determination of bismuth by dielectric barrier discharge atomic absorption spectrometry coupled with hydride generation: method optimization and evaluation of analytical performance*. Anal. Chem. 2014, 86, 9620–9625.
DOI: 10.1021/ac502093y
[124] M. Li, Y. Deng, C. Zheng, X. Jiang, X. Hou. *Hydride generation-point discharge microplasma-optical emission spectrometry for the determination of trace As, Bi, Sb and Sn*. J. Anal. At. Spectrom. 2016, 31, 2427–2433.
DOI: 10.1039/C6JA00341A
[125] T. Sahraeian, H. Sereshti, A. Rohanifar. *Simultaneous Determination of Bismuth, Lead, and Iron in Water Samples by Optimization of USAEME and ICP–OES via Experimental Design*. J. Anal. Test. 2018, 2, 98–105.
DOI: 10.1007/s41664-017-0046-0
[126] J. Proch, P. Niedzielski. *In-spray chamber hydride generation by multi-mode sample introduction system (MSIS) as an interface in the hyphenated system of high performance liquid chromatography and inductivity coupled plasma optical emission spectrometry (HPLC/HG-ICP-OES) in arsenic species determination*. Talanta 2020, 208, 120395.
DOI: 10.1016/j.talanta.2019.120395

[127] X. Peng, Z. Wang. *Ultrasensitive Determination of Selenium and Arsenic by Modified Helium Atmospheric Pressure Glow Discharge Optical Emission Spectrometry Coupled with Hydride Generation*. Anal. Chem. 2019, 91, 10073–10080.
DOI: 10.1021/acs.analchem.9b02006
[128] A. Garcia-Figueroa, F. Pena-Pereira, I. Lavilla, C. Bendicho. *Headspace single-drop microextraction coupled with microvolume fluorospectrometry for highly sensitive determination of bromide*. Talanta 2017, 170, 9–14.
DOI: 10.1016/j.talanta.2017.03.090
[129] P. Pohl, I. Jimenez Zapata, M. A. Amberger, N. H. Bings, J. A.C. Broekaert. *Characterization of a microwave microstrip helium plasma with gas-phase sample introduction for the optical emission spectrometric determination of bromine, chlorine, sulfur and carbon using a miniaturized optical fiber spectrometer*. Spectrochim. Acta B 2008, 63, 415–421.
DOI: 10.1016/j.sab.2007.12.005

JAAS

PAPER

View Article Online
View Journal | View Issue

Cite this: *J. Anal. At. Spectrom.*, 2021, **36**, 165

Determination of bismuth by optical emission spectrometry with liquid anode/cathode atmospheric pressure glow discharge†

Monika Gorska, * Krzysztof Greda and Pawel Pohl

Novel atmospheric pressure glow discharge (APGD) microplasma systems, sustained between a miniaturized flowing liquid anode (FLA) or cathode (FLC) and a He nozzle jet were investigated for the determination of Bi with the aid of optical emission spectrometry (OES). The most influential working conditions, *i.e.*, the acid type, the acid concentration, the discharge current, the He flow rate, the sample flow rate, and the discharge gap, were optimized for both studied methods. Furthermore, the effect of the addition of low molecular weight organic compounds (LMWOCs) into FLA/FLC solutions on the signal intensity of Bi was investigated. It was found that the addition of formic acid (5%) into the FLC solution enhanced the signal intensity 10 times. Under the optimized conditions, detection limits (DLs, assessed on the basis of the 3σ criterion) reached 33 μg L^{-1} for the FLC-APGD system and 0.34 μg L^{-1} in the case of the FLA-APGD system. The DL of Bi offered by the FLA-APGD-OES method was better than those reported for other microplasma techniques. The latter method was successfully applied for a quantitative determination of Bi in spiked water samples. The influence of concomitant ions on the signal intensity of Bi was thoroughly studied and the recoveries of Bi added to these water samples (at a concentration of 100 μg L^{-1}) were within the range of 86–101%, confirming the good accuracy and usefulness of the developed FLA-APGD-OES method.

Received 11th September 2020
Accepted 10th November 2020

DOI: 10.1039/d0ja00401d

rsc.li/jaas

1. Introduction

Bismuth is considered as an environmentally significant element, due to numerous applications of its compounds in different areas, which include: semiconductors, cosmetics and medicine production as well as chemical and metallurgical industries. The increasing use of Bi in the abovementioned areas augments its environmental distribution and the organism exposure to this element.[1,2] Additionally, a great number of toxic effects related to Bi compounds have been reported.[3] For all of the aforesaid reasons, Bi is widely determined in medicines,[4,5] human hair,[6,7] urine,[8,9] soil,[10,11] sediments,[12,13] different water samples,[14,15] and food samples.[16,17]

Several spectrometric methods have been applied to Bi determination, *e.g.*, atomic absorption spectrometry (AAS),[6,12] hydride generation atomic absorption spectrometry (HG-AAS),[11,18] hydride generation atomic fluorescence spectrometry (HG-AFS),[2,8] inductively coupled plasma optical emission spectrometry (ICP-OES),[19,20] hydride generation inductively coupled plasma optical emission spectrometry (HG-ICP-OES),[21,22] hydride generation microwave induced plasma optical emission spectrometry (HG-MIP-OES),[23,24] and inductively coupled plasma mass spectrometry (ICP-MS).[10,25] The aforesaid commercially available techniques are valued for providing good selectivity, sensitivity, low detection limits (DLs), high precision and trueness as well as the possibility of performing multi-element analysis. However, a number of disadvantages have been recognized in regard to the application of these methods, *e.g.*, bulky and complex instrumentation, and high power and gas consumption, resulting in high operating costs.

To overcome these disadvantages, the attention of many researchers has been directed to the development of miniaturized excitation sources which would provide a similar or better analytical performance at low costs and reduced power and gas consumption, concurrently requiring a simplified device design.[26,27] Among numerous systems proposed for the time being,[27–32] discharges generated in contact with flowing solutions enjoy a special interest. They provide a simple design, and operation at a low power (<100 W) and often in an open to air atmosphere (no discharge gas is required) as well as the transport of analytes directly from a sample solution, which eliminates the need for nebulizers or spray chamber application. All of this results in notably reduced operation costs, contemporaneously offering sensitivity and detectability comparable to or better than those obtained with conventionally used bulky instruments.[33–35]

Wroclaw University of Science and Technology, Faculty of Chemistry, Division of Analytical Chemistry and Chemical Metallurgy, Wybrzeze Stanislawa Wyspianskiego 27, 50-370 Wroclaw, Poland. E-mail: monika.gorska@pwr.edu.pl

† Electronic supplementary information (ESI) available. See DOI: 10.1039/d0ja00401d

Surprisingly, there are only a few reports of such microplasma systems being applied in the quantitative determination of Bi. They include the following techniques: hydride generation dielectric barrier discharge atomic fluorescence spectrometry (HG-DBD-AFS),[36] hydride generation dielectric barrier discharge atomic absorption spectrometry (HG-DBD-AAS),[37] hydride generation point discharge optical emission spectrometry (HG-PD-OES),[38] solution anode glow discharge atomic emission spectrometry (SAGD-AES),[39] and hydride generation flowing liquid anode atmospheric pressure glow discharge optical emission spectrometry (HG-FLA-APGD-OES).[40] It is noteworthy that the majority of the aforesaid techniques employ the HG technique. Although the application of the HG reaction enhances the sensitivity and improves the transport efficiency of analytes, it is well known that this method suffers from interference in the liquid phase coming from the sample matrix and significant memory effects. In addition, it requires the use of a toxic and unstable reducing agent and the pre-reduction step is often needed in real sample analysis to obtain lower oxidation states of elements.[41–43]

The last from the above listed techniques, *i.e.*, SAGD, known also as flowing liquid anode atmospheric pressure glow discharge (FLA-APGD),[44] was repeatedly proven to be a promising tool for highly sensitive determination of Ag, Bi, Cd, Hg, In, Pb, Tl, and Zn.[39,44–46] It offers high precision, wide linearity ranges, good trueness, and DLs of the above-mentioned analytes improved up to 3 orders of magnitude in comparison with those achievable with other microplasma techniques as well as commercially available instruments, such as ICP-OES. Very recently, Bi was successfully determined by two independent research groups using the FLA-APGD excitation source combined with OES detection. In the first case,[40] the obtained DL of Bi was 0.8 μg L^{-1}; however, in this approach the HG technique was applied. On the other hand, Yuan *et al.*[39] proposed a simplified design for the SAGD device but the DL obtained in this work was over two times higher, *i.e.*, 2.0 μg L^{-1}.

Therefore, the aim of this work was to improve the sensitivity and detectability of Bi determination by the FLA-APGD-OES method, but without applying the HG technique. To reach this goal, the optimization of crucial working parameters was performed at first. Afterwards, the influence of the addition of low molecular weight organic compounds (LMWOCs) on the signal intensity of Bi was investigated. Under optimal operating conditions, the analytical performance of the FLA-APGD-OES method (in terms of the DL of Bi, the linearity range of the calibration curve, and the precision of measurements) was evaluated. Moreover, the effect of the selected foreign ions on the signal intensity of Bi was evaluated and the analysis of the selected water samples was carried out. Additionally, the optimization, the evaluation of the analytical performance and the study of the effect of the addition of LMWOCs were also conducted for flowing liquid cathode atmospheric pressure glow discharge (FLC-APGD) sustained and operated in the discharge system similar to FLA-APGD. The results attained for both methods were compared and discussed comprehensively.

2. Experimental

2.1. Instrumentation

A schematic drawing of the FLA-APGD system is presented in Fig. 1. The FLC-APGD system was almost the same but differed from the FLA-APGD system only in electrode polarization and a sample inlet tube construction. In both cases, the discharge was sustained in an open-to-air chamber between a tungsten nozzle (OD/ID 3/1 mm, length 50 mm) and a vertically oriented quartz tube (OD/ID 4/2 mm). In the case of the FLA-APGD system, the electrical contact was provided directly to the tungsten nozzle and with the aid of a platinum spiral wrapped around the quartz tube. In the case of the FLC-APGD system, a graphite tube (OD/ID 6/4 mm, length 20 mm) was inserted into the quartz tube to provide appropriate electrical contact and stabilize solution surface formation. The sample solutions acidified with HCl or HNO_3, which served as either the anode or the cathode, were pumped through the quartz tube by means of a 3-channel REGLO ICC peristaltic pump (Ismatec, USA) at a flow rate up to 4.5 mL min^{-1}. As the solution reached

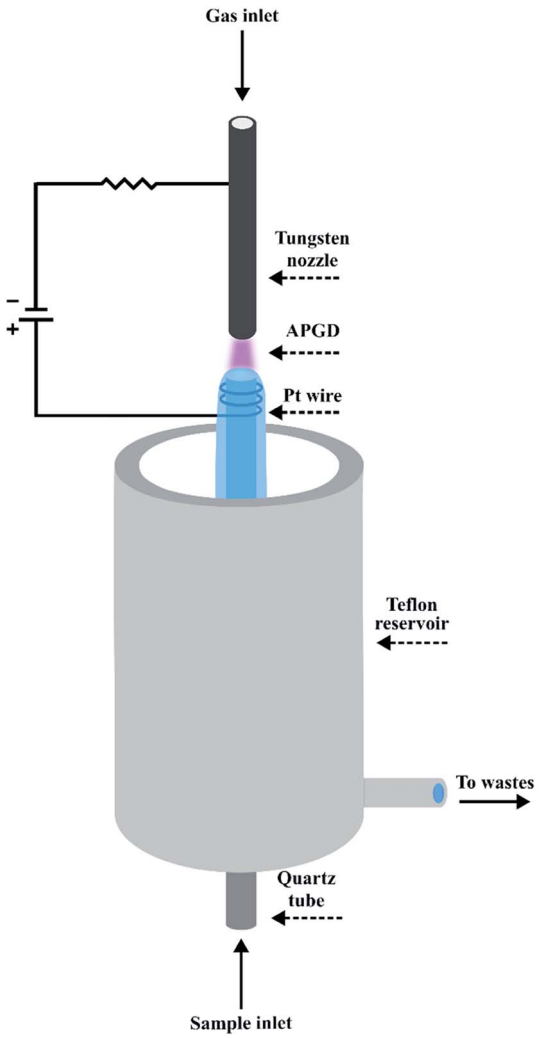

Fig. 1 A schematic drawing of the FLA-APGD system.

the top of the quartz tube it flowed down to a PTFE reservoir, from which it was pumped out. The tungsten nozzle was fed with He at a flow rate up to 350 mL min^{-1}, which was controlled using an FC-2900 flow controller and an RO-28 digital flow meter (Tylan General, USA). The distance between the solution surface and the anode/cathode nozzle was set in the 1–5 mm range.

A voltage of 800–1200 V was applied to both electrodes by a HV DC power supply (model DP50H-024PH, DSC-Electronics, Germany). Its exact value depended on the applied He flow rate, the discharge current, and the acid concentration. To stabilize the discharge, a 2.2 kΩ (FLA-APGD) or 6.9 kΩ (FLC-APGD) ballast resistor was connected into the circuit.

The radiation emitted by APGD was imaged (1 : 1) on the entrance slit (10 μm) of a Shamrock 500i imaging spectrometer (Andor, UK), using an achromatic quartz lens (f = 80). The spectrometer was equipped with a holographic grating (1800 lines per mm) and a Newton DU-920P-OE UV-Vis CCD camera (Andor, UK). The integration time was 10 s during all experiments and the intensities of atomic emission lines of Bi were background corrected.

2.2. Reagents and sample preparation

Deionized water (18.2 MΩ cm^{-1}) from an Easypure water purification system (Thermolyne Corp., USA) was used throughout the study. All chemicals were at least of analytical grade. He of 99.999% purity was supplied by Air Products (Poland). Stock standard solutions of Ag, Bi, Ca, Cu, Fe, Hg, K, Mg, Mn, Na, Pb, Sn, and Zn (1000 mg L^{-1}), obtained from Sigma-Aldrich (Germany), were utilized to prepare all working standard solutions. Solutions of methanol (100%), ethanol (96%), and formic acid (85%), applied for the investigation of the influence of organic compounds on the signal intensity of Bi, were provided by Avantor Performance Materials (Poland). To acidify the FLA/FLC solutions, concentrated HNO_3 (65% m m^{-1}) or HCl (37% m m^{-1}) solutions (Merck, Germany) were employed.

Mineral water was purchased from a local store. Bystrzyca river water (sampled in the city of Swidnica, Poland) and municipal tap water (Wroclaw, Poland) were collected into pre-cleaned 1 L PE bottles. River water was initially filtered through cellulose filter paper (grade 595) and subsequently acidified with concentrated HNO_3 to reach its final concentration of 0.015 mol L^{-1}.

A portion of 10.0 g of each water sample was transferred into a twist cup container. The samples of mineral and tap waters were then acidified with concentrated HNO_3, spiked with the stock standard of Bi, and subsequently filled with deionized water to the final mass of 30.0 g. The resulting concentrations of HNO_3 and Bi were 0.005 mol L^{-1} and 100 μg L^{-1}, respectively. Such prepared sample solutions were divided into three separate parts and the standard addition was performed on the last two of them. All the above-mentioned water samples were prepared in triplicate; besides, appropriate procedural blanks were prepared and considered in the final results.

3. Results and discussion

3.1. Identification of the emission lines of Bi

Initially, in order to identify the emission lines of Bi, a solution containing 10 mg L^{-1} of this element, acidified with 0.01 (FLA-APGD) or 0.1 (FLC-APGD) mol L^{-1} HNO_3, was prepared. The measurement conditions were as follows: a discharge current of 50 mA, a He flow rate of 300 (FLA-APGD) or 50 (FLC-APGD) mL min^{-1}, and a sample flow rate of 3.5 mL min^{-1}. The emission spectrum was recorded in the 200–280 nm range, for both the investigated discharge systems (see Fig. SI-1†).

Table 1 presents the values of the signal to background ratio (SBR) for all acquired atomic emission lines. Although 8 of such lines were identified in the FLA-APGD spectrum, the sensitivity of most of them was rather poor (except for Bi 223.1 nm). In the case of FLC-APGD, a weak emission from the resonance line of Bi (223.1 nm) as well as three other lines at 202.1 nm, 206.2 nm, and 262.8 nm was noted. The obtained results are in line with the outcomes reported in other studies, concerning FLA- and FLC-APGD systems, indicating that only a few most prominent atomic lines are observed for most of the elements.[44,47] Based on the received signal intensities of Bi for the studied discharge systems, it could be expected that FLA-APGD would provide much better excitation conditions for Bi (because of lower saturation of the discharge gas with water vapor), as compared to FLC-APGD. The enhanced transport of Bi can contribute to its improved analytical response as well; the efficiency of the volatile species generation of Bi in the case of FLA-APGD is much higher than the transport of this element through the solution sputtering in the case of FLC-APGD. Previously, such a difference was reported for other elements, specifically Ag, Cd, Pb, Tl, and Zn.[44] It is also noteworthy that the background intensity in the whole studied spectral range was perceptibly lower (up to 21 times) for the FLC-APGD system. A similar observation was also previously made in both above cited studies. This is likely due to increased water evaporation into the FLC-APGD system (by about 3–4 times, as compared to FLA-APGD),[44,48] leading to a limited diffusion of the surrounding air into the discharge phase. As a result, the emission from molecular bands such as NO in the investigated spectral range was lowered.

Table 1 Atomic emission lines of Bi identified in the spectra of the FLA-APGD and FLC-APGD systems with the corresponding signal to background ratios (SBRs)

Line (nm)	Excitation energy [eV]	SBR[a]
202.1	6.13	0.67/0.09
206.2	6.01	14.3/0.23
211.0	5.87	1.55/ND
223.1	5.56	46.3/0.92
227.7	5.44	9.41/ND
262.8	4.71	6.21/0.33
269.7	4.59	1.12/ND
278.0	4.45	1.02/ND

[a] The SBR obtained for FLA-APGD/and FLC-APGD. ND – not detected.

As the SBR of the resonance line of Bi (223.1 nm) was 3–69 times higher than that for the other lines in both APGD systems, this atomic line was considered in all subsequent experiments.

3.2. Optimization of working parameters

In order to successfully use the proposed APGD excitation sources for Bi determination by OES, it was necessary to optimize the most influential operating parameters. The following ones were identified to have a significant impact on the emission from Bi atoms: the acid type (HCl, and HNO_3), the acid concentration (0.001–0.01 mol L^{-1} for FLA-APGD and 0.01–0.1 mol L^{-1} for FLC-APGD), the discharge current (30–70 mA), the He flow rate (50–350 mL min^{-1}), the sample flow rate (1.0–4.5 mL min^{-1}), and the discharge gap (1–5 mm). Optimization was performed using either a Bi standard solution of 300 μg L^{-1} (for FLA-APGD) or a Bi standard solution of 10 mg L^{-1} (for FLC-APGD). If not stated otherwise, the measurement conditions were as follows: a discharge current of 50 mA, a He flow rate of 350 mL min^{-1}, a sample flow rate of 3.5 mL min^{-1}, and the discharge gap set to approximately 1 mm.

3.2.1. The effect of the acid type and its concentration. The influence of the acid type on the obtained SBR in the case of the FLA-APGD system was studied using freshly prepared sample solutions of Bi acidified with HNO_3 or HCl, both at a concentration of 0.01 mol L^{-1}. When HCl was used, the attained SBR was 35% lower (as compared to that obtained for HNO_3), which likely resulted from the formation of insoluble species of BiOCl (for more details, see Comment SI-1 in the ESI†). Taking this into account, the effect of the acid type was not further investigated in the FLC-APGD system, and HNO_3 was applied to acidify all sample solutions in the subsequent experiments.

As for the FLA-APGD system, the influence of the HNO_3 concentration was studied in the range of 0.001–0.01 mol L^{-1}. It was established that when the lower acidification of the introduced solutions was employed, poorer discharge stability was observed. As the acid concentration was equal to 0.001 mol L^{-1}, it was impossible to ignite the discharge; likely due to the insufficient solution conductivity. In the case of the FLC-APGD system, it is expected that the acid concentration in the analyzed solution needs to be higher than this for the FLA-APGD system.[44,49] Hence, for FLC-APGD, the investigated HNO_3 concentrations ranged between 0.01 and 0.1 mol L^{-1} (lower and higher acid concentrations than given destabilized the discharge).

The highest emission from Bi was observed at HNO_3 concentrations of 0.005 mol L^{-1} and 0.1 mol L^{-1}, respectively for the FLA-APGD and FLC-APGD systems (see Comment SI-2†). For both studied systems, as the acid concentration increased, the background intensity slightly dropped (less than 10% over the whole studied ranges), hence the fluctuations in SBRs resulted predominantly from the changes in the Bi signal intensities (see Fig. SI-2 and SI-3†). As a result, the maximum SBRs were obtained at 0.005 mol L^{-1} and 0.1 mol L^{-1}, for FLA- and FLC-APGD, respectively (see Fig. 2).

The results obtained for the FLC-APGD system are in good agreement with other literature data,[50,51] reported for that system, indicating that the signal intensities of different elements decreased with lowering sample acidification. For this system, it was proved[52,53] that at a high acid concentration, the cathode voltage drop is reduced, leading to the enhanced recombination of the sputtered element species with the electrons and hence, increasing their transport efficiency into the discharge.

Concerning the results obtained for the FLA-APGD system, their clarification is more troublesome due to a much smaller number of studies devoted to this excitation source. Similar observations regarding the changes in the signal intensity of the analytes with the increasing acid concentration were made by Liu *et al.* for Cd and Zn (regardless of the kind of acid used, *i.e.*, HCl or HNO_3)[45] and Greda *et al.* for Ag, Cd, Pb, Tl, and Zn (in HNO_3 media).[54] A supposed reason for the decrease of the Bi signal intensity (with the increase of the acid concentration) was likely the scavenging of the solvated electrons by H_3O^+ ions present in the FLA solution (see Comment SI-3†).[48]

Regardless of the specific reason for the observed effect of HNO_3, acid concentrations of 0.005 mol L^{-1} (for FLA-APGD) and 0.1 mol L^{-1} (for FLC-APGD) offered the highest SBRs, and hence they were applied in further experiments.

3.2.2. The effect of the discharge current and the He flow rate. As was shown in our previous paper,[54] the influence of the

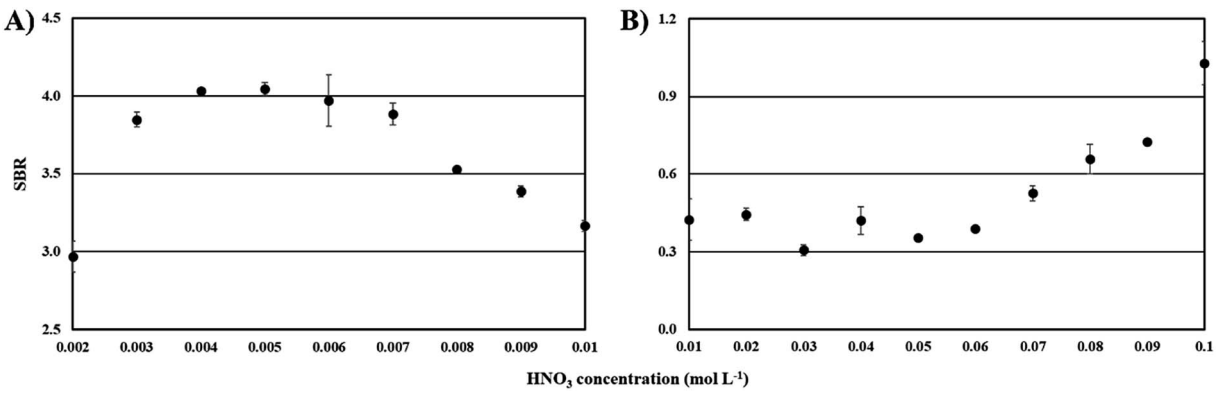

Fig. 2 The effect of the acid concentration on the SBR for Bi in the case of the FLA-APGD (A) and FLC-APGD (B) systems.

discharge current on the response of analytes is dependent on the He flow rate and *vice versa*. The preliminary studies performed in this work led us to a conclusion that this could be also the case regarding Bi. For that reason, the discharge current and the He flow rate were optimized simultaneously. The He flow rate was changed in the range of 50–350 mL min^{-1}, while the discharge current range was quite narrow, *i.e.*, 30–70 mA, since lower and higher discharge currents destabilized the discharge. The FLA- and FLC-APGD systems could be stably operated at discharge currents above 70 mA using more acidified solutions (in the case of FLA-APGD) or higher He flow rates (FLC-APGD). However, the preliminary study showed that the signal intensity drop of Bi, caused by the enhanced HNO_3 concentration or He flow rate, was not compensated by the higher discharge currents. For that reason, the discharge currents above 70 mA was not investigated in detail.

It was repeatedly shown in the literature[44,45,54–57] that the increase of the discharge current leads to a linear enhancement of the signal intensity of analytes in the case of both FLA- and FLC-APGD systems. This signal intensity enhancement of elements is usually associated with a more efficient introduction of the analytes into the discharge.[54] That being so, unsurprisingly, an enhancement of the Bi signal intensity (over the whole studied range) was observed in this work as well, for both investigated systems. A linear rise in the background intensity was observed as the discharge current increased (for both the FLC- and FLA-APGD system). The only small exception occurred for the FLA-APGD system operated at He flow rates ≤100 mL min^{-1} (see Comment SI-4†). In regard to the effect of the He flow rate in the case of FLA-APGD, the higher the gas flow rate, the higher the analytical signal observed. This signal enhancement was especially remarkable for the discharge system operating at currents exceeding 50 mA. In contrast to FLA-APGD, for FLC-APGD the maximum response from Bi was noted at lower He flow rates, *i.e.*, 100–150 mL min^{-1}. These observations are in agreement with the previous ones,[58] and may result from a hindered diffusion of the analyte atoms into the discharge phase at a stronger He atom flux used.

As for the background intensity, it was increasing over the whole range of the He flow rates, regardless of the discharge current applied, in both the studied systems. Noteworthily, the background intensity enhancement for FLA-APGD was remarkably higher as compared to that observed for FLC-APGD (see Comment SI-5†). All of this resulted in receiving the SBR patterns presented in Fig. 3 (see Comment SI-6†). In the case of the FLC-APGD system, the discharge current and the He flow rate corresponding to the highest SBR obtained were 50 mA and 50 mL min^{-1}, respectively. These settings were used in subsequent experiments. As for FLA-APGD, the best results were obtained at a discharge current of 70 mA. However, at 60 mA the discharge seemed to be more stable and for that reason the discharge current of 60 mA and a He flow rate of 350 mL min^{-1} were applied in the following experiments.

3.2.3. The effect of the sample flow rate. The sample flow rate is an important factor when element determination is performed in discharge systems with overflowing solutions, as

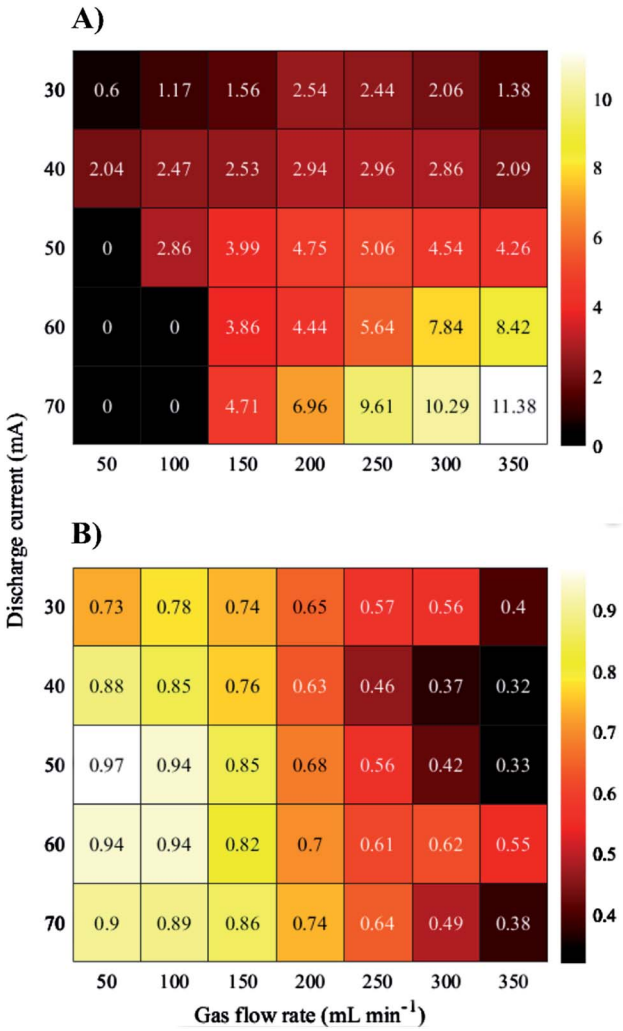

Fig. 3 The effect of the discharge current and the gas flow rate on the SBR for Bi. (A) FLA-APGD, and (B) FLC-APGD. "0" indicates the parameter combination at which the discharge was unstable and measurements could not be carried out.

they provide electrical contact. The solution flow rate cannot be too low because its discontinuous overflow destabilizes the discharge. On the other hand, it should not be too high to avoid much sample consumption. Taking this into account, the effect of the solution flow rate was investigated in the range of 1.0–4.5 mL min^{-1}. In regard to FLA-APGD, it could be maintained over the whole studied range of the solution flow rates; however, its lower stability was noted when the solution was flowing at 1.0–1.5 mL min^{-1}. As for FLC-APGD, it could be stably operated only from the sample flow rate starting at 2.0 mL min^{-1}. This could be related to water evaporation, which was previously established to be 3 times greater for FLC-APGD than in the case of FLA-APGD.[44] In such a case, the higher sample consumption would result in a discontinuous solution overflow in the FLC-APGD system.

Considering the FLA-APGD system, the signal intensity of Bi was increasing as the solution flow rate was enhanced up to 3.5 mL min^{-1} and then reached a *plateau*. A quite similar

observation was made by other researchers dealing with FLA-APGD.[55] It is likely that by increasing the solution flow rate the amount of Bi volatile species released from the analyzed sample increased. Moreover, it was found that by increasing the solution flow rate (in the range of 2.0–4.5 mL min^{-1}) the water evaporation rate declined from 26% to 9%. As a result, the saturation of the discharge gas phase with water vapor is lower, yielding improved excitation conditions. In regard to FLC-APGD, the signal intensity of Bi reduced by 29% as the sample flow rate increased from 2.0 up to 4.5 mL min^{-1}. The received outcomes are in good agreement with the results obtained previously for other elements, such as Ca, Cd, Cu, Mg, and Zn.[47,59,60] The reliable explanation for these observations has not been given up to now, and a more detailed study is needed.

Regarding the background intensity, its apparent drop was noted for both the studied discharge systems, *i.e.*, 24% (for FLA-APGD) and 17% (for FLC-APGD), when the solution flow rate increased from the lowest studied value up to 4.5 mL min^{-1}.

The abovementioned changes in the signal and background intensities are charted in Fig. SI-2 and SI-3† and resulted in obtaining the SBRs given in Fig. 4A and B. In the case of the FLA-APGD system, although the highest SBR was obtained for a solution flow rate of 4.5 mL min^{-1}, the differences in the SBR values obtained between 3.5 and 4.5 mL min^{-1} were negligible. Considering the need for lowering the sample consumption, a sample flow rate of 3.5 mL min^{-1} was used in all subsequent experiments. In regard to the FLC-APGD system, although the highest signal intensity of Bi was acquired at a sample flow rate of 2.0 mL min^{-1}, the discharge stability and the measurement precision were poor under these conditions. Therefore, the sample flow rate of 3.0 mL min^{-1} was applied in further experiments.

3.2.4. The effect of the discharge gap. The effect of the discharge gap on the SBR of Bi for both the FLA- and FLC-APGD systems was investigated in the range of 1–5 mm. The highest emission from Bi was observed when discharge gaps were 2.5 mm and 1.0 mm, respectively for FLA- and FLC-APGD systems (see Comment SI-7†). Regarding the background intensity, it was increasing as the discharge gap was increasing, in both the investigated systems (see Fig. SI-2 and SI-3†). Noteworthily, the observed increase of the background level was much higher for the FLA-APGD system (see Comment SI-7†). Intuitively, one could expect that the increase of the discharge gap should lead to the boosted intensity of both the atomic lines and the background – as a result of the radiation imaging from a greater area. Indeed, that seemed to be the case for the background intensity; however, for the atomic emission line of Bi such a behavior was noted only in the case of the FLA-APGD and only when the discharge gap increased up to 2.5 mm. The

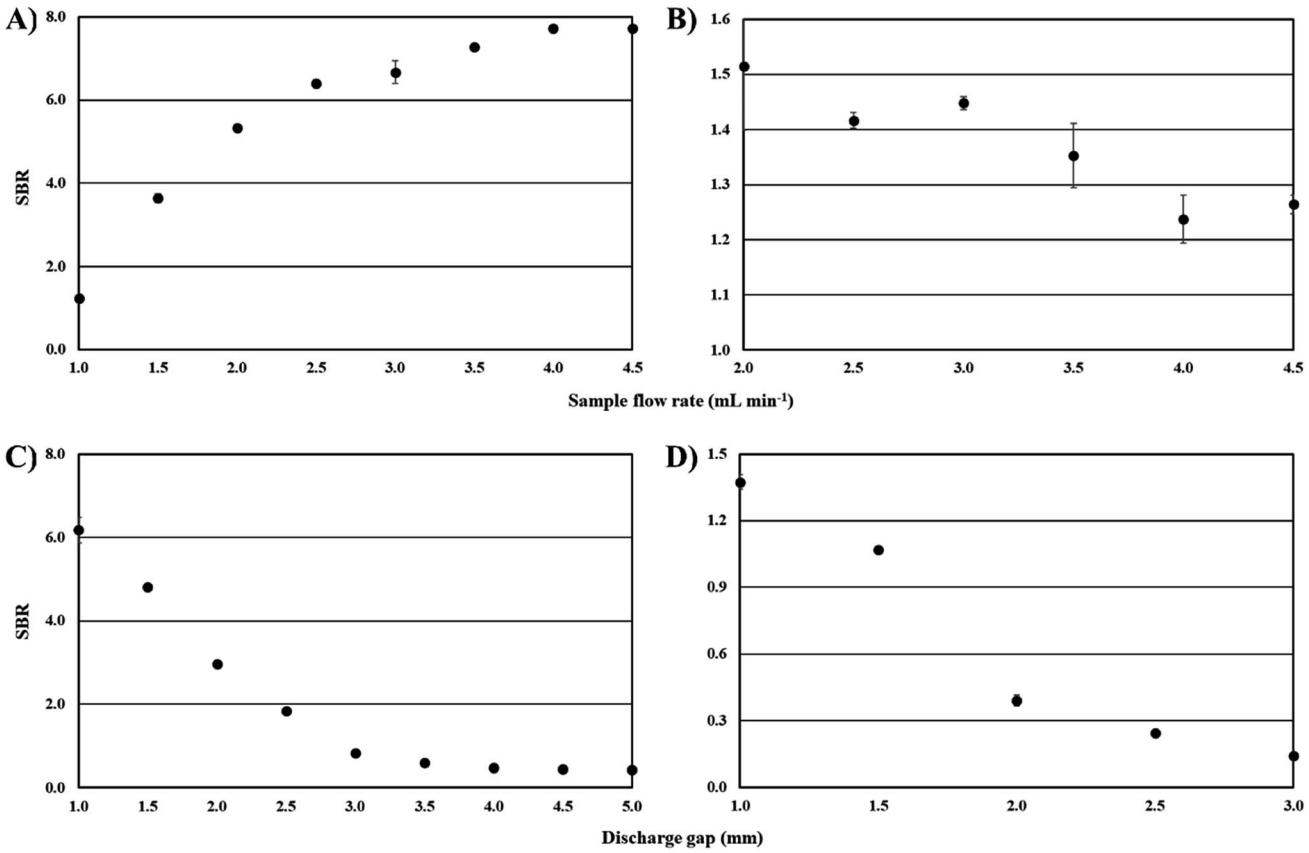

Fig. 4 The effect of the sample flow rate and the discharge gap on the SBR for Bi in the case of the FLA-APGD (A and C) and FLC-APGD (B and D) systems.

background level enhancement resulted not only from the imaging from a greater area of the discharge but also due to the higher intensity of the NO molecular bands. Boosted emission from NO molecules could be the effect of higher amounts of the surrounding air being diffused into the plasma at higher discharge gaps.

Considering the outcomes for the Bi emission line, their explanation is much more troublesome. It seems unlikely that the increasing discharge gap deteriorated the efficiency of the Bi volatile species generation. In that case, the only suspected reason for the observed suppression in the Bi emission (with the increasing discharge gap) is impaired atomization/excitation conditions. There are only residual data on the effect of the discharge gap on the microplasma performance (both in the case of FLA- and FLC-APGD), and what is worse, they unanimously indicate that with the discharge gap expansion, the spectroscopic temperatures increase,[54,56,59] which rather improves the atomization/excitation conditions. Undoubtedly, to make a plausible hypothesis explaining the influence of the discharge gap on the signal intensity of Bi, a more-in-depth study would be necessary.

Nevertheless, the SBRs were highest at a discharge gap of 1 mm (see Fig. 4C and D), regardless of the studied system, which in both cases was a consequence of the rapid growth of the background intensity with increasing gap. Therefore, the discharge gap of 1 mm was chosen for further experiments.

3.3. The effect of foreign anions

In order to investigate the endurance of the FLA-APGD-OES method to the interference from concomitant elements, the effect of the presence of Ag, Ca, Cu, Fe, Hg, K, Mg, Mn, Na, Pb, Sn, and Zn on the signal intensity of Bi was assessed. Each of the potentially interfering elements was added separately to a single-element solution of Bi. The concentration of Bi was equal to 0.5 mg L^{-1}, whereas the concentration of the concomitant elements was either 1 or 10 mg L^{-1}. The same effect for the FLC-APGD-OES method was not studied due to the low signal intensity of Bi at its concentration of 10 mg L^{-1}.

The results are presented in Fig. 5. It was found that the addition of Fe, Mn, Pb, and Sn at a concentration being only two times higher than the analyte content (*i.e.*, 1 mg L^{-1}), strongly lowered the recovery of Bi (ranging from 26% in the case of Sn to 77% in the case of Pb). The impact of the remaining metals (at the same concentration) was less significant and the recoveries obtained in their presence ranged between 81% for K to 103% for Cu. As for the concomitant elements at a concentration of 10 mg L^{-1}, their negative influence was apparently stronger; the obtained recoveries of Bi ranged from 11% (in the presence of Sn) to 75% (for Mg). Surprisingly, alkali and alkaline earth metals seemed to have a minor impact on the signal intensity of Bi, as compared to the remaining metals at a concentration of 10 mg L^{-1}. It was previously shown that the presence of Ca, Mg, Na, and K at a concentration similar to the one investigated herein influenced the recoveries of other analytes, *i.e.*, Ag, Cd, Hg, In, Pb, Tl, and Zn, in a greater degree than other studied interferents, *e.g.*, Al, Cu, Cd, Pb, Fe, and Mn.[54,55,61] Very recently, Greda *et al.*[61] proved that matrix effects in the FLA-APGD system results from the decreased efficiency of the volatile species generation (in the presence of foreign ions). Moreover, they noticed that the highest ionic radius of the concomitant element showed the greater interfering effect. Herein, a similar correlation between the degree of matrix effects and the ionic radius of the interfering element was not observed. The elements that affected the response of Bi to the greatest extent were not alkali and alkaline earth metals but Sn, Mn, and Fe. The determined matrix effects for Bi were quite similar to those reported in chemical vapor generation (CVG), *e.g.*, in the reaction with sodium tetrahydroborate (THB), where transition metals are considered to have a more adverse effect as compared to alkali metals.[62] This observation indicates that the mechanism of Bi volatile species generation (assisted by FLA-APGD) likely differs from that of Ag, Cd, Hg, Pb, Tl, and Zn.

Nevertheless, it was revealed that the presence of different elements in a sample solution is a serious limitation for the investigated method. Therefore, the standard addition method

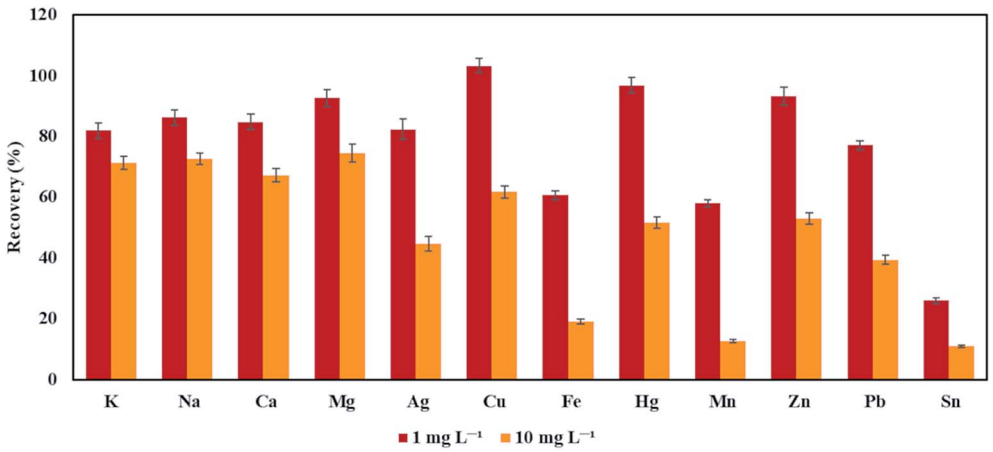

Fig. 5 The effect of the foreign ions (at concentrations of 1 and 10 mg L^{-1}) on the recovery of Bi.

or selected separation techniques should be applied in order to eliminate the matrix effects.

3.4. The effect of the addition of low molecular weight organic compounds

Low molecular weight organic compounds (LMWOCs), such as methanol, ethanol, formic acid, and acetic acid, are known to intensify the signals of the analytes and lower their DLs in the FLC-APGD-OES method.[34] As for the FLA-APGD system, the effect of LMWOCs was investigated only twice.[46,48] Greda *et al.*[46] found that the presence of methanol and ethanol remarkably enhanced the signal intensity of In, over 30 times at an alcohol concentration of 0.5%. However, in the case of other elements, *i.e.*, Ag, Cd, Hg, Pb, Tl, and Zn, the addition of the studied alcohols either did not result in apparent signal intensity improvement or even suppressed the response (Ag and Pb). Also Swiderski *et al.*[48] investigated the influence of LMWOCs on the signals intensity of Ag, Cd, and Pb in FLA-APGD-OES, and they found that under the optimized conditions it was possible to boost the emission from Ag, Cd, and Pb up to 5-fold.

Neither in FLA- nor in FLC-APGD systems, the influence of LMWOCs on the response of Bi has been investigated so far. Therefore, the effect of the addition of methanol, ethanol, and formic acid, in the concentration range of 0.1–10%, was investigated herein in both the studied systems. The concentration of Bi in the solution was 0.5 mg L^{-1} (FLA) and 10 mg L^{-1} (FLC). Table 2 shows the relative intensities of the Bi signal in the presence of the studied organic media (calculated in reference to the signal obtained for the solution without any organic additives). In the case of FLA-APGD, it was found that the presence of all studied organic media significantly reduced the signal intensity of Bi (around 1 order of magnitude). The highest intensity drop occurred as the concentration of LMWOCs increased in the range of 0–1%, and above 1%; the analytical response was approximately constant. Concurrently, the background intensity in the presence of LMWOCs was roughly constant. Small exceptions occurred in the case of methanol and ethanol; as their concentrations increased in the range of 1–10%, the background intensity increased by 11% and 48%, respectively. Considering the FLC-APGD system, the signal intensity of Bi was significantly higher in the presence of the studied LMWOCs (especially formic acid). For the investigated alcohols, the maximum analytical response occurred as the concentrations of methanol and ethanol were 1% and 5%, respectively. In both cases, the factor of intensity enhancement was roughly 1.8. Even higher improvement of the analytical response, *i.e.*, 10-fold, was observed as formic acid was added in the concentration ranging from 3% to 10%. The impact of LMWOCs on the background intensity was similar to the one observed for the FLA-APGD system. In the presence of methanol and ethanol, the background intensity did not significantly change up to their concentration of 1% and afterward, it increased by 20% or 2-fold for methanol and ethanol, respectively. In the case of formic acid, it remained constant over the whole examined concentration range.

Table 2 The effect of the addition of low molecular weight organic compounds (at concentrations 0.1–10%) on the relative intensity of Bi

Organic compound	Concentration (%)	Relative intensity (a.u.) FLA-APGD	FLC-APGD
Methanol	0.1	0.30	1.30
	0.3	0.14	1.39
	0.5	0.07	1.50
	1	0.07	1.75
	3	0.06	1.18
	5	0.07	0.74
	10	0.09	—[a]
Ethanol	0.1	0.33	1.07
	0.3	0.16	1.17
	0.5	0.11	1.26
	1	0.09	1.34
	3	0.09	1.47
	5	0.10	1.81
	10	0.10	—[a]
Formic acid	0.1	0.11	0.96
	0.3	0.03	1.47
	0.5	0.10	2.65
	1	0.18	6.98
	3	0.15	10.2
	5	0.13	10.2
	10	0.09	9.74

[a] Not measured due to the discharge instability.

Additionally, in the spectra of both discharges, the CO bands (the fourth positive $A^1\Pi \rightarrow X^1\Sigma$ system) and the CO^+ bands (the first negative $B^2\Pi \rightarrow {}^2\Sigma$) were observed (see Fig. SI-4†), which proves that the LMWOCs were decomposed and transported into the discharge in both the systems. As can be seen from this figure, although the intensity of these bands was roughly equal, they were much more noticeable in the FLC-APGD spectrum. This is due to a significantly lower emission from the NO molecules for this discharge system. Thus, in the vicinity of the Bi atomic emission line there were mainly the CO bands (FLC-APGD) and the CO bands overlapped by the NO bands (FLA-APGD). Therefore, the increase of the background intensity for the FLC-APGD system in the case of the increased alcohol concentration was directly related to the increase in the emission from the CO and CO^+ bands.

Considering the impact of the studied organic additives on the response of the analytes, it was repeatedly suggested that their signal intensity enhancement, observed for the FLC-APGD systems, could be a result of a change in the boiling point, the surface tension and/or the viscosity of the FLC solutions.[58,63,64] However, in such a case, a similar effect would also be expected in the case of the FLA-APGD system, which apparently was not a case herein. Moreover, it was previously established that the boiling point changes of water mixtures with methanol, ethanol, and formic acid (at concentrations similar to those used in this work) are negligible.[65]

The observed differences in the influence of the LMWOCs on the signal intensities of Bi in both the studied systems could be clarified regarding the mechanisms of the analyte transport in these discharges. As for FLA-APGD, it is believed that it takes place by analyte reduction with the solvated electrons in the

liquid phase, leading to form some kind of volatile species, which are then transported into the discharge.[44,48] In such a case, a likely reason for lowering the Bi signal intensity in the presence of the LMWOCs could be the scavenging of solvated electrons by these compounds in the liquid phase, yielding the lowered efficiency of the volatile species generation.[48] In the case of the FLC-APGD, the analytes are transported to the plasma phase most likely by cathode sputtering. It is suspected that in the presence of LMWOCs, organic radicals (*e.g.*, $^{\bullet}CO_2^-$, $^{\bullet}CO_2H$, and $^{\bullet}CH_2OH$) are additionally formed, and they could improve the transport efficiency of Bi by the formation of some volatile species. The confirmation of this theory could be the results obtained by Doroski *et al.*,[63] indicating that the addition of LMWOCs enhances the signal intensity of elements forming the volatile species (*e.g.*, Ag, Hg, Pb, and Se) to a higher degree. Although it would then be expected to observe the same effect for FLA-APGD, the scavenging of the solvated electrons by the added LMWOCs could be the predominant effect. Bearing all this in mind, the addition of LMWOCs was no longer used in further studies on the FLA-APGD system.

3.5. Analytical performance and sample analysis

The analytical performance of the studied systems, *i.e.*, FLA- and FLC-APGD, on the determination of Bi by OES detection was evaluated under the optimized conditions, as summarized in Table 3. Additionally, the analytical performance with the addition of 5% formic acid for the FLC-APGD system was also established. For this purpose, the DLs of Bi, the extent of linearity of the calibration curves, and the precision were determined. Instrumental DLs were calculated to be $3\sigma/a$, where "3σ" stands for 3 times the standard deviation of 30 consecutive measurements of an appropriate blank solution, and "a" stands for the sensitivity of a corresponding calibration curve. The linearity extents were examined using 9 (for FLA-APGD-OES) or 7 (for FLC-APGD-OES) single-element standard solutions in concentration ranges of 0.01–1 mg L^{-1} (FLA-APGD), 10–100 mg L^{-1} (FLC-APGD without formic acid) or 1–10 mg L^{-1} (FLC with the addition of 5% formic acid). The precision was expressed as the relative standard deviation (RSD) for 10 consecutive measurements of the standard solutions. The RSD was measured 3 times for each method and the averaged results were given. The concentration of Bi for the precision measurements was as follows: 30 μg L^{-1} for FLA-APGD, 10 mg L^{-1} for FLC-APGD without the addition of formic acid, and 1 and 10 mg L^{-1} for FLC-APGD with the presence of 5% formic acid in the FLC solution.

Table 4 exhibits the abovementioned figures of merit achieved by the proposed methods. It is noteworthy that the addition of 5% formic acid allowed lowering the DL of Bi over 8 times, in the case of the FLC-APGD system. It was established that the presence of formic acid did not influence the background fluctuations and their level, and therefore the lowered DL of the element was the result of the improved sensitivity. However, the DL obtained with the aid of the FLA-APGD system was incomparably better, being almost 100 times lower than the one obtained for the FLC-APGD system when formic acid was added to the solution and over 800 times better, as compared to conditions without the additive of the organic media. The achieved DLs of Bi were also compared to those reported for other spectrometric methods, constituting both miniaturized plasma excitation sources and conventionally employed bulky plasmas (see Table 5). As can be noticed from this table, each of the presented methods provided significantly better DLs of Bi than that with FLC-APGD. On the other hand, the proposed FLA-APGD excitation source with OES detection assured a better DL than the majority of techniques in which bulky[20,37] and miniaturized plasma sources[38–40] were used. Moreover, the obtained DL of Bi for FLA-APGD-OES was also improved, as compared to DLs of this element achievable with the methods combined with the HG technique,[37,38] including the HG-FLA-APGD-OES method, previously studied by our group.[40] Although, a few of the cited studies[21,23,36] reported better DLs of Bi than the one obtained in this work, the applied methods were premised upon bulky instruments[21,23] and/or required the HG technique.[21,23,36] It is also worth mentioning that – to the best of our knowledge –

Table 3 The optimal operating conditions for the FLA-APGD and FLC-APGD systems

Method	Acid type	Acid concentration (mol L^{-1})	Discharge current (mA)	Gas flow rate (mL min^{-1})	Sample flow rate (mL min^{-1})	Discharge gap (mm)
FLA-APGD	HNO_3	0.005	60	350	3.5	1
FLC-APGD		0.1	50	50	3.0	

Table 4 The analytical performance of the FLA-APGD and FLC-APGD systems combined with the OES detection

Method	Instrumental detection limit (μg L^{-1})	Linearity range[a] (mg L^{-1})	R^2	Sensitivity (a.u. per μg per L)	RSD (%)
FLA-APGD	0.34	0.001–1	0.9968	1301.7	3.76
FLC-APGD	274	0.9–100	0.9988	0.56	2.22
FLC-APGD[b]	33	0.1–10	0.9963	3.60	1.99/0.52[c]

[a] Given as the range between the quantification limit and the highest standard concentration measured in this work (yielding a linear response). [b] With the addition of 5% formic acid to the solution. [c] For Bi concentrations of 1 and 10 mg L^{-1}, respectively.

Table 5 A comparison of the detection limits of Bi obtained for the proposed FLA-APGD-OES and FLC-APGD-OES methods and other spectrometric methods

Method	Detection limit (μg L^{-1})	Reference
FLA-APGD	0.34	This work
FLC-APGD	274/33[a]	This work
SAGD-AES	1.98	39
HG-FLA-APGD	0.85	40
HG-PD-OES	1.0	38
ICP-OES	0.78	20
HG-MIP-OES	0.09	23
HG-ICP-OES	0.16	21
HG-DBD-AFS	0.07	36
HG-DBD-AAS	1.1	37

[a] Without and with the addition of 5% formic acid, respectively. FLA – flowing liquid anode, APGD – atmospheric pressure glow discharge, FLC – flowing liquid cathode; SAGD – solution anode glow discharge, AES – atomic emission spectrometry, HG – hydride generation, PD – point discharge, OES – optical emission spectrometry, ICP – inductively coupled plasma, MIP – microwave induced plasma, DBD – dielectric barrier discharge, AFS – atomic fluorescence spectrometry, and AAS – atomic absorption spectrometry.

the microplasma techniques cited in the table are the only ones by which Bi has ever been determined.

As for the other analytical figures of merit, the precision was established to be <4% for both the studied methods, being slightly better for the FLC-APGD-OES method. Nonetheless, the observed differences in the precision between FLA- and FLC-APGD excitation sources was likely related to the Bi concentrations in the solutions, as the SBRs for Bi were 0.71, 1.09, and 8.52 for FLA-APGD, FLC-APGD and FLC-APGD with the presence of 5% formic acid in the solution, respectively. The calibration curves for the atomic emission line of Bi were linear ($R^2 > 0.995$) over the whole studied concentration ranges. The linearity ranges of the calibration curves covered at least 3 orders of magnitude for the FLA-APGD and at least 2 orders of magnitude for the FLC-APGD systems (higher concentrations were not studied).

Based on these findings, it was concluded that the proposed FLA-APGD-OES method is a promising alternative to the competitive ones (especially, in terms of the DL). As for the FLC-APGD-OES method, although it provides a much worse DL of Bi, it could be used for the determination of Bi in samples containing higher abundances of this element, *e.g.*, drugs or wastes, especially with the addition of formic acid as a matrix modifier.

To demonstrate the trueness of the proposed FLA-APGD-OES method, an attempt was made to determine Bi in river, tap, and mineral waters. Due to the matrix effects from the concomitant ions, the standard addition method was applied. The reliability of the method was checked by the spike and recovery test. It was established, that the matrix of the analyzed samples lowered the response of Bi by similar values, *i.e.*, 64%, 66%, and 58% for river, tap, and mineral water, respectively (as compared to the solution not containing any matrix). As it had been expected that the primary minerals present in all water samples would be

Table 6 The results of the determination of Bi in different water samples by the developed FLA-APGD-OES method

Water type	Added (μg L^{-1})	Found[a] (μg L^{-1})	Recovery (%)
River water	100	100.7 ± 6.2	100.7
Tap water		86.5 ± 8.3	86.5
Mineral water		90.3 ± 7.0	90.3

[a] Average values ($n = 3$) ± standard deviations.

alkali and alkaline earth metals, the quantification of Ca, K, Mg, and Na was performed using an Agilent ICP-OES instrument, model 5110. It was revealed that the total amount of these elements was equal to 46.7, 116.5, and 123.3 mg L^{-1} in river, tap, and mineral water, respectively. Although the content of the studied alkali and alkaline earth metals was over 2 times lower in river water (as compared to tap and mineral waters), apparently it was high enough to cause a serious reduction of the Bi response and a further increase of the interfering elements did not lead to the reduction of the Bi signal intensity. With regard to the DLs of Bi in the analyzed water samples they covered the range of 0.7–1.1 μg L^{-1}, and were in good agreement with the observed suppression in the Bi signal intensity.

The obtained recovery values ranged between 86 and 101% (see Table 6), which confirms the good trueness of the developed method. The precision of the real sample analysis was slightly worse and fell within the range of 6–10%, which was a consequence of a reduced signal intensity. The trueness of the FLC-APGD-OES method in reference to the determination of Bi in the collected water samples was not studied because it would require their spiking with Bi in an amount of the order of several mg L^{-1}, which is rather not found in naturally occurring and drinking water.

4. Conclusions

The use of FLA- and FLC-APGD systems for Bi determination by OES was studied and the results were compared. It was established that the FLA-APGD excitation source provides a much better analytical performance (as compared to FLC-APGD) in terms of the DL of Bi and sensitivity. Although the matrix effects from the concomitant ions became a serious limitation, water sample analysis could be performed with the standard addition method. The developed method seems to be a reliable alternative to methods involving the conventionally employed large-scale spectrometric instruments, especially for the analysis of samples containing lower abundances of foreign ions, *i.e.*, drugs. It offers the advantages of a small size, a stable operation at a relatively low discharge current, reduced gas consumption, and no requirement for the use of the HG technique.

Despite the fact that the FLC-APGD-OES method is a well-known and efficient tool for the sensitive determination of a wide group of elements, in the case of Bi determination it seems to be less useful than the FLA-APGD-OES method. Nevertheless, it was demonstrated that the addition of formic acid improved the DL of Bi by almost one order of magnitude.

Moreover, this method offers a very good precision, an admittable linearity range, and all the abovementioned advantages of the microplasma system, and therefore it could be still applied for the determination of higher concentrations of Bi.

Conflicts of interest

There are no conflicts to declare.

Acknowledgements

This work was funded by the National Science Centre (Poland) based on decision no. DEC-2017/24/C/ST4/00325.

References

1 A. K. Das, R. Chakraborty, M. L. Cervera and M. de La Guardia, Analytical techniques for the determination of bismuth in solid environmental samples, *TrAC, Trends Anal. Chem.*, 2006, **25**, 599–608.
2 W. N. L. dos Santos, A. de Freitas Santos Junior, L. O. B. Silva, B. R. da Silva Santos and D. L. F. da Silva, Multivariate optimization of a digestion procedure for bismuth determination in urine using continuous flow hydride generation and atomic fluorescence spectrometry, *Microchem. J.*, 2017, **130**, 147–152.
3 A. Slikkerveer and F. A. de Wolff, Pharmacokinetics and toxicity of bismuth compounds, *Med. Toxicol. Adverse Drug Exper.*, 1989, **4**, 303–323.
4 P. C. A. Jeronimo, A. N. Araujo, M. C. B. S. M. Montenegro, D. Satinsky and P. Solich, Colorimetric bismuth determination in pharmaceuticals using a xylenol orange sol–gel sensor coupled to a multicommutated flow system, *Anal. Chim. Acta*, 2004, **504**, 235–241.
5 A. P. Argekar and A. K. Shetty, Extraction and spectrophotometric determination of bismuth(III) with Cyanex 301, *Analyst*, 1995, **120**, 1819–1822.
6 H. Ashkenani and M. A. Taher, Application of a new ion-imprinted polymer for solid-phase extraction of bismuth from various samples and its determination by ETAAS, *Int. J. Environ. Anal. Chem.*, 2013, **93**, 1132–1145.
7 A. S. Amin, Cloud-Point Extraction and Spectrophotometric Determination of Trace Quantities of Bismuth in Environmental Water and Biological Samples, *Spectrosc. Lett.*, 2011, **44**, 424–431.
8 H. Wu, B. Du and C. Fang, Flow Injection On-line Preconcentration Coupled with Hydride Generation Atomic Fluorescence Spectrometry for Ultra-Trace Amounts of Bismuth Determination in Biological and Environmental Water Samples, *Anal. Lett.*, 2007, **40**, 2772–2782.
9 S. Moyano, R. G. Wuilloud, R. A. Olsina, J. A. Gasquez and L. D. Martinez, On-line preconcentration system for bismuth determination in urine by flow injection hydride generation inductively coupled plasma atomic emission spectrometry, *Talanta*, 2001, **54**, 211–219.
10 T. Tokumaru, H. Ozaki, S. Onwona-Agyeman, J. Ofosu-Anim and I. Watanabe, Determination of the Extent of Trace Metals Pollution in Soils, Sediments and Human Hair at e-Waste Recycling Site in Ghana, *Arch. Environ. Contam. Toxicol.*, 2017, **73**, 377–390.
11 M. C. Saha, R. Baskey, S. Lahiri and S. Dutta, Quantitative determination of antimony, bismuth, and tellurium in geological samples by inductively coupled plasma mass spectrometry and flow injection hydride generation atomic absorption technique, *At. Spectrosc.*, 2017, **38**, 7–11.
12 R. Dobrowolski, J. Dobrzynska and B. Gawronska, Determination of bismuth in environmental samples by slurry sampling graphite furnace atomic absorption spectrometry using combined chemical modifiers, *Environ. Monit. Assess.*, 2015, **187**, 4125.
13 M. A. Taher and B. K. Puri, Differential Pulse Polarographic Determination of Trace Amount of Bismuth in Various Complex Samples After Preconcentration of Its 1-(2-Pyridylazo)-2-naphthol Complex by Column and Microcrystalline Naphthalene Methods, *Electroanalysis*, 1999, **11**, 899–904.
14 C. Calderilla, J. Avivar, L. O. Leal and V. Cerda, Multivariate optimisation of a rapid and simple automated method for bismuth determination in well water samples exploiting long path length spectrophotometry, *Int. J. Environ. Anal. Chem.*, 2016, **96**, 653–666.
15 A. S. Bashammakh, Extractive Spectrophotometric Determination of Bismuth(III) in Water Using Some Ion Pairing Reagents, *E-J. Chem.*, 2011, **8**, 1462–1471.
16 J. F. Ventura-Gayete, E. Rodenas-Torralba, A. Morales-Rubio, S. Garrigues and M. de La Guardia, A Multicommutated Flow System for Determination of Bismuth in Milk Shakes by Hydride Generation Atomic Fluorescence Spectrometry Incorporating On-Line Neutralization of Waste Effluent, *J. AOAC Int.*, 2004, **87**, 1252–1259.
17 R. J. Medeiros, L. M. G. dos Santos, A. S. Freire, R. E. Santelli, A. M. C. B. Braga, T. M. Krauss and S. d. C. Jacob, Determination of inorganic trace elements in edible marine fish from Rio de Janeiro State, Brazil, *Food Control*, 2012, **23**, 535–541.
18 C. Moscoso-Perez, J. Moreda-Pineiro, P. Lopez-Mahia, S. Muniategui-Lorenzo, E. Fernandez-Fernandez and D. Prada-Rodrigez, Bismuth determination in environmental samples by hydride generation-electrothermal atomic absorption spectrometry, *Talanta*, 2003, **61**, 633–642.
19 D. D. Afonso, S. Baytak and Z. Arslan, Simultaneous generation of hydrides of bismuth, lead and tin in the presence of ferricyanide and application to determination in biominerals by ICP-AES, *J. Anal. At. Spectrom.*, 2010, **25**, 726–729.
20 T. Sahraeian, H. Sereshti and A. Rohanifar, Simultaneous Determination of Bismuth, Lead, and Iron in Water Samples by Optimization of USAEME and ICP–OES via Experimental Design, *J. Anal. Test.*, 2018, **2**, 98–105.
21 E. Kilinc and F. Aydin, Optimization of Continuous Flow Hydride Generation Inductively Coupled Plasma Optical Emission Spectrometry for Sensitivity Improvement of Bismuth, *Anal. Lett.*, 2012, **45**, 2623–2636.

22 M. Welna, A. Szymczycha-Madeja and P. Pohl, Critical evaluation of strategies for single and simultaneous determinations of As, Bi, Sb and Se by hydride generation inductively coupled plasma optical emission spectrometry, *Talanta*, 2017, **167**, 217–226.
23 R. C. Machado, C. D. B. Amaral, J. A. Nobrega and A. R. Araujo Nogueira, Multielemental Determination of As, Bi, Ge, Sb, and Sn in Agricultural Samples Using Hydride Generation Coupled to Microwave-Induced Plasma Optical Emission Spectrometry, *J. Agric. Food Chem.*, 2017, **65**, 4839–4842.
24 A. Matsumoto and T. Nakahara, Determination of Some Trace Elements in Steels by High Power Nitrogen Microwave Induced Plasma Atomic Emission Spectrometry Coupled with Hydride Generation Technique, *Tetsu to Hagane*, 2003, **89**, 881–889.
25 P. Schramel, I. Wendler and J. Angerer, The determination of metals (antimony, bismuth, lead, cadmium, mercury, palladium, platinum, tellurium, thallium, tin and tungsten) in urine samples by inductively coupled plasma-mass spectrometry, *Int. Arch. Occup. Environ. Health*, 1997, **69**, 219–223.
26 Z. Wang, R. Gai, L. Zhou and Z. Zhang, Design modification of a solution-cathode glow discharge-atomic emission spectrometer for the determination of trace metals in titanium dioxide, *J. Anal. At. Spectrom.*, 2014, **29**, 2042–2049.
27 J. A. C. Broekaert, Plasma bubbles detect elements, *Nature*, 2008, **455**, 1185–1186.
28 S. Weagant and V. Karanassios, Helium-hydrogen microplasma device (MPD) on postage-stamp-size plastic-quartz chips, *Anal. Bioanal. Chem.*, 2009, **395**, 577–589.
29 M. Miclea, K. Kunze, G. Musa, J. Franzke and K. Niemax, The dielectric barrier discharge—a powerful microchip plasma for diode laser spectrometry, *Spectrochim. Acta, Part B*, 2001, **56**, 37–43.
30 A. Kitano, A. Iiduka, T. Yamamoto, Y. Ukita, E. Tamiya and Y. Takamura, Highly sensitive elemental analysis for Cd and Pb by liquid electrode plasma atomic emission spectrometry with quartz glass chip and sample flow, *Anal. Chem.*, 2011, **83**, 9424–9430.
31 W. C. Davis and R. K. Marcus, Role of powering geometries and sheath gas composition on operation characteristics and the optical emission in the liquid sampling-atmospheric pressure glow discharge, *Spectrochim. Acta, Part B*, 2002, **57**, 1473–1486.
32 J. C. T. Eijkel, H. Stoeri and A. Manz, A Molecular Emission Detector on a Chip Employing a Direct Current Microplasma, *Anal. Chem.*, 1999, **71**, 2600–2606.
33 A. J. Schwartz, K. L. Williams, G. M. Hieftje and J. T. Shelley, Atmospheric-pressure solution-cathode glow discharge: a versatile ion source for atomic and molecular mass spectrometry, *Anal. Chim. Acta*, 2017, **950**, 119–128.
34 P. Pohl, P. Jamroz, K. Swiderski, A. Dzimitrowicz and A. Lesniewicz, Critical evaluation of recent achievements in low power glow discharge generated at atmospheric pressure between a flowing liquid cathode and a metallic anode for element analysis by optical emission spectrometry, *TrAC, Trends Anal. Chem.*, 2017, **88**, 119–133.
35 K. Swiderski, P. Pohl and P. Jamroz, A miniaturized atmospheric pressure glow microdischarge system generated in contact with a hanging drop electrode – a new approach to spectrochemical analysis of liquid microsamples, *J. Anal. At. Spectrom.*, 2019, **34**, 1287–1293.
36 Z. Xing, J. Wang, S. Zhang and X. Zhang, Determination of bismuth in solid samples by hydride generation atomic fluorescence spectrometry with a dielectric barrier discharge atomizer, *Talanta*, 2009, **80**, 139–142.
37 J. Kratzer, J. Bousek, R. E. Sturgeon, Z. Mester and J. Dedina, Determination of bismuth by dielectric barrier discharge atomic absorption spectrometry coupled with hydride generation: method optimization and evaluation of analytical performance, *Anal. Chem.*, 2014, **86**, 9620–9625.
38 M. Li, Y. Deng, C. Zheng, X. Jiang and X. Hou, Hydride generation-point discharge microplasma-optical emission spectrometry for the determination of trace As, Bi, Sb and Sn, *J. Anal. At. Spectrom.*, 2016, **31**, 2427–2433.
39 M. Yuan, X. Peng, F. Ge, Q. Li, K. Wang, D.-G. Yu and Z. Wang, Simplified design for solution anode glow discharge atomic emission spectrometry device for highly sensitive detection of Ag, Bi, Cd, Hg, Pb, Tl, and Zn, *Microchem. J.*, 2020, **155**, 104785.
40 M. Gorska, K. Greda and P. Pohl, On the coupling of hydride generation (HG) with flowing liquid anode atmospheric pressure glow discharge (FLA-APGD) for simultaneous determination of traces of As, Bi, Hg, Sb and Se by optical emission spectrometry (OES), *Talanta*, 2021, **222**, 121510.
41 Y. Gao, R. Liu and L. Yang, Application of chemical vapor generation in ICP-MS: a review, *Chin. Sci. Bull.*, 2013, **58**, 1980–1991.
42 X. Liu, Z. Zhu, Z. Bao, D. He, H. Zheng, Z. Liu and S. Hu, Simultaneous Sensitive Determination of Selenium, Silver, Antimony, Lead, and Bismuth in Microsamples Based on Liquid Spray Dielectric Barrier Discharge Plasma-Induced Vapor Generation, *Anal. Chem.*, 2019, **91**, 928–934.
43 P. Pohl and P. Jamroz, Recent achievements in chemical hydride generation inductively coupled and microwave induced plasmas with optical emission spectrometry detection, *J. Anal. At. Spectrom.*, 2011, **26**, 1317–1337.
44 K. Greda, K. Swiderski, P. Jamroz and P. Pohl, Flowing Liquid Anode Atmospheric Pressure Glow Discharge as an Excitation Source for Optical Emission Spectrometry with the Improved Detectability of Ag, Cd, Hg, Pb, Tl, and Zn, *Anal. Chem.*, 2016, **88**, 8812–8820.
45 X. Liu, Z. Zhu, D. He, H. Zheng, Y. Gan, N. Stanley Belshaw, S. Hu and Y. Wang, Highly sensitive elemental analysis of Cd and Zn by solution anode glow discharge atomic emission spectrometry, *J. Anal. At. Spectrom.*, 2016, **31**, 1089–1096.
46 K. Greda, S. Burhenn, P. Pohl and J. Franzke, Enhancement of emission from indium in flowing liquid anode atmospheric pressure glow discharge using organic media, *Talanta*, 2019, **204**, 304–309.
47 P. Jamroz, P. Pohl and W. Zyrnicki, An analytical performance of atmospheric pressure glow discharge

generated in contact with flowing small size liquid cathode, *J. Anal. At. Spectrom.*, 2012, **27**, 1032–1037.

48 K. Swiderski, A. Dzimitrowicz, P. Jamroz and P. Pohl, Influence of pH and low-molecular weight organic compounds in solution on selected spectroscopic and analytical parameters of flowing liquid anode atmospheric pressure glow discharge (FLA-APGD) for the optical emission spectrometric (OES) determination of Ag, Cd, and Pb, *J. Anal. At. Spectrom.*, 2018, **33**, 437–451.

49 X. Liu, Z. Zhu, P. Xing, H. Zheng and S. Hu, Plasma induced chemical vapor generation for atomic spectrometry: a review, *Spectrochim. Acta, Part B*, 2020, **167**, 105822.

50 Y. S. Park, S. H. Ku, S. H. Hong, H. J. Kim and E. H. Piepmeier, Fundamental studies of electrolyte-as-cathode glow discharge-atomic emission spectrometry for the determination of trace metals in flowing water, *Spectrochim. Acta, Part B*, 1998, **53**, 1167–1179.

51 M. A. Mottaleb, Y.-A. Woo and H.-J. Kim, Evaluation of open-air type electrolyte-as-cathode glow discharge-atomic emission spectrometry for determination of trace heavy metals in liquid samples, *Microchem. J.*, 2001, **69**, 219–230.

52 P. Mezei, T. Cserfalvi and M. Janossy, Pressure Dependence of the Atmospheric Electrolyte Cathode Glow Discharge Spectrum, *J. Anal. At. Spectrom.*, 1997, **12**, 1203–1208.

53 P. Mezei, T. Cserfalvi, H. J. Kim and M. A. Mottaleb, The influence of chlorine on the intensity of metal atomic lines emitted by an electrolyte cathode atmospheric glow discharge, *Analyst*, 2001, **126**, 712–714.

54 K. Greda, M. Gorska, M. Welna, P. Jamroz and P. Pohl, In-situ generation of Ag, Cd, Hg, In, Pb, Tl and Zn volatile species by flowing liquid anode atmospheric pressure glow discharge operated in gaseous jet mode - Evaluation of excitation processes and analytical performance, *Talanta*, 2019, **199**, 107–115.

55 X. Liu, Z. Liu, Z. Zhu, D. He, S. Yao, H. Zheng and S. Hu, Generation of Volatile Cadmium and Zinc Species Based on Solution Anode Glow Discharge Induced Plasma Electrochemical Processes, *Anal. Chem.*, 2017, **89**, 3739–3746.

56 M. R. Webb, F. J. Andrade, G. Gamez, R. McCrindle and G. M. Hieftje, Spectroscopic and electrical studies of a solution-cathode glow discharge, *J. Anal. At. Spectrom.*, 2005, **20**, 1218–1225.

57 Q. He, Z. Zhu, S. Hu and L. Jin, Solution cathode glow discharge induced vapor generation of mercury and its application to mercury speciation by high performance liquid chromatography-atomic fluorescence spectrometry, *J. Chromatogr. A*, 2011, **1218**, 4462–4467.

58 K. Greda, P. Jamroz and P. Pohl, Comparison of the performance of direct current atmospheric pressure glow microdischarges operated between a small sized flowing liquid cathode and miniature argon or helium flow microjets, *J. Anal. At. Spectrom.*, 2013, **28**, 1233–1241.

59 P. Jamroz and W. Zyrnicki, Spectroscopic Characterization of Miniaturized Atmospheric-Pressure dc Glow Discharge Generated in Contact with Flowing Small Size Liquid Cathode, *Plasma Chem. Plasma Process.*, 2011, **31**, 681–696.

60 A. Shaltout, Micro Plasma Generation Using Liquid Sampling-Atmospheric Pressure Glow Discharge, *Microchim. Acta*, 2006, **155**, 447–452.

61 K. Greda, A. Szymczycha-Madeja and P. Pohl, Study and reduction of matrix effects in flowing liquid anode - atmospheric pressure glow discharge - optical emission spectrometry, *Anal. Chim. Acta*, 2020, **1123**, 81–90.

62 A. R. Kumar and P. Riyazuddin, Chemical interferences in hydride-generation atomic spectrometry, *TrAC, Trends Anal. Chem.*, 2010, **29**, 166–176.

63 T. A. Doroski and M. R. Webb, Signal enhancement in solution-cathode glow discharge—optical emission spectrometry via low molecular weight organic compounds, *Spectrochim. Acta, Part B*, 2013, **88**, 40–45.

64 R. Shekhar, Improvement of sensitivity of electrolyte cathode discharge atomic emission spectrometry (ELCAD-AES) for mercury using acetic acid medium, *Talanta*, 2012, **93**, 32–36.

65 C. G. Decker and M. R. Webb, Measurement of sample and plasma properties in solution-cathode glow discharge and effects of organic additives on these properties, *J. Anal. At. Spectrom.*, 2016, **31**, 311–318.

Supporting Information

Determination of bismuth by optical emission spectrometry with liquid anode/cathode atmospheric pressure glow discharge.

Monika Gorska*, Krzysztof Greda, Pawel Pohl

Wroclaw University of Science and Technology, Faculty of Chemistry, Division of Analytical Chemistry and Chemical Metallurgy, Wybrzeze Stanislawa Wyspianskiego 27, 50-370 Wroclaw, Poland

* Corresponding author. E-mail address: monika.gorska@pwr.edu.pl (Monika Gorska)

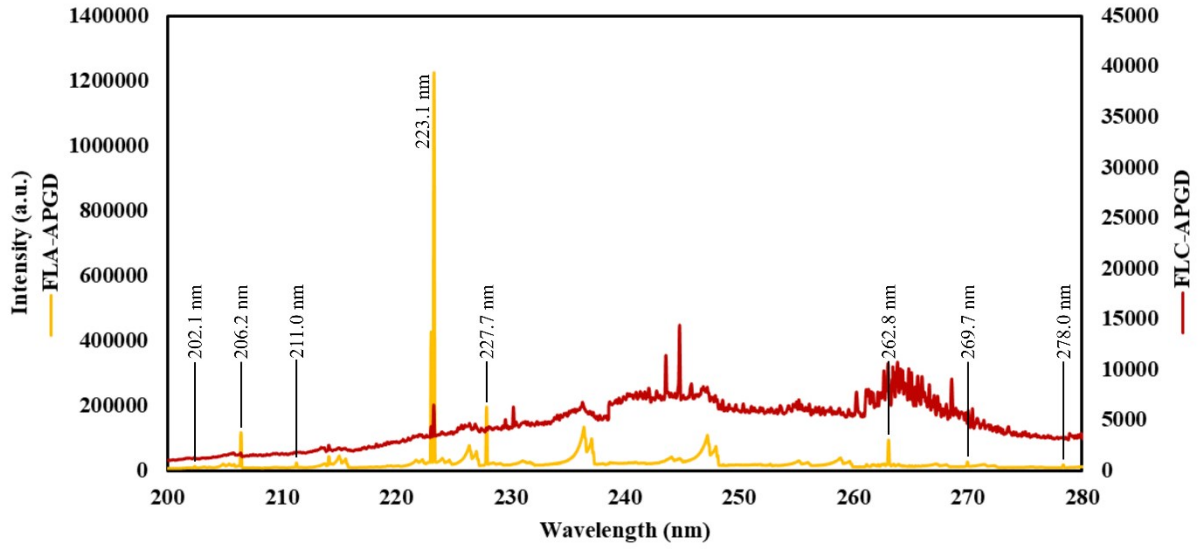

Fig. SI-1. Emission spectra of APGD generated in contact with a Bi-containing solution (serving as the FLA or the FLC) in the spectral range of 200-280 nm.

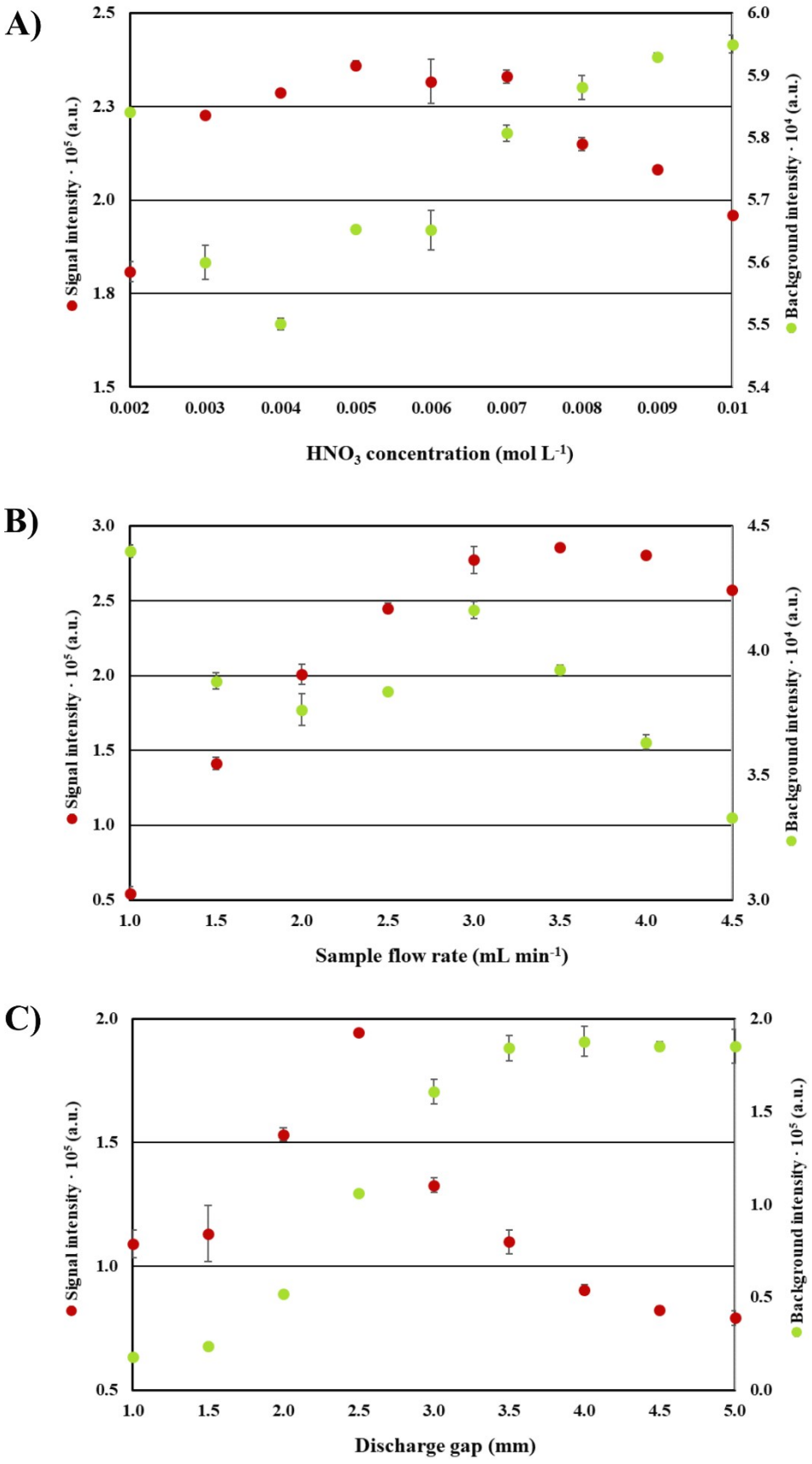

Fig. SI-2. The effect of the acid concentration (A), the sample flow rate (B), and the discharge gap (C) on the intensities of the Bi emission line and the background emission in the case of the FLA-APGD system.

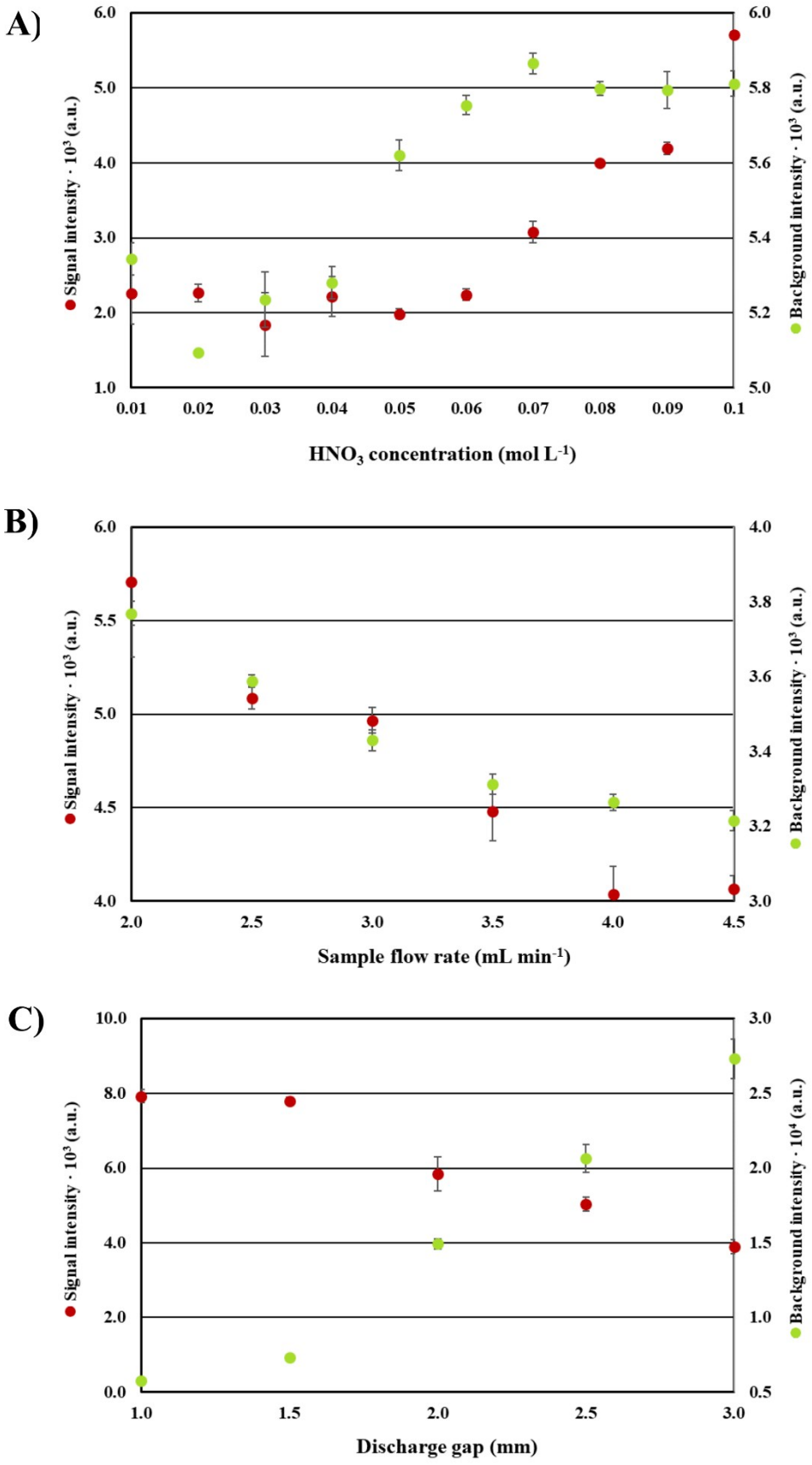

Fig. SI-3. The effect of the acid concentration (A), the sample flow rate (B), and the discharge gap (C) on the intensities of the Bi emission line and the background emission in the case of the FLC-APGD system.

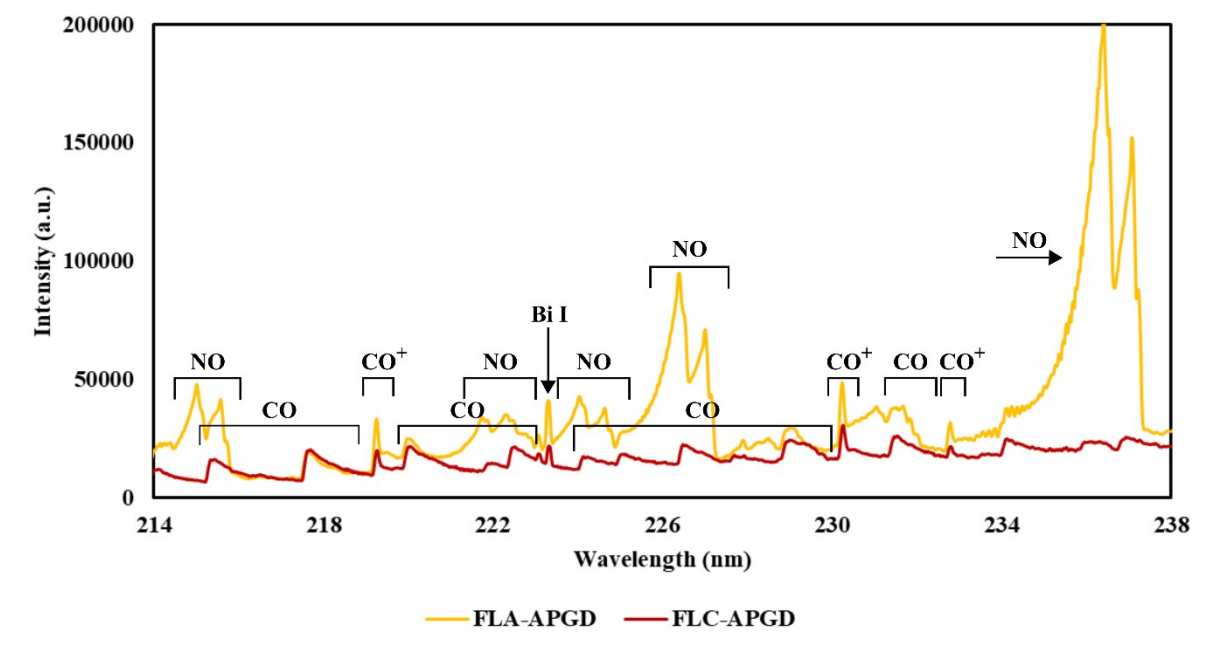

Fig. SI-4. The emission spectra of APGD generated in contact with a Bi-containing solution (serving as the FLA or the FLC) with the addition of 5% methanol, acquired in the spectral range of 214-238 nm.

Comment SI-1
The effect of acid kind and its concentration
The use of HCl for the sample preparation caused an inconvenience due to the reaction of the analyte with Cl^- ions, leading to the formation of BiOCl species. This resulted in a great suppression of the Bi signal intensity after some time since the sample preparation. That being so, the Bi standard solution in HCl had to be prepared just before measurements. Although it was not the aim of this work, it was established that after only a 3 hour storage from the preparation of the Bi solution acidified with HCl, the SBR of the Bi emission line was 4 times lower than the corresponding one obtained for a freshly prepared solution. Additionally, there was almost no measurable signal from Bi in the spectrum recorded the next day.

Comment SI-2
The effect of acid kind and its concentration
In the FLA-APGD system, the growth in the acid concentration up to 0.005 mol L^{-1} resulted in an enhancement of the Bi signal intensity (by 30%) following by a gradual decline as the acid concentration was further increased. In the case of the FLC-APGD system, conversely, an initial fall of the Bi signal intensity was noted (by 12%) at acid concentrations up to 0.05 mol L^{-1} and then, it rocketed with a succedent growth in the acid concentration up to 0.1 mol L^{-1}.

Comment SI-3
The effect of acid kind and its concentration
Normally, solvated electrons take part in the reduction of the analyte ions, which the process is privileged at lower acidities of the FLA solution, and are responsible for the generation of the reduced forms of these analytes, as reported for Ag(I) and Cd(II).[1] Hence, alike for the latter analytes, it can be expected that at higher HNO_3 concentrations, *i.e.*, up to 0.01 mol L^{-1} as studied here, a contribution of the solvated electrons was very low, while other reactive species present in these conditions in the solution, *e.g.*, H radicals,[1] could react much slower or not at all with Bi(III) ions as compared to the solvated electrons. Therefore, the Bi signal intensity was decreased when the HNO_3 concentration was increased.

Comment SI-4
The effect of the discharge current and the He flow rate
Generally, as the discharge current increased, the background intensity in FLA-APGD was lifted; its behavior was akin to that reported for the FLC-APGD system. However, at the He flow rate of 100 mL min^{-1}, the background intensity did not depend on the discharge current, whereas at the lowest studied He flow rate (50 mL min^{-1}), the background intensity decreased with the increasing discharge current.

Comment SI-5
The effect of the discharge current and the He flow rate
The remarked background intensity growth was different for both investigated systems. In the case of FLA-APGD, it was noted that the background level enhanced around 4.5-fold as the gas flow rate rose from 150 to 350 mL^{-1} (lower He flow rates were not considered due to the discharge instability when the gas flow rates of 50-100 mL min^{-1} were applied at higher discharge currents), regardless of the discharge current used. However, for FLC-APGD, the observed background enhancement (assessed in the same range of the He flow rates) was much lower, *i.e.*, 2-fold (at discharge currents of 30-50 mA) or 1.4-fold (at discharge currents

of 60-70 mA), apparently being slightly dependent on the discharge current applied and dropping with its growth.

Comment SI-6

The effect of the discharge current and the He flow rate

The results shown in Fig. 3 as well as the abovementioned intensity shifts of both the Bi emission line and the background level clearly indicate that there is a strong and intricate relationship between the discharge current and the He flow rate. This relationship could point that except for the collisions with electrons, the collisions with the excited He atoms and/or the metastable He atoms might play an important role in the excitation processes of Bi atoms, particularly in the case of the FLA-APGD system operated at higher He flow rates and higher discharge currents. As reported by Swiderski *et al.*[1], the later excitation source is more energetic than the FLC-APGD system and with a negligible contribution of the quenching processes due to the collisions of water molecules with the excited states of the molecular and atomic species. The water evaporation from the surface of the FLC solution and the flux of water molecules in the discharge phase was much higher than this in the FLA-APGD system, but its effect was less deteriorating at lower He flow rates and lower discharge currents.

Comment SI-7

The effect of the discharge gap

Considering the FLA-APGD system, the signal intensity of Bi was growing as the discharge gap was increased from 1 mm up to 2.5 mm (the observed intensity amplification was equal to 78% at the discharge gap of 2.5 mm) and then dropped with the further increase of the discharge gap up to 5 mm (by 60% at 5 mm). As for FLC-APGD, the signal intensity of Bi was decreasing up to 3 mm by 50%. At discharge gaps above that value, the response from Bi was not observed.

Regarding the background intensity, it was established that, with the rise of the discharge gap up to 3 mm, the background intensity was enhanced almost 5-fold in the case of FLC-APGD and over 9-fold in the case of FLA-APGD. Moreover, at discharge gaps of 4-5 mm, the background level for the FLA-APGD system was roughly constant, which resulted in an overall 10-fold background intensity enhancement as the discharge gap was changed from 1 to 5 mm.

References

1. K. Swiderski, A. Dzimitrowicz, P. Jamroz, P. Pohl, Influence of pH and low-molecular weight organic compounds in solution on selected spectroscopic and analytical parameters of flowing liquid anode atmospheric pressure glow discharge (FLA-APGD) for the optical emission spectrometric (OES) determination of Ag, Cd, and Pb, *J. Anal. At. Spectrom.*, 2018, **33**, 437–451.

Talanta 237 (2022) 122921

Contents lists available at ScienceDirect

Talanta

journal homepage: www.elsevier.com/locate/talanta

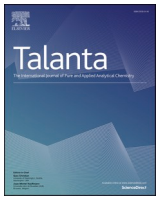

Application of atmospheric pressure glow discharge generated in contact with liquids for determination of chloride and bromide in water and juice samples by optical emission spectrometry

Monika Gorska *, Pawel Pohl

Wroclaw University of Science and Technology, Faculty of Chemistry, Division of Analytical Chemistry and Chemical Metallurgy, Wybrzeze Stanislawa Wyspianskiego 27, 50-370, Wroclaw, Poland

A R T I C L E I N F O

Keywords:
Atmospheric pressure glow discharge
Flowing liquid anode
Flowing liquid cathode
Chloride
Bromide
Optical emission spectrometry

A B S T R A C T

Novel atmospheric pressure glow discharge (APGD) microplasma systems, sustained between a miniaturized flowing anode (FLA) or cathode (FLC) and a He jet, were investigated for the direct determination of Br and Cl, using optical emission spectrometry (OES). The impact of the most crucial operating parameters, *i.e.*, the acid type and its concentration, the discharge current, the gas flow rate, and the sample flow rate, was studied for each of the proposed APGD-based systems. Under the optimized conditions, the analytical figures of merit were determined. The susceptibility to the matrix effects of both developed methods was verified as well. It was found that the mechanism of the analytes transport into the discharge likely relied on the cathode sputtering in the case of FLC-APGD and the formation of the volatile Br and Cl species for FLA-APGD. The DLs of Br and Cl were established to be relatively high, *i.e.*, 0.15 and 1.5 mg L^{-1} for FLA-APGD and 2.1 and 18 mg L^{-1} for FLC-APGD. However, both studied methods turned out to be resistant to the presence of foreign ions in a sample, at relatively high concentrations. Hence, the proposed methods could be successfully applied for the determination of Br and Cl in water and juices samples and no major differences between the results obtained using the external standard calibration and the standard addition method were found.

1. Introduction

Owing to rapid urbanization and industrial development, observed in the course of the last decades, there is a growing need of a reliable determination of elements in different kind of samples, such as environmental, metallurgical or food samples [1–3]. Apart from the requirement of a given method reliability, it is expected that modern techniques would be founded upon compact and portable instrumentation to be able to perform on-line analyses [4]. Among various analytical techniques that are applied to meet those needs, spectrometric techniques are the most appreciated ones. Nowadays, several commercially available techniques are commonly used for this purpose and they include: flame atomic absorption spectrometry (FAAS), graphite furnace atomic absorption spectrometry (GF-AAS), atomic fluorescence spectrometry (AFS), inductively coupled plasma optical emission spectrometry (ICP-OES), and inductively coupled plasma mass spectrometry (ICP-MS). They share numerous joint advantages such as detection limits (DLs) ranging from relatively low (AAS) to ultra-low (ICP-MS), the linearity ranges of calibration curves covering several orders of magnitude, good sensitivity and precision, and – in some techniques – the possibility of performing fast multi-element analyses. A wide variety of the mentioned available techniques, along with both instruments and sample preparation techniques modifications, proposed by researchers, have currently enabled to determine almost each element in every sample.

Nevertheless, certain drawbacks are pointed out regarding the abovementioned techniques. First of all, those instruments usually require a special pre-treatment of samples containing organic matter and/or dissolved solids, due to matrix effects and/or the apparatus parts vulnerability to sample viscosity or dissolved solids [5–7]. This is usually done by performing the digestion procedure with the aid of concentrated acids, elevated temperature and – sometimes – microwave energy [7,8]. However, the digestion procedure is time-consuming and may lead to measurement errors due to a sample contamination and/or an analytes loss [7,9,10]. Moreover, the ICP-based techniques require large amounts of gas or even vacuum, for stable operation [11]. On the other hand, the

* Corresponding author.
E-mail address: monika.gorska@pwr.edu.pl (M. Gorska).

https://doi.org/10.1016/j.talanta.2021.122921
Received 5 August 2021; Received in revised form 14 September 2021; Accepted 30 September 2021
Available online 2 October 2021

AAS and AFS techniques require separate radiation sources for each element, meaning the number of analytes that may be determined at once is limited. Apart from all of that, all aforesaid techniques require a complex and bulky instrumentation. That being so, the application of those techniques translates to both purchasing and operating costs being extremely high and the techniques themselves do not address the criteria of compactness and portability.

On this account, there is a continuant need for developing compact and portable spectrochemical instrumentation which would assure similar or better analytical characteristics at reduced costs. For this reason, miniaturized plasma sources have become an attractive alternative for the commercially available instrumentation and directed the attention of many researchers into their development. Among various groups of such microplasma sources, developed for the time being, discharges generated in contact with liquids enjoy a special interest. They include electrolyte cathode discharge (ELCAD) [12], solution cathode glow discharge (SCGD) [13], flowing liquid cathode – atmospheric pressure glow discharge (FLC-APGD) [14], solution anode glow discharge (SAGD) [15], flowing liquid anode – atmospheric pressure glow discharge (FLA-APGD) [16], liquid drop anode – atmospheric pressure glow discharge (LDA-APGD) [17], and hanging drop electrode – atmospheric pressure glow discharge (HDE-APGD) [4]. FLC- and FLA-APGD seem to be very promising tools for spectrochemical analysis. The FLC-APGD systems enable to determine a wide range of different elements, offer the DLs comparable to those achieved with the ICP-OES technique, are quite resistant to matrix effects, and allow to determine the metal content in certain samples containing complex organic matter with omitting the digestion procedure [5,18]. In the case of samples of relatively simple matrices, *e.g.*, waters, they often may be analyzed using the external standard calibration, due to the lack of significant interferences, found for this method [19–22]. On the other hand, the elements determination with the aid of the FLA-APGD system is restricted only to 8 elements which are known to form volatile species (Ag, Bi, Cd, Hg, In, Pb, Tl, and Zn) and suffers from matrix effects coming from other ions, present in the analyzed samples, which usually force to perform their analysis using the standard addition method for calibration [15,16,23–25]. However, the DLs offered by FLA-APGD are improved up to several orders of magnitude, as compared to other microplasma sources as well as some conventional techniques, *e.g.*, FAAS or ICP-OES [16,23,24,26]. Therefore, the FLA-APGD system still allows to determine small quantities of the above listed elements though the analytes signals are usually reduced in real samples, due to the matrix effects [26].

It is worth to note, however, that the application of microplasma sources – in the vast majority of cases – is reported only to the direct determination of metals and metalloids. Nonetheless, three microplasma techniques were applied to the determination of halogens as well. The first one showed the potential of dielectric barrier discharge (DBD) for the determination of Br, Cl and I, arisen from the introduction of Br_2, Cl_2, and I_2 vapors as produced in the reaction of an acidified solution of Br^-, Cl^-, and I^- ions with a $KMnO_4$ solution [27]. Another one studied the performance of microwave microstrip helium plasma for the determination of Br and Cl also preceded by the reaction of their anions with $KMnO_4$ to form Br_2 and Cl_2, respectively [28]. In the third one, a capillary microplasma analytical system (C-μPAS) was applied for the separation of mixture containing different Br- and Cl-containing compounds, followed by a sensitive detection of Br and Cl by glow discharge optical emission spectrometry (GD-OES) [29]. It is noteworthy that the application of the first two aforesaid methods with chemical vapor generation (CVG) of Br and Cl required the system construction modifications to perform this analyte introduction mean. On the other hand, the determination of non-metals such as halogens, S, P, and N by the conventional techniques has been reported much more often [30–35].

Apart from metals, the reliable determination of halides is particularly important since they are widely distributed in environment, living organisms as well as occur in many water and food samples, indicating their quality and safety. Therefore, as to the best of our knowledge neither FLA- nor FLC-APGD has been ever applied for the direct determination of halides, the aim of this work was to examine the suitability of the mentioned APGD-based methods for the determination of Br and Cl. For better overview, the potential of both FLA- and FLC-APGD systems was studied and the results were compared and discussed.

To reach this goal, at first, the analytical lines of each studied elements were identified in the APGD spectra. Subsequently, the optimization of crucial working parameters was performed for each studied system and the analytical figures of merit were evaluated under the optimized conditions. Furthermore, the impact of selected concomitant salts on the analytes signals intensity was examined to evaluate the method endurance to matrix effects coming from potential inorganic constituents of real samples. Finally, to verify the reliability of the proposed methods, Br and Cl were determined in water and juice samples, using two calibration methods. The obtained results were additionally compared to those provided by the ICP-OES technique.

2. Experimental

2.1. Instrumentation

A schematic drawing of the developed APGD-based systems is presented in Fig. 1. The construction of the developed APGD-based systems was almost the same; they differed only in the electrodes polarization

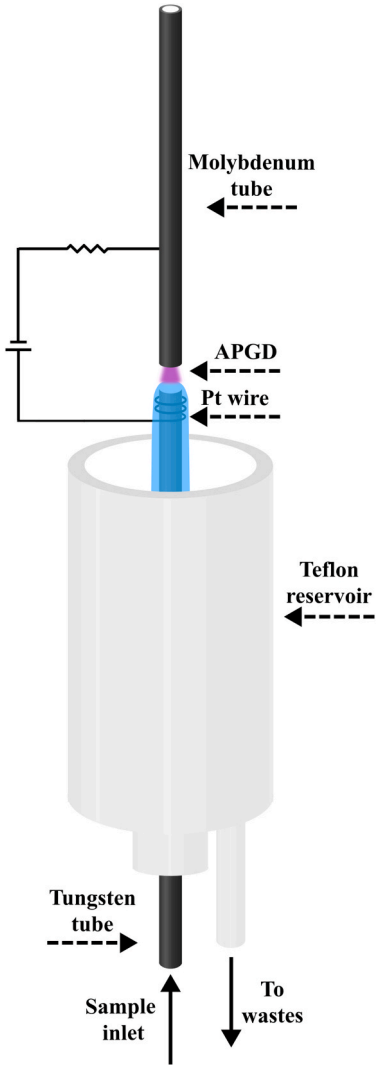

Fig. 1. A schematic drawing of the developed FLA- and FLC-APGD systems.

(for that reason it was omitted in the figure). The developed systems consisted of an open-to-air chamber with a Mo tube (OD/ID 3/2 mm, length 100 mm) placed at the top and, a vertically oriented, W tube (OD/ID 3/2 mm, length 100 mm), placed at the bottom. The discharge was sustained between the surface of sample solutions, pumped through the W tube by means of a 3-channel REGLO ICC peristaltic pump (Ismatec, USA), and a gaseous (He) jet carried through the Mo tube. The He flow rate was controlled using a FC-2900 flow controller and a RO-28 digital flow meter (Tylan General, USA). The sample solutions served either as the FLC or the FLA. The sample flow rate was changed in the 1–4 mL min^{-1} range, whereas the gas flow rate ranged between 150 and 350 mL min^{-1}. As the solution reached the W tube's top it flowed down to a PTFE reservoir, from which it was pumped out. The distance between the solution surface and the Mo tube (so-called discharge gap) was set to approximately 1.5 mm. The electrical contact was provided directly to the Mo tube and with the aid of a Pt spiral wrapped around the W tube. The voltage being around 500–1000 V was applied to both electrodes by a HV dc power supply (model DP50H–024 PH, DSC-Electronics, Germany). Its exact value was dependent on the electrodes polarization, the applied discharge current, the sample flow rate, the gas flow rate as well as the type of acid, used to acidify the sample solutions and its concentration. To stabilize the discharge, a 6.9 kΩ ballast resistor was connected into the circuit.

The radiation emitted by both APGD systems was imaged (1:1) on the entrance slit (10 μm) of a Shamrock 500i imaging spectrometer (Andor, UK), using an achromatic quartz lens (f = 80). The spectrometer was equipped with a holographic grating (1200 lines mm^{-1}) and a Newton DU-920P-OE UV–Vis CCD camera (Andor, UK). The integration time was 10 s during all experiments and intensities of atomic emission lines of the studied elements were background corrected.

2.2. Reagents and sample preparation

Deionized water (18.2 MΩ cm) from a Polwater water purification system (Labopol-Polwater, Poland) was used throughout the study. All chemicals were at least of analytical grade. He of 99.999% purity was supplied by Air Products (Poland). All working standard solutions of Br and Cl were prepared using solid NH_4Br and NH_4Cl, provided by Sigma-Aldrich (Germany) and Avantor Performance Materials (Poland), respectively. To acidify the analyzed solutions, concentrated HNO_3 (65% m/m) or H_2SO_4 (95–98% m/m) obtained from Sigma-Aldrich (Germany) were used. Solid $Fe(NO_3)_3$, NH_4NO_3, K_2SO_4, $MgSO_4$, KI, NH_4F, $KMnO_4$, $NaHCO_3$, KH_2PO_4, $K_2Cr_2O_7$, Na_2S, and $Ca(NO_3)_2$ were applied for the matrix effects investigation and they were provided by Avantor Performance Materials (Poland).

To show the reliability of the proposed methods for the real samples analysis, mineral medicinal water, river water, sea water, and tap water as well as beetroot and tomato juices were analyzed on the content of Br and Cl. Mineral medicinal water "Hanna" (Polish Healing Waters, Poland), beetroot juice (Dawtona, Poland), and tomato juice (Fortuna, Poland) were purchased in local stores. Samples of municipal tap water, the Oder (river) water (sampled in Wroclaw city), and the Mediterranean Sea water (sampled in Marsaskala, Malta) were collected into precleaned 0.5 L PE bottles and immediately acidified with HNO_3. Followingly, appropriate portions of each water and juice samples were transferred into a twist cup container, to reach their dilutions of 2 (tap water), 5 (river water), 10 (mineral water), 60 (juices), and 100 (sea water) for FLA-APGD and 0 (tap and river water), 2 (mineral water), 20 (juices), and 100 (sea water) for FLC-APGD. Subsequently, deionized water was added to around 80% of the final volume of 30 mL (v/v). After that, appropriate amounts of concentrated H_2SO_4 were added to reach its final concentration of 0.01 (FLC-APGD) or 1 (FLA-APGD) mol L^{-1}. Finally, all samples were filled with deionized water to the final volume. All samples were prepared in triplicates (along with the relevant procedural blanks) and – for the determination of Br – they were divided into three separate parts and the standard addition was performed on the last two of them. For the measurements with the aid of the APGD-based techniques, the external standard calibration as well as the standard addition method were used for calibration.

Regarding the ICP-OES measurements, the water samples were diluted 0 (river and tap water), 5 (mineral medicinal water), and 100 (sea water) times. To achieve that, the appropriate amounts of each of the aforesaid samples were transferred into a twist cup container and subsequently acidified with concentrated HNO_3, to achieve its concentration of 0.7 mol L^{-1}. Such prepared samples were analyzed in regard to the external standard calibration. In the case of the juice samples, the digestion procedure could not be performed due to possibility of the analytes loss. Therefore, they were only centrifuged at 15 000 rpm for 10 min to remove any dissolved particles. After that, their preparation procedure was similar to the abovementioned one, however, the prepared samples were divided into three parts and the standard solution addition was performed on the last two of them. All samples for the ICP-OES measurements were prepared in triplicates along with the relevant procedural blanks.

3. Results and discussion

3.1. Emission spectra of the studied APGD systems

At the beginning, the emission spectra of both investigated APGD-based systems were acquired in order to identify the analytical lines of Br and Cl. Also, the background intensity for both investigated systems in the measured spectral region was compared. For this purpose, a mixed solution of Br and Cl (1000 mg L^{-1}), acidified with HNO_3 to its concentration of 0.1 mol L^{-1} was prepared. The emission spectra were recorded in the 700–900 nm range. The measurements conditions were as follows: the discharge current of 40 mA, the gas flow rate of 150 mL min^{-1}, and the sample flow rate of 3.0 mL min^{-1}.

The received results are given in Table 1 and Fig. SI-1. Regarding the analytical lines found for both analytes, there were 14 of them in the

Table 1
The emission lines of Br and Cl (both at the concentration of 1000 mg L^{-1}) identified in the FLA-APGD and FLC-APGD spectra (in the 700–900 nm range) along with their intensities and SBR values.

Element	λ (nm)	FLA-APGD		FLC-APGD	
		Intensity (a.u.)	SBR	Intensity (a.u.)	SBR
Br	700.52	$1.05{\cdot}10^5$	1.19	$1.59{\cdot}10^4$	0.34
	734.85	$2.81{\cdot}10^4$	0.30	$2.01{\cdot}10^4$	0.70
	751.30	$4.55{\cdot}10^4$	0.44	$3.48{\cdot}10^4$	1.57
	780.30	$2.00{\cdot}10^4$	0.13	$1.57{\cdot}10^4$	0.84
	827.24	$3.09{\cdot}10^5$	1.15	$1.95{\cdot}10^5$	14.87
	833.47	$2.54{\cdot}10^4$	0.09	$1.99{\cdot}10^4$	1.58
	834.37	$2.91{\cdot}10^4$	0.10	$2.08{\cdot}10^4$	1.62
	847.75	$3.89{\cdot}10^4$	0.13	$2.89{\cdot}10^4$	2.27
	863.87	$9.31{\cdot}10^4$	0.26	$6.53{\cdot}10^4$	5.94
	869.85	$1.83{\cdot}10^4$	0.06	$2.09{\cdot}10^4$	1.67
	882.52	$7.16{\cdot}10^4$	0.21	$4.88{\cdot}10^4$	4.24
	889.76	$1.63{\cdot}10^5$	0.45	$1.05{\cdot}10^5$	8.91
	893.24	$2.73{\cdot}10^3$	0.01	$1.92{\cdot}10^3$	0.16
	896.40	$7.96{\cdot}10^3$	0.02	$7.38{\cdot}10^3$	0.66
Cl	725.66	ND		$4.54{\cdot}10^3$	0.12
	741.41			$5.88{\cdot}10^3$	0.21
	754.71			$5.18{\cdot}10^3$	0.19
	771.76			$2.74{\cdot}10^3$	0.13
	774.50			$5.87{\cdot}10^3$	0.30
	808.67			$5.76{\cdot}10^3$	0.40
	837.59	$1.82{\cdot}10^3$	0.01	$3.20{\cdot}10^4$	2.25
	842.83	ND		$6.02{\cdot}10^3$	0.52
	857.52			$5.40{\cdot}10^3$	0.48
	858.60			$1.50{\cdot}10^4$	1.41
	891.29			$3.69{\cdot}10^3$	0.34
	894.81			$7.76{\cdot}10^3$	0.78

SBR – signal to background ratio.
ND – not detected.

case of Br (for both studied systems) and 12 in the case of Cl. Nevertheless, such a multitude of analytical lines for Cl were identified only in the spectrum of the FLC-APGD system, whereas only one weak analytical line was found in the spectrum of FLA-APGD. As for Br, however, it is noteworthy that although the intensities of corresponding analytical lines were similar or better in the case of FLA-APGD, their signal-to-background ratios (SBRs) were higher for the FLC-APGD system. This was due to a significantly higher background intensity noted for FLA-APGD (see Fig. SI-1), at chosen measurement conditions.

For the time being, the background intensity for FLA- and FLC-APGD had been previously compared in two papers [16,23]. Nonetheless, those spectra were recorded within 200–400 nm range, where the emission bands of the NO, OH, and N_2 molecules is observed. It was found in those works that the emission coming from the N-containing molecules was higher for FLA-APGD, whereas the intensity of the OH band was higher in the FLC-APGD spectrum. A higher intensity of the OH bands and lower emission from the NO and N_2 molecules for the FLC-APGD system could be easily explained (and proven) by a higher amount of the water vapor entering the discharge [16,36]. However, in the spectral region observed herein, no molecular bands were found and only the analytical lines of Br, Cl, He, and O were identified. Therefore, the enhanced background emission for FLA-APGD could be related rather to the operating conditions applied in this part of study, which – apparently – were not favorable for generating APGD in contact with the FLA solution.

It is an interesting issue that there was a significant difference between the intensity of the He and O analytical lines. The atomic lines of He were notably increased for the FLA-APGD system, whereas the signals coming from the O atoms were higher in FLC-APGD. Since the He flow rate was identical for both systems, the observed variations in those signals intensity likely resulted from the abovementioned discharge saturation with the water vapor.

Nevertheless, prescinding from the background intensity, the mechanism of the analytes transport to the discharge regarding both APGD systems should be also taken into consideration. Although for none of the investigated systems it was experimentally proven, it is strongly believed that in the case of FLC-APGD the analytes are likely transported into the discharge as a result of the liquid cathode sputtering, whereas for FLA-APGD it is presumed that some kind of volatile species of the analytes are generated as a result of the reduction reactions with solvated electrons and/or the H radicals, as only a few elements that are known to form volatile species may be observed in the spectra of this system [4,16,24]. In the case of the analytes studied herein, the reduction reactions could not take place, since they are present in the FLA solution in the anionic form. However, the OH radicals, which are known to present oxidative properties, are also widely distributed in the discharge [37,38]. Therefore, the presence of the Br lines, along with one for Cl in the FLA-APGD spectrum might suggest that Br^- and Cl^- ions reacted with the OH radicals in the plasma-liquid interfacial layer, resulting in the formation of volatile Br_2 and Cl_2. Although there is no evidence of such reactions taking place in the studied systems, some possible reactions between Br and Cl ions and OH radicals had been described previously [39,40]. Hence, the differences in the signal intensities of Br and Cl, obtained for both APGD systems, could be related to the acid type and/or its concentration, applied herein, that were not optimal for the analytes transport processes through the sputtering and/or the mentioned reaction with the OH radicals.

Regardless of a particular reason responsible for the differences in the analytes signals intensities and the SBR values, the analytical lines of 827.24 nm (Br) and 837.59 nm (Cl) were found to assure the highest emission and they were traced in the further experiments.

3.2. Optimization of working parameters

Bearing in mind observations and hypotheses given in the previous section, the optimization of the most crucial operating parameters was found to be essential for a reliable comparison of the performance of both systems as well as turning the spotlight on the way the analytes are transported into the discharge in the case of FLA-APGD. The optimization was carried out taking the following parameters into account: the acid type (HNO_3, H_2SO_4) and its concentration (0.01–2 mol L^{-1}), the discharge current (30–50 mA), the gas flow rate (150–350 mL min^{-1}), and the sample flow rate (1–4 mL min^{-1}). The optimization process was divided into two parts. In the first one, the acid type and its concentration were optimized using the one factor at the time (OFAT) approach and the remaining parameters were optimized together, using the design of experiment (DoE) approach. The measured response, during the whole optimization, were the SBRs of the Br and Cl analytical lines. If not stated otherwise, the analytes concentration was equal to 1000 mg L^{-1}.

3.2.1. Preliminary optimization of the acid type and its concentration

The acid primarily applied for the acidification of the FLA and FLC solutions is HNO_3. This acid is the preferable one since it does not form any precipitates with common metal cations and is commonly used during the digestion procedure performed in the case of samples that are solid and/or contain any organic matter [41]. On the other hand, H_2SO_4 is habitually applied for the acidic oxidation of halides and their subsequent determination [27,28,31]. Therefore, the impact of both those acids on the analytes signal intensities was tested. The measurements conditions were as follows: the discharge current of 40 mA, the He flow rate of 150 mL min^{-1}, and the sample flow rate of 3.0 mL min^{-1}. In the case of the acid type optimization, the acid concentration was increased to 0.2 mol L^{-1}, as preliminary study showed it assured higher signals in the FLA-APGD system which was expected to result in better credibility of the obtained results.

The obtained results are presented in Tables SI–1 and Fig. 2. As it can be seen from the table, the samples acidification with H_2SO_4 indeed translated to higher SBRs for analytical lines of both analytes and both systems, however, the differences between the two acids were usually small. Since H_2SO_4 assured better results, with particular reference to Cl in the FLA-APGD system, this acid was applied in the further part of this study.

In the next step, the H_2SO_4 concentration was optimized. In the case of FLC-APGD, the discharge could not be maintained over the whole investigated range, *i.e.*, 0.01–2 mol L^{-1} as the plasma became unstable above the acid concentration of 0.2 mol L^{-1}. The increasing H_2SO_4 concentration did not affect significantly the Br signal as the difference between the lowest and highest obtained values was merely 6%. The same difference for Cl was equal 37%. Nevertheless, as it can be noted in Fig. 2, the highest SBR value (especially for Cl) was received for the acid concentration of 0.01 mol L^{-1}. Also, the best visual stability as well as the lowest RSD values were noted for the same acid concentration.

Regarding the FLA-APGD system, the discharge could be stably maintained over the whole studied range and the visual stability of the discharge remained unchanged with increasing acid concentrations. As for the impact of its growing concentration on the SBR values of the analytical lines, the tendency was opposite to the one obtained for the FLC-APGD system; a significant signal intensity boost was observed with the growing acid concentration, particularly in the range of 0.01–1 mol L^{-1}.

These results were quite unexpected considering previously published works regarding the impact of the acid concentration on analytical response for different elements in both studied systems. For FLC-APGD, the increase of the acid concentration is typically found to enhance the analytes signals [23,42]. Such a tendency is attributed to the reduced cathode voltage drop (at high acid concentrations) and the corresponding drop of the electric field strength in the cathode dark space (CDS) zone of the discharge (see Comment SI-1). On the other hand, lower acid concentrations are favorable for obtaining high analytes signals for the FLA-APGD system [15,23–25], likely due to the

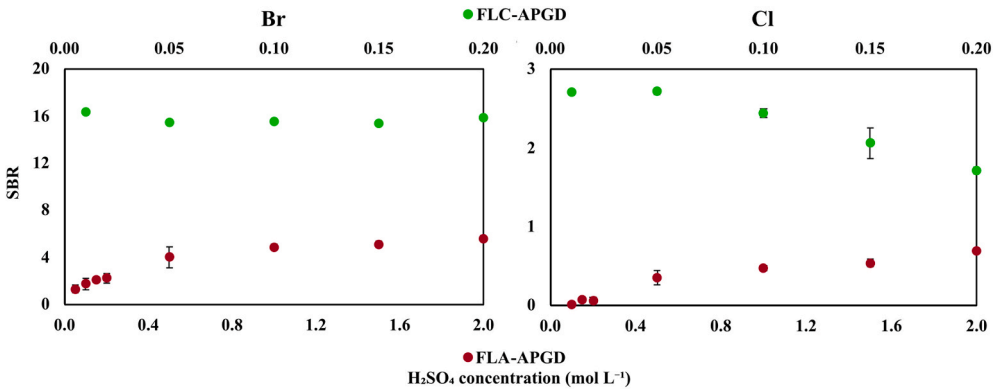

Fig. 2. The effect of the H_2SO_4 concentration on the signal-to-background ratios (SBRs) of the Br and Cl analytical lines for both developed APGD-based systems.

scavenging of the solvated electrons by H_3O^+ ions taking place at higher acid concentrations, leading to the reduced analytes signals [23].

The opposite results obtained in this work could be explained based on the abovementioned presumptions. In the case of FLC-APGD, assuming that the Br and Cl anions are sputtered from the FLC solution surface, high cathode voltage in the CDS zone was actually conducing to the anions transport into the NG zone, as they were accelerated towards the anode. Therefore it should be expected that for the anionic analytes lower FLC solutions acidification would result in higher signal intensities and this is exactly what was observed in this work. Assuming the analytes were transported into the FLA-APGD discharge as Br_2 and Cl_2 formed with the OH radicals in the plasma-liquid interfacial layer, the received results could suggest that either the number of the OH radicals grew with the increasing acid concentration or the mentioned reaction was more efficient at lower pH. Since it was previously established the production rate of those radicals is independent on pH [37] and considering the differences between the signals enhancement factor, observed for Br and Cl (see Fig. 2), it could be concluded that the second hypothesis seems to be more likely. More details regarding the proposed mechanism of the analytes transport into the discharge were given in Comment SI-2.

To sum up, it was concluded that the formation of volatile Br_2 and Cl_2 likely took place in both FLA- and FLC-APGD systems. However, in the case of the FLC-APGD system, its impact was less significant than the transport mechanism through the cathode sputtering, whereas for the FLA-APGD system it could be the main factor responsible for the analytes transportation.

Taking into account the obtained results, the optimal H_2SO_4 concentration was decided to be 0.01 mol L^{-1} for FLC-APGD, since it assured the highest SBRs of both analytes and the best discharge stability, and 1 mol L^{-1} for FLA-APGD, as a further increase of the acid concentration did not have such a great impact on the analytes signals.

3.2.2. *Further optimization of the remaining parameters*

As it was shown in our previous works regarding both FLA- and FLC-APGD [23,24], some of operating parameters might depend on each other. For instance, the impact of the discharge current on the SBRs of the analytical lines of different elements may vary depending on the applied gas flow rate. Also, the discharge stability is restricted by the combination of the discharge current, the gas flow rate, and the sample flow rate. Exemplary, the higher sample flow rate, the higher discharge current may be applied. Therefore, the optimization of the remaining parameters (*i.e.*, the ones listed above) was carried out using the DoE approach. The Box-Behnken response surface design was applied for this purpose. It was used to model the curvature of the experimental data with fewer design points. The received response surface regression equations (see Table 2) allowed to model how the investigated parameters affected the SBRs of the Br and Cl analytical lines. To determine how well the established regression equations fitted the data, the goodness-of-fit statistics is shown in Tables SI–2, including values of the coefficient of determination (R^2) that shows the percentage of variation in the response that is explained by the model, values of the adjusted R^2 ($R^2_{(adj)}$) that accounts for the terms that are not significant in the model, and values of the predicted R^2 ($R^2_{(pred)}$) that determines how well the model predicts responses for new observation. The Box-Behnken response surface design comprised 15 runs and included 3 center points. A more detailed description of the applied measurement method is given in Ref. [43]. A quadratic model was chosen for describing the influence of the investigated operating parameters on the SBR values, nonetheless, insignificant terms (at the significance level $\alpha > 0.15$, meaning the confidence level <85%) were removed from it.

At this stage of research, the analytes concentration was lowered to 100 mg L^{-1} for the FLA-APGD system and remained 1000 mg L^{-1} in the case of the FLC-APGD system.

Analyzing the data depicted in Table 2 and in Figs. SI-2 and SI-3, it might be noted that the dependency of the SBRs of the Br and Cl analytical lines on all optimizing parameters was meaningful for both studied systems. In the case of the FLA-APGD system, the increase of the discharge current lowered the analytes signals intensity and this effect was independent on the remaining parameters values. This finding differed from the vast majority of the literature data concerning FLA-APGD, indicating that the analytes response was actually boosted with the discharge current growth, which was attributed to an improved transport efficiency of the studied elements into the discharge [15,

Table 2
Statistically significant terms in the regression equations modeling the effect of the studied parameters A, B, and C on the signal to background ratio (SBR) of the analytical lines of Br and Cl.

System	Analyte	Coefficients of regression equation									
		Const.	A	B	C	A^2	B^2	C^2	A·B	A·C	B·C
FLA-APGD	Br	33.50	−1.191	−0.0274	0.420	0.00910	–	–	0.000767	–	–
	Cl	3.71	−0.2044	0.00635	0.383	0.002431	–	–	−0.000080	−0.00450	−0.000772
FLC-APGD	Br	6.28	−0.1157	0.0235	5.343	–	−0.000151	−0.9845	0.000672	0.0597	−0.00300
	Cl	0.890	−0.00129	0.00611	0.1794	–	−0.000016	−0.0754	–	0.00667	–

A – discharge current (mA), B – gas flow rate (mL min^{-1}), C – sample flow rate (mL min^{-1}).

23–25,44]. Nevertheless, this effect could not affect the analytes signal intensities herein, due to molecular forms, in which the analytes were introduced into the discharge (see Comment SI-3 for a more detailed follow-up on this issue). Therefore, it could be stated that there was another factor, strictly related to Br and Cl themselves, having a bigger impact on the analytes responses in FLA-APGD than the improvement of the atomization/excitation conditions. For instance, assuming that the examined analytes are introduced into the discharge mostly as Br_2 and Cl_2 and considering the fact that an increase in the discharge current leads to the enhanced water evaporation [45], it could be concluded that the enhanced water evaporation limited the amount of Br_2 and Cl_2 that could enter the discharge, leading to the observed decline of the SBRs of the Br and Cl analytical lines.

Regarding the He flow rate for the FLC-APGD system, its increase resulted in a gradual decline of the SBRs of the analytical lines of both analytes, which did not depend on the values on the remaining parameters either. Those results are in good agreement with some previous literature data concerning FLC-APGD [23,46]. Such outcomes were likely a result of a hindered diffusion of the analyte atoms or their molecular species into the discharge phase at a stronger gas flux applied. Utterly diverse findings were obtained in the case of the FLA-APGD system. For Br, the growth of the He flow rate resulted in its signal intensity boost, regardless of the applied sample flow rate. However, this parameter was found to be dependent on the discharge current as for higher discharge currents the Br signal intensity still grew with the increased gas flow rate but for lower discharge currents it was declined. Moreover, this kind of dependency was not the case for Cl; the SBRs of the analytical line of this element were enhanced with the growing gas flow rate, regardless of the applied discharge current but the impact of the He flow rate was found to be affected by the sample flow rate.

In the case of the sample flow rate, its growth led to a general increase of the SBRs of the analytical lines for the FLC-APGD system. Only small dependency on the remaining parameters was noted as the mentioned increase was stronger for higher discharge currents and lower gas flow rates. Those outcomes were again in good agreement with the majority of the previously reported ones [19,23,42]. A likely clarification of the received outcomes might be attributed to a lower water evaporation rate observed at higher sample flow rates, which would facilitate the transport of the studied elements and/or improve the excitation conditions in the plasma. Regarding the FLA-APGD system, the growing sample flow rate was found to enhance the SBRs, regardless of the discharge current and the sample flow rate applied but only in the case of the Br analytical line. For Cl, the impact of the sample flow rate on the SBRs of its analytical line was dependent on both the discharge current and the gas flow rate. For lower discharge currents and higher gas flow rates the SBR values increased along with the grow of the sample flow rate, whereas the opposite was observed for higher discharge currents and lower He flow rates.

All abovementioned observations concerning the impact of the gas and sample flow rates on the analytes signal intensities found for the FLA-APGD system are much more troublesome to explain. Nonetheless, it could be assumed that the observed tendencies were a resultant of the way the studied analytes were transported into discharge and the impact of those parameters on the discharge itself, *e.g.*, the atomization/excitation conditions, the electrical conductivity of the FLA solution, the analytes residence time in the discharge, etc. Bearing in mind that there was no such obvious dependency of the same parameters on themselves for the FLC-APGD system, it could be presumed they were related to the mechanism of the analyte transport to the discharge to a larger extent. It was also evident that there was a strong relationship between all tested parameters for the FLA-APGD system, which would be certainly overlooked using the OFAT approach, likely resulting in choosing less favorable operating conditions for further experiments.

Therefore the optimal operating conditions were as follows: the discharge current of 50 mA, the gas flow rate of 150 mL min^{-1}, and the sample flow rate of 4.0 mL min^{-1} for FLC-APGD as well as the discharge current of 30 mA, the gas flow rate of 150 (Br) or 350 (Cl) mL min^{-1}, and the sample flow rate of 4.0 mL min^{-1} for FLA-APGD. However, the sample flow rate of 4.0 mL min^{-1} was considered to be relatively high taking into account possibly limited amounts of samples or the samples preparation procedure involving their digestion as well as small differences of the SBRs of the Br analytical line in the range of 2.5–4.0 mL min^{-1}. Hence, the sample flow rate of 3.0 mL min^{-1}, along with the abovementioned values of the remaining parameters, was applied in the further part of this study as compromise conditions. Moreover, the optimal values of the He flow rate varied for FLA-APGD, depending on the analyte, therefore the gas flow rate of 300 mL min^{-1} was applied as a compromise condition, considering a lower sensitivity of the Cl analytical line in this case.

As can be seen from Tables SI–2, the values of the goodness-of-fit statistics were mostly over 90%, meaning the received regression equations well explained the experimental data and could be applied for predicting new data with fair credibility. To further validate the established models, the SBRs of the analytical lines of both analytes were measured under the compromise conditions and the received results were compared to those, predicted by the models. It was established that the obtained SBRs were in good agreement with the predicted ones (relative errors changing in the 10–19% range), which proved that the models could predict new data with fine reliability.

3.3. Analytical performance

The analytical performance of the studied APGD-based systems for the determination of Br and Cl with the OES detection was evaluated under the previously mentioned compromise conditions. For this purpose, the DLs of the studied elements, the upper linearity ranges of calibration curves, the sensitivity of the analytical lines, and the precision were assessed for both investigated systems. DLs were calculated as 3σ/a, where “3σ" stands for 3 times the standard deviation of 30 consecutive measurements of an appropriate blank solution, and “a" stands for the sensitivity of a corresponding calibration curve. The upper linearity ranges were determined using 9 mixed standard solutions of Br and Cl at concentrations ranging either from 1 (FLA-APGD) or 30 (FLC-APGD) mg L^{-1} up to 5000 mg L^{-1}. The precision was expressed as the relative standard deviation (RSD) for 10 consecutive measurements of a mixed solution containing either 10 (FLA-APGD) or 50 (FLC-APGD) mg L^{-1} of each analyte. The RSD was measured 3 times and the averaged results were given. The analytical figures of merit achieved by both studied systems are shown in Table 3.

The DLs obtained under the compromise conditions for Br were equal 0.15 and 2.1 mg L^{-1} for FLA- and FLC-APGD, respectively. In the case of Cl, the DLs were around one order of magnitude higher, giving values of 1.5 and 18 mg L^{-1} for FLA- and FLC-APGD, respectively. Similar relationships between the DLs provided by the FLA- and FLC-APGD systems were earlier presented by Greda et al. [16], for other elements. Although the attained DLs were relatively high, with particular

Table 3
The analytical performance of the studied APGD-based systems combined with the OES detection for the determination of Br and Cl.

	FLA-APGD		FLC-APGD	
	Br	Cl	Br	Cl
Detection limit (mg L^{-1})	0.15	1.5	2.1	18
ULR (mg L^{-1})	1000	500	5000	1000
R^2	0.9994	0.9999	0.9994	0.9973
Sensitivity (a.u. per mg L^{-1})	$1.95{\cdot}10^3$	$3.00{\cdot}10^2$	$3.45{\cdot}10^2$	$3.9.0{\cdot}10^1$
RSD (%)[a]	1.24	2.86	0.60	2.82

FLA-APGD – flowing liquid anode atmospheric pressure glow discharge.
FLC-APGD – flowing liquid cathode atmospheric pressure glow discharge.
ULR – upper linearity range.
RSD – relative standard deviation.
[a] For the analytes concentration of 10 (FLA-APGD) or 50 (FLC-APGD) mg L^{-1}.

reference to FLC-APGD, real samples contain usually high amounts of those analytes (see Comment SI-4).

The upper linearity ($R^2 > 0.995$) ranges varied depending on the element and the discharge type. Generally, they were lower for FLA-APGD and – for each studied system – they were higher for Br. The extents of the linearity of calibration curves were over 2 (Cl) or 3 (Br) orders of magnitude for FLA-APGD and only over 1 (Cl) and 3 (Br) for FLC-APGD (in reference to the DLs).

The measurements precision was not dependent on the discharge type and was excellent for both of them. For Br the RSD was around 1%, whereas for Cl it was around 3%. Higher RSDs received for Cl in both APGD-based systems was an obvious consequence of its lower sensitivity. Nevertheless, it was still established to be very good, considering the fact that the concentration of Cl in the analyzed solution exceeded its DL only 6.7 (FLA-APGD) and 2.8 (FLC-APGD) times.

Therefore, it could be concluded that the DLs, being notably lower as compared to the analytes concentration in real samples (especially in the case of the FLA-APGD system), along with acceptable upper linearity ranges and excellent precision, make the proposed APGD-based systems very attractive for the determination of Br and Cl by OES. Especially, when compared to the currently applied large-scale and expensive instrumentation such as ionic chromatography, or ICP-based techniques (see Comment SI-4 and the values of DLs of Br and Cl achievable with ICP-OES using a standard pneumatic nebulization sample introduction system and the measurement parameters listed in Table SI-3). The proposed systems could be also competitive for conventional titration techniques as, although they do not require any expensive and complex instrumentation, they do not allow to determine the Br^- and Cl^- anions simultaneously and/or in the presence of other analytes (*e.g.*, I^- or SCN^- anions).

3.4. The effect of foreign ions

As mentioned in the earlier parts of this paper, it is believed that the analytes are transported into the discharge by the liquid cathode sputtering in the case of FLC-APGD and as some kind of volatile forms, generated in the gas-liquid phase in the reaction with solvated electrons, in the case of analyte cations introduced into FLA-APGD. Thus, it could be expected that the presence of foreign ions would affect the analytes signal intensities for the FLC-APGD system, as those ions are sputtered into the discharge as well, and would not have major impact on the analytes signals for the FLA-APGD system, since – except for a few elements that may be determined with the aid of this source – foreign ions do not reach the plasma. However, according to results presented previously, regarding both those sources, the opposite is valid. For FLC-APGD, interferences caused by the presence (even at high concentrations) of foreign ions are not usually observed [4,42] or their extent is small [19], whereas even low concentrations of many commonly occurred foreign ions (particularly alkali and alkaline earth metals as well as transition metals) cause serious matrix effects for the FLA-APGD system [16,25,26]. Therefore, since the APGD-based systems, studied herein, have never been applied for the determination of any anionic analytes, the impact of ions that commonly occur in many environmental, food, and metallurgical samples on the Br and Cl signal intensities was investigated.

Considering the need of applying relatively high analytes concentrations (in case their signals would be significantly suppressed by the interfering ions), even higher concentrations of potentially interfering elements had to be studied. Hence, the impact of the foreign ions on the analytes signals intensities was tested using salts of commonly occurred ions, instead of adding single ions separately. That being said, appropriate amounts of solid $Fe(NO_3)_3$, NH_4NO_3, K_2SO_4, $MgSO_4$, KI, NH_4F, $KMnO_4$, $NaHCO_3$, KH_2PO_4, $K_2Cr_2O_7$, Na_2S, and $Ca(NO_3)_2$ were used to prepare their standard solutions, which were subsequently added to a mixed solution of Br and Cl (at the concentration of 100 and 1000 mg L^{-1} for FLA- and FLC-APGD, respectively) to reach the final salts concentrations of 2 and 20 g L^{-1} (for both systems). Such concentrations of the tested salts were chosen in order to cover both a level of interfering elements close to the actual one, occurring in real samples (2 g L^{-1}), as well as a relatively high analyte-to-interfering ions concentration ratio (20 g L^{-1}). The measured response of Br and Cl was their signal intensities which was normalized in regard to the signal intensities obtained for a solution that did not contain any interfering ions.

The obtained results are depicted in Fig. 3 and indicate that no major interferences took place for the salts concentration of 2 g L^{-1}, regardless of the system type; except NH_4F and Na_2S, whose presence resulted in suppressing the normalized signal intensity of Cl in FLC-APGD up to 0.59 and 0.52, respectively. Also, some matrix effects were observed for the FLA-APGD system after adding 2 g L^{-1} of KI (the normalized signal intensity was equal to 0.76) as well as 2 g L^{-1} of $KMnO_4$ (the normalized signal intensity equal to 0.58). As for the interfering ions concentration of 20 g L^{-1}, some matrix effects could be noted. In the case of FLA-APGD, although the presence of 20 g L^{-1} of K_2SO_4, $MgSO_4$, $NaHCO_3$ KH_2PO_4, and – for Br – NH_4F still did not cause any interfering effects, the presence of the remaining salts resulted in receiving the normalized signal intensities being from 0.06 (KI) to 0.75 (Na_2S) and 0 (KI) to 0.75 (NH_4F) for Br and Cl, respectively. In the case of the FLC-APGD system, the discharge could not be stably sustained in the presence of 20 g L^{-1} of K_2SO_4 and Na_2S. Concerning the rest of the studied salts (at the same concentration), the matrix effects were observed for all of them (except $Fe(NO_3)_3$ that did not interfered with Cl), however, the presence of Fe $(NO_3)_3$, NH_4NO_3, $MgSO_4$, NH_4F, and $Ca(NO_3)_2$ suppressed the signal intensity of Br to a lower extent (the normalized signal intensities ranged within 0.69–0.79). The impact of KI on the response of both analytes was again the most devastating as the normalized signal intensities in the presence of this salt were equal to 0.18 and 0.05 for Br and Cl, respectively.

The above described results were quite unexpected, with particular reference to the FLA-APGD system. Taking into account that the other analytes are supposedly transported into the discharge in the form of some kind of volatile species and assuming the same is true for Br and Cl, it should be expected the presence of foreign ions in the FLA solutions would affect the Br and Cl signals as well. This indeed seemed to be the case for KI and – when higher concentrations were studied – for Na_2S (particularly when concerning Cl). A likely clarification for that were the competitive reactions, resulting in the formation of gaseous I_2 and H_2S, taking place in both the FLA and FLC solutions. However, the lack of significant matrix effects for the vast majority of the remaining salts in the case of the FLA-APGD system suggests that the presence of foreign ions in the FLA solutions interferes with the reduction process (in the case of cations) but have no major impact on the formation of gaseous Br_2 and Cl_2 in the analyzed solution and/or is not an issue for the oxidation process of the anionic analytes.

Considering the matrix effects observed for the FLC-APGD system, it was previously hypothesized [42] that they may result from some secondary reactions/processes taking place in the discharge and yielding the formation of some kind of analytes species that are unviable to be further atomized and excited. This postulate could be actually supported by the results presented herein, indicating the presence of the matrix effects is dependent rather on the analyte-to-interfering ions concentration ratio that the foreign ions concentration itself.

To sum up, it was concluded that the matrix effects that occurred for the studied APGD-based systems were not significant (especially in the case of FLA-APGD) since foreign ions rarely are present in real samples at concentrations as high as 20 g L^{-1}.

3.5. Real sample analysis

To demonstrate the trueness of the proposed methods and turn the spotlight on the impact of the organic matrix on the signals of the studied analytes, an attempt was made to determine both analytes in several water and juices samples, with the aid of both investigated

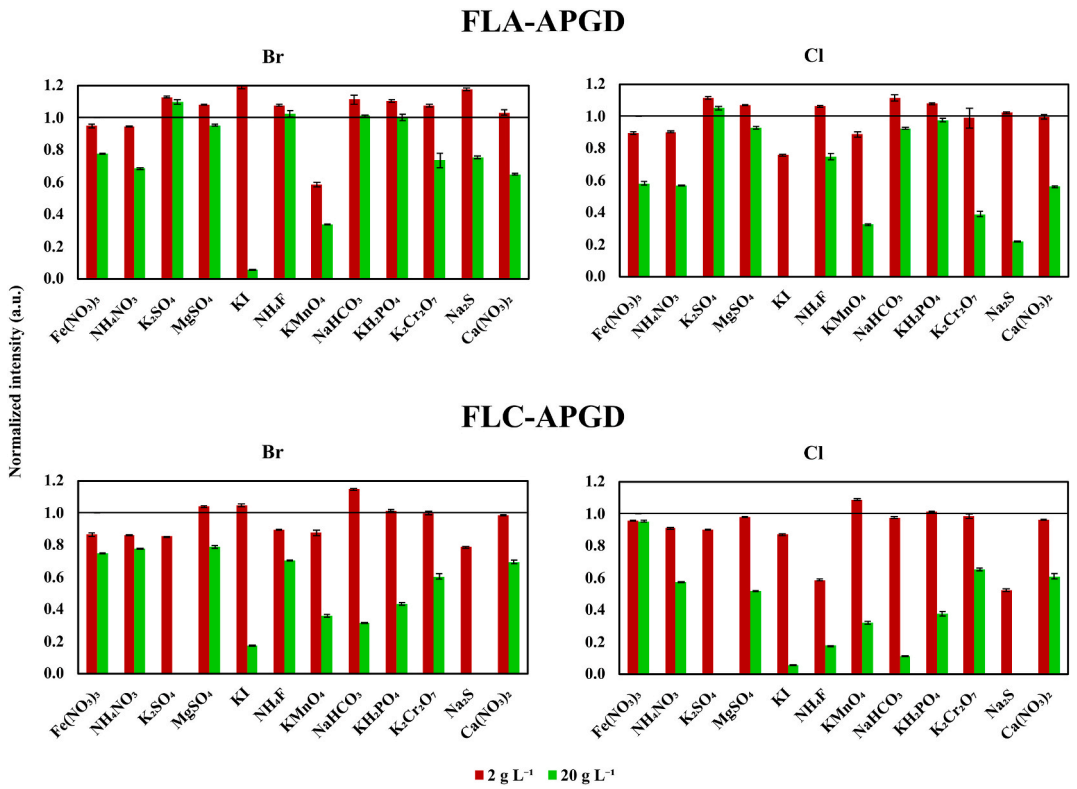

Fig. 3. The effect of different salts (at a concentration of 2 and 20 g L^{-1}) on the signal intensity of Br and Cl for the studied APGD-based systems. The missing bars for 20 g L^{-1} of K_2SO_4 and Na_2S are due to the plasma instability in contact with those solutions, which precluded taking measurements.

excitation sources. As no suitable reference material was available in our laboratory, samples of mineral medicinal water, river, sea, and tap waters as well as beetroot and tomato juices were chosen for this purpose. To assure the best possible credibility of the obtained results, all samples were analyzed in regard to both the external standard calibration and using the standard addition method. Moreover, the Cl concentration in the analyzed samples was additionally determined by the ICP-OES technique, due to the lack of the ion chromatography instrumentation in our laboratory. In the latter case, the water samples were analyzed *versus* the external standard calibration. As for juices, they could not be reliably analyzed with the aid of the same calibration method, due to a complex organic matrix, present in them [5]. On the other hand, the conventional digestion process likewise could not be applied due to a potential oxidation of the Cl^- ions to Cl_2, leading to the analyte loss. Therefore, the application of the standard additions method was considered to be the best solution for this issue. Nevertheless, the DL of Cl for the ICP-OES technique, assessed on this occasion, was really high, *i.e.*, 96 mg L^{-1}. Hence, the ICP-OES measurements were treated rather as additional ones, but not the reference ones. The suitability of the proposed methods for the real samples analysis was evaluated by comparing all results, obtained for a given sample, *i.e.*, of both methods and both calibration strategies as well as the outcomes provided by the ICP-OES technique or comparing the received results with the spiked concentrations.

In order to show the effectiveness of the proposed methods for the real samples analysis, an attempt was made to determine both analytes at relatively low concentration levels. Therefore, after performing some preliminary studies, the analyzed samples were diluted 2- (tap water), 5- (river water), 10- (mineral water), 60- (juices), and 100-fold (sea water) for FLA-APGD and 0- (undiluted, tap and river water), 2- (mineral water), 20- (juices), and 100-fold (sea water) for FLC-APGD.

At first, the samples were analyzed with the aid of both studied systems. It was established (analyzing the results obtained for both systems, and considering especially the FLA-APGD measurements, due to lower DL of Br for that system) that Br was not present in any of the analyzed samples. Therefore, the samples were spiked with 50 (FLA-APGD) or 100 (FLC-APGD) mg L^{-1} of Br.

As can be seen from Table 4, the ICP-OES technique did not allow to measure the Cl concentration in tap and river waters, due to too high DL of this element. Nevertheless, the results obtained for FLA- and FLC-APGD-OES techniques and both calibration methods, generally were in good agreement with each other; the coefficients of variations (CVs) between the results for each sample (calculated for all results obtained for a given sample, *i.e.*, of both methods and both calibration strategies), usually ranged within 5–7%. Only the results concerning the Cl concentration in river water (FLC-APGD) and tomato juice (FLA-APGD) (both determined using the external standard calibration) misfitted the remaining obtained values. This was likely due to the organic matrix present in those samples, which possibly affected the analyte signal as well as the plasma stability (with particular reference to FLC-APGD).

Similar results were obtained for Br (see Table 5). Although the Br content could not be determined with the aid of the ICP-OES technique due to its high DL (44 mg L^{-1}), the received, results – in most cases – agreed well with the spiked concentrations as well as between themselves. However, the concentrations obtained for FLC-APGD, using the external standard calibration, were significantly higher, especially in the case of river water and both juices.

Regarding the standard deviations (SDs) received for individual results, in the vast majority of cases, they corresponded to the RSDs of obtained individual results being <5% for all applied methods and proved their good precision. Hence, it was concluded that all three methods provided accurate results and both studied APGD-based methods could be applied for the real sample analysis. Obviously, the standard addition method assured better results, however, significant differences between the two calibration strategies were observed only in a few cases and particularly for FLC-APGD. The agreement, observed in most cases, between the values received using both calibration methods supported the earlier assumption that the presence of foreign ions in the

Table 4
The results of the determination of the Cl concentration (in mg L^{-1}) in waters and juices by the developed APGD-OES methods as well as the ICP-OES method.

Method	Calibration	Sample					
		Mineral medicinal water	River water	Sea water	Tap water	Beetroot juice	Tomato juice
FLA-APGD	ESC	1082 ± 19	109.2 ± 5.2	25300 ± 851	39.64 ± 0.36	3617 ± 180	3583 ± 223
	SAM	910.2 ± 16.3	97.61 ± 3.77	23410 ± 930	34.14 ± 0.76	3792 ± 144	4462 ± 116
FLC-APGD	ESC	972.3 ± 32.3	144.1 ± 11.2	25580 ± 570	39.16 ± 0.35	3453 ± 148	4429 ± 73
	SAM	1069 ± 68	105.9 ± 9.0	22080 ± 900	37.44 ± 2.18	3940 ± 239	4708 ± 11
ICP-OES	ESC	1010 ± 7	<DL	24640 ± 2009	<DL	–	–
	SAM	–	–	–	–	3522 ± 198	4858 ± 166

ESC – external standard calibration.
SAM – standard addition method.
DL – detection limit.

Table 5
The results of the determination of Br spiked into waters and juices by the developed APGD-OES methods. The concentration of the spiked Br was 50 mg L^{-1} for FLA-APGD and 100 mg L^{-1} for FLC-APGD.

Method	Calibration	Sample					
		Mineral medicinal water	River water	Sea water	Tap water	Beetroot juice	Tomato juice
FLA-APGD	ESC	45.85 ± 0.28	45.54 ± 1.70	44.85 ± 0.29	48.61 ± 0.48	45.61 ± 1.61	44.14 ± 0.42
	SAM	48.43 ± 0.26	49.23 ± 3.21	46.34 ± 1.78	46.10 ± 0.15	48.50 ± 1.58	54.89 ± 2.98
FLC-APGD	ESC	103.9 ± 4.4	134.1 ± 5.6	114.9 ± 2.4	115.6 ± 2.1	140.8 ± 2.8	135.0 ± 3.5
	SAM	104.8 ± 0.5	100.6 ± 3.3	109.4 ± 2.5	103.8 ± 0.4	108.7 ± 3.9	100.4 ± 4.6

ESC – external standard calibration.
SAM – standard addition method.

analyzed samples is not an issue as long as their concentration is not significantly higher, compared to the analytes concentration. Furthermore, even the organic matrix was not as troublesome as in our recent work concerning the determination of K, Na, Ca and Mg in juices [5], most likely due to the inability of halides to form complexes with organic constituents of samples as it is the case with Ca and Mg. However, it had some impact on the discharge stability in the case of FLC-APGD.

Based on the present work findings, it was concluded that the developed APGD-based methods were appropriate for determining Br and Cl concentrations in commonly analyzed samples, such as waters or juices and could be a suitable alternative for other frequently applied techniques as they offer the advantages of miniaturized construction, reduced power and gas consumption as well as manufacturing and operation costs that are meaningfully lower as compared to the currently used bulky instrumentation, *e.g.*, ion chromatography, ICP-OES, and ICP-MS.

4. Conclusions

In this work, the performance of the FLA- and FLC-APGD systems for the determination of Br and Cl by OES was evaluated. This was the first time when the abovementioned systems were applied for the determination of anions. Some conclusions regarding the mechanism of the studied analytes transport into the discharge as well as the transport taking place when other elements are introduced into discharge were drawn by analyzing the emission spectra, acquired for both systems, the results obtained during the optimization step as well as the impact of the presence of foreign ions on the analytes signals. The application of the DoE approach for performing optimization contributed to drawing some of the aforesaid conclusions and choosing the most suitable operating conditions, which could be overlooked when using the conventional (OFAT) approach.

Although the obtained DLs were relatively high, as compared to those achievable for metals, they turned out to be low enough for determining the Cl content in some real samples. An effort was made to determine the analytes concentration in the selected samples with the best possible credibility, by using two calibration methods, and compare the received results between FLA- and FLC-APGD-OES as well as with outcomes provided by an additional technique (ICP-OES) or obtained from the spike-and-recovery test (Br). It was established that all those results well agreed with each other, especially in the case of the FLA-APGD technique, which means that not only the analysis could be carried out using the two systems and gave reliable results, but also that – in most cases – it could be performed using the external standard calibration.

Both of the developed methods turned out to be quite insusceptible to matrix effects coming from foreign ions, present in real samples. Noteworthy, FLA-APGD was found to be more resistant to interferences than FLC-APGD, which had never been the case before. Moreover, the operation of FLA-APGD was more stable when a sample contained huge amounts (20 g L^{-1}) of interfering constituents. Regarding the stability of FLA-APGD, it is also worth to note that it could be operated in a wider range of the acid concentrations, which could be helpful in analyzing previously digested samples. Lower DLs provided by the FLA-APGD system were another advantage of this technique. However, although this was not studied in this work, it is well known that FLC-APGD system can be easily operated with a solid (*e.g.*, tungsten) anode instead of the He jet, which could further reduce the operating costs of analysis. Taking all of this into account, it was concluded that FLA-APGD generally is more suitable for the determination of Br and Cl in real samples. Nevertheless, both methods assured reliable results, therefore, in the case of higher analytes concentrations, FLC-APGD is also an accurate and efficient tool, especially if it could be operated without the He jet.

Author statements

Conceptualization – Monika Gorska, Pawel Pohl; Data curation – Monika Gorska; Formal analysis – Monika Gorska; Funding acquisition – Pawel Pohl; Investigation – Monika Gorska; Methodology – Monika Gorska; Project administration – Monika Gorska; Resources – Pawel Pohl; Software – Monika Gorska; Supervision – Pawel Pohl; Validation – Monika Gorska; Visualization – Monika Gorska; Writing - original draft – Monika Gorska; Writing - review & editing – Pawel Pohl, Monika Gorska.

Declaration of competing interest

The author declares that he has no known competing financial interests or personal relationships that could have appeared to influence the work reported in this paper.

Appendix A. Supplementary data

Supplementary data to this article can be found online at https://doi.org/10.1016/j.talanta.2021.122921.

References

[1] H. Jeong, J. Young Choi, J. Lee, J. Lim, K. Ra, Heavy metal pollution by road-deposited sediments and its contribution to total suspended solids in rainfall runoff from intensive industrial areas, Environ. Pollut. 265 (2020) 115028, https://doi.org/10.1016/j.envpol.2020.115028.

[2] C. Femina Carolin, P. Senthil Kumar, A. Saravanan, G. Janet Joshiba, M. Naushad, Efficient techniques for the removal of toxic heavy metals from aquatic environment: a review, J. Environ. Chem. Eng. 5 (2017) 2782–2799, https://doi.org/10.1016/j.jece.2017.05.029.

[3] H. Tian, K. Cheng, Y. Wang, D. Zhao, L. Lu, W. Jia, J. Hao, Temporal and spatial variation characteristics of atmospheric emissions of Cd, Cr, and Pb from coal in China, Atmos. Environ. 50 (2012) 157–163, https://doi.org/10.1016/j.atmosenv.2011.12.045.

[4] K. Swiderski, P. Pohl, P. Jamroz, A miniaturized atmospheric pressure glow microdischarge system generated in contact with a hanging drop electrode – a new approach to spectrochemical analysis of liquid microsamples, J. Anal. At. Spectrom. 34 (2019) 1287–1293, https://doi.org/10.1039/C9JA00038K.

[5] M. Gorska, P. Pohl, Simplified and rapid determination of Ca, K, Mg, and Na in fruit juices by flowing liquid cathode atmospheric glow discharge optical emission spectrometry, J. Anal. At. Spectrom. 36 (2021) 1455–1465, https://doi.org/10.1039/D1JA00127B.

[6] P. Pohl, A. Bielawska-Pohl, A. Dzimitrowicz, P. Jamroz, M. Welna, Impact and practicability of recently introduced requirements on elemental impurities, Trends Anal. Chem. 101 (2018) 43–55, https://doi.org/10.1016/j.trac.2017.09.011.

[7] T.L. Marques, H. Wiltsche, J.A. Nobrega, M. Winkler, G. Knapp, Performance evaluation of a high-pressure microwave-assisted flow digestion system for juice and milk sample preparation, Anal. Bionanal. Chem. 409 (2017) 4449–4458, https://doi.org/10.1007/s00216-017-0388-5.

[8] G. Cristea, A. Dehelean, C. Voica, I. Feher, R. Puscas, D. Alina Magdas, Isotopic and elemental analysis of apple and orange juice by isotope ratio mass spectrometry (IRMS) and inductively coupled plasma – mass spectrometry (ICP-MS), Anal. Lett. 54 (2021) 212–226, https://doi.org/10.1080/00032719.2020.1743717.

[9] N. Khan, I. Seon Jeong, I. Min Hwang, J. Sung Kim, S. Hwa Choi, E. Yeong Nho, J. Yeon Choi, K. Su Park, K. Su Kim, Analysis of minor and trace elements in milk and yogurts by inductively coupled plasma-mass spectrometry (ICP-MS), Food Chem. 147 (2014) 220–224, https://doi.org/10.1016/j.foodchem.2013.09.147.

[10] A. Giorgia Potorti, G. Di Bella, V. Lo Turco, R. Rando, G. Dugo, Non-toxic and potentially toxic elements in Italian donkey milk by ICP-MS and multivariate analysis, J. Food Compos. Anal. 31 (2013) 161–172, https://doi.org/10.1016/j.jfca.2013.05.006.

[11] S.M. El-Safty, M.A. Khorshed, M.M. Ghuniem, Rapid determination of mercury in dust emission using cold vapour inductively coupled plasma optical emission spectrometer (CV ICP OES), Int. J. Environ. Anal. Chem. (2020) 1–23, https://doi.org/10.1080/03067319.2020.1720012.

[12] T. Cserfalvi, P. Mezei, P. Apai, Emission studies on a glow discharge in atmospheric pressure air using water as a cathode, J. Phys. D Appl. Phys. 26 (1993) 2184–2188, https://doi.org/10.1088/0022-3727/26/12/015.

[13] M.R. Webb, F.J. Andrade, G. Gamez, R. McCrindle, G.M. Hieftje, Spectroscopic and electrical studies of a solution-cathode glow discharge, J. Anal. At. Spectrom. 20 (2005) 1218–1225, https://doi.org/10.1039/B503961D.

[14] P. Jamroz, W. Zyrnicki, Spectroscopic characterization of miniaturized atmospheric-pressure dc glow discharge generated in contact with flowing small size liquid cathode, Plasma Chem. Plasma Process. 31 (2011) 681–696, https://doi.org/10.1007/s11090-011-9307-2.

[15] X. Liu, Z. Zhu, D. He, H. Zheng, Y. Gan, N. Stanley Belshaw, S. Hu, Y. Wang, Highly sensitive elemental analysis of Cd and Zn by solution anode glow discharge atomic emission spectrometry, J. Anal. At. Spectrom. 31 (2016) 1089–1096, https://doi.org/10.1039/C6JA00017G.

[16] K. Greda, K. Swiderski, P. Jamroz, P. Pohl, Flowing liquid anode atmospheric pressure glow discharge as an excitation source for optical emission spectrometry with the improved detectability of Ag, Cd, Hg, Pb, Tl, and Zn, Anal. Chem. 88 (2016) 8812–8820, https://doi.org/10.1021/acs.analchem.6b02250.

[17] P. Jamroz, K. Greda, A. Dzimitrowicz, K. Swiderski, P. Pohl, Sensitive determination of Cd in small-volume samples by miniaturized liquid drop anode atmospheric pressure glow discharge optical emission spectrometry, Anal. Chem. 89 (2017) 5729–5733, https://doi.org/10.1021/acs.analchem.7b01198.

[18] K. Greda, P. Jamroz, A. Dzimitrowicz, P. Pohl, Direct elemental analysis of honeys by atmospheric pressure glow discharge generated in contact with a flowing liquid cathode, J. Anal. At. Spectrom. 30 (2015) 154–161, https://doi.org/10.1039/C4JA00261J.

[19] J. Yu, Z. Zhang, Q. Lu, D. Sun, S. Zhu, X. Zhang, X. Wang, W. Yang, High-sensitivity determination of K, Ca, Na, and Mg in salt mines samples by atomic emission spectrometry with a miniaturized liquid cathode glow discharge, J. Anal. Methods Chem. (2017) 7105831, https://doi.org/10.1155/2017/7105831, 2017.

[20] J. Yu, X. Zhang, Q. Lu, L. Yin, F. Feng, H. Luo, Y. Kang, Liquid cathode glow discharge as an excitation source for the analysis of complex water samples with atomic emission spectrometry, ACS Omega 5 (2020) 19541–19547, https://doi.org/10.1021/acsomega.0c01906.

[21] P. Zheng, W. Li, J. Wang, X. Zhai, X. Mao, X. Wang, C. Lai, Spatially resolved characteristics of solution cathode glow discharge source coupled with an interference filter wheel as spectral discrimination device, Anal. Lett. 53 (2020) 31–39, https://doi.org/10.1080/00032719.2019.1636060.

[22] Y.-J. Zhou, J. Ma, F. Li, T. Xian, Q.-H. Yuan, Q.-F. Lu, Sensitivity improvement of solution cathode glow discharge-optical emission spectrometry by external magnetic field for optical determination of elements, Microchem. J. 158 (2020) 105224, https://doi.org/10.1016/j.microc.2020.105224.

[23] M. Gorska, K. Greda, P. Pohl, Determination of bismuth by optical emission spectrometry with liquid anode/cathode atmospheric pressure glow discharge, J. Anal. At. Spectrom. 36 (2021) 165–177, https://doi.org/10.1039/D0JA00401D.

[24] K. Greda, M. Gorska, M. Welna, P. Jamroz, P. Pohl, In-situ generation of Ag, Cd, Hg, In, Pb, Tl and Zn volatile species by flowing liquid anode atmospheric pressure glow discharge operated in gaseous jet mode - evaluation of excitation processes and analytical performance, Talanta 199 (2019) 107–115, https://doi.org/10.1016/j.talanta.2019.02.058.

[25] X. Liu, Z. Liu, Z. Zhu, D. He, S. Yao, H. Zheng, S. Hu, Generation of volatile cadmium and zinc species based on solution anode glow discharge induced plasma electrochemical processes, Anal. Chem. 89 (2017) 3739–3746, https://doi.org/10.1021/acs.analchem.7b00126.

[26] M. Gorska, P. Pohl, K. Greda, The application of antioxidant compounds to minimize matrix effects in flowing liquid anode atmospheric pressure glow discharge optical emission spectrometry, Microchem. J. 164 (2021) 105975, https://doi.org/10.1016/j.microc.2021.105975.

[27] D.-J. Zhang, Y. Cai, M.-L. Chen, Y.-L. Yu, J.-H. Wang, Dielectric barrier discharge-optical emission spectrometry for the simultaneous determination of halogens, J. Anal. At. Spectrom. 31 (2016) 398–405, https://doi.org/10.1039/C5JA00266D.

[28] P. Pohl, I. Jimenez Zapata, M.A. Amberger, N.H. Bings, J.A.C. Broekaert, Characterization of a microwave microstrip helium plasma with gas-phase sample introduction for the optical emission spectrometric determination of bromine, chlorine, sulfur and carbon using a miniaturized optical fiber spectrometer, Spectrochim. Acta B 63 (2008) 415–421, https://doi.org/10.1016/j.sab.2007.12.005.

[29] X. Jiang, X. Xu, X. Hou, Z. Long, Y. Tian, X. Jiang, F. Xu, C. Zheng, A novel capillary microplasma analytical system: interface-free coupling of glow discharge optical emission spectrometry to capillary electrophoresis, J. Anal. At. Spectrom. 31 (2016) 1423–1429, https://doi.org/10.1039/C6JA00142D.

[30] F. Cacho, L. Machynak, M. Nemecek, E. Beinrohr, Determination of bromide in aqueous solutions via the TlBr molecule using high-resolution continuum source graphite furnace molecular absorption spectrometry, Spectrochim. Acta B 144 (2018) 63–67, https://doi.org/10.1016/j.sab.2018.03.010.

[31] A. Garcia-Figueroa, F. Pena-Pereira, I. Lavilla, C. Bendicho, Headspace single-drop microextraction coupled with microvolume fluorospectrometry for highly sensitive determination of bromide, Talanta 170 (2017) 9–14, https://doi.org/10.1016/j.talanta.2017.03.090.

[32] G.F. Kirkbright, A.F. Ward, T.S. West, The determination of sulphur and phosphorus by atomic emission spectrometry with an induction-coupled high-frequency plasma source, Anal. Chim. Acta 62 (1972) 241–251, https://doi.org/10.1016/0003-2670(72)80030-8.

[33] Z. Kowalewska, Feasibility of high-resolution continuum source molecular absorption spectrometry in flame and furnace for sulphur determination in petroleum products, Spectrochim. Acta B 66 (2011) 546–556, https://doi.org/10.1016/j.sab.2011.06.004.

[34] R.E. Sturgeon, Detection of bromine by ICP-oa-ToF-MS following photochemical vapor generation, Anal. Chem. 87 (2015) 3072–3079, https://doi.org/10.1021/ac504747a.

[35] M.H. Timperley, J.C. Priscu, Determination of nitrogen-15 by optical emission spectrometry using an atomic absorption spectrometer, Analyst 111 (1986) 23–28, https://doi.org/10.1039/AN9861100023.

[36] P. Mezei, T. Cserfalvi, Electrolyte cathode atmospheric glow discharges for direct solution analysis, Appl. Spectrosc. Rev. 42 (2007) 573–604, https://doi.org/10.1080/05704920701624451.

[37] K. Swiderski, A. Dzimitrowicz, P. Jamroz, P. Pohl, Influence of pH and low-molecular weight organic compounds in solution on selected spectroscopic and analytical parameters of flowing liquid anode atmospheric pressure glow discharge (FLA-APGD) for the optical emission spectrometric (OES) determination of Ag, Cd, and Pb, J. Anal. At. Spectrom. 33 (2018) 437–451, https://doi.org/10.1039/C7JA00374A.

[38] P.J. Bruggeman, M.J. Kushner, B.R. Locke, J.G.E. Gardeniers, W.G. Graham, D. B. Graves, R.C.H.M. Hofman-Caris, D. Maric, J.P. Reid, E. Ceriani, D. Fernandez Rivas, J.E. Foster, S.C. Garrick, Y. Gorbanev, S. Hamaguchi, F. Iza, H. Jablonowski, E. Klimova, J. Kolb, F. Krcma, P. Lukes, Z. Machala, I. Marinov, D. Mariotti, S. Mededovic Thagard, D. Minakata, E.C. Neyts, J. Pawlat, Z. Lj Petrovic, R. Pflieger, S. Reuter, D.C. Schram, S. Schröter, M. Shiraiwa, B. Tarabová, P.A. Tsai, J.R.R. Verlet, T. von Woedtke, K.R. Wilson, K. Yasui, G. Zvereva, Plasma–liquid interactions: a review and roadmap, Plasma Sources Sci. Technol. 25 (2016) 53002, https://doi.org/10.1088/0963-0252/25/5/053002.

[39] D. Zehavi, J. Rabani, Oxidation of aqueous bromide ions by hydroxyl radicals. Pulse radiolytic investigation, J. Phys. Chem. 76 (1972) 312–319, https://doi.org/10.1021/j100647a006.
[40] M. Saran, I. Beck-Speier, B. Fellerhoff, G. Bauer, Phagocytic killing of microorganisms by radical processes:consequences of the reaction of hydroxyl radicals with chloride yielding chlorine atoms, Free Radic. Biol. Med. 26 (1999) 482–490, https://doi.org/10.1016/s0891-5849(98)00187-7.
[41] P. Pohl, P. Jamroz, K. Greda, M. Gorska, A. Dzimitrowicz, M. Welna, A. Szymczycha-Madeja, Five years of innovations in development of glow discharges generated in contact with liquids for spectrochemical elemental analysis by optical emission spectrometry, Anal. Chim. Acta 1169 (2021) 338399, https://doi.org/10.1016/j.aca.2021.338399.
[42] Q. Lu, F. Feng, J. Yu, L. Yin, Y. Kang, H. Luo, D. Sun, W. Yang, Determination of trace cadmium in zinc concentrate by liquid cathode glow discharge with a modified sampling system and addition of chemical modifiers for improved sensitivity, Microchem. J. 152 (2020) 104308, https://doi.org/10.1016/j.microc.2019.104308.
[43] K. Greda, K. Kurcbach, K. Ochromowicz, T. Lesniewicz, P. Jamroz, P. Pohl, Determination of mercury in mosses by novel cold vapor generation atmospheric pressure glow microdischarge optical emission spectrometry after multivariate optimization, J. Anal. At. Spectrom. 30 (2015) 1743–1751, https://doi.org/10.1039/C5JA00170F.
[44] M. Gorska, K. Greda, P. Pohl, On the coupling of hydride generation (HG) with flowing liquid anode atmospheric pressure glow discharge (FLA-APGD) for determination of traces of As, Bi, Hg, Sb and Se by optical emission spectrometry (OES), Talanta 222 (2021) 121510, https://doi.org/10.1016/j.talanta.2020.121510.
[45] M. Yuan, X. Peng, F. Ge, Q. Li, K. Wang, D.-G. Yu, Z. Wang, Simplified design for solution anode glow discharge atomic emission spectrometry device for highly sensitive detection of Ag, Bi, Cd, Hg, Pb, Tl, and Zn, Microchem. J. 155 (2020) 104785, https://doi.org/10.1016/j.microc.2020.104785.
[46] K. Greda, P. Jamroz, P. Pohl, Comparison of the performance of direct current atmospheric pressure glow microdischarges operated between a small sized flowing liquid cathode and miniature argon or helium flow microjets, J. Anal. At. Spectrom. 28 (2013) 1233–1241, https://doi.org/10.1039/C3JA50062D.

Supporting Information

Application of atmospheric pressure glow discharge generated in contact with liquids for the determination of chlorides and bromides in water and juice samples by the optical emission spectrometry

Monika Gorska*, Pawel Pohl

Wroclaw University of Science and Technology, Faculty of Chemistry, Division of Analytical Chemistry and Chemical Metallurgy, Wybrzeze Stanislawa Wyspianskiego 27, 50-370 Wroclaw, Poland

* Corresponding author. E-mail address: monika.gorska@pwr.edu.pl (Monika Gorska)

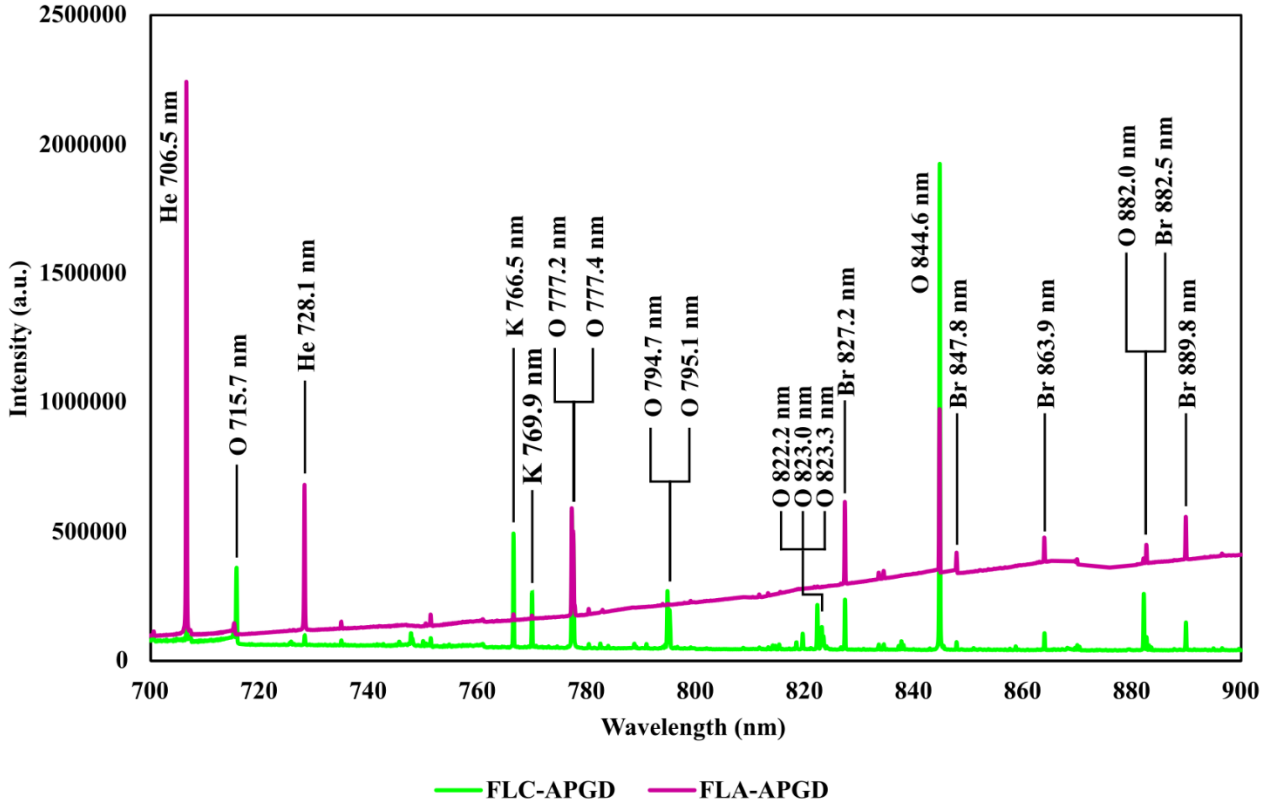

Fig. SI-1. The emission spectra of FLA- and FLC-APGD acquired for a solution containing Br and Cl (at the concentration of 1000 mg L^{-1}) in the spectral range of 700–900 nm.

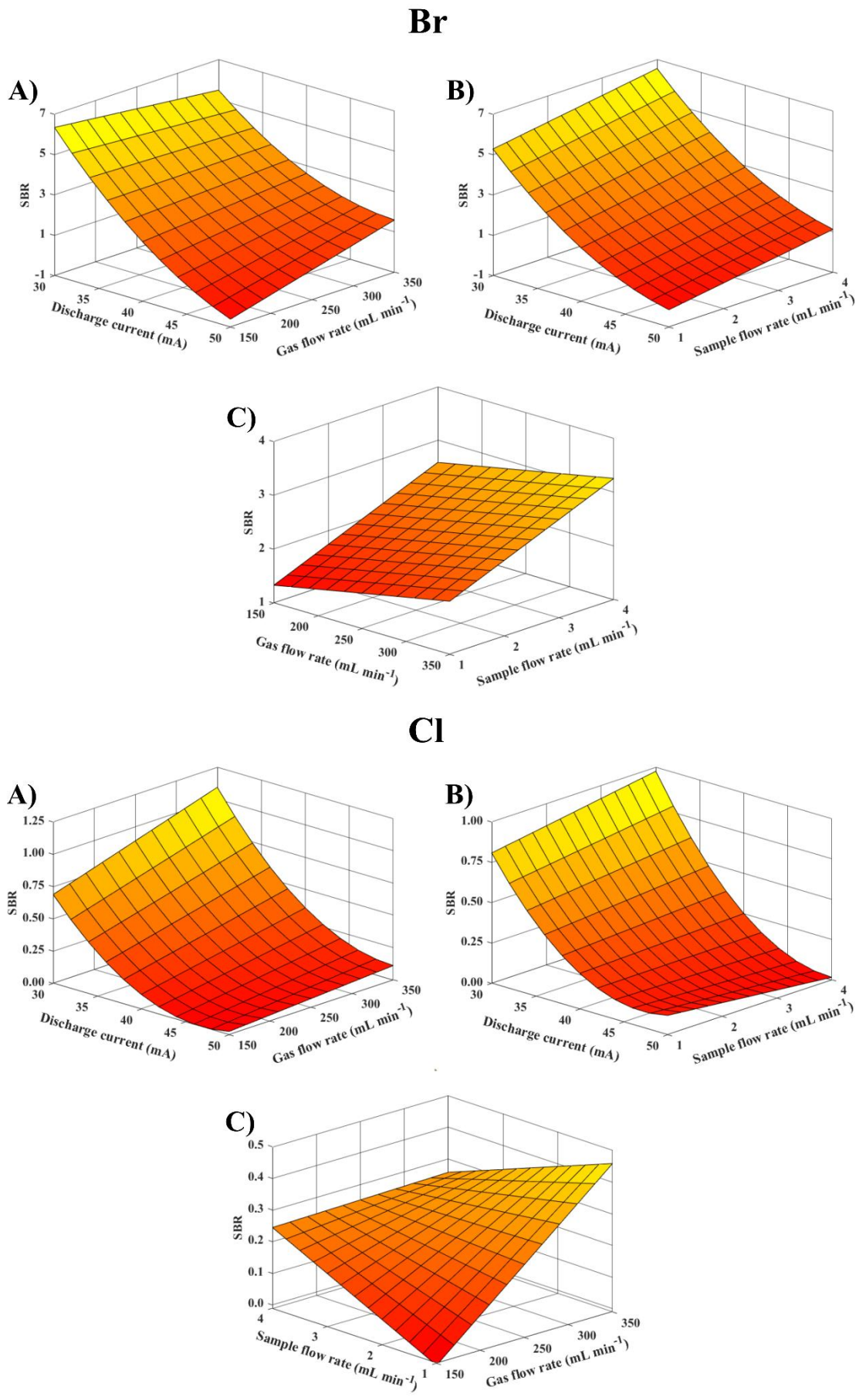

Fig. SI-2. The effect of the discharge current, the He flow rate, and the sample flow rate on the signal to background (SBR) of the Br and Cl analytical lines for the FLA-APGD system.

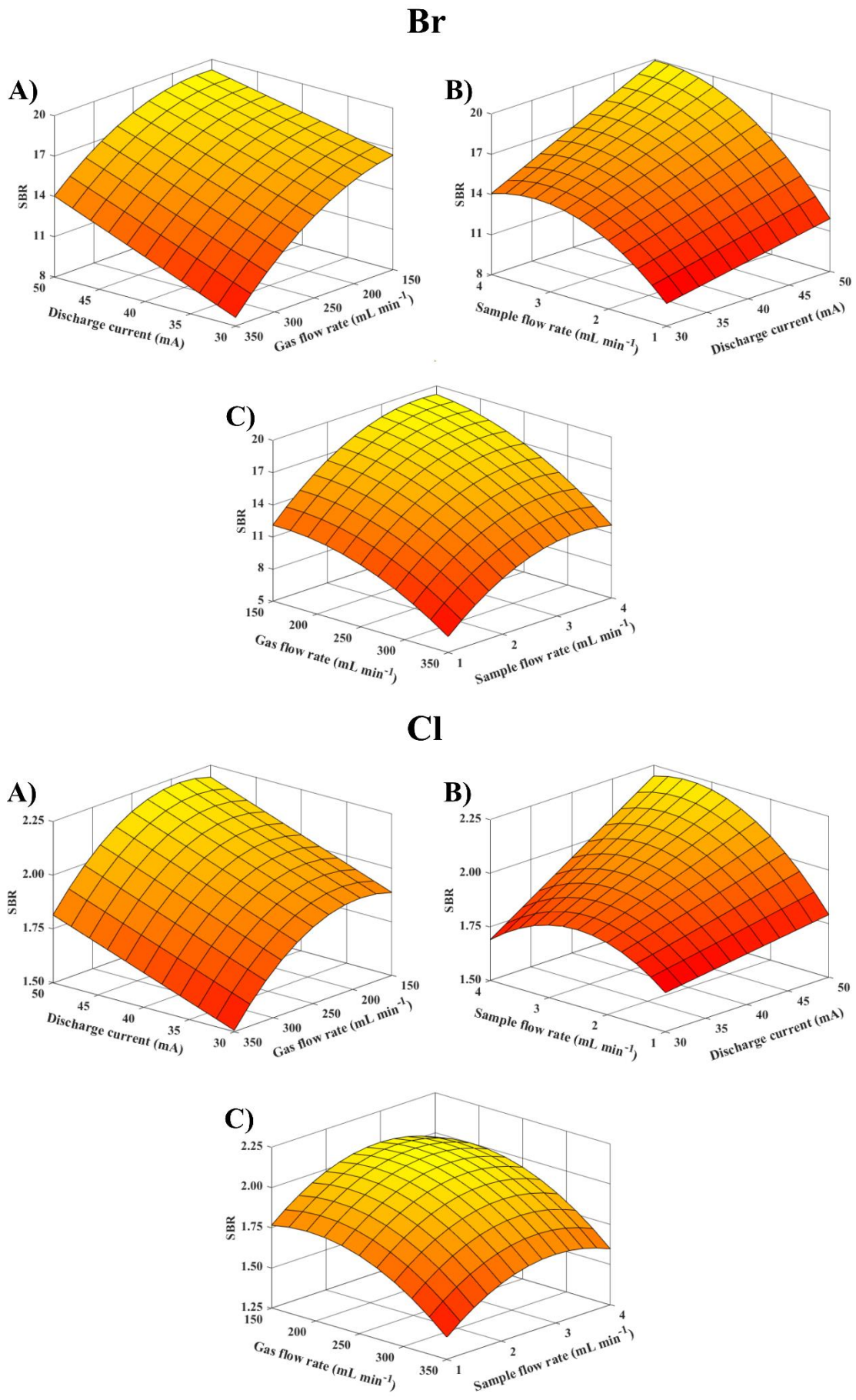

Fig. SI-3. The effect of the discharge current, the He flow rate, and the sample flow rate on the signal to background (SBR) of the Br and Cl analytical lines for the FLC-APGD system.

Table SI-1. The comparison of SBR values of the analytical lines of Br and Cl for two different acid types (concentration of each of them equal 0.2 mol L^{-1}).

System	Acid	SBR	
		Br	Cl
FLA-APGD	HNO_3	1.29	0.03
	H_2SO_4	1.53	0.06
FLC-APGD	HNO_3	14.07	2.30
	H_2SO_4	14.71	2.46

Table SI-2. The comparison of SBR values predicted by the models and the measured ones.

System	Analyte	R-statistics of models			Model validation		
		R^2	$R^2_{(adj)}$	$R^2_{(pred)}$	Predicted	Measured	Relative error (%)
FLA-APGD	Br	92.61	88.51	67.29	5.91	5.38	-10.03
	Cl	95.49	90.98	71.39	1.02	1.21	+18.63
FLC-APGD	Br	99.57	98.99	95.66	20.57	17.55	-14.68
	Cl	97.73	96.03	89.98	2.25	1.88	-16.44

R^2 Coefficient of determination.
$R^2_{(adj)}$ Adjusted R^2.
$R^2_{(pred)}$ Predicted R^2.

Table SI-3. The operating parameters of an Agilent 5110 SVDV ICP OES instrument.

RF power (kW)	1.50
Plasma Ar flow rate (L min^{-1})	12.0
Nebulizing Ar flow rate (L min^{-1})	0.7
Auxiliary Ar flow rate (L min^{-1})	1.0
Uptake delay time (s)	10
Read time (s)	5
Number of replicates	3
Stabilization time (s)	15
Viewing mode	SVDS (both axial and radial viewing)
Viewing height (mm)	8
Pump speed (rpm)	12
Background correction	Off-peak, fitted, 2 pixels
Analytical line (nm)	447.26 (Br), 774.50 (Cl)

Comment SI-1

Preliminary optimization of the acid type and its concentration

The cathode dark space (CDS) zone is found below the negative glow (NG) zone, at which the analytes atoms emission was proven to be the highest. That means the electric field turns the sputtered cations back to the FLC solution, inhibiting their transport into the NG zone. Therefore, as the acid concentration is growing, the cathode voltage drop extends the residence time of the sputtered cations in the CDS zone, enhancing their recombination with electrons and other reactive species, thus leading to the increased transport efficiency of analytes into the discharge [1, 2].

Comment SI-2

Preliminary optimization of the acid type and its concentration

It is also worth to take a deeper look into the tendencies observed for higher acid concentrations, presented in Fig. 2. First of all, it could be noted that for FLC-APGD the Br signal intensity was increased at the H_2SO_4 concentration of 0.2 mol L^{-1} (as compared to the previous point), whereas the Cl signal intensity was further declined. This observation, in the case of Br, also suggested that Br_2 was additionally generated in the plasma-liquid interfacial layer, meaning this analyte was introduced into the discharge by both the FLC solution sputtering and in the form of the volatile Br species. In such a case, the initial signal drop might be attributed to the cathode voltage drop and its subsequent growth was likely related to the volatile Br species production, playing a predominant role in the Br transportation into the discharge. Hence, the Br signal intensity at the acid concentration of 0.2 mol L^{-1} would be a resultant of those two tendencies. In the case of Cl, the abovementioned observations could mean that Cl_2 either was not generated at all or it was generated with much lower efficiency. Nonetheless, it is worth to note that at the acid concentration range of 1-2 mol L^{-1}, the signal intensity of Br remained roughly the same, whereas for Cl, its further enhancement was smaller than for lower acid concentrations. Similar observations were made previously, when Br_2 and Cl_2 were generated in the reaction with $KMnO_4$ and it was found out the production of Cl_2 required higher concentrations of both H_2SO_4 and $KMnO_4$ [3].

Comment SI-3

Further optimization of the remaining parameters

On the other hand, it could be expected that the growth of discharge current would provide better atomization/excitation conditions by enhancing the energy density in the discharge, thus leading to increased intensity of the analytical lines. This effect seemed to be the case in our previous work where the analytes were introduced to the discharge in the form of hydrides, generated in the reaction with $NaBH_4$ [4]. The latter explanation would be also supported by the results obtained herein for the FLC-APGD system, in which the increase of the discharge current resulted in the corresponding growth of the SBRs of the Br and Cl analytical lines. Similar results for FLC-APGD were reported by other researchers [5, 6].

Comment SI-4

Analytical performance

The concentration levels of Cl in different types of water varies from <1-10 mg L^{-1} for fresh and tap waters to >1000-10000 mg L^{-1} for brines and seawater [7], while in the case of various food samples it is from up to 4 mg g^{-1} (unprocessed meat and fish) to less than 1 mg g^{-1} (fruits and vegetables) [8]. The content of Br is from 40 to 8000 times less than the content of Cl [7]. Similar data was provided by the WHO [9], which stated that the Cl concentration in different types of water may vary from 11 mg L^{-1} in river water to 141 mg L^{-1} (on average) in water sampled from contaminated wells. Even higher Cl concentrations (up to 460 mg L^{-1}) were reported for aquifers prone to the seawater intrusion in the USA. On the other hand, unpolluted water usually contains Cl at levels being below 10 mg L^{-1}. Regarding food samples, the same document stated that natural levels of Cl in foodstuff does not exceed 360 mg kg^{-1}, however, its actual concentration in food is usually significantly higher due to the salt addition during processing, cooking, and eating food.

For comparison of the analytical results, an Agilent 5110 synchronous vertical dual view (SVDV) ICP-OES instrument was used to measure total concentrations of Br and Cl in prepared water samples, including river and tap waters, mineral medicinal water and sea water, *versus* external standard calibration and in prepared beetroot and tomato juices *versus* standard solution additions. The ICP-OES spectrometer was equipped with an easy-fit vertical quartz torch with a standard 1.8 mm injector and a pneumatic nebulization sample introduction system comprising a Seaspray nebulizer and a double-pass glass cyclonic spray chamber. The instrument was operated using the parameters listed in Table SI-3. In addition, the values of the DLs of Br and Cl obtained with the applied ICP-OES instrument were assessed, using the "3σ" criterion, and compared with those obtained with the examined excitation sources, *i.e.*, FLA- and FLC-APGD systems, and the OES detection. These DLs assessed for the ICP-OES technique, including the selected sample preparation, were 44 mg L^{-1} (Br) and 96 mg L^{-1} (Cl) and were 5-293 times higher than those obtained with the studied APGD-based methods.

References

[1] P. Mezei, T. Cserfalvi, M. Janossy, Pressure Dependence of the Atmospheric Electrolyte Cathode Glow Discharge Spectrum, J. Anal. At. Spectrom. 12 (1997) 1203–1208. https://doi.org/10.1039/A608528H.

[2] P. Mezei, T. Cserfalvi, H. J. Kim, M. A. Mottaleb, The influence of chlorine on the intensity of metal atomic lines emitted by an electrolyte cathode atmospheric glow discharge, Analyst 126 (2001) 712–714. https://doi.org/10.1039/B010057I.

[3] P. Pohl, I. Jimenez Zapata, M. A. Amberger, N. H. Bings, J. A.C. Broekaert, Characterization of a microwave microstrip helium plasma with gas-phase sample introduction for the optical emission spectrometric determination of bromine, chlorine, sulfur and carbon using a miniaturized optical fiber spectrometer, Spectrochim. Acta B 63 (2008) 415–421. https://doi.org/10.1016/j.sab.2007.12.005.

[4] M. Gorska, K. Greda, P. Pohl, On the coupling of hydride generation (HG) with flowing liquid anode atmospheric pressure glow discharge (FLA-APGD) for determination of traces of As, Bi, Hg, Sb and Se by optical emission spectrometry (OES), Talanta 222 (2021) 121510. https://doi.org/10.1016/j.talanta.2020.121510.

[5] J. Wang, P. Tang, P. Zheng, X. Zhai, Analysis of metal elements by solution cathode glow discharge-atomic emission spectrometry with a modified pulsation damper, J. Anal. At. Spectrom. 32 (2017) 1925–1931. https://doi.org/10.1039/C7JA00212B.

[6] V. A. Titov, V. V. Rybkin, A. I. Maximov, H.-S. Choi, Characteristics of Atmospheric Pressure Air Glow Discharge with Aqueous Electrolyte Cathode, Plasma Chem. Plasma Process. 25 (2005) 503–518. https://doi.org/10.1007/s11090-005-4996-z.

[7] S. N. Davis, D. O. Whittemore, J. Fabryka-Martin, Uses of Chloride/Bromide Ratios in Studies of Potable Water, Ground Water 36 (1998) 338–350. https://doi.org/10.1111/j.1745-6584.1998.tb01099.x.

[8] Anses, 2016. French food composition table. Table Ciqual version 2016. Available online: https://pro.anses.fr/tableciqual/.

[9] Guidelines for Drinking-water Quality, Chloride in Drinking-water, 2nd ed. Vol. 2. Health criteria and other supporting information, World Health Organization, Geneva, 1996.

Microchemical Journal 178 (2022) 107391

Contents lists available at ScienceDirect

Microchemical Journal

journal homepage: www.elsevier.com/locate/microc

Coupling of chemical vapor generation with atmospheric pressure glow discharge optical emission spectrometry generated in contact with flowing liquid electrodes for determination of Br in water samples

Monika Gorska *, Pawel Pohl

Wroclaw University of Science and Technology, Faculty of Chemistry, Division of Analytical Chemistry and Chemical Metallurgy, Wybrzeze Stanislawa Wyspianskiego 27, 50-370 Wroclaw, Poland

ARTICLE INFO

Keywords:
Atmospheric pressure glow discharge
Flowing liquid anode
Flowing liquid cathode
Chemical vapor generation
Bromide
Optical emission spectrometry

ABSTRACT

Miniaturized atmospheric pressure glow discharge (APGD) microplasma devices, operated in contact with a flowing liquid anode (FLA) or a flowing liquid cathode (FLC) and a He jet, were studied for the determination of Br by optical emission spectrometry (OES), after oxidizing the Br^- ions to volatile Br_2 in the reaction with $KMnO_4$. The concentrations of all reagents needed for the successful operation of the proposed systems were found to be the most crucial parameters and their impact on the intensity of the Br analytical line was studied. Under the optimal conditions, the analytical figures of merit were assessed. The endurance to the matrix effects of both developed methods was also investigated and both of them were found to be strongly insusceptible to the presence of foreign ions. The detection limits (DLs) of Br and was established to be 0.05 and 0.2 mg L^{-1} for CVG-FLA- and CVG-FLC-APGD, respectively. The developed methods were successfully applied for the determination of relatively low concentrations of Br in selected water samples, spiked with this element, with very good precision (0.9–6.1% as RSD) and trueness (94–110% as recovery). In addition, no significant differences between the results obtained using the external standard calibration and the standard addition method were noted.

1. Introduction

Bromide (Br^-) ions occur naturally in many water sources at concentrations varying from trace amounts in freshwater to even over 80 mg L^{-1} in seawater [1–4]. When present in waters and/or being an impurity of NaClO, the Br^- ions are involved in the reactions taking place during chlorination disinfections process between the Cl^- ions and organic matter, leading to form some Br-containing by-products such as brominated acetic acids. In the case of the ozonation process, the BrO_3^- ions also may be produced [2,4,5]. Among those Br-containing by-products, the latter ones are classified by the International Agency for Research on Cancer as potentially carcinogen for humans [6,7]. Apart from the natural occurrence, Br-containing compounds may be also released to environmental waters due to their wide application in industrial and agricultural products [8–10]. Since the Br^- ions were found to be the precursor of the BrO_3^- ions in waters [11], their impact on the waters quality is significant. Therefore, it is of great importance to determine the Br^- ions concentration in waters using fast, low-cost, and reliable methods.

For the time being, a number of analytical techniques have been applied for this purpose, including: spectrophotometry [9], laser-induced plasma spectroscopy (LIPS) [12], X-ray fluorescence [13], inductively coupled plasma–optical emission spectrometry (ICP-OES) [14], inductively coupled plasma–mass spectrometry (ICP-MS) [15], gas chromatography (GC) [16], ion chromatography (IC) [17], liquid chromatography (LC) [18], and capillary electrophoresis (CE) [19]. However, some of those techniques are characterized with poor sensitivity (*e.g.*, spectrophotometry), which either limits their application or requires a complex and time-consuming sample preparation procedure leading to the analyte preseparation and preconcentration [3]. On the other hand, the techniques that provide very good sensitivity (ICP-OES, ICP-MS) require bulky and complex instrumentation, which not only limits their portability but also involves high costs of their purchasing, operation and maintenance.

To address the abovementioned issues, the attention of many research groups has been drawn to the development of miniaturized, low-cost, compact, and portable spectrochemical instrumentation, which is concurrently expected to provide high sensitivity along with

* Corresponding author.
E-mail address: monika.gorska@pwr.edu.pl (M. Gorska).

https://doi.org/10.1016/j.microc.2022.107391
Received 1 February 2022; Received in revised form 9 March 2022; Accepted 10 March 2022
Available online 15 March 2022

good reproducibility and credibility of the results. Although a wide group of such devices has been proposed for the time being, their application is limited mostly to the determination of metals and metalloids. Nevertheless, a few of them were also applied for the Br^- determination, namely: dielectric barrier discharge [20], microwave microstrip helium plasma (MSP) [21], capillary microplasma (C-μPAS) [22], flowing liquid anode atmospheric pressure glow discharge (FLA-APGD), and flowing liquid cathode atmospheric pressure glow discharge (FLC-APGD) [23].

It is noteworthy, however, that only in the case of a few abovementioned works, the Br^- ions were determined directly in the solutions [22,23]. The obtained detection limits (DLs) were 0.5, 0.15, and 2.1 mg L^{-1}, respectively for C-μPAS, FLA- and FLC-APGD. The other methods based on microplasma sources, *i.e.*, DBD [2,20] or MSP [21], as well as other methods, premised upon bulky home-made or commercially available instrumentation with ICP sources [14,24,25] or microwave induced plasma (MIP) devices operated in surfatrons [26,27], Beenakker cavities [28–30] or a microwave plasma torch [31], usually use a separate reaction chamber in which volatile Br species are generated from the Br^- ions (*e.g.*, bromine, methyl bromide) and subsequently transported into the (micro)plasma-based excitation source in a flux of carrier gas. This approach is similar to the well-known hydride generation (HG) technique and just as it, the mentioned chemical vapor generation (CVG) technique certainly has advantages of high efficiency of the volatile species formation and significant reduction of interferences [20,24].

Therefore, the present work is a continuation of our recent study [23] in which the Br^- and Cl^- ions where directly determined in some water and juice samples with the aid of FLA- and FLC-APGD and the OES detections. In this work, it was aimed to couple both aforesaid excitation sources with the CVG technique for the OES determination of the Br^- ions in selected water samples. Specifically, volatile Br_2 was generated in an acidified solution in the reaction of the Br^- ions with a $KMnO_4$ solution. The present research put forward a hypothesis that the coupling of the FLA- and FLA-APGD systems with the CVG technique will improve the element detectability by enhancing the efficiency of the Br_2 generation. This work was limited only to the determination of Br since it was established previously [21] as well as in our preliminary study that the application of the mentioned CVG technique for the generation of volatile Cl_2 requires unreasonably high concentrations of both H_2SO_4 and $KMnO_4$.

To attain the abovementioned goal, in the first part of this study, the most prominent analytical line of Br was recorded and its signal was compared when using all four techniques (FLA-, FLC-, CVG-FLA-, and CVG-FLC-APGD). In the next step, the optimal values of the most crucial operating parameters were assessed for both studied CVG-based systems. Followingly, the analytical figures of merit were assessed for each system, working under the optimal conditions. Subsequently, the methods insusceptibility to the matrix effects, caused by inorganic matrix of real samples, was established by measuring the Br signal intensity in the presence of several concomitant salts. Lastly, to verify the credibility of the proposed methods, Br was determined in selected water samples, applying two calibration methods, *i.e.*, the external standards calibration and with two standard additions.

2. Experimental

2.1. Experimental setup

A schematic picture of the developed CVG-FLA- and CVG-FLC-APGD systems is shown in Fig. 1. Volatile Br_2 was generated in a glass cylindrical chamber (total volume 25 mL, OD 20 mm) and then transferred to the FLA/FLC-APGD system. The analyzed Br-containing solutions, acidified with H_2SO_4, and solutions of $KMnO_4$ were separately introduced to the glass chamber through a T-piece connector with the aid of a 4-channel Perimax peristaltic pump (AHF Analysentechnik, Germany),

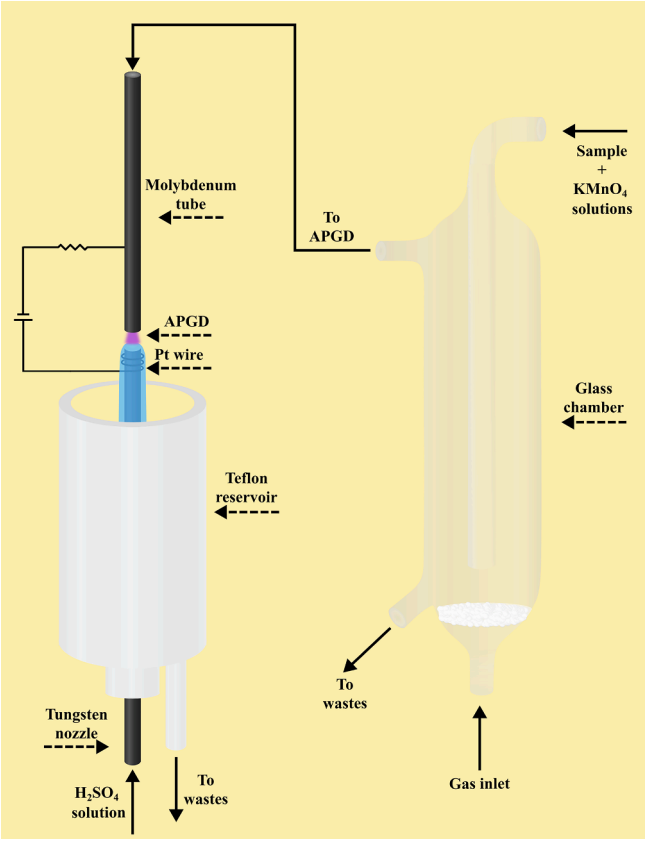

Fig. 1. A schematic picture of the proposed CVG-FLA- and CVG-FLC-APGD systems.

working at a constant flow rate of 2.0 mL min^{-1}. The carrier gas (He) was introduced from the bottom of the chamber *via* a glass frit and carried Br_2 into the discharge. The post-reaction solution was drained into a waste container with the aid of the aforesaid peristaltic pump.

The general construction of the developed APGD-based systems was basically the same; the only difference between them was the electrodes polarization (due to that fact, it was skipped in Fig. 1). In the developed systems, a Mo tube (OD/ID 3/2 mm, length 100 mm) and a W tube (OD/ID 3/2 mm, length 100 mm) were placed vertically to each other in an open-to-air chamber. Since the analyte (Br as Br_2) was introduced into the discharge *via* the He jet, the discharge was sustained between the surface of the H_2SO_4 solution (at different concentrations), which served as either FLA or FLC, and the He jet introduced through the Mo tube. The He flow rate of 350 mL min^{-1} was applied for both studied systems and it was adjusted using a FC-2900 flow controller and a RO-28 digital flow meter (Tylan General, USA). The FLA/FLC solutions were pumped through the W tube with the aid of a 3-channel REGLO ICC peristaltic pump (Ismatec, USA), with the flow rate set to 3.0 mL min^{-1}. The solution flowing down to a PTFE reservoir, was pumped out. The distance between the Mo tube and the surface of the H_2SO_4 (so-called discharge gap) was constant and set to approximately 1.5 mm. A Pt wire, wound on the W tube, was used to connect one crocodile clip cable from a HV dc power supply (model DP50H-024PH, DSC-Electronics, Germany). The second crocodile clip cable was directly attached to the Mo tube. The voltage of 700–1100 V was supplied and ballast resistor of 6.9 kΩ was introduced into the circuit to stabilize the discharge.

An achromatic quartz lens (f = 80) was used to focus the radiation coming from APGD and image it (1:1) on the entrance slit (10 μm) of an imaging spectrometer (Shamrock 500i, Andor, UK). The spectrometer was equipped with a Newton DU-920P-OE UV–Vis CCD camera (Andor, UK) and a holographic grating (1200 lines mm^{-1}) and. The integration time was constant and equal 10 s for all recordings. The Br analytical

line of 827.2 nm was traced and its intensity was background corrected by subtracting the intensity of the same wavelength measured for the blank solution (so-called background intensity) from the overall intensity of the Br analytical line.

2.2. Reagents and sample preparation

Deionized water (18.2 MΩ cm), used during the whole study, was obtained from a Polwater water purification system (Labopol-Polwater, Poland). He of 99.999% purity was provided by Air Products (Poland). The standard solutions of Br were prepared using solid NH_4Br, provided by Sigma-Aldrich (Germany). To prepare these solutions, concentrated H_2SO_4 (95–98% m/m) obtained from Sigma-Aldrich (Germany) was used. In addition, Sigma-Aldrich solid $KMnO_4$ was applied for the CVG reaction. Solid NH_4NO_3, $(NH_4)_2SO_4$, K_2SO_4, $MgSO_4$, KI, NaF, KH_2PO_4, $K_2Cr_2O_7$, KCl, Na_2S, $Ca(NO_3)_2$, and $Fe(NO_3)_3$, employed for the investigation of potential matrix effects, were supplied by Avantor Performance Materials (Poland). All chemicals were at least of analytical grade.

Samples of the Oder (river) water (sampled in Wroclaw, Poland), municipal tap water, and reservoir water (sampled in Swidnica, Poland) were collected into pre-cleaned 0.5 L PE bottles and immediately acidified with H_2SO_4 to a concentration of 0.1 mol L^{-1}. Followingly, 25.0 mL of such water samples were transferred into twist cup containers. Furthermore, concentrated H_2SO_4 was added to these samples to reach its final concentration of 1.5 mol L^{-1}. Subsequently, each water sample was spiked with a previously prepared standard solution of Br (100 mg L^{-1} of Br^- ions) to reach its concentration of 1 (CVG-FLA-APGD) or 10 (CVG-FLC-APGD) mg L^{-1}. Lastly, the samples were filled to the final volume of 30.0 mL with deionized water. All the aforesaid samples were prepared in triplicates (along with the relevant procedural blanks) and each of such parallel sample was divided into three separate parts. Appropriate amounts of the standard were added the last two such subsamples, in order to perform the standard addition method. Both calibration method, *i.e.*, the external standard calibration as well as the standard addition method were used to compare the results.

3. Results and discussion

3.1. The emission spectra of both APGD systems before and after coupling with the CVG technique

In the first part of this study, an attempt was made to compare the intensity and signal-to-background ratio (SBR) of the Br analytical line obtained for the FLA-, FLC-, CVG-FLA-, and CVG-FLC-APGD systems. In the case of the FLA- and FLC-APGD systems, where Br_2 was generated directly in the FLA or FLC solution due to the oxidation reactions with reactive forms accompanying the APGD operation (most likely with the OH radicals), it was established in our recent work [23] that the optimal H_2SO_4 concentrations were 1 and 0.01 mol L^{-1}, respectively. Therefore, two solutions containing 1000 mg L^{-1} of Br and acidified with H_2SO_4 to the previously mentioned concentrations were prepared. The measurement conditions for those two systems were the ones that were established to be optimal in the same previous work, *i.e.*, the discharge current of 30 mA for FLA-APGD or 50 mA for FLC-APGD, the He flow rate of 300 (FLA-APGD) or 150 (FLC-APGD) mL min^{-1}, and the FLA or FLC solution flow rate of 3.0 mL min^{-1}. As for the CVG-FLA- and CVG-FLC-APGD systems, it was expected that low acid concentrations will not be favorable for the Br_2 generation [21], therefore, another solution containing 1000 mg L^{-1} of Br in 1 mol L^{-1} H_2SO_4 was prepared along with a 3% $KMnO_4$ solution. The FLA and FLC solutions consisted only H_2SO_4 at 0.01 and 0.1 mol L^{-1}, respectively, and were used just to sustain the both APGD systems. The remaining operating parameters were as follows: the sample and $KMnO_4$ solutions flow rate of 2.0 mL min^{-1}, the FLA or FLC solution flow rate of 3.0 mL min^{-1}, the discharge current of 30 (CVG-FLA-APGD) or 50 (CVG-FLC-APGD) mA, and the He flow rate of 350 mL min^{-1}..

The comparison of the intensity of the Br analytical line for all studied systems is presented in Fig. 2 and the corresponding SBR values are given in Table SI-1. As compared to the corresponding FLC-APGD system, the Br signals obtained for the FLA-based systems were found to be higher (see Fig. 2), which is in accordance with the outcomes shown in previous studies comparing the response of different elements between the FLA- and FLC-APGD systems [23,32–35]. Unsurprisingly, it was also noted that the intensity of the Br analytical line was enhanced when the abovementioned systems were coupled with the CVG unit. This finding is also in good agreement with other works related to either the determination of Br using the PVG technique [24] or the determination of other elements using the HG technique [36,37].

However, it is worth to note that although the Br signal intensity was enhanced around 11-fold in the case of the CVG-FLA-APGD system (as compared to FLA-APGD), the corresponding SBR increase was about 14-fold (see Table SI-1 for details). This was because the introduction of gaseous Br_2 led to the background intensity decrease of about 22%. Similar results were previously observed for the HG-FLA-APGD system [37]. In the case of the CVG-FLC-APGD system, the intensity of the Br analytical line was increased around 12-fold (in comparison to FLC-APGD) but the corresponding SBR value was elevated only 4.5 times. This was because the background intensity increased almost 3 times when gaseous Br_2 was introduced into the APGD phase. The reason why the introduction of Br_2 affected the background intensity differently in those two systems is troublesome to explain and needs a more detailed investigation. However, a likely clarification might rely on different atomization and excitation conditions occurring between FLA- and FLC-based discharges arisen from different electrodes polarity.

The results obtained at this stage of research clearly indicated that gaseous Br_2 was actually generated in those conditions. The coupling of the CVG unit with the FLA- and FLC-APGD systems indeed allowed to enhance the intensity of the Br analytical line, which was most likely a result of the increased efficiency of the analyte transport into the discharge as it is the case for the HG technique [36].

3.2. Optimization of reagent concentrations

In the next step, the optimization of crucial operating parameters was performed. Of those established to be crucial for the efficient systems operation, several were excluded from the optimization step, after performing some preliminary trials. First of those was the discharge current. It was proven in the past that the optimal current is usually one of the highest value, regardless of the polarization of the liquid electrode or the way of the analytes introduction [36–41]. On the other hand, lower discharge current was found to be optimal for the Br

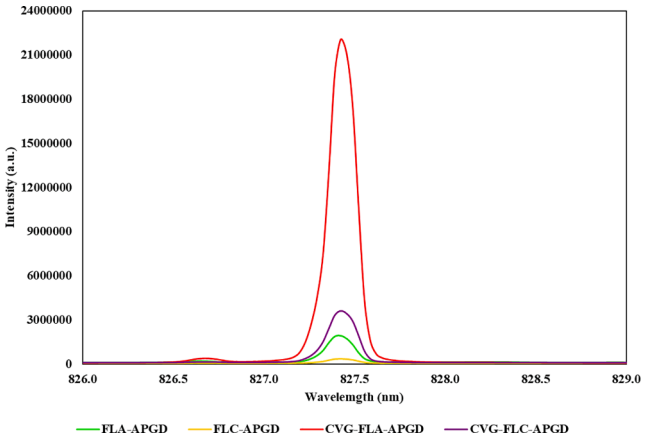

Fig. 2. The emission profiles of the Br analytical line (827.2 nm) recorded for different APGD-based systems.

determination in our recent work but only in the case of the FLA-APGD system [23]. Nevertheless, there was no reason to expect the same results herein, since the mentioned effect seemed to be affected by the way of the analytes were introduced into the discharge rather than the atomization and excitation conditions. A preliminary study, carried out at the beginning of this step, confirmed this assumption. However, it was also revealed that the operation of the CVG-FLA-APGD system became notably unstable for the discharge currents above 30 mA. Due to that fact, the discharge current of 30 and 50 mA for CVG-FLA- and CVG-FLC-APGD, respectively was applied for all further parts of this study. As for the He flow rate, it was repeatedly shown that the signals of the analytes introduced into the discharge in a stream of jet-supporting gas are enhanced along with the increasing gas flow rate [36,37,41]. Another preliminary study showed a similar tendency herein, for both studied systems, therefore, the He flow rate of 350 mL min^{-1} was used for all posterior experiments. Regarding the flow rate of the sample solution and the $KMnO_4$ solution, it could be expected that the increase of their flow rate would enhance the Br signal intensity due to more Br_2 entering the discharge per unit time [40]. Nevertheless, taking into account the back-pressure from the T-connector and the overall volume of the post-reaction solution pumped out the reaction/separation chamber, the solution flow rate of 2.0 mL min^{-1} was used for all experiments. Finally, the FLA/FLC solution flow rate was not actually expected to change significantly the analyte response, since it did not contain the analyte. Therefore, the optimal value of 3.0 mL min^{-1}, assuring the best discharge stability, was used in any further part of this study.

Nevertheless, the concentration of H_2SO_4 in the sample solution, the concentration of $KMnO_4$ in the oxidant solution, and the concentration of H_2SO_4 in the FLA/FLC solutions were needed to be optimized as they were expected to directly impact on the Br_2 generation efficiency, thus influencing the Br signal intensity [21]. Although it was established in our recent work [23] that the optimal H_2SO_4 concentration in the FLA and FLC solutions were 1 and 0.01 mol L^{-1}, respectively, it was not expected to be the case when coupling those APGD-based excitation sources with the CVG unit. This was because the FLA and FLC solutions served only as an part of the electrical circuit and the results of our previous work indicated that such unusual optimal values might be attributed to the anionic form of the analytes introduced into the discharge which had been not the case before. Therefore, the findings of this work were expected to confirm the previous hypotheses about the impact of the FLA/FLC solution concentration on the analytes and the plasma behavior.

The Box-Behnken response surface design was used to study the effect of the selected operating parameters, *i.e.*, A – the H_2SO_4 concentration in the FLA/FLC solution (mol L^{-1}), B – the $KMnO_4$ concentration in the oxidant solution (%), and C – the H_2SO_4 concentration in the sample solution (mol L^{-1}), on the SBR of the Br analytical line (at this phase of research, the Br^- concentration was decreased to 100 mg L^{-1} for both studied APGD systems). All planned treatments within this design were carried out in one experimental block and included 15 single randomized experiments, combining the parameters at three different levels (-1, 0, +1), *i.e.*, A: 0.01–1 and 0.01–0.2 mol L^{-1} in the case of the FLA and FLC solution, respectively, B: 1–5%, and C: 0.2–2 mol L^{-1}. There were also 3 center points included within these treatments to assess the precision of this experimental design. The coefficients in the full quadratic response surface regression equations modeling the SBR of the Br analytical line versus the studied parameters A, B, and C were established using the forward-selection-of-terms algorithm at the 85% significance level ($\alpha = 0.15$). Such significance level was chosen in accordance with the recommendations of the software manufacturer to obtain a suitable curvature in the regression equations describing the acquired analytical response. These regression coefficients of the developed statistically significant models are given in Table SI-2. Their visualization, showing the effect of the studied parameters, on the determined response is given in Fig. 3. The goodness-of-fit of for these models was shown by the coefficients of determination (R^2) and the adjusted R^2, while their predictive power – by the predicted R^2 (see Table SI-3).

Regarding the CVG-FLA-APGD system, the Br response was found to increase along with the increase of all three reagent concentrations. In the case of the CVG-FLC-APGD system, the SBR of the Br analytical line was also noted to be enhanced with increasing concentrations of H_2SO_4 in the sample solution and $KMnO_4$ in the oxidant solution, however, the growth of the H_2SO_4 concentration in the FLC solution resulted in an initial increase of the Br response, followed by its further drop starting from 0.1 mol L^{-1}. Similar results regarding the effect of the concentration of H_2SO_4 in the sample solution and the concentration of $KMnO_4$ in the oxidant solution on the Br response were obtained in other studies that relied on the Br_2 generation before its introducing to the plasma excitation source [21,42]. Since the effect of those two reagents did not depend on the discharge polarization, it could be concluded that their higher concentration likely contributed to a higher Br_2 generation efficiency.

More surprising outcomes were obtained when considering the effect of the H_2SO_4 concentration in the FLA/FLC solution. As seen in Fig. 3 and Table SI-2, the SBR value of the Br analytical line was growing over the whole range of the H_2SO_4 concentration in the case of the FLA solution. This was not expected in this case as it was repeatedly shown that lower acid concentrations in the FLA solutions are favorable for obtaining the highest signals of various analytes [32,43,44]. Nevertheless, it is worth noting that, although none of possible explications for this phenomenon has been proven, a likely reason for that is the scavenging effect of the increased concentration of the H_3O^+ ions on the solvated electrons in the plasma-solution interfacial zone [23,44]. However, the scavenging effect was not the case herein as the analyte was introduced into the discharge in the stream of He. Therefore, a likely clarification for the results observed in this work could be rather related to the atomization and excitation conditions in the discharge, which apparently are affected by the presence of higher H_3O^+ ions in the interfacial zone. At these conditions, higher concentrations of certain reactive species, *e.g.*, the H and OH radicals, could be formed and directly contribute to the atomization and excitation conditions in the discharge. Apart from that, it was previously shown [45] that at higher acid concentrations the water evaporation is lower which could also concur to the improvement of the conditions of the atomization and excitation (by reducing the probability of competitive processes taking place and/or the negative impact of the H and OH radicals on the atomization and excitation conditions). Even though, the same observations would be then expected in the conventional FLA-APGD system, the scavenging process still may take place and be the predominant factor determining the analyte response.

As for the FLC solution, its H_2SO_4 concentration of 0.1 mol L^{-1} is established to be optimal in the vast majority of cases [32,46–48] and the same value was found to provide the highest SBR of the Br analytical line herein. In the case of the conventional FLC-APGD system, the signals enhancement observed with growing acid concentrations is imputed to the decreased cathode voltage drop and the corresponding decline of the electric field strength in the part of the discharge called cathode dark space (CDS), resulting in facilitating the analytes transport to the discharge. Nevertheless, since the FLC solutions did not contain any analytes, the behavior of the SBR of the Br analytical line versus the H_2SO_4 concentration could be explained by the changes in the atomization and excitation conditions, *i.e.*, its initial growth due to the lower water evaporation and improvement of these conditions as well as its further decline due to the intensive production of the H radicals and their recombination to H_2, introduced into the discharge and deteriorating these conditions.

Regardless of the specific reason for the observed tendencies, the optimal concentrations were found to be as follows: the H_2SO_4 concentration of 1.8 mol L^{-1} and the $KMnO_4$ concentration of 5% for both systems, the H_2SO_4 concentration in the FLA solution concentration of 1 mol L^{-1}, and the H_2SO_4 concentration in the FLC solution concentration

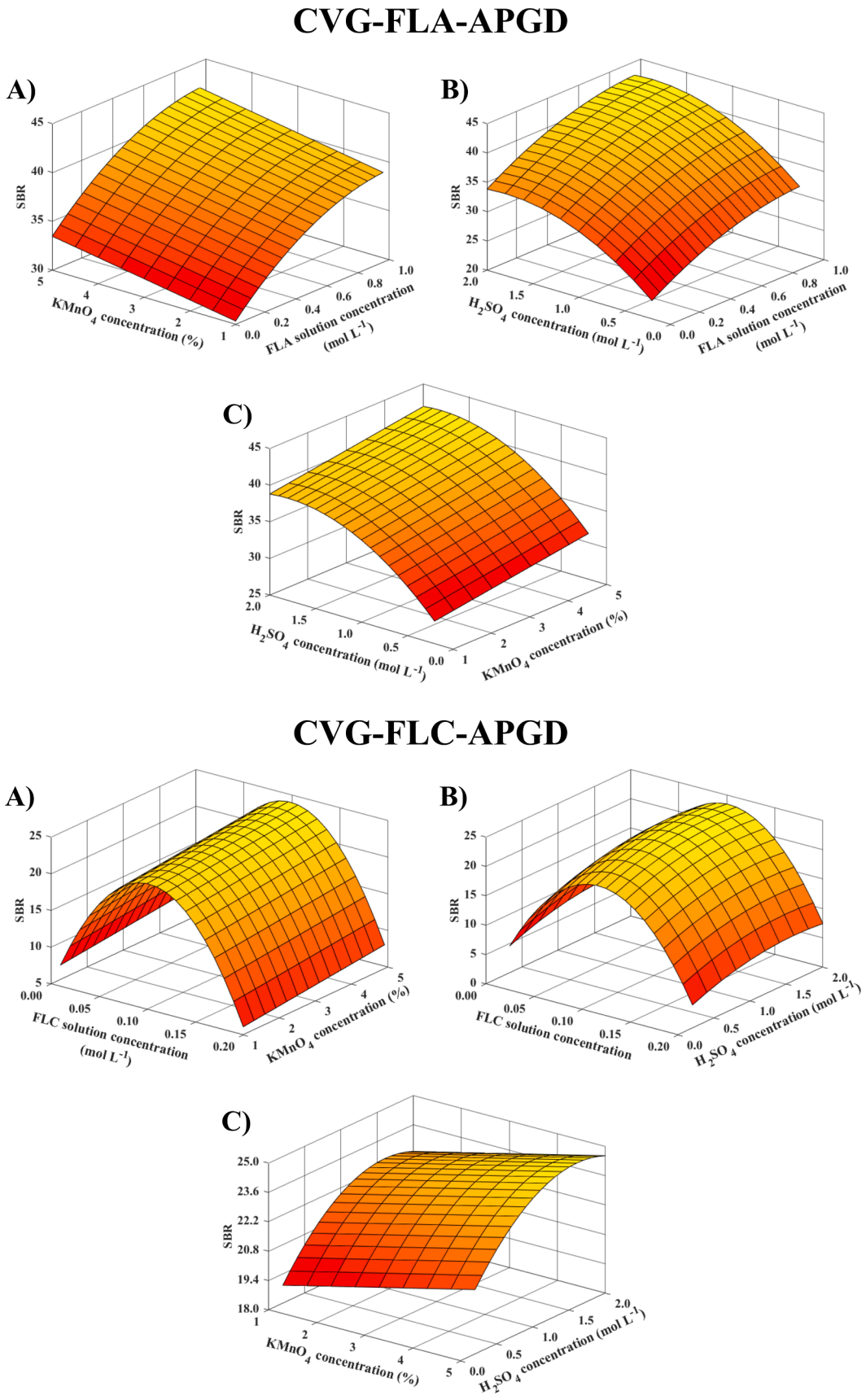

Fig. 3. The impact of the H_2SO_4 concentration in the FLA/FLC solution, the $KMnO_4$ concentration in the oxidant solution and the H_2SO_4 concentration in the sample solution on the signal to background (SBR) of the Br analytical line for both studied systems. The concentration of the Br^- ions in the sample solution: 100 mg L^{-1}.

of 0.1 mol L^{-1}. Nevertheless, since no significant difference was observed between the predicted SBR values for the H_2SO_4 concentration of 1.8 and 1.5 mol L^{-1}, the latter one along with the abovementioned remaining concentration settings were established to be optimal and applied for all further experiments.

As demonstrated in Table SI-3, the R-statistics values were in almost all cases around or higher than 90%, meaning that the models obtained for the Br response with the CVG-FLA- or CVG-FLC-APGD systems were able to describe and predict new experimental data with great trustworthiness. To further confirm the usefulness of the obtained models, the SBR values received for both studied methods were measured under the optimal operating conditions and compared to those predicted by the models. It was found that the received SBRs agreed well with the predicted ones since relative errors were equal −4.68 and −3.30% for CVG-FLA- and CVG-FLC-APGD, respectively. This approach proved the reliability of the new data prediction by the models.

3.3. Analytical figures of merit

The analytical figures of merit of the investigated APGD systems coupled with the CVG technique were assessed for the Br determination under the aforesaid optimal working conditions. To achieve that, the DLs of Br, the sensitivity of the Br analytical line, the upper linearity ranges (ULRs) of calibration curves, and the precision (expressed as RSD) were determined for both developed systems. DLs were assessed using the 3σ/a criterion, in which "3σ" is the triple of the standard deviation of 10 measurements of an suitable blank solution and "a" is the sensitivity of the Br analytical line. The ULRs were assessed using 8 standard solutions of Br at concentrations within the 10 to 2000 mg L^{-1} range. To evaluate the precision, a total of 10 consecutive measurements performed on a solution containing either 1 (CVG-FLA-APGD) or 10 (CVG-FLC-APGD) mg L^{-1} of the analyte were recorded and the average relative standard deviation (RSD) obtained from 3 series of those 10 measurements was calculated. The results of the analytical figures of merit determination are depicted in Table 1.

The DLs of Br received under the optimal conditions were equal to 0.05 and 0.2 mg L^{-1} for CVG-FLA- and CVG-FLC-APGD, respectively. Regarding the CVG-FLA-APGD technique, the sensitivity enhancement (as compared to the results obtained in our recent work [23]) was 9.2-fold. Unfortunately, the SD of the background increased by 2.4-fold, which resulted in the DL of Br being improved only over 3 times. As the background intensity in the vicinity of the Br analytical line was actually lower in the case of the CVG-FLA-APGD system, the worsened SD likely resulted from a slightly impaired discharge stability while introducing gaseous Br_2. In the case of the CVG-FLC-APGD system, the sensitivity improved 7.9-fold, whereas the SD of the background remained unchanged, which allowed to lower the DL of Br by around 8 times (in comparison to this evaluated for the FLC-APGD system).

The linearity of the calibration curves was proved by the $R^2 > 0.995$

Table 1
The analytical figures of merit obtained for the studied CVG-APGD-based systems coupled with the OES detection for the Br determination.

System	Detection limit (mg L^{-1})	ULR (mg L^{-1})	R^2	Sensitivity (a.u. per mg L^{-1})	RSD (%)[a]
CVG-FLA-APGD	0.05	2000	0.9972	$1.79 \cdot 10^4$	2.55
CVG-FLC-APGD	0.2	500	0.9981	$2.73 \cdot 10^3$	3.97

FLA-APGD – flowing liquid anode atmospheric pressure glow discharge.
FLC-APGD – flowing liquid cathode atmospheric pressure glow discharge.
CVG – chemical vapor generation.
ULR – upper linearity range.
RSD – relative standard deviation.
[a] For the Br concentration of 1 (CVG-FLA-APGD) or 10 (CVG-FLC-APGD) mg L^{-1}.

values (see Fig. SI-1) but the ULRs were various depending on the discharge type and were dissimilar, comparing them to our previous work [23]. Coupling the FLA-APGD with the CVG unit allowed to broaden the ULR from 1000 to 2000 mg L^{-1}. The opposite outcomes were received for the CVG-FLC-APGD system; the ULR was reduced from 5000 to 500 mg L^{-1}. Therefore, the scopes of the linearity of the calibration curves were improved up to at least 4 orders of magnitude for CVG-FLA-APGD and remained 3 orders of magnitude for CVG-FLC-APGD (in reference to the respective DLs).

Although a growth in the SD value for the CVG-FLA-APGD system may suggest a slight deterioration in its operation, the RSD measured for this system was 2.55%, which was an excellent result, considering the fact that the Br concentration was merely around 20-fold higher from its DL. Nevertheless, this value was around 2-fold worse as compared to this achieved with the FLA-APGD system alone. As for CVG-FLC-APGD, the obtained RSD was significantly higher, compared to this obtained with FLC-APGD, being equal 3.97%. However, such a value is still acceptable in the spectrochemical analysis.

Therefore, it could be concluded that the application of the CVG technique allowed to decrease the DLs of Br for both systems, with particular reference to the FLC-APGD system, giving the DL of Br for the CVG-FLC-APGD system comparable with the one obtained previously for the FLA-APGD system. It is also worth to note that the DLs of Br received herein were ~ 180 times (CVG-FLC-APGD) or ~ 960 times (CVG-FLA-APGD) lower than this, established in our recent work [23] for the conventional ICP-OES instrumentation, available in our laboratory (being equal 44 mg L^{-1}). Combining the improved DLs values with relatively wide linearity ranges and the acceptable measurement precision, it could be stated that both developed systems are an attractive alternative for commercially applied bulky and expensive instruments such as ionic chromatography or ICP-OES.

3.4. The effect of foreign ions

One of the most crucial factors contributing to the practical application of any analytical method is its endurance to the matrix effects related to the presence of organic and inorganic concomitants in real samples. In the case of the FLC-APGD systems, the presence of high concentrations of foreign ions does not usually cause serious interfering effects, even though the constituents of the FLC solution are sputtered into the discharge [38]. On the other hand, the FLA-APGD system is recognized to be poorly resistant to the presence of even low concentrations of different elements in real samples, especially when considering alkali and alkaline earth metals [32,33,43]. However, it was demonstrated in our previous work that the matrix effects were not an issue in the case of Br and Cl [23], which ions (Br^- and Cl^-) were oxidized to produce volatile Br_2 and Cl_2, respectively. This, along with previously observed lack of the impact of foreign elements on plasma temperatures and the electron density of this excitation source [49], seemed to confirm the theory that the source of the matrix effects in the case of the FLA-APGD system is the impaired analytes reduction caused by the existence of other elements (metals cations) in a sample, which compete in this process with the analytes cations, *e.g.*, Ag(I), Cd(II), Hg(II), Pb(II), Zn(II), vulnerable to the production of their volatile species [49,50]. Nonetheless, it was not expected to observe any negative impact from most of the coexisting ions when considering the CVG or HG techniques as only elements that are able to form such volatile forms may be co-introduced into the discharge and this assumption seems to be reflected in literature data, regarding the application of the CVG technique for the determination of Br [20,21].

Nevertheless, since the CVG technique, based on the analytes reaction with $KMnO_4$ had been ever previously coupled to the FLA/FLC-APGD system, the impact of the foreign ions on the response of Br obtained for these systems was tested. It was decided to investigate the matrix effects using selected salts instead for multi-element standard solutions. Hence, a series of solutions of Br at the concentration of 20

(CVG-FLA-APGD) or 100 (CVG-FLC-APGD) mg L^{-1} were prepared and solid NH_4NO_3, $(NH_4)_2SO_4$, K_2SO_4, $MgSO_4$, KI, NaF, KH_2PO_4, $K_2Cr_2O_7$, KCl, Na_2S, $Ca(NO_3)_2$, and $Fe(NO_3)_3$ were added separately to each of them to the final concentration of the salts being 200 and 2000 mg L^{-1} (CVG-FLA-APGD) or 1000 and 10000 mg L^{-1} (CVG-FLC-APGD). The signal intensity of Br was measured and it was normalized in regard to the intensity of the Br signal received for a solution not containing any additional matrix constituents.

Except KI at the concentration of 2000 mg L^{-1}, the normalized signal of Br in the CVG-FLA-APGD system ranged within 0.84–1.07 (see Fig. 4). Those outcomes indicated that only the presence of KI at the concentration corresponding to the interfering salt-to-analyte concentration ratio being equal 100 caused a serious interfering effect, since the Br signal was reduced 4-fold. This was likely due to the I_2 formation, whose atomization and excitation could be a competitive process to the atomization and excitation of Br_2. It is interesting that similar effects were not observed for NaF, KCl, and Na_2S for which F_2, Cl_2, and H_2S could be possibly formed. However, as mentioned in the Introduction section, the H_2SO_4 and $KMnO_4$ concentrations were not favorable for the Cl_2 formation and this could be also the case with the F^- and S^{2-} ions.

As for the CVG-FLC-APGD system, the existence of the majority of the studied salts led to the normalized signal of Br fallen within the 0.88–1.12 range. The only significant interfering effect was noted after adding $K_2Cr_2O_7$ into the solution, regardless of its concentration, however, providing a specific reason for this observation is troublesome at the present stage and likely requires a more in-depth study on this phenomenon.

It is also worth to emphasize that although the FLA- and FLC-APGD systems turned out to be quite unsusceptible to the matrix effects (in the case of the Br determination) [23], their coupling with the CVG unit allowed to reduce them even further. That being said, it can be stated that both investigated CVG-APGD-based methods were interference-free as the I^- and $Cr_2O_7^{2-}$ ions are rarely present in samples at such high concentrations as the ones studied herein, especially considering the interfering ion-to-analyte concentration ratios.

3.5. Water sample analysis

To prove the suitability of the developed methods to the real sample analysis, the determination of the Br concentration in several water samples was carried out. Since no appropriate certified reference material was accessible in our laboratory, samples of river, tap, and reservoir waters were chosen for this purpose, as relevant environmental matrices. The preliminary study carried out at this point showed that no Br was found in the selected water samples at detectable levels, therefore, the samples were spiked with certain amounts of Br. The trueness of the CVG-FLA- and CVG-FLC-APGD-OES methods was assessed in this case by determining the recoveries of Br from these samples since such an approach to substitute the reference values by using suitable prepared known samples is recommended by the ISO guidelines [51]. To ascertain the best possible credibility of the attained results, two calibration methods (namely the external standard calibration and with the aid of the standard addition method) were applied for performing the analysis. The reliability of the received results for the water samples analysis was established by comparing the whole set of results, obtained for a given sample, *i.e.*, using both calibration methods as well as the values of the recoveries of the spiked concentrations.

Due to possible discharge stability issues, coming from too much of the sample matrix, the analyzed solutions usually need to be diluted before the analysis in the case of the FLA- and FLC-APGD systems. However, a great convenience of the applied CVG technique is that only the volatile products are introduced into the discharge, which results in not only significantly reduced matrix effects but also uninterrupted discharge operation. That being said, it was decided to not perform any sample dilution. Hence, the samples were only acidified with appropriate amounts of concentrated H_2SO_4 and spiked with a previously prepared standard solution of Br (to its final concentration of 1 and 10 mg L^{-1} for CVG-FLA- and CVG-FLC-APGD, respectively).

The attained results are given in Table 2. showing that the measured concentrations values were in line with the spiked values, resulting in the recoveries falling within the 94–109% range for CVG-FLA-APGD and the 101–110% range for CVG-FLC-APGD. The RSD values of the measured concentrations were similar for both developed techniques and changed from 0.9 to 6.1% for CVG-FLA-APGD and from 1.1 to 6.1% for CVG-FLC-APGD. In addition, there were no significant variations between the results received with both applied calibration methods, proving the endurance of the developed methods to the interferences coming from the inorganic constituents of the analyzed water samples.

Considering all findings described above, it can be stated that both developed CVG-APGD-based techniques assured good accuracy of the received results, which turned out to be both true and precise. That being said, it was concluded that both proposed methods may be a reliable substitution for currently applied large-scale instrumentation

Table 2
The results of the Br determination in waters received with the aid of the developed CVG-APGD-OES methods. The spiked concentration of Br was 1 mg L^{-1} for CVG-FLA-APGD and 10 mg L^{-1} for CVG-FLC-APGD.

Method	Calibration	Sample		
		River water	Tap water	Reservoir water
CVG-FLA-APGD	ESC	1.09 ± 0.02	1.03 ± 0.05	0.97 ± 0.04
	SAM	0.98 ± 0.06	1.09 ± 0.01	0.94 ± 0.01
CVG-FLC-APGD	ESC	10.39 ± 0.26	10.13 ± 0.62	10.99 ± 0.27
	SAM	10.29 ± 0.11	10.56 ± 0.38	10.22 ± 0.13

ESC – external standard calibration.
SAM – standard addition method.
FLA-APGD – flowing liquid anode atmospheric pressure glow discharge.
FLC-APGD – flowing liquid cathode atmospheric pressure glow discharge.
CVG – chemical vapor generation.

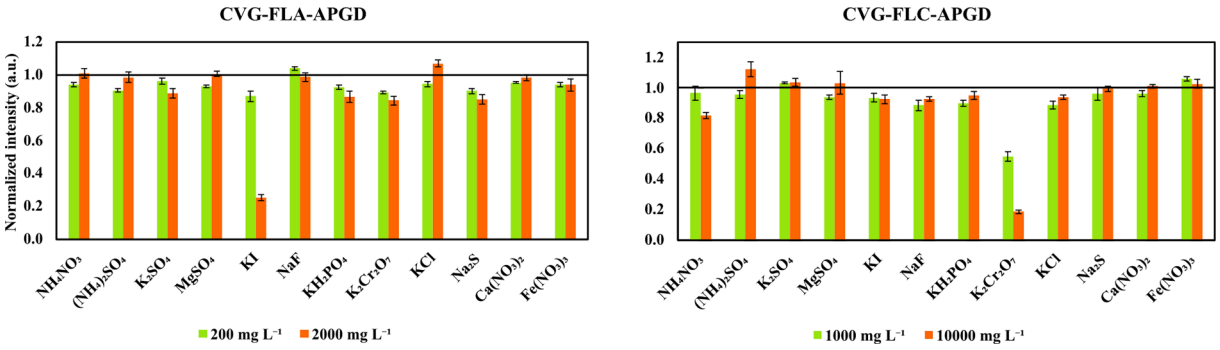

Fig. 4. The impact of presence of different salts in the analyzed solutions on the signal intensity of the Br analytical line for the studied APGD-based systems. The black horizontal line indicates the Br response for a solution not containing any interfering element.

due to their compactness, low manufacturing and operating costs as well as relatively low DLs of Br (especially in the case of CVG-FLA-APGD) and reliable analysis results received with the external standard calibration.

4. Conclusions

The application of the CVG-FLA- and CVG-FLC-APGD systems for the Br determination by OES was studied and the results obtained for both techniques were collated. This was the second time when the above-mentioned systems were applied for the determination of anions and the first time when their reaction with $KMnO_4$ was applied for this purpose. It was found that the optimal operating conditions of both studied systems were basically the same, except the discharge current which was limited in the case of the CVG-FLA-APGD system, due to the discharge stability, and the H_2SO_4 concentration in the FLA/FLC solution.

Coupling the FLA- and FLC-APGD excitation sources with the CVG unit led to the Br signal intensity enhancement around 10-fold. However, the SD of the background was significantly boosted in the case of the CVG-FLA-APGD system, as compared to FLA-APGD alone, which led to the DL of Br being improved only over 3-fold. On the other hand, the SD of the background remained unchanged for CVG-FLC-APGD (as compared to FLC-APGD), which allowed to lower the DL of Br by around 8 times.

Both studied methods were found to be resistant to matrix effects coming from the vast majority of the studied foreign anions (NO_3^-, SO_4^{2-}, F^-, Cl^-, $H_2PO_4^-$, S^{2-}) and cations (NH_4^+, K^+, Mg^{2+}, Na^+, Ca^{2+}, Fe^{3+}). It was revealed that the application of the CVG technique allowed to reduce those matrix effects almost completely, as compared to the FLA- and FLC-APGD systems. The endurance of the developed methods to the existence of foreign ions was then further confirmed after performing the analysis of selected water samples, which demonstrated no qualitative difference between the results received for the external standard calibration and the standard addition method.

Both studied methods provided reliable results of the samples analysis, making them an interesting alternative for the commercially available techniques, being currently applied for the Br determination.

Unfortunately, the proposed methods did not allow to determine Cl with the use of reasonable amounts of reagents needed for the CVG process. However, their application could be possibly broadened in the future by the determination of other anionic analytes, *e.g.*, F^-, I^-, or S^{2-}.

CRediT authorship contribution statement

Monika Gorska: Conceptualization, Data curation, Formal analysis, Investigation, Methodology, Project administration, Software, Validation, Visualization, Writing – original draft, Writing – review & editing. **Pawel Pohl:** Conceptualization, Formal analysis, Funding acquisition, Resources, Supervision, Writing – review & editing.

Declaration of Competing Interest

The authors declare that they have no known competing financial interests or personal relationships that could have appeared to influence the work reported in this paper.

Appendix A. Supplementary data

Supplementary data to this article can be found online at https://doi.org/10.1016/j.microc.2022.107391.

References

[1] X. Zhang, J.W. Talley, B. Boggess, G. Ding, D. Birdsell, Fast selective detection of polar brominated disinfection byproducts in drinking water using precursor ion scans, Environ. Sci. Technol. 42 (2008) 6598–6603, https://doi.org/10.1021/es800855b.

[2] Y.-L. Yu, Y. Cai, M.-L. Chen, J.-H. Wang, Development of a miniature dielectric barrier discharge-optical emission spectrometric system for bromide and bromate screening in environmental water samples, Anal. Chim. Acta 809 (2014) 30–36, https://doi.org/10.1016/j.aca.2013.11.054.

[3] M.O. Gorbunova, M.S. Garshina, M.S. Kulyaginova, V.V. Apyari, A.A. Furletov, A. V. Garshev, S.G. Dmitrienko, Y.A. Zolotov, A dynamic gas extraction-assisted paper-based method for colorimetric determination of bromides, Anal. Methods 12 (2020) 587–594, https://doi.org/10.1039/C9AY02640A.

[4] World Health Organization, Guidelines for Drinking-Water Quality, 4th edition, Geneva, 2011 .

[5] S.D. Richardson, A.D. Thruston, C. Rav-Acha, L. Groisman, I. Popilevsky, O. Juraev, V. Glezer, A. Bruce McKague, M.J. Plewa, E.D. Wagner, Tribromopyrrole, brominated acids, and other disinfection byproducts produced by disinfection of drinking water rich in bromide, Environ. Sci. Technol. 37 (2003) 3782–3793, https://doi.org/10.1021/es030339w.

[6] K.C. Thompson, J.L. Guinamant, V. Ingrand, A.R. Elwaer, C.W. McLeod, F. Schmitz, G. de Swaef, P. Quevauviller, Interlaboratory trial to determine the analytical state-of-the-art of bromate determination in drinking water, J. Environ. Monit. 2 (2000) 416–419, https://doi.org/10.1039/B004226I.

[7] R. Butler, L. Lytton, A.R. Godley, I.E. Tothill, E. Cartmell, Bromate analysis in groundwater and wastewater samples, J. Environ. Monit. 7 (2005) 999–1006, https://doi.org/10.1039/B505833C.

[8] L. Li, C.M. Barshick, J.T. Millay, A.V. Welty, F.L. King, Determination of bromine in flame-retardant plastics using pulsed glow discharge mass spectrometry, Anal. Chem. 75 (2003) 3953–3961, https://doi.org/10.1021/ac034567k.

[9] J.F. van Staden, L.V. Mulaudzi, R.I. Stefan, On-line speciation of bromine and bromide using sequential injection analysis with spectrophotometric detection, Anal. Bioanal. Chem. 375 (2003) 1074–1082, https://doi.org/10.1007/s00216-003-1814-4.

[10] A. Takeda, S. Yamasaki, H. Tsukada, Y. Takaku, S. Hisamatsu, N. Tsuchiya, Determination of total contents of bromine, iodine and several trace elements in soil by polarizing energy-dispersive X-ray fluorescence spectrometry, Soil Sci. Plant Nutr. 57 (2011) 19–28, https://doi.org/10.1080/00380768.2010.548313.

[11] S.E. Duirk, R.L. Valentine, Bromide oxidation and formation of dihaloacetic acids in chloraminated water, Environ. Sci. Technol. 41 (2007) 7047–7053, https://doi.org/10.1021/es070753m.

[12] I. Radivojevic, R. Niessner, C. Haisch, S. Florek, H. Becker-Ross, U. Panne, Detection of bromine in thermoplasts from consumer electronics by laser-induced plasma spectroscopy, Spectrochim. Acta B 59 (2004) 335–343, https://doi.org/10.1016/j.sab.2004.01.003.

[13] T. Vander Hoogerstraete, S. Jamar, S. Wellens, K. Binnemans, Determination of halide ions in solution by Total Reflection X-ray Fluorescence (TXRF) spectrometry, Anal. Chem. 86 (2014) 1391–1394, https://doi.org/10.1021/ac403583u.

[14] E.A. Vtorushina, A.I. Saprykin, G. Knapp, Optimization of the conditions of oxidation vapor generation for determining chlorine, bromine, and iodine in aqueous solutions by inductively coupled plasma atomic-emission spectrometry, J. Anal. Chem. 63 (2008) 643–648, https://doi.org/10.1134/S1061934808070071.

[15] J. Hu, H. Chen, X. Jiang, X. Hou, Photochemical Vapor Generation of Halides in Organic-Acid-Free Media: Mechanism Study and Analysis of Water Samples, Anal. Chem. 93 (2021) 11151–11158, https://doi.org/10.1021/acs.analchem.1c01639.

[16] A.M. Carro, R.A. Lorenzo, F. Fernandez, R. Phan-Tan-Luu, R. Cela, Microwave-assisted extraction followed by headspace solid-phase microextraction and gas chromatography with mass spectrometry detection (MAE-HSSPME-GC-MS/MS) for determination of polybrominated compounds in aquaculture samples, Anal. Bioanal. Chem. 388 (2007) 1021–1029, https://doi.org/10.1007/s00216-007-1220-4.

[17] H. Wenzhi, C. Shun-an, M. Tominaga, A. Miyazaki, Direct determination of bromide ions in sea water by ion chromatography using water as the mobile phase, Anal. Chim. Acta 322 (1996) 43–47, https://doi.org/10.1016/0003-2670(95)00573-0.

[18] W. Liu, H. Yang, B. Li, S. Xu, Determination of Bromine and Iodine Speciation in Drinking Water Using High Performance Liquid Chromatography-Inductively Coupled Plasma-Mass Spectrometry, Geostand. Geoanalytical Res. 35 (2011) 69–74, https://doi.org/10.1111/j.1751-908X.2010.00033.x.

[19] J.-H. Chen, K. Wang, S.-J. Jiang, Determination of iodine and bromine compounds in foodstuffs by CE-inductively coupled plasma MS, Electrophoresis 28 (2007) 4227–4232, https://doi.org/10.1002/elps.200700241.

[20] D.-J. Zhang, Y. Cai, M.-L. Chen, Y.-L. Yu, J.-H. Wang, Dielectric barrier discharge-optical emission spectrometry for the simultaneous determination of halogens, J. Anal. At. Spectrom. 31 (2016) 398–405, https://doi.org/10.1039/C5JA00266D.

[21] P. Pohl, I. Jimenez Zapata, M.A. Amberger, N.H. Bings, J.A.C. Broekaert, Characterization of a microwave microstrip helium plasma with gas-phase sample introduction for the optical emission spectrometric determination of bromine, chlorine, sulfur and carbon using a miniaturized optical fiber spectrometer, Spectrochim. Acta, Part B 63 (2008) 415–421, https://doi.org/10.1016/j.sab.2007.12.005.

[22] X. Jiang, X. Xu, X. Hou, Z. Long, Y. Tian, X. Jiang, F. Xu, C. Zheng, A novel capillary microplasma analytical system: interface-free coupling of glow discharge optical emission spectrometry to capillary electrophoresis, J. Anal. At. Spectrom. 31 (2016) 1423–1429, https://doi.org/10.1039/C6JA00142D.

[23] M. Gorska, P. Pohl, Application of atmospheric pressure glow discharge generated in contact with liquids for determination of chloride and bromide in water and juice samples by optical emission spectrometry, Talanta 237 (2022), 122921, https://doi.org/10.1016/j.talanta.2021.122921.

[24] R.E. Sturgeon, Detection of bromine by ICP-oa-ToF-MS following photochemical vapor generation, Anal. Chem. 87 (2015) 3072–3079, https://doi.org/10.1021/ac504747a.
[25] M. Bebek, K. Mitko, Some aspects of bromine determination by ICP-OES in salinated waters, At. Spectrosc. (2004) 64–69.
[26] M.D. Calzada, M.C. Quintero, A. Gamero, J. Cotrino, J. Uría, A. Sanz-Medel, Determination of bromide by low power surfatron microwave induced plasma after bromine continuous generation, Talanta 39 (1992) 341–347, https://doi.org/10.1016/0039-9140(92)80146-5.
[27] M. Dolores, M.C. Calzada, A. Quintero, M.G. Gamero, Chemical generation of chlorine, bromine and iodine for sample introduction into a surfatron-generated argon microwave-induced plasma, Anal. Chem. 64 (1992) 1374–1378, https://doi.org/10.1021/ac00037a013.
[28] T. Nakahara, S. Morimoto, T. Wasa, Application of atmospheric pressure helium microwave induced plasma atomic emission spectrometry with gas-phase sample introduction to the continuous-flow determination of bromine in seawaters, Anal. Sci. 7 (1991) 463–466, https://doi.org/10.2116/analsci.7.Supple_463.
[29] F. Camuna, J. Uria, A. Medel, Continuous flow and flow injection halogen generation for chloride, bromide and iodide determinations by microwave induced plasma atomic emission spectroscopy, Spectrochim. Acta B 48 (1993) 1115–1125, https://doi.org/10.1016/0584-8547(93)80102-Z.
[30] J.F. Camuna, M. Montes, R. Pereiro, A. Sanz Medel, C. Katschthaler, R. Gross, G. Knapp, Determination of halides by microwave induced plasma and stabilized capacitive plasma atomic emission spectrometry after on-line continuous halogen generation, Talanta 44 (1997) 535–544, https://doi.org/10.1016/S0039-9140(96)02055-3.
[31] Y. Duan, M. Wu, Q. Jin, G.M. Hieftje, Vapor generation of nonmetals coupled to microwave plasma-torch mass spectrometry, Spectrochim. Acta B 50 (1995) 1095–1108, https://doi.org/10.1016/0584-8547(95)01306-Y.
[32] M. Gorska, K. Greda, P. Pohl, Determination of bismuth by optical emission spectrometry with liquid anode/cathode atmospheric pressure glow discharge, J. Anal. At. Spectrom. 36 (2021) 165–177, https://doi.org/10.1039/D0JA00401D.
[33] K. Greda, K. Swiderski, P. Jamroz, P. Pohl, Flowing Liquid Anode Atmospheric Pressure Glow Discharge as an Excitation Source for Optical Emission Spectrometry with the Improved Detectability of Ag, Cd, Hg, Pb, Tl, and Zn, Anal. Chem. 88 (2016) 8812–8820, https://doi.org/10.1021/acs.analchem.6b02250.
[34] X. Liu, Z. Zhu, D. He, H. Zheng, Y. Gan, N. Stanley Belshaw, S. Hu, Y. Wang, Highly sensitive elemental analysis of Cd and Zn by solution anode glow discharge atomic emission spectrometry, J. Anal. At. Spectrom. 31 (2016) 1089–1096, https://doi.org/10.1039/C6JA00017G.
[35] K. Swiderski, A. Dzimitrowicz, P. Jamroz, P. Pohl, Influence of pH and low-molecular weight organic compounds in solution on selected spectroscopic and analytical parameters of flowing liquid anode atmospheric pressure glow discharge (FLA-APGD) for the optical emission spectrometric (OES) determination of Ag, Cd, and Pb, J. Anal. At. Spectrom. 33 (2018) 437–451, https://doi.org/10.1039/C7JA00374A.
[36] K. Greda, P. Jamroz, D. Jedryczko, P. Pohl, On the coupling of hydride generation with atmospheric pressure glow discharge in contact with the flowing liquid cathode for the determination of arsenic, antimony and selenium with optical emission spectrometry, Talanta 137 (2015) 11–17, https://doi.org/10.1016/j.talanta.2014.11.073.
[37] M. Gorska, K. Greda, P. Pohl, On the coupling of hydride generation (HG) with flowing liquid anode atmospheric pressure glow discharge (FLA-APGD) for determination of traces of As, Bi, Hg, Sb and Se by optical emission spectrometry (OES), Talanta 222 (2021), 121510, https://doi.org/10.1016/j.talanta.2020.121510.
[38] P. Pohl, P. Jamroz, K. Greda, M. Gorska, A. Dzimitrowicz, M. Welna, A. Szymczycha-Madeja, Five years of innovations in development of glow discharges generated in contact with liquids for spectrochemical elemental analysis by optical emission spectrometry, Anal. Chim. Acta 1169 (2021), 338399, https://doi.org/10.1016/j.aca.2021.338399.
[39] Z. Zhu, G.-C.-Y. Chan, S.J. Ray, X. Zhang, G.M. Hieftje, Use of a solution cathode glow discharge for cold vapor generation of mercury with determination by ICP-atomic emission spectrometry, Anal. Chem. 80 (2008) 7043–7050, https://doi.org/10.1021/ac8011126.
[40] C. Yang, G. Cheng, S.-Q. Cheng, X. Liu, Y. Liu, H.-T. Zheng, S.-H. Hu, Z.-L. Zhu, Direct and Sensitive Determination of Antimony in Water by Hydrogen-Doped Solution Anode Glow Discharge-Optical Emission Spectrometry Without Hydride Generation, Anal. Chem. 93 (2021) 16393–16400, https://doi.org/10.1021/acs.analchem.1c02940.
[41] X. Peng, M. Zhao, M. Yuan, Z. Wang, Solution anode glow discharge optical emission spectrometry: Volatile hydride introduction from the gas jet nozzle cathode for ultrasensitive determination of lead, Talanta 225 (2021), 121995, https://doi.org/10.1016/j.talanta.2020.121995.
[42] A. Garcia-Figueroa, F. Pena-Pereira, I. Lavilla, C. Bendicho, Headspace single-drop microextraction coupled with microvolume fluorospectrometry for highly sensitive determination of bromide, Talanta 170 (2017) 9–14, https://doi.org/10.1016/j.talanta.2017.03.090.
[43] X. Liu, Z. Liu, Z. Zhu, D. He, S. Yao, H. Zheng, S. Hu, Generation of Volatile Cadmium and Zinc Species Based on Solution Anode Glow Discharge Induced Plasma Electrochemical Processes, Anal. Chem. 89 (2017) 3739–3746, https://doi.org/10.1021/acs.analchem.7b00126.
[44] P. Jamroz, K. Greda, A. Dzimitrowicz, K. Swiderski, P. Pohl, Sensitive Determination of Cd in Small-Volume Samples by Miniaturized Liquid Drop Anode Atmospheric Pressure Glow Discharge Optical Emission Spectrometry, Anal. Chem. 89 (2017) 5729–5733, https://doi.org/10.1021/acs.analchem.7b01198.
[45] K. Greda, M. Gorska, M. Welna, P. Jamroz, P. Pohl, In-situ generation of Ag, Cd, Hg, In, Pb, Tl and Zn volatile species by flowing liquid anode atmospheric pressure glow discharge operated in gaseous jet mode - Evaluation of excitation processes and analytical performance, Talanta 199 (2019) 107–115, https://doi.org/10.1016/j.talanta.2019.02.058.
[46] M. Gorska, P. Pohl, Comparison of the performance of atmospheric pressure glow discharges operated between a flowing liquid cathode and either a pin-type anode or a helium jet anode for the Ga and In determination by the optical emission spectrometry, Talanta 226 (2021), 122155, https://doi.org/10.1016/j.talanta.2021.122155.
[47] Y.S. Park, S.H. Ku, S.H. Hong, H.J. Kim, E.H. Piepmeier, Fundamental studies of electrolyte-as-cathode glow discharge-atomic emission spectrometry for the determination of trace metals in flowing water, Spectrochim. Acta B 53 (1998) 1167–1179, https://doi.org/10.1016/S0584-8547(98)00154-2.
[48] M.A. Mottaleb, Y.-A. Woo, H.-J. Kim, Evaluation of open-air type electrolyte-as-cathode glow discharge-atomic emission spectrometry for determination of trace heavy metals in liquid samples, Microchem. J. 69 (2001) 219–230, https://doi.org/10.1016/S0026-265X(01)00087-X.
[49] K. Greda, A. Szymczycha-Madeja, P. Pohl, Study and reduction of matrix effects in flowing liquid anode - Atmospheric pressure glow discharge - Optical emission spectrometry, Anal. Chim. Acta 1123 (2020) 81–90, https://doi.org/10.1016/j.aca.2020.05.026.
[50] M. Gorska, P. Pohl, K. Greda, The application of antioxidant compounds to minimize matrix effects in flowing liquid anode atmospheric pressure glow discharge optical emission spectrometry, Microchem. J. 164 (2021), 105975, https://doi.org/10.1016/j.microc.2021.105975.
[51] International Standard, Accuracy (trueness and precision) of measurement methods and results - Part 4: Basic methods for the determination of the trueness of a standard measurement method. Reference number ISO 5725-4: 2020.

Supporting Information

Coupling of chemical vapor generation with atmospheric pressure glow discharge optical emission spectrometry generated in contact with flowing liquid electrodes for determination of Br in water samples

Monika Gorska*, Pawel Pohl

Wroclaw University of Science and Technology, Faculty of Chemistry, Division of Analytical Chemistry and Chemical Metallurgy, Wybrzeze Stanislawa Wyspianskiego 27, 50-370 Wroclaw, Poland

* Corresponding author. E-mail address: monika.gorska@pwr.edu.pl (Monika Gorska)

Table SI-1. The comparison of the signal-to-background ratio (SBR) values of the Br analytical line (827.2 nm) for FLA- and FLC-APGD systems with and without the chemical vapor generation (CVG) technique.

FLA-APGD	**FLC-APGD**	**CVG-FLA-APGD**	**CVG-FLC-APGD**
22.9	16.7	328.2	74.5

Table SI-2. Statistically significant terms in the regression equations modeling the effect of the studied parameters A, B and C on the signal-to-background ratio (SBR) of the analytical lines of Br.

Coefficients of regression equation	**CVG-FLA-APGD**	**CVG-FLC-APGD**
Const.	17.78	-0.31
A	17.49	342.0
B	0.78	0.55
C	15.21	6.11
A^2	-8.43	-1674
B^2	-	-
C^2	-4.22	-1.90
A·B	-	-
A·C	-	-
B·C	-	-

A – the H_2SO_4 concentration in the FLA/FLC solution (mol L^{-1}), B – the $KMnO_4$ concentration in the oxidant solution (%), C – the H_2SO_4 concentration in the sample solution (mol L^{-1}).

Table SI-3. The comparison of SBR values predicted by the models and the measured ones.

System	R-statistics of models			Model validation		
	R^2	$R^2_{(adj)}$	$R^2_{(pred)}$	Predicted	Measured	Relative error (%)
CVG-FLA-APGD	93.39	89.72	80.69	44.42	42.34	-4.68
CVG-FLC-APGD	96.49	94.55	89.44	24.82	24.00	-3.30

R^2 Coefficient of determination.

$R^2_{(adj)}$ Adjusted R^2.

$R^2_{(pred)}$ Predicted R^2.

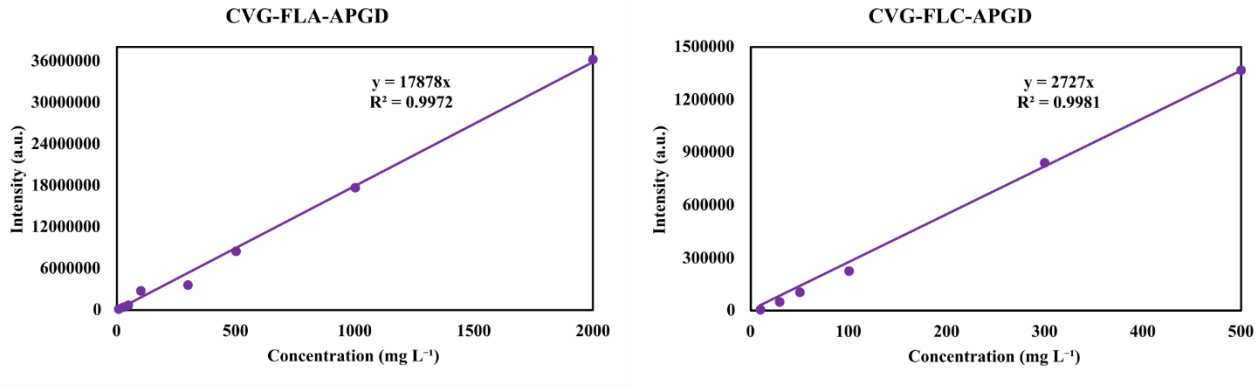

Fig. SI-1. The calibration curves of the analytical line of Br established for the CVG-FLA-APGD and CVG-FLC-APGD systems.

Talanta 222 (2021) 121510

Contents lists available at ScienceDirect

Talanta

journal homepage: www.elsevier.com/locate/talanta

On the coupling of hydride generation (HG) with flowing liquid anode atmospheric pressure glow discharge (FLA-APGD) for determination of traces of As, Bi, Hg, Sb and Se by optical emission spectrometry (OES)

Monika Gorska *, Krzysztof Greda, Pawel Pohl

Wroclaw University of Science and Technology, Faculty of Chemistry, Division of Analytical Chemistry and Chemical Metallurgy, Wybrzeze Stanislawa Wyspianskiego 27, 50-370, Wroclaw, Poland

ARTICLE INFO

Keywords:
Atmospheric pressure glow discharge
Flowing liquid anode
Solution anode glow discharge
Cold vapor generation
Hydride generation
Miniaturized plasma
Optical emission spectrometry

ABSTRACT

A novel atmospheric pressure glow discharge (APGD) microplasma system, sustained between a miniaturized flowing liquid anode (FLA) and a He jet nozzle cathode, was combined with a hydride generation (HG) technique to improve the determination performance of As, Bi, Hg, Sb, and Se with the aid of optical emission spectrometry (OES). The discharge current, the He flow rate, and the concentrations of HCl and $NaBH_4$ were considered to affect both the HG reaction and the excitation conditions in the discharge, thus they were thoroughly studied. Under the optimized conditions, the detections limits (LODs), assessed on the basis of the 3σ criterion, reached 1.7, 0.85, 0.04, 0.51, and 2.9 μg L^{-1} for As, Bi, Hg, Sb, and Se, respectively. The HG and transport efficiency for these elements was evaluated to be 88–100%, which is notably better, as compared to their transport efficiency in the conventional FLA-APGD system, without the HG technique. This yielded an improvement of the LODs achievable in this system and, simultaneously, enabled to determine As, Sb, and Se at a level, which is unobtainable with the use of the FLA-APGD system alone. The proposed methodology was then successfully applied for a quantitative determination of the examined elements in wastewater (ERM-CA713) and spiked water samples. The recoveries of the elements added to these waters (at the maximum acceptable levels in drinking water set by the U.S. Environmental Protection Agency) ranged between 81 and 104%, confirming the excellent accuracy, usefulness, and reliability of the developed HG-FLA-APGD technique.

1. Introduction

The use of miniaturized plasma sources in spectrochemical analysis has gained much attention over the course of the last several dozen years due to their numerous advantages, which include: a small size, low manufacturing and operating costs, a low power and gas consumption, portability and a possibility for performing real-time measurements [1–5]. Moreover, these systems provide similar or better analytical characteristics, in terms of detection limits (LODs), precision and linearity extents, than bulky and costly conventionally used techniques, such as ICP-OES [4,6–8].

Discharges generated in contact with liquids constitute a large group of those systems. The numerous examples of such techniques can be distinguished: electrolyte jet cathode glow discharge (EJC-GD) [9], discharge on boiling in a channel (DBC) [10], liquid electrode plasma (LEP) [11], electrolyte cathode discharge (ELCAD) [12], solution cathode glow discharge (SCGD) [13], flowing liquid cathode - atmospheric pressure glow discharge (FLC-APGD) [14], liquid sampling - atmospheric pressure glow discharge (LS-APGD) [15], solution anode glow discharge (SAGD) [16], liquid drop anode - atmospheric pressure glow discharge (LDA-APGD) [17], hanging drop electrode – atmospheric pressure glow discharge (HDE-APGD) [18] or flowing liquid anode - atmospheric pressure glow discharge (studied herein) [19]. From the abovementioned methods, FLA-APGD is one of the newest techniques being developed. When first described in 2016 by Liu et al. [16] and shortly after by Greda et al. as well [19], it offered LODs of the studied elements improved up to 3 orders of magnitude, in comparison with other plasma systems operated in contact with liquids. Additionally, those systems provided wide linearity ranges, high precision, and good trueness of the results in real samples analysis. Later on, it was shown that LODs of the studied elements and precision provided by the system could be further improved by operating FLA-APGD with the aid of a He

* Corresponding author.
E-mail address: monika.gorska@pwr.edu.pl (M. Gorska).

https://doi.org/10.1016/j.talanta.2020.121510
Received 1 June 2020; Received in revised form 29 July 2020; Accepted 3 August 2020
Available online 7 August 2020
0039-9140/

jet [20] and/or by using selected organic media [21,22]. Considering the aforesaid results, it was concluded that FLA-APGD is a promising analytical tool for optical emission spectrometry (OES).

Nevertheless, it was demonstrated that, despite a great number of elements introducing into FLA-APGD, measurable signals could be observed only in the case of Ag, Bi, Cd, Hg, In, Pb, Tl, and Zn [19,20,23]. It was concluded that the reason for this phenomenon is related to the mechanism of the analytes transport into the discharge phase of the FLA-APGD system. Since all the abovementioned elements are well-known to form volatile species, *e.g.,* hydrides, vapors, and other forms [24–27], it is assumed that they are released from the liquid phase into the discharge in a form of some kind of such volatile species. The mentioned species are likely a consequence of the electrochemical reactions taking place while bombarding the solution surface with the high-energy electrons [19,20]. There are also other elements that are recognized to form their volatile species, *e.g.,* As, Os, Sb, Se, and Sn [27,28], however, no emission from those elements was remarked in the investigated FLA-APGD systems. Despite a few attempts [16,19,20] to either explain the mechanism taking place in FLA-APGD or to collect and assay the nature of the volatile species formed, up to now, it has not been managed yet to do this.

The other disadvantage of the FLA-APGD system is its strong vulnerability to interferences from concomitant ions [19,20,29]. Although it was evidenced that transition metals, as well as alkali and alkaline earth metals reduce the sensitivity of the analytical emission lines, the matrix effects are especially inconvenient when sample solutions contain high concentrations of alkali and alkaline earth metals. The results published so far revealed that the presence of Ca, K, Mg and Na in the sample solutions at the concentrations of 10 mg L^{-1} may decline the recoveries of the studied elements (Ag, Cd, Hg, In, Pb, Tl, Zn) by 20–80% [20,29]. Very recently, Greda et al. [30] found that matrix effects result from chemical interactions in a liquid phase (plasma parameters remain unaffected), and they can be reduced by the use of different complexing agents. It was possible to significantly mitigate matrix effects originating from transition metals, however, interferences coming from alkali and alkaline earth metals were more difficult to be minimized. Considering this, the matrix effects from concomitant ions became a serious limitation in the quantitative determination of elements by the FLA-APGD-OES method even in very common samples, *e.g.,* waters, especially mineral and tap waters, which contain large amounts of alkali and alkaline earth metals. Hence, in the papers published until now, the FLA-APGD system was used to the analysis of samples, which either did not contain alkali and alkaline earth metals [19,23,29], or the standard addition method was applied to overcome the interference effects [29].

Cold vapor generation (CVG) and hydride generation (HG) are widely employed sample introduction techniques being coupled to both conventional instruments such as ICP-OES [31], as well as microplasma sources [6,32–34]. Both mentioned analytes introduction techniques assure high transport and atomization efficacies leading to boosted emission from investigated elements and – as a consequence – improving their sensitivity and lowering the obtained LODs [33,35,36]. Furthermore, the matrix interferences are eliminated in both techniques due to their selectivity. As a result, the use of CVG or HG techniques enables to determine traces of selected analytes in different kind of real samples with no particular sample preparation or calibration method required [33–35,37].

Therefore, the aim of the present work was to improve the analytical characteristics of APGD sustained between a He jet nozzle cathode and a solution of a miniaturized FLA by coupling it with the HG sample introduction technique. It was expected that the use of HG would open the possibility for determining the elements, which signals were not previously observed in the FLA-APGD system operating in contact with a metallic pin cathode, namely As, Sb, and Se. Regarding the elements which were determined before in the later FLA-APGD system, *i.e.,* Bi [23] and Hg [19–21,23], it was foreseen that the replacement of a traditional way of the analytes introduction from an FLA solution with a HG unit would enhance their sensitivity and the achieved detectability.

To begin with, the emission spectra of the FLA-APGD system with the traditional analytes introduction *via* the FLA solution was compared to those obtained when the HG unit was connected to APGD through the He nozzle jet. Subsequently, the effects of selected working conditions, including the discharge current, the He flow rate, as well as the HCl and $NaBH_4$ concentrations, were investigated to improve the sensitivity and the detectability of the proposed system. Under the optimized conditions, the analytical figures of merit, *i.e.,* the linearity range, precision, and LODs of As, Bi, Hg, Sb, and Se were assessed. Finally, the developed HG-FLA-APGD method was successfully applied for the quantitative determination of As, Bi, Hg, Sb, and Se in different water samples spiked with those elements.

2. Experimental

2.1. Instrumentation

A schematic drawing of the HG-FLA-APGD system is shown in Fig. 1. The device described in previous papers [20,36] were the basis of the developed system. FLA-APGD was sustained in an open-to-air discharge chamber between a tungsten nozzle (OD/ID 3/1 mm, length 50 mm) and a vertically oriented quartz tube (OD/ID 5/3 mm) through which an FLA solution (HNO_3, 0.01 mol L^{-1}) was pumped. The tungsten nozzle was fed with He at a flow rate up to 350 mL min^{-1} which was controlled using a Tylan General (CA, USA) FC-2900 flow controller and a RO-28 digital flow meter. The FLA solution was delivered through the quartz tube by means of a 3-channel REGLO ICC peristaltic pump (Ismatec, USA) at a flow rate of 3.5 mL min^{-1}. The overflowing solution was pumped out from the anode compartment using the very same peristaltic pump. The FLA solution did not contain the analytes (As, Bi, Hg, Sb, Se) as it served only for sustaining the discharge. The distance between the tungsten nozzle and the solution surface (so called the discharge gap) was set to approximately 1 mm. The electrical contact was provided directly in case of the tungsten nozzle and with the aid of a Pt spiral wrapped around the quartz tube in case of the FLA solution. The voltage of 600–1000 V was applied to both electrodes by an HV dc power supply (model DP50H–024 PH, DSC-Electronics, Germany) and its exact value was depended on the discharge current, the He flow rate, and the H_2 amount fed into the discharge (corresponding to the respective $NaBH_4$ concentration). To stabilize the discharge, a 2.2 kΩ ballast resistor was connected into the circuit.

Cold vapors of Hg and volatile hydrides of As, Bi, Sb, and Se were generated in a separate cylindrical chamber (ID 34 mm, total volume 90 mL) connected to the FLA-APGD system. The sample solutions acidified with HCl as well as the $NaBH_4$ solutions alkalized with 0.1% NaOH were introduced separately to the chamber through a Y-junction by a 4-channel Perimax peristaltic pump (AHF Analysentechnik, Germany). The flow rate of 2.0 mL min^{-1} was adjusted through all experiments for the solutions of samples and the reductant. The chamber had a glass frit at the bottom and a drainage inserted from the top. The He flow was introduced to the same chamber from the bottom through the glass frit and swept the gaseous reaction products into the discharge. The post-reaction solution was pumped out into a waste container using the abovementioned peristaltic pump. To decrease the water vapor content in the gas mixture, an additional glass coil (length 70 cm, dead volume 9 mL) was inserted between the chamber and the tungsten nozzle.

The radiation emitted by APGD was imaged (1:1) on the entrance slit (10 μm) of a Shamrock 500i imaging spectrometer (Andor, UK), using an achromatic quartz lens (f = 80). The spectrometer was equipped with a holographic grating (1800 lines mm^{-1}) and a Newton DU-920P-OE UV–Vis CCD camera (Andor, UK). The integration time was 10 s during all experiments. The intensities of the atomic emission lines of As, Bi, Hg, Sb, and Se were background corrected.

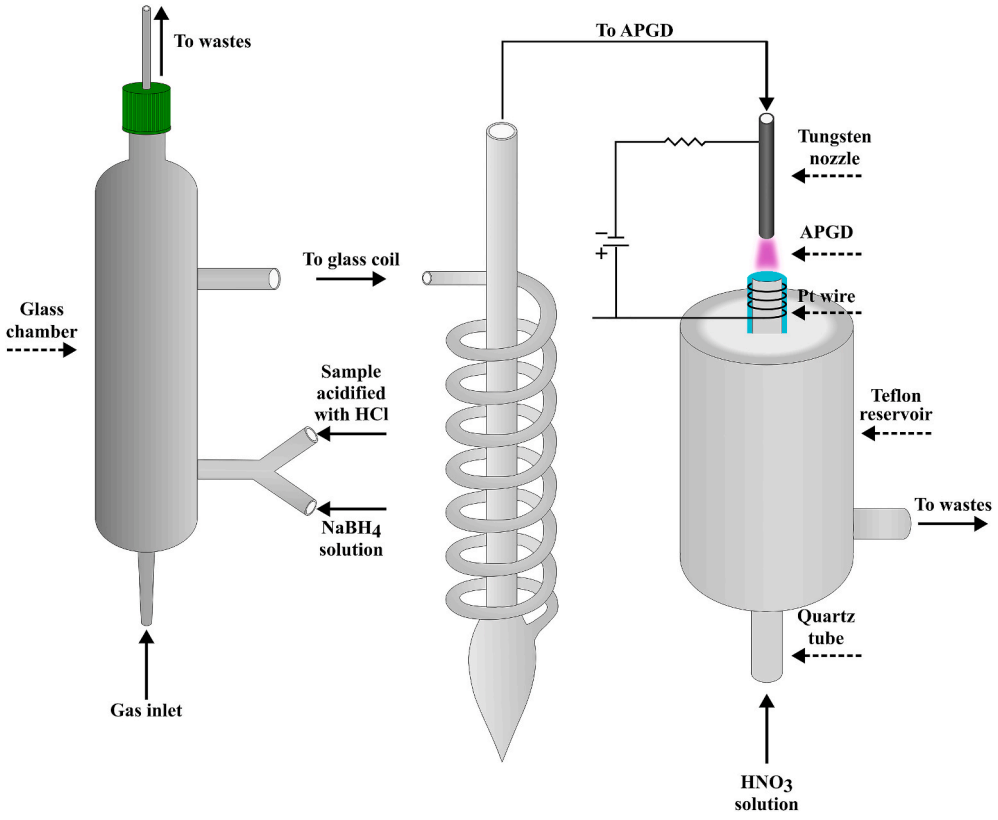

Fig. 1. A schematic drawing of the developed HG-FLA-APGD system.

2.2. Reagents and samples

Deionized water (18.2 MΩ cm^{-1}) from an Easypure water purification system (Thermolyne Corp., USA) was used throughout the study. All chemicals were at least of analytical grade. He of 99.999% purity was supplied by Air Products (Poland). Stock standard solutions of As(III), Bi (III) and Hg(II) (1000 mg L^{-1}) obtained from Sigma-Aldrich (Germany), as well as As(V), Sb(III) from Merck KGaA (Germany) were used to prepare all working standard solutions. Stock standard solutions of Sb (V) and Se(IV) (1000 mg L^{-1}) were prepared from the respective salts, *i.e.,* $K[Sb(OH)_6]$ and Na_2SeO_3 (Sigma-Aldrich, Germany), while a stock standard solution of Se(VI) (1000 mg L^{-1}) was obtained by heating solid Na_2SeO_3 with an appropriate amount of concentrated 65% (m/m) HNO_3 solution (Merck, Germany). The same concentrated HNO_3 solution was employed to prepare the FLA solution. A concentrated 37% (m/m) HCl solution from Merck (Germany) was utilized to acidify all sample solutions for HG/CVG reactions and pre-reduce the Se(VI) species to the Se (IV) species. Additionally, solid thiourea (Sigma-Aldrich, Germany) and ascorbic acid (Eurochem BGD, Poland) were used to pre-reduce the As and Sb species from their pentavalent to trivalent forms. The reducing agent solutions were prepared by dissolving solid $NaBH_4$ (Sigma-Aldrich, Germany) in a 0.1% NaOH solution, obtained from solid NaOH (Avantor Performance Materials, Poland). All the $NaBH_4$ solutions were freshly prepared and filtered through cellulose filter papers (grade 595).

Mineral water was purchased in a local store. The Oder river water (sampled in the city of Wroclaw, Poland) and municipal tap water (Wroclaw, Poland) were collected into pre-cleaned 1 L bottles made of PE. The river water was initially filtered through the cellulose filter paper. The certified reference material of wastewater (ERM-CA713) was obtained from Sigma-Aldrich (Germany).

2.3. Sample preparation

With the aim of determining the content of As, Hg and Sb in mineral, river and tap waters, a portion of 15.0 mL of each type of water was transferred into a twist cup container and acidified with an appropriate amount of a concentrated HCl to reach its final concentration of 7.5% (m/m). To assure that As and Sb existed in the sample only in their reduced forms, ascorbic acid and thiourea were added to obtain their final concentration of 0.5% (m/m), and the resulting solutions were diluted with deionized water to 20.0 mL. Moreover, the analysis of wastewater (ERM-CA713) on the content of Hg was carried out. The sample was prepared as described above (except that ascorbic acid and thiourea were not added). As it had not been expected to acquire any signals from As, Hg, and Sb in mineral, river and tap waters (due to the absence of those elements in analyzed types of water), a second series of the samples was prepared. In this case, all the aforesaid preparation steps were repeated but the water samples were previously spiked with As, Hg, and Sb to reach their final concentrations of 10, 2, and 6 μg L^{-1}, respectively; these are the maximum contaminant levels in drinking water set by the U.S. Environmental Protection Agency (EPA).

Considering the determination of Bi and Se, these elements could not be measured in the same samples because the mixture of ascorbic acid and thiourea suppresses signals of those elements [38]. Therefore, separate samples of each water were prepared to determine the Bi and Se content. The analyzed water (5.3 mL) and concentrated HCl (5.3 mL) were transferred into a DigiPrep tube and the samples were being heated for 2 h at 120 °C. After cooling, the samples were filled with deionized water to the final volume of 30.0 mL. As previously, to perform the recovery study, analyzed waters were spiked with Bi and Se (prior to pre-reduction) to reach the concentrations of 50 μg L^{-1} (this concentration of Se is the maximum acceptable level in drinking water set by the EPA).

All abovementioned water samples were prepared in triplicates, besides, appropriate procedural blanks were prepared and considered in the final results. All sample solutions were analyzed with the aid of the HG-FLA-APGD-OES method against solutions of simple standards and procedural blanks.

3. Results and discussion

3.1. Comparison of the emission spectra of the FLA-APGD systems with and without HG

To compare the emission spectra of both the conventional FLA-APGD system and the FLA-APGD system combined with the HG unit, three multi-element solutions of As, Bi, Hg, Sb, and Se were prepared. First of them (Standard 1) comprised of Bi (10 mg L^{-1}), Hg (1 mg L^{-1}), and the reduced forms of As, Sb, and Se, at concentrations of 10 mg L^{-1} in 0.01 mol L^{-1} HNO_3. The second solution (Standard 2) contained the same elements (at the same concentrations) with the difference that oxidized forms of As, Sb, and Se were used. These solutions were analyzed by the conventional FLA-APGD. The last standard solution (Standard 3) contained Bi, Hg, and reduced forms of As, Sb and Se at concentrations of 200 μg L^{-1} (for each element) and it was acidified with 10% HCl (m/m). This solution was intended to be analyzed by HG-FLA-APGD. It should be noted that for this standard, a separate solution containing oxidized forms of As, Sb, and Se was not prepared as their HG efficiency is lower than this of the reduced forms [39]. The measurements were taken at the discharge current of 50 mA and the He flow rate of 350 mL min^{-1}. As for the HG-FLA-APGD system, either 0.05% (Hg) or 0.3% (As, Bi, Sb, and Se) $NaBH_4$ solutions were employed.

Fig. 2 demonstrates the emission spectra of FLA-APGD (Standard 1) and HG-FLA-APGD (Standard 3), recorded in the 190–270 nm spectral range. The additional information about signal to background ratios (S/B) for different atomic emission lines obtained for both systems is presented in Table S1. As compared to the classical FLA-APGD, for HG-FLA-APGD the intensity of NO molecular bands, and thus the background intensity in the vicinity of emission lines, was lowered even up to 16 times. This beneficial phenomenon may likely result from the presence of H_2 (reducing agent, introduced with carrier gas) that swept NO radicals (strong oxidant), causing a decrease in the NO concentration. Considering the most sensitive atomic emission lines of the studied elements, which signals could be observed in both explored systems (Bi 223.1 nm and Hg 253.7 nm), the background level in their vicinity was descended about 2–5 times when the mentioned elements were introduced to the discharge with the aid of the HG unit.

With regard to the conventional FLA-APGD, despite a great concentration of the elements, strong signals were remarked only for Bi and Hg. Considering the other elements, only weak signals (for Sb) or no signals at all (for As and Se) were detected when using that system. As regard to the HG-FLA-APGD system, measurable signals for all examined elements were obtained. In this case, the extraordinary emission from Hg and Sb was observed, whereas the signals coming from As, Bi and Se were slightly weaker.

Taking into account that for most of the studied elements several signals were obtained, 2 or 3 most sensitive atomic emission lines of As (193.8, 228.8 and 235.0 nm), Sb (206.8, 217.6 and 231.1 nm) and Se (196.1 and 204.0 nm) were analyzed in the subsequent experiments. When it comes to Bi, even 5 atomic lines were identified in the studied spectral range, but the relatively strong emission (S/B higher than 1) was registered only at 223.1 nm and this line was assayed throughout all experiments. Finally, in the case of Hg, only the resonance line (253.7 nm) was identified and analyzed in further experiments.

3.2. Optimization of the HG-FLA-APGD system parameters

With the object of boosting the obtained S/B of the studied elements, the optimization of crucial working parameters of the HG-FLA-APGD system was performed. The following parameters were considered as the most influential on the signals and the background intensities: the discharge current, the He flow rate, and the HCl and $NaBH_4$ concentrations. For this purpose, multi-element solutions containing As(III), Bi, Hg, Sb (III), and Se(IV) at concentrations of 200, 300, 10, 100, and 500 μg L^{-1}, respectively, were prepared. Unless otherwise stated, the measurement conditions were as follows: the discharge current of 50 mA, the He flow rate of 350 mL min^{-1}, the HCl concentration of 10%, and the $NaBH_4$ concentration of 0.05% (for Hg) or 0.3% (for As, Bi, Sb, and Se), respectively.

3.3. The effect of discharge current

The influence of the discharge current on the emission intensity and S/B for all the studied elements was examined in the range of 20–60 mA; it was found that discharge currents beyond that scope destabilized the plasma. It was established that an increase in the discharge current yielded a linear rise of the emission intensity from As, Bi, Sb, and Se; the observed rise was between 1.5 and 2.2 (depending on the line) over the investigated range. The background intensity in the vicinity of the studied emission lines changed dissimilarly. Its enhancement was noticed as the discharge current increased from 20 to 30 mA, but afterward, the background intensity either slightly dropped (in the spectral range up to 220 nm) or remained roughly constant (above 220 nm). As a result of these changes, the higher the discharge current was, the higher S/B value for As, Bi, Sb, and Se was noted (see Fig. S1). Utterly

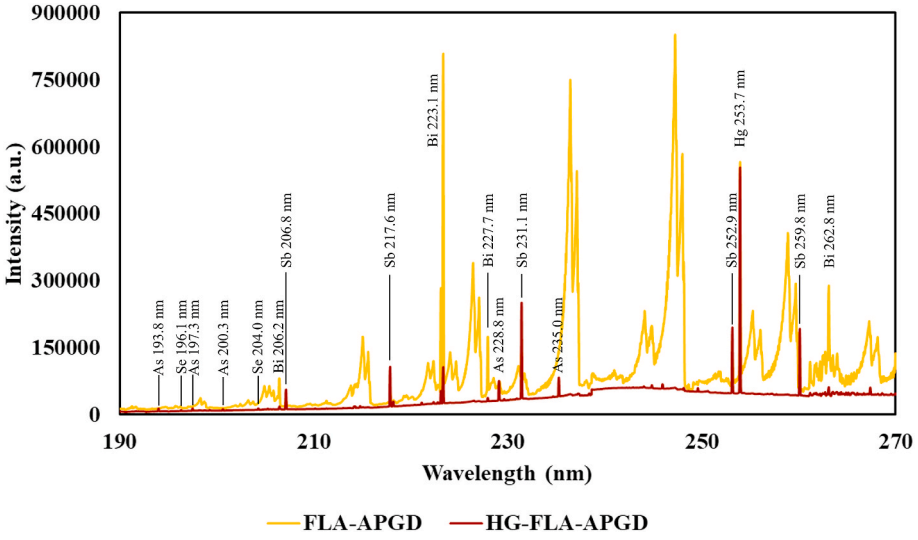

Fig. 2. Emission spectra of FLA-APGD and HG-FLA-APGD systems. Elements concentration: Bi(III) 10 mg L^{-1}; Hg(II) 1 mg L^{-1}; As(III), Sb(III), and Se (IV) 10 mg L^{-1} for FLA-APGD and Bi(III), Hg(II), As(III), Sb(III), and Se (IV), all at a concentration of 0.20 mg L^{-1} for HG-FLA-APGD.

diverse findings were obtained for the emission line of Hg; its maximum was observed at 30–40 mA, and above that value, a slight suppression could be noticed. As a consequence, the highest S/B value was obtained at the discharge current of 30 mA.

In conventional FLC-APGD and FLA-APGD [13,19] systems with tungsten pin electrodes, it was established that higher discharge currents resulted in an improved transport efficiency of the studied elements into the discharge, which yielded an increased intensity of their emission lines. Nonetheless, this phenomenon could not explain the outcomes presented in this paper, as in the case of the HG-FLA-APGD system the FLA solution did not contain the analytes. On the other hand, it could be expected that the growth of the discharge current might increase the energy density in the discharge, which would provide better atomization/excitation conditions for the analytes leading to a boosted intensity of the atomic emission lines. Indeed, this theory seems to be reflected in the results obtained for As, Bi, Sb, and Se signals. Although the Hg behavior is more troublesome to explain and it departs from the other investigated elements, it is in line with previously reports for the HG-FLC-APGD [36] and classical FLA-APGD systems [20]. In the last of the aforesaid papers [20], it was established that, for Hg, lower discharge currents are preferred when high He flow rates are applied. Moreover, a combination of the highest studied He flow rate with the lowest investigated discharge current led to obtain the prime results in terms of the atomic emission Hg line intensity and the LOD of this element. The He flow rate employed in the experiment of the present work was even higher than the one utilized in the abovementioned work, which likely elucidates the optimal S/B value acquired for Hg.

A reasonable explanation for the reduced background intensity could be an observation made by Greda and co-workers [19], who noted that at higher discharge currents the greater evaporation of water appeared, which, being introduced into the discharge phase, hindered the access of the surrounding air to it. As a consequence, the formation of the excited states of the NO and N_2 molecules was likely suppressed, which yielded a decline in their emission bands intensity.

Bearing in mind the fact that for almost all elements the highest S/B values were obtained as the discharge current increased, and having regard to relatively small differences in the S/B fluctuations of the Hg emission line, it was concluded that the use of higher discharge currents was preferred, as a compromised condition for all analytes. Although the best S/B values were obtained when the discharge current of 60 mA was applied, at the same point the discharge started to be unstable. Taking this fact into consideration, the discharge current of 50 mA was used in further experiments to assure a better stability of the developed HG-FLA-APGD system.

3.4. The effect of gas flow rate

In conventional glow discharge systems generated in contact with liquids, the use of an additional discharge gas (*e.g.*, gaseous jet) is unneeded because they are sustained in the surrounding air atmosphere. Regarding the systems in which the HG technique is applied, an additional gas flow is required to separate the volatile hydrides from a reaction chamber and carry them into the discharge [33,40]. In this case, it could be expected that the highest S/B values would be reached with the enhanced gas flow rate, as a consequence of the improved analytes transport and excitation efficiency. On the other hand, the increasing gas flow rate could also be responsible for shortened residence time of the analytes in the discharge phase which would lead to decline their emission. Thus, the impact of the He flow rate on the S/B value of the studied elements was examined within 100–350 mL min^{-1}.

As can be seen in Fig. S2, the growth of the He flow rate yielded a boost of the S/B values. However, it was also noted that this increasing tendency was dissimilar for various elements. For example, considering As, Sb, and Se, the observed enhancement was quite minor, while in the case of Bi and Hg it was much stronger. Due to the abovementioned differences in shifts of the S/B values for different elements, the intensities of the atomic emission lines of the analytes and the background level in their vicinity were additionally analyzed. It was revealed that the background intensity in the vicinity of all the examined emission lines dropped up to 200 mL min^{-1}, and went up afterward. A similar observation was made for the intensity of the As, Sb and Se atomic emission lines, while this for the Bi and Hg emission lines was increasing over the whole studied range. Considering the observed changes in the response from all the analytes, it could be stated that at lower He flow rates, the analytes separation in the HG unit and the transport efficiency were poor and presumably the residence time of the analytes in the discharge phase played a more significant role. Hence, the initial drop of the atomic emission lines intensities could be explicated by a shortened residence time in the discharge core with the He flow rate enhancement up to 200 mL min^{-1}. The lack of Bi and Hg vulnerability to the shortened residence time could be possibly related to a lower excitation energy of these elements in comparison to the rest of the investigated elements. Consequently, the improved analytes separation and transport efficacy could be responsible for a further increase of the intensity of their emission lines. A quite different explanation seemed to be reasonable, regarding the background intensity. Mohamed et al. [41] and Jamroz et al. [42] demonstrated that in other microplasma systems, namely microhollow cathode discharge and FLC-APGD, generated with the aid of different gaseous jets, a gas flow shift from laminar to turbulent took place at relatively low flow rates. Therefore, at low He flow rates, its growth could result in a decreased diffusion of N_2 and O_2 to the discharge phase. At high He flow rates the turbulent flow rate could facilitate the diffusion of N_2 and O_2 from the outer layers of the discharge into its core, where the conditions of the excitation processes are more favorable and thus, the formation of different molecular excited states, *e.g.*, N_2, N_2^+, NO, could be higher [43–45].

That being so, the He flow rate of 350 mL min^{-1} was applied in further experiments, as the highest S/B values were acquired at this point for almost all examined elements. The only exception from that rule was Se, however, the differences between the highest S/B value obtained at 300 mL min^{-1} and the one gained for the He flow rate of 350 mL min^{-1} were negligible.

3.5. The effect of the HCl and $NaBH_4$ concentration

To achieve the maximum CVG/HG generation efficiency, the intensity of the atomic emission lines of the studied elements, the background intensity in their vicinity, and the respective S/B values were analyzed in relation to different HCl and $NaBH_4$ concentrations, investigated within the range of 5–20% and 0.005–0.5%, respectively.

Fig. 3 presents the impact of the HCl concentration on the S/B values acquired for the examined elements. Apparently, the changes in the HCl concentrations did not affect the S/B values of As and Se, slightly changed the S/B value of Hg, and had a strong influence on the S/B values of Bi and Sb. Considering the emission lines intensities of the studied elements, they declined as the HCl concentration was raised from 5.0 to 20.0% for all elements, with exception of Hg. However, the observed changes in the intensities varied between elements. For instance, the shift of the HCl concentration from 5.0 to 20.0% yielded an intensity drop of the As emission lines by 25–30%, while the same intensity drop was around 55% for Sb. As for Hg, the intensity of its line was roughly equal for almost the whole studied scope. Regarding the background level in the vicinity of the emission lines of the studied elements, it fell averagely by 16% as the HCl concentration grew. The only exception was the background level in the vicinity of the Hg emission line which was virtually constant over the whole examined range.

The observed decline of both the emission lines intensities and the background level could be explained by the enhanced amount of the water aerosol, likely containing some remnants of HCl and $NaBH_4$ that was introduced into the discharge phase and led to worsening the excitation conditions in the discharge. This could particularly happen at higher HCl concentrations because the course of the HG reaction was

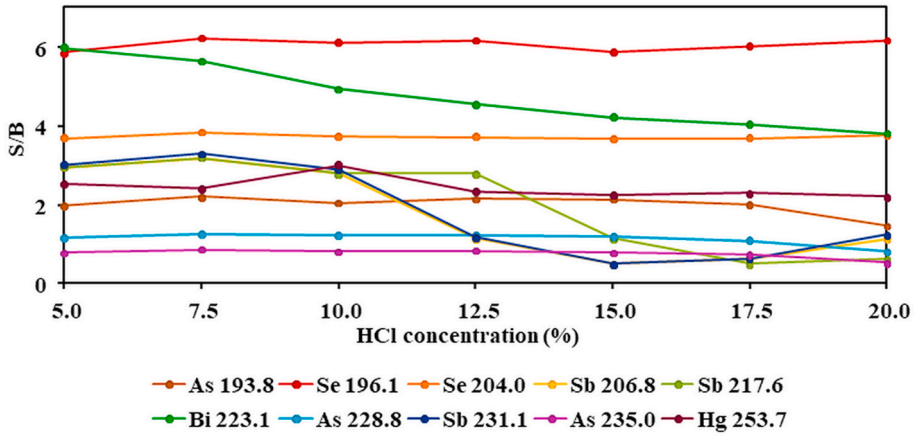

Fig. 3. The effect of the HCl concentration on the signal to background ratio (S/B) of all studied elements.

more violent and vigorous in these conditions, and the abovementioned water aerosol could be introduced. With regard to the abovementioned results, there was no doubt that lower HCl concentrations were preferred. The best S/B values of the emission lines of the studied elements were acquired in the range of 5–10% HCl and they were different for each element. To simplify the determination procedure, the HCl concentration of 7.5% was used for the sample acidification in further experiments, as a compromised value for all studied elements.

Contrary to the influence of the HCl concentration, the variations in the $NaBH_4$ concentration strongly affected the gained S/B values (see Fig. 4). The highest S/B values were obtained at various $NaBH_4$ concentrations for different elements, *i.e.,* 0.005% (Hg); 0.01% (Sb); 0.05% (Bi) and 0.1% (As and Se). To provide a clarification to what caused different $NaBH_4$ concentrations to be optimal for different analytes, their emission lines intensities and the background levels in the vicinity of these lines were analyzed at first. It was established that changes in the $NaBH_4$ concentrations had a diverse impact on both the atomic emissions lines intensities and the background intensity. Considering the emission lines intensities of the analytes, they enhanced as the $NaBH_4$ concentration was risen up to 0.01% (Sb), 0.1% (Bi), 0.2% (Se), and 0.5% (As) and subsequently dropped. For the Hg emission line, it came out that the increase of the $NaBH_4$ concentration resulted in a remarkable suppression of its intensity over the whole examined range of the reductant concentration. A similar behavior of the Hg emission line was previously observed in the CVG-FLC-APGD systems [32,36]. The effect of the $NaBH_4$ concentration on the background intensity was independent of the investigated spectral range; as the reductant concentration increased, the constant growth in the background level could be observed.

In light of so divaricated outcomes, the CVG/HG efficiency was

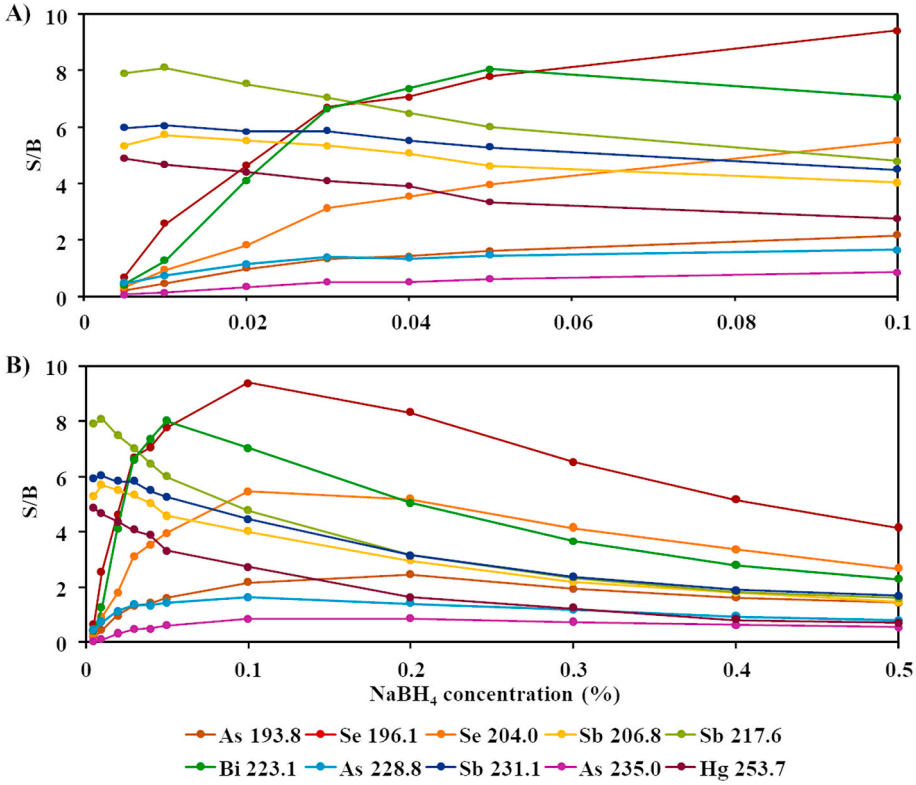

Fig. 4. The effect of the $NaBH_4$ concentration on the signal to background ratio (S/B) of all studied elements. A) A close-up of the 0–0.1% range, B) The whole studied range.

additionally investigated at the $NaBH_4$ concentrations equal to 0.005, 0.01, 0.05 and 0.1% (see Fig. 5). To assess the CVG/HG efficacy, mixed solutions containing studied elements were prepared and delivered into the HG-FLA-APGD system with corresponding $NaBH_4$ solutions. Followingly, the quantification of the examined elements was performed in the resulting post-reaction solutions using an Agilent ICP-OES instrument, model 5110. Taking into account the LODs of the studied elements achievable with the ICP-OES instrument, the concentrations of As, Bi, Sb and Se in the solutions used in this experiment were equal to those previously applied, while the concentration of Hg was ten times higher, *i.e.,* 100 μg L^{-1}.

With regard to the CVG/HG efficiency, it rendered that Bi, Hg, and Sb achieved around 100% efficiencies of their conversion into the corresponding volatile species at the $NaBH_4$ concentrations at which the highest S/B values were reached for these elements. Considering As and Se, the highest HG efficiency was also achieved at the $NaBH_4$ concentration corresponding to the highest S/B values for those elements, *i.e.,* 0.1%, however, it reached only 88 and 90%, respectively. Comparing these results with the emission lines intensity of the studied elements, one could notice that the maximum of the response from Hg and Sb correlated well to the $NaBH_4$ concentration at which the HG reaction took place with the 100% efficiency and the highest S/B values were obtained. In such a case, it could be stated that the initial enhancement of the emission lines intensity (in case of Sb) was related to the growing HG efficacy and its subsequent drop was related to the atomization of H_2 and the excitation of the H atoms as a process competitive to the atomization of the hydrides and the excitation of the mentioned elements atoms. Considering intensities of the emission lines of As, Bi and Se, possibly the HG efficiency for these elements reached 100% at higher $NaBH_4$ concentrations, *i.e.,* 0.1% (Bi), 0.2% (Se) and at least 0.5% (As), however, the background intensity was relatively high at these $NaBH_4$ concentrations that deteriorated the overall S/B values of these emission lines.

Taking into account variations of the S/B values at different $NaBH_4$ concentrations for each element, it was impossible to choose one $NaBH_4$ concentration, which would be optimal for all elements. Therefore, for As, Bi, Sb, and Se, the $NaBH_4$ concentrations corresponding to the highest S/B values were applied in further experiments, *i.e.,* 0.01% (Sb), 0.05% (Bi) and 0.1% (As, Se). In case of Hg, although the best S/B value was achieved at the $NaBH_4$ concentration of 0.005%, it was decided to use a 0.01% $NaBH_4$ solution in the following experiments due to a possibility of some competitive reactions of the reducing agent with other sample components.

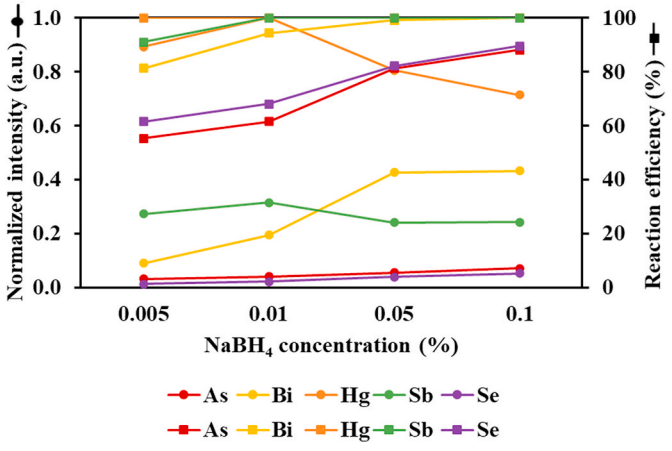

Fig. 5. The effect of the $NaBH_4$ concentration on the response from the studied elements and their hydrides generation efficiency.

3.6. Analytical performance and application

Under optimal operating conditions (the discharge current of 50 mA, the He flow rate of 350 mL min^{-1}, the HCl concentration of 7.5% and the $NaBH_4$ concentration of 0.01% (Hg, Sb), 0.05% (Bi), and 0.1% (As, Se)), the analytical performance of the developed HG-FLA-APGD-OES method was evaluated. For this purpose, LODs of As, Bi, Hg, Sb, and Se, the extent of linearity of the calibration curves of their analytical lines, and the precision were investigated.

Table 1 presents the LODs achieved by the proposed method (calculated as 3σ/a, where "3σ" stands for 3 times the standard deviation of 30 consecutive measurements of an appropriate blank solution, and "a" stands for the sensitivity of a corresponding emission line). For simplification, in case of As, Sb, and Se, the results were shown only for one atomic emission line, corresponding to the lowest LODs obtained, *i.e.,* 228.8 nm, 231.1 nm and 196.1 nm, respectively. In addition, the attained LOD values were compared with those reported for other systems, working with a continuous flow mode sample introduction, constituting both the miniaturized plasma excitation sources and conventionally employed spectroscopy techniques, being premised upon bulky instruments. The comparison revealed that LODs of Hg and Sb were similar to those obtained by all methods they were compared to. Regarding the other elements (As, Bi, Se), it was concluded that their LODs achieved using the HG-FLA-APGD system were up to 1 order of magnitude higher than those offered by commercially utilized techniques, such as ICP-OES and MIP-OES, however they were still better than those achievable with other microplasma sources, such as DBD or APGD generated between a solid anode and a liquid cathode (FLC-APGD). It is also noteworthy that coupling the FLA-APGD system with CVG/HG provided better LODs of Bi and Hg than the same system with a traditional sample introduction technique [19,20,23] (through the FLA solution) and simultaneously – enabled to determine As, Sb and Se, which is not achievable with the aid of the FLA-APGD system without HG.

Table 2 exhibits the linearity ranges and the precision for all studied emission lines of As, Bi, Hg, Sb, and Se. The linearity extents were examined using 10 single-element standard solutions in the concentration range of 1–10000 μg L^{-1}. It was found that the calibration curves of the atomic emission lines of the studied elements were linear ($R^2 > 0.995$) within 2 (Bi, Se) or 3 (As, Hg, Sb) orders of magnitude. The precision was expressed as relative standard deviation (RSD) for 10 consecutive measurements of multi-element standard solutions. The RSD was measured 3 times for each separate emission line and the averaged results were given. This figure of merit was evaluated separately for 2 concentrations of each element (quoted in in Table 2). The

Table 1
The comparison of limits of detection (LODs) of As, Bi, Hg, Sb and Se obtained for the HG-FLA-APGD system with those obtained for different excitation sources reported in the literature.

Method	LOD (μg L^{-1})					Reference
	As	Bi	Hg	Sb	Se	
HG-FLA-APGD	1.7	0.85	0.04	0.51	2.9	This work
HG-DBD-AFS	30	-[a]	-[a]	70	60	[40]
CVG-μAPGD	-[a]	-[a]	0.06	-[a]	-[a]	[32]
HG-ICP-OES	0.87	-[a]	-[a]	0.80	0.99	[46]
HG-APGD-OES	4.2	-[a]	-[a]	1.2	3.1	[34]
HG-MIP-OES	0.46	0.09	-[a]	0.46	-[a]	[47]
HG-SAGD-OES	-[a]	-[a]	0.03	-[a]	-[a]	[33]

HG Hydride generation. FLA Flowing liquid anode. (μ)APGD Atmospheric pressure glow (micro)discharge. AAS Atomic absorption spectrometry. DBD Dielectric barrier discharge. AFS Atomic fluorescence spectrometry. CVG Cold vapor generation. ICP Inductively coupled plasma. OES Optical emission spectrometry. MIP Microwave-induced plasma. SAGD Solution anode glow discharge.

[a] Not studied.

Table 2
Analytical figures of merit of the proposed HG-FLA-APGD-OES method for As, Bi, Hg, Sb and Se.

Element	Wavelength (nm)	LR (μg L^{-1})	R^2	S (a.u. per μg L^{-1})	RSD (%) (concentration, μg L^{-1})
As	193.8	32–10000	0.9993	1.05×10^1	18.7 (32)/6.3 (100)
	228.8	10–10000	0.9993	9.32×10^1	8.9 (32)/3.0 (100)
	235.0	32–10000	0.9987	8.89×10^1	21.3 (32)/2.2 (100)
Bi	223.1	10–3200	0.9997	3.17×10^2	3.3 (32)/2.2 (100)
Hg	253.7	1–3200	0.9995	3.18×10^3	21.5 (1)/6.9 (3.2)
Sb	206.8	3.2–3200	0.9969	5.56×10^1	6.5 (10)/3.3 (32)
	217.6	1–3200	0.9998	1.09×10^2	4.9 (10)/1.8 (32)
	231.1	3.2–3200	0.9957	2.52×10^2	3.3 (10)/1.8 (32)
Se	196.1	10–1000	0.9979	2.31×10^1	6.5 (32)/3.2 (100)
	204.0	10–3200	0.9996	2.71×10^1	9.9 (32)/3.0 (100)

LR Linearity range. R^2 Coefficient of determination. S Sensitivity.

results indicated that for the most sensitive lines of As (228.8 nm), Bi (223.1 nm), Sb (231.1 nm), and Se (204.0 nm), the precision was equal to 3.0% or better, considering higher concentrations of the analytes. Nevertheless, the measured precision for the Hg emission line was slightly worse, equal to 6.9%.

To ascertain the trueness of the offered method, the determination of the studied elements in wastewater (ERM-CA713), river, mineral and tap waters was performed under the optimized conditions. The external standard calibration curves were used to quantify the studied elements in all analyzed samples. The determined concentration of Hg in wastewater was in line with certified value (see Table 3). As for river, mineral and tap waters, they were initially analyzed with no addition of any of the examined elements. As no signal from those elements was detected, the analysis was repeated, but this time, the spiked samples were analyzed. The analyzed samples were spiked at concentrations corresponding to maximum contaminant levels in drinking water set by the EPA, *i.e.,* 10, 2, 6, and 50 μg L^{-1} of As, Hg, Sb, and Se, respectively. In the case of Bi (no EPA recommendation), it was added at a concentration of 50 μg L^{-1}. The percent recoveries along with RSDs of the analysis of the samples to which the targeted analytes were added are shown in Table 3. The results confirm the good trueness of the method since the recovery values of the added analytes were fallen within the range of 81–104%, which is still admittable in the trace analysis. The only exception was Se that could not be reliably quantified in the studied waters; the sample had to be diluted over 5-times prior to analysis, hence the resulting concentration of Se was slightly below LOQ (9.6 μg L^{-1}). Nevertheless, in all the examined samples, apparent analytical signals at 204.0 nm were detected. A comparison of the limits of quantification (LOQs) of As (5.6 μg L^{-1}), Hg (0.13 μg L^{-1}), and Sb (1.7 μg L^{-1}) achievable with the developed HG-FLA-APGD-OES method with the maximum contaminant levels adopted by U.S. EPA for ground and drinking waters, *i.e.*, As (10 μg L^{-1}), Hg (2 μg L^{-1}), and Sb (6 μg L^{-1}) [48], let us state that the proposed method is appropriate for assessing water quality and safety. Based on the work findings, it was concluded that the proposed method is a reliable alternative to the commercially used large instruments, which require much higher power and gas consumption.

Table 3
The results of the determination of As, Bi, Hg, Sb, and Se in different water samples by the developed HG-FLA-APGD-OES method.

Water type	Element	Measured (μg L^{-1})	Added (μg L^{-1})	Found[a] (μg L^{-1})	Recovery[b] (%)
River water	As	<LOD	10	8.98 ± 0.47	89.8 ± 4.9
	Bi		50	50.8 ± 1.3	102 ± 6
	Hg		2.0	2.07 ± 0.07	104 ± 4
	Sb		6.0	6.12 ± 0.09	102 ± 3
	Se		50	<LOQ	–
Mineral water	As		10	9.66 ± 0.56	96.6 ± 9.8
	Bi		50	50.9 ± 2.9	102 ± 5
	Hg		2.0	1.83 ± 0.09	91.5 ± 4.9
	Sb		6.0	6.01 ± 0.06	100 ± 2
	Se		50	<LOQ	–
Tap water	As		10	8.13 ± 0.81	81.3 ± 5.0
	Bi		50	42.5 ± 2.9	85.0 ± 6.3
	Hg		2.0	1.85 ± 0.11	92.5 ± 5.8
	Sb		6.0	6.07 ± 0.8	101 ± 2
	Se		50	<LOQ	–
CRM type		**Element**	**Certified (μg L^{-1})**	**Measured (μg L^{-1})**	**Relative error (%)**
Wastewater (ERM-CA713)		Hg	1.85 ± 0.11	1.77 ± 0.08	−4.3

LOD - limit of detection.
LOQ - limit of quantification.
[a] Average values (n = 3) ± type A standard uncertainty.
[b] Percent recoveries ± relative standard deviation (RSD).

4. Conclusions

As compared to previously reported APGD systems, all operated in contact with solutions of differently constructed liquid electrodes, the use of the FLA-APGD system combined with the HG unit gives a real possibility to determine traces of As, Sb and Se, which is normally infeasible when the transport of these elements takes place in a traditional way, *i.e.,* by releasing them from the FLA solution. Moreover, when it comes to Bi and Hg, LODs of these elements were notably improved in comparison to the use of the FLA-APGD system for their determination. This is the novelty of this work and the benefit for the spectrochemical element analysis carried out by OES with new microplasma based excitation sources. The use of the CVG/HG technique with the aid of the $NaBH_4$ reductant allows to avoid matrix effects from concomitant components, hence the trace analysis of samples containing large amount of them can be performed. However, due to the memory effects observed for Hg and Se, some longer washing times of the CVG/HG unit are required in case of the measurements of (ultra)traces of these elements. A good tolerance of H_2 derived from up to 0.5% $NaBH_4$ decomposition and a quite simple emission spectrum with a relatively low background level leads to the high sensitivity offered for determining the analytes and the good precision (3–4% for 30–100 μg L^{-1} of the analytes in the solutions). Although the obtained LODs of the studied elements (0.04–2.9 mg L^{-1}) are slightly worse than those reported for conventionally employed large-scale spectrometric instruments, the developed miniaturized excitation source seems to be competitive to those currently used, particularly in case of the monitoring of the quality and safety of ground and drinking waters in reference to the content of As, Hg, Sb and Se. In contrast to the mentioned bulky ICP sources combined with the OES detection, it offers the advantages of a small size, a stable operation at a relatively low discharge current and a reduced gas consumption, as well as a requirement of a low $NaBH_4$ concentration to be applied. It was demonstrated that the HG-FLA-APGD system developed in this study is an accurate (precise and true) and efficient tool for reliable determinations of traces of As, Bi, Hg, Sb, and Se in different water samples. Finally, the replacement of the metallic cathode with the He gaseous jet certainly broadens the capability of the system, which could be used as an atomic emission detector for gas chromatography.

Author statement

Monika Gorska: Conceptualization, Data curation, Investigation,

Methodology, Project administration, Software, Validation, Visualization, Writing - original draft, Writing - review & editing. Krzysztof Greda: Conceptualization, Funding acquisition, Methodology, Resources, Software, Supervision, Writing - review & editing. Pawel Pohl: Conceptualization, Formal analysis, Funding acquisition, Supervision, Writing - review & editing.

Declaration of competing interest

The author declares that he has no known competing financial interests or personal relationships that could have appeared to influence the work reported in this paper.

Acknowledgments

This work was funded by the National Science Centre (Poland) based on decision no. DEC-2017/24/C/ST4/00325.

Appendix A. Supplementary data

Supplementary data to this article can be found online at https://doi.org/10.1016/j.talanta.2020.121510.

References

[1] Y. Cai, X.-G. Gao, Z.-N. Ji, Y.-L. Yu, J.-H. Wang, Nonthermal optical emission spectrometry for simultaneous and direct determination of zinc, cadmium and mercury in spray, Analyst 143 (2018) 930–935, https://doi.org/10.1039/c7an01633f.

[2] B. Han, X. Jiang, X. Hou, C. Zheng, Miniaturized dielectric barrier discharge carbon atomic emission spectrometry with online microwave-assisted oxidation for determination of total organic carbon, Anal. Chem. 86 (2014) 6214–6219, https://doi.org/10.1021/ac501272m.

[3] E.D. Hoegg, R.K. Marcus, D.W. Koppenaal, J. Irvahn, G.J. Hager, G.L. Hart, Determination of uranium isotope ratios using a liquid sampling atmospheric pressure glow discharge/Orbitrap mass spectrometer system, Rapid Comm. Mass Spectrom. 31 (2017) 1534–1540, https://doi.org/10.1002/rcm.7937.

[4] P. Pohl, P. Jamroz, K. Swiderski, A. Dzimitrowicz, A. Lesniewicz, Critical evaluation of recent achievements in low power glow discharge generated at atmospheric pressure between a flowing liquid cathode and a metallic anode for element analysis by optical emission spectrometry, TrAC Trends Anal. Chem. (Reference Ed.) 88 (2017) 119–133, https://doi.org/10.1016/j.trac.2017.01.002.

[5] C. Yang, G.C.-Y. Chan, D. He, Z. Liu, Q. Deng, H. Zheng, S. Hu, Z. Zhu, Highly sensitive determination of arsenic and antimony based on an interrupted gas flow atmospheric pressure glow discharge excitation source, Anal. Chem. 91 (2019) 1912–1919, https://doi.org/10.1021/acs.analchem.6b05158.

[6] X. Peng, Z. Wang, Ultrasensitive determination of selenium, arsenic by modified helium atmospheric pressure glow discharge optical emission spectrometry coupled with hydride generation, Anal. Chem. 91 (2019) 10073–10080, https://doi.org/10.1021/acs.analchem.9b02006.

[7] Y. Cai, Y.-J. Zhang, D.-F. Wu, Y.-L. Yu, J.-H. Wang, Nonthermal optical emission spectrometry: direct atomization and excitation of cadmium for highly sensitive determination, Anal. Chem. 88 (2016) 4192–4195, https://doi.org/10.1021/acs.analchem.6b00830.

[8] J. Yu, Z. Zhang, Q. Lu, D. Sun, S. Zhu, X. Zhang, X. Wang, W. Yang, High-sensitivity determination of K, Ca, Na, and Mg in salt mines samples by atomic emission spectrometry with a miniaturized liquid cathode glow discharge, J. Anal. Methods Chem. 2017 (2017) 7105831, https://doi.org/10.1155/2017/7105831.

[9] V.V. Yagov, M.L. Getsina, B.K. Zuev, Use of electrolyte jet cathode glow discharges as sources of emission spectra for atomic emission detectors in flow-injection analysis, J. Anal. Chem. 59 (2004) 1037–1041, https://doi.org/10.1023/B:JANC.0000047005.47648.f0.

[10] B.K. Zuev, V.V. Yagov, M.L. Getsina, B.A. Rudenko, Discharge on boiling in a channel as a new atomization and excitation source for the flow determination of metals by atomic emission spectrometry, J. Anal. Chem. 57 (2002) 907–911, https://doi.org/10.1023/A:1020475025336.

[11] A. Kitano, A. Iiduka, T. Yamamoto, Y. Ukita, E. Tamiya, Y. Takamura, Highly sensitive elemental analysis for Cd and Pb by liquid electrode plasma atomic emission spectrometry with quartz glass chip and sample flow, Anal. Chem. 83 (2011) 9424–9430, https://doi.org/10.1021/ac2020646.

[12] T. Cserfalvi, P. Mezei, P. Apai, Emission studies on a glow discharge in atmospheric pressure air using water as a cathode, J. Phys. D Appl. Phys. 26 (1993) 2184–2188, https://doi.org/10.1088/0022-3727/26/12/015.

[13] M.R. Webb, F.J. Andrade, G. Gamez, R. McCrindle, G.M. Hieftje, Spectroscopic and electrical studies of a solution-cathode glow discharge, J. Anal. At. Spectrom. 20 (2005) 1218–1225, https://doi.org/10.1039/B503961D.

[14] P. Jamroz, W. Zyrnicki, Spectroscopic characterization of miniaturized atmospheric-pressure dc glow discharge generated in contact with flowing small size liquid cathode, Plasma Chem. Plasma Process. 31 (2011) 681–696, https://doi.org/10.1007/s11090-011-9307-2.

[15] H.W. Paing, K.A. Hall, R.K. Marcus, Sheathing of the liquid sampling – atmospheric pressure glow discharge microplasma from ambient atmosphere and its implications for optical emission spectroscopy, Spectrochim. Acta B 155 (2019) 99–106, https://doi.org/10.1016/j.sab.2019.03.002.

[16] X. Liu, Z. Zhu, D. He, H. Zheng, Y. Gan, N.S. Belshaw, S. Hu, Y. Wang, Highly sensitive elemental analysis of Cd and Zn by solution anode glow discharge atomic emission spectrometry, J. Anal. At. Spectrom. 31 (2016) 1089–1096, https://doi.org/10.1039/C6JA00017G.

[17] P. Jamroz, K. Greda, A. Dzimitrowicz, K. Swiderski, P. Pohl, Sensitive determination of Cd in small-volume samples by miniaturized liquid drop anode atmospheric pressure glow discharge optical emission spectrometry, Anal. Chem. 89 (2017) 5729–5733, https://doi.org/10.1021/acs.analchem.7b01198.

[18] K. Swiderski, P. Pohl, P. Jamroz, A miniaturized atmospheric pressure glow microdischarge system generated in contact with a hanging drop electrode – a new approach to spectrochemical analysis of liquid microsamples, J. Anal. At. Spectrom. 34 (2019) 1287–1293, https://doi.org/10.1039/c9ja00038k.

[19] K. Greda, K. Swiderski, P. Jamroz, P. Pohl, Flowing liquid anode atmospheric pressure glow discharge as an excitation source for optical emission spectrometry with the improved detectability of Ag, Cd, Hg, Pb, Tl, and Zn, Anal. Chem. 88 (2016) 8812–8820, https://doi.org/10.1021/acs.analchem.6b02250.

[20] K. Greda, M. Gorska, M. Welna, P. Jamroz, P. Pohl, In-situ generation of Ag, Cd, Hg, In, Pb, Tl and Zn volatile species by flowing liquid anode atmospheric pressure glow discharge operated in gaseous jet mode - evaluation of excitation processes and analytical performance, Talanta 199 (2019) 107–115, https://doi.org/10.1016/j.talanta.2019.02.058.

[21] K. Greda, S. Burhenn, P. Pohl, J. Franzke, Enhancement of emission from indium in flowing liquid anode atmospheric pressure glow discharge using organic media, Talanta 204 (2019) 304–309, https://doi.org/10.1016/j.talanta.2019.06.015.

[22] K. Swiderski, A. Dzimitrowicz, P. Jamroz, P. Pohl, Influence of pH and low-molecular weight organic compounds in solution on selected spectroscopic and analytical parameters of flowing liquid anode atmospheric pressure glow discharge (FLA-APGD) for the optical emission spectrometric (OES) determination of Ag, Cd, and Pb, J. Anal. At. Spectrom. 33 (2018) 437–451, https://doi.org/10.1039/c7ja00374a.

[23] M. Yuan, X. Peng, F. Ge, Q. Li, K. Wang, D.-G. Yu, Z. Wang, Simplified design for solution anode glow discharge atomic emission spectrometry device for highly sensitive detection of Ag, Bi, Cd, Hg, Pb, Tl, and Zn, Microchem. J. 155 (2020) 104785, https://doi.org/10.1016/j.microc.2020.104785.

[24] J.A. Nobrega, R.E. Sturgeon, P. Grinberg, G.J. Gardner, C.S. Brophy, E.E. Garcia, UV photochemical generation of volatile cadmium species, J. Anal. At. Spectrom. 26 (2011) 2519–2523, https://doi.org/10.1039/C1JA10252D.

[25] A.S. Luna, R.E. Sturgeon, R.C. de Campos, Chemical vapor generation: atomic absorption by Ag, Au, Cu, and Zn following reduction of aquo ions with sodium tetrahydroborate(III), Anal. Chem. 72 (2000) 3523–3531, https://doi.org/10.1021/ac000221n.

[26] M.L. Garrido, R. Munoz-Olivas, C. Camara, Determination of cadmium in aqueous media by flow injection cold vapour atomic absorption spectrometry. Application to natural water samples, J. Anal. At. Spectrom. 13 (1998) 295–300, https://doi.org/10.1039/A707419K.

[27] P. Smichowski, S. Farias, S.P. Arisnabarreta, Chemical vapour generation of transition metal volatile species for analytical purposes: determination of Zn by inductively coupled plasma-optical emission spectrometry, Analyst 128 (2003) 779–785, https://doi.org/10.1039/B212844F.

[28] E.T. Mansur, S.-J. Barnes, D. Savard, P.C. Webb, Determination of Te, as, Bi, Sb and Se (TABS) in geological reference materials and geo PT proficiency test materials by hydride generation-atomic fluorescence spectrometry (HG-AFS), Geostand. Geoanal. Res. 44 (2020) 143–167, https://doi.org/10.1111/ggr.12289.

[29] X. Liu, Z. Liu, Z. Zhu, D. He, S. Yao, H. Zheng, S. Hu, Generation of volatile cadmium and zinc species based on solution anode glow discharge induced plasma electrochemical processes, Anal. Chem. 89 (2017) 3739–3746, https://doi.org/10.1021/acs.analchem.7b00126.

[30] K. Greda, A. Szymczycha-Madeja, P. Pohl, Study and reduction of matrix effects in flowing liquid anode - atmospheric pressure glow discharge - optical emission spectrometry, Anal. Chim. Acta https://doi.org/10.1016/j.aca.2020.05.026.

[31] J. Proch, P. Niedzielski, In-spray chamber hydride generation by multi-mode sample introduction system (MSIS) as an interface in the hyphenated system of high performance liquid chromatography and inductivity coupled plasma optical emission spectrometry (HPLC/HG-ICP-OES) in arsenic species determination, Talanta 208 (2020) 120395, https://doi.org/10.1016/j.talanta.2019.120395.

[32] K. Greda, K. Kurcbach, K. Ochromowicz, T. Lesniewicz, P. Jamroz, P. Pohl, Determination of mercury in mosses by novel cold vapor generation atmospheric pressure glow microdischarge optical emission spectrometry after multivariate optimization, J. Anal. At. Spectrom. 30 (2015) 1743–1751, https://doi.org/10.1039/c5ja00170f.

[33] M. Yuan, X. Peng, F. Ge, M. Zhao, Q. Li, Z. Wang, Ultrasensitive determination of mercury by solution anode glow discharge atomic emission spectrometry coupled with hydride generation, Chin. Chem. Lett. (2020), https://doi.org/10.1016/j.cclet.2020.03.055.

[34] K. Greda, P. Jamroz, D. Jedryczko, P. Pohl, On the coupling of hydride generation with atmospheric pressure glow discharge in contact with the flowing liquid cathode for the determination of arsenic, antimony and selenium with optical emission spectrometry, Talanta 137 (2015) 11–17, https://doi.org/10.1016/j.talanta.2014.11.073.

[35] C. Huang, Q. Li, J. Mo, Z. Wang, Ultratrace determination of tin, germanium, and selenium by hydride generation coupled with a novel solution-cathode glow discharge-atomic emission spectrometry method, Anal. Chem. 88 (2016) 11559–11567, https://doi.org/10.1021/acs.analchem.6b02807.

[36] K. Greda, P. Jamroz, P. Pohl, Coupling of cold vapor generation with an atmospheric pressure glow microdischarge sustained between a miniature flow helium jet and a flowing liquid cathode for the determination of mercury by optical emission spectrometry, J. Anal. At. Spectrom. 29 (2014) 893–902, https://doi.org/10.1039/c3ja50395j.

[37] J. Cheng, Q. Li, M. Zhao, Z. Wang, Ultratrace Pb determination in seawater by solution-cathode glow discharge-atomic emission spectrometry coupled with hydride generation, Anal. Chim. Acta 1077 (2019) 107–115, https://doi.org/10.1016/j.aca.2019.06.003.

[38] M. Welna, A. Szymczycha-Madeja, P. Pohl, Critical evaluation of strategies for single and simultaneous determinations of As, Bi, Sb and Se by hydride generation inductively coupled plasma optical emission spectrometry, Talanta 167 (2017) 217–226, https://doi.org/10.1016/j.talanta.2017.01.029.

[39] P. Cava-Montesinos, A. de La Guardia, C. Teutsch, M. Luisa Cervera, M. de La Guardia, Non-chromatographic speciation analysis of arsenic and antimony in milk hydride generation atomic fluorescence spectrometry, Anal. Chim. Acta 493 (2003) 195–203, https://doi.org/10.1016/S0003-2670(03)00876-6.

[40] M. Yang, J. Xue, M. Li, G. Han, Z. Xing, S. Zhang, X. Zhang, Low temperature hydrogen plasma assisted chemical vapor generation for Atomic Fluorescence Spectrometry, Talanta 126 (2014) 1–7, https://doi.org/10.1016/j.talanta.2014.03.009.

[41] A.-A.H. Mohamed, J.F. Kolb, K.H. Schoenbach, Low temperature, atmospheric pressure, direct current microplasma jet operated in air, nitrogen and oxygen, Eur. Phys. J. D 60 (2010) 517–522, https://doi.org/10.1140/epjd/e2010-00220-7.

[42] P. Jamroz, W. Zyrnicki, P. Pohl, The effect of a miniature argon flow rate on the spectral characteristics of a direct current atmospheric pressure glow microdischarge between an argon microjet and a small sized flowing liquid cathode, Spectrochim. Acta B 73 (2012) 26–34, https://doi.org/10.1016/j.sab.2012.06.008.

[43] K. Greda, P. Jamroz, P. Pohl, Comparison of the performance of direct current atmospheric pressure glow microdischarges operated between a small sized flowing liquid cathode and miniature argon or helium flow microjets, J. Anal. At. Spectrom. 28 (2013) 1233–1241, https://doi.org/10.1039/c3ja50062d.

[44] K. Greda, P. Jamroz, P. Pohl, Ultrasonic nebulization atmospheric pressure glow discharge — preliminary study, Spectrochim. Acta B 121 (2016) 22–27, https://doi.org/10.1016/j.sab.2016.04.008.

[45] P. Jamroz, K. Greda, P. Pohl, Direct current atmospheric pressure microdischarge generated between a miniature flow helium microjet and a flowing liquid cathode, Plasma Process. Polym. 11 (2014) 755–762, https://doi.org/10.1002/ppap.201400012.

[46] M. Welna, A. Szymczycha-Madeja, Effect of sample preparation procedure for the determination of As, Sb and Se in fruit juices by HG-ICP-OES, Food Chem. 159 (2014) 414–419, https://doi.org/10.1016/j.foodchem.2014.03.046.

[47] R.C. Machado, C.D.B. Amaral, J.A. Nobrega, A.R.A. Nogueira, Multielemental determination of as, Bi, Ge, Sb, and Sn in agricultural samples using hydride generation coupled to microwave-induced plasma optical emission spectrometry, J. Agric. Food Chem. 65 (2017) 4839–4842, https://doi.org/10.1021/acs.jafc.7b01448.

[48] US EPA National Primary Drinking Water Regulations (EPA 816-F-09-004), United States Environmental Protection Agency, Office of Ground Water and Drinking Water, Washington, DC, 2009.

Table S1

Comparison of signal to background ratios (S/B) of the most sensitive atomic emission lines for FLA-APGD and HG-FLA-APGD systems. Considering S/B, please take into account differences in the standard solution composition (see footnote).

Element (line)	Signal to background ratio		
	FLA-APGD		HG-FLA-APGD
	Standard 1[a]	Standard 2[b]	Standard 3[c]
As (193.8 nm)	ND	ND	3.47
Se (196.1 nm)	ND	ND	0.88
As (197.3 nm)	ND	ND	1.22
As (200.3 nm)	ND	ND	1.18
Se (204.0 nm)	ND	ND	0.53
Bi (206.2 nm)	6.99	6.35	0.93
Sb (206.8 nm)	1.16	0.29	6.76
Sb (217.6 nm)	1.63	0.48	6.81
Bi (223.1 nm)	10.86	9.44	3.48
Bi (227.7 nm)	2.59	2.13	0.26
As (228.8 nm)	ND	ND	1.69
Sb (231.1 nm)	0.87	0.31	7.06
As (235.0 nm)	ND	ND	1.17
Sb (252.9 nm)	0.76	ND	3.48
Hg (253.7 nm)	5.21	8.08	11.68
Sb (259.8 nm)	ND	ND	4.19
Bi (262.8 nm)	1.38	1.40	1.28

ND Not detected.

Solution composition:

[a] Bi(III) 10 mg L^{-1}; Hg(II) 1 mg L^{-1}; As(III), Sb(III), and Se (IV) 10 mg L^{-1}.

[b] Bi(III) 10 mg L^{-1}; Hg(II) 1 mg L^{-1}; As(V), Sb(V), and Se (VI) 10 mg L^{-1}.

[c] Bi(III), Hg(II), As(III), Sb(III), and Se (IV), all at a concentration of 0.20 mg L^{-1}.

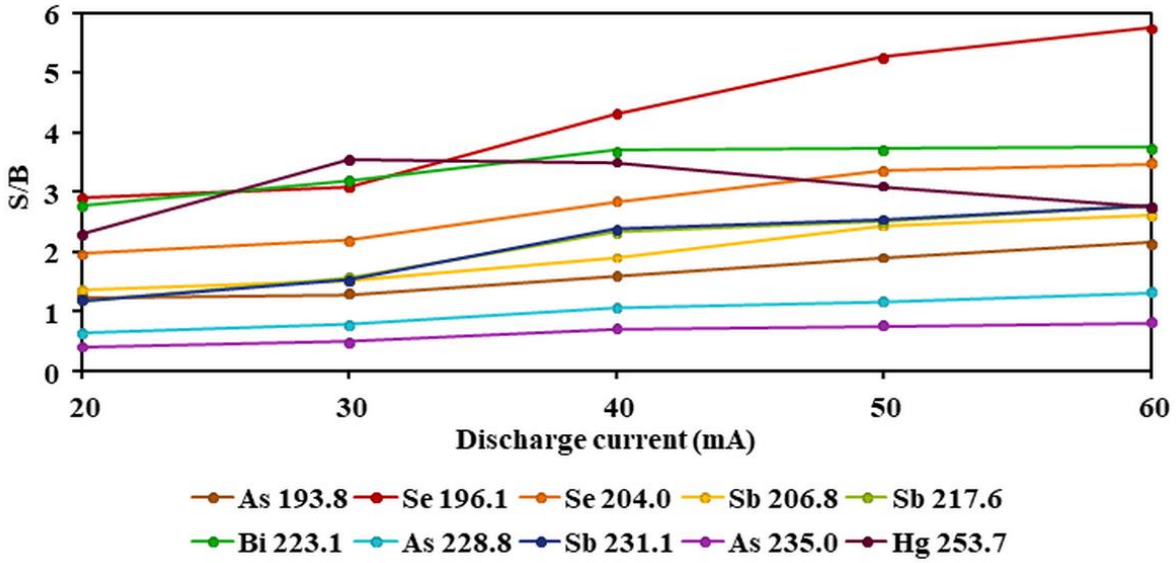

Fig. S1. The effect of the discharge current on the signal to background ratio (S/B) of all studied elements.

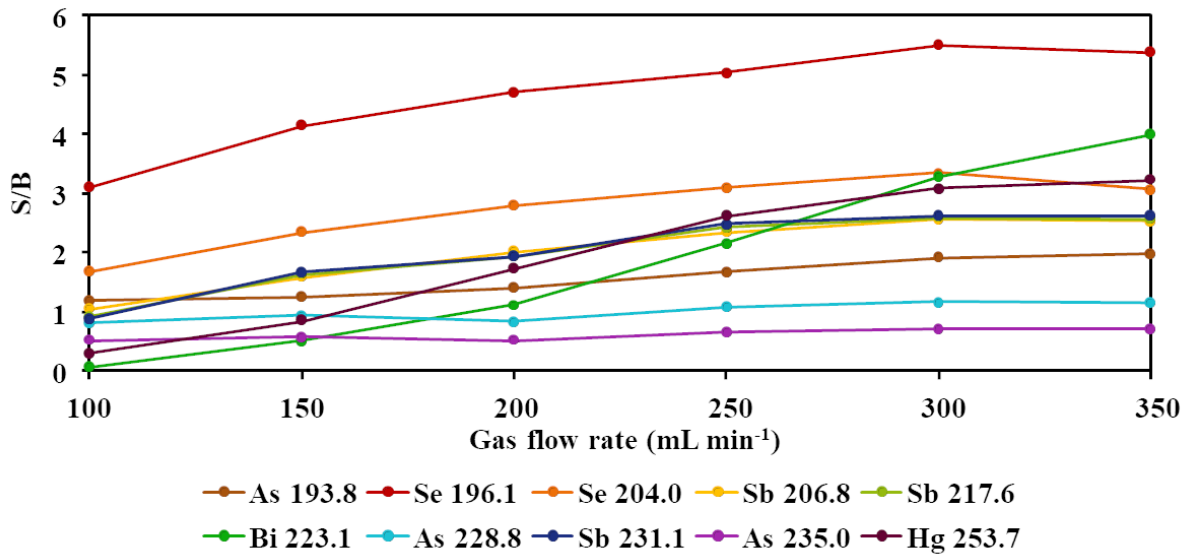

Fig. S2. The effect of the discharge current on the signal to background ratio (S/B) of all studied elements.

JAAS

PAPER

View Article Online
View Journal | View Issue

Cite this: *J. Anal. At. Spectrom.*, 2021, **36**, 1455

Simplified and rapid determination of Ca, K, Mg, and Na in fruit juices by flowing liquid cathode atmospheric glow discharge optical emission spectrometry†

Monika Gorska * and Pawel Pohl

Received 13th April 2021
Accepted 26th May 2021

DOI: 10.1039/d1ja00127b

rsc.li/jaas

Novel atmospheric pressure glow discharge (APGD) plasma sustained between a miniaturized flowing liquid cathode (FLC) and a pin-type anode was applied as an excitation source for the determination of Ca, K, Mg, and Na in fruit (apple, banana, blackcurrant, lemon, lime, pomegranate, quince, and tomato) juices by optical emission spectrometry. A simplified sample preparation procedure of juices, involving only their 1000-fold dilution and acidification with HNO_3 to a concentration of 0.1 mol L^{-1}, was proposed. The content of K and Na was determined using simple standard solutions for calibration, while the determination of Ca and Mg required the use of the standard addition method, due to matrix effects. Under the optimal conditions, the developed method assured instrumental detection limits of 5.69 (Ca), 0.14 (K), 0.63 (Mg), and 0.02 (Na) μg L^{-1}. Owing to such low detection limits, the content of all studied metals could be determined using only one sample dilution. The proposed FLC APGD OES method was established to provide reliable results with high accuracy and very good precision.

1. Introduction

Fruit juices are a rich source of nutritionally important compounds, such as antioxidants, carbohydrates, carotenoids, flavonoids, macroelements, phenolic acids, pectins, proteins, vitamins and others.[1–3] Due to increasing knowledge about their nutritional and health benefits, along with their good taste, fruit juices are widely consumed beverages by different age groups all over the world.[2,4,5] Considering elements that are present in different types of juices, they can be divided into three groups: macroelements (*e.g.*, Ca, K, Mg, Na), microelements (*e.g.*, Cu, Fe, Zn), and trace elements (*e.g.*, Cd, Cr, Mn, Pb).[1,2,6] As the total content of elements in these beverages may reach 10 g L^{-1}, their contribution to the human diet is significant.[1] It was previously revealed that the consumption of fruit juices on a daily basis significantly covers recommended daily allowances (RDAs) of many nutritionally important elements, such as Al (up to 19%), Ca (up to 32%), Cr (up to 87%), Cu (up to 35%), Fe (up to 26%), K (up to 55%), Mg (up to 22%), Na (up to 14%), and Zn (up to 21%).[6] Hence, it is of great concern to develop quick and simple methods for the elements determination in different types of juices.[3,7]

Among various methods that are applied for elemental analysis of juices, spectrometric techniques are the prevailing ones and they include: flame atomic absorption spectrometry (FAAS),[3,8,9] graphite furnace atomic absorption spectrometry (GF AAS),[9,10] inductively coupled plasma optical emission spectrometry (ICP OES),[11–14] and inductively coupled plasma mass spectrometry (ICP MS).[15–17] However, direct analysis of juices with the aid of the aforesaid techniques causes many troubles due to a complex organic matrix of samples, their high viscosity as well as the presence of dissolved solids in them.[1] For this reason, samples of juices usually have to be either digested before the analysis, in order to remove the organic matter, or significantly diluted to lower the organic substances concentration.[1,15,16,18] Although these procedures allow to overcome the adverse impact of the matrix substances, they require the use of relevant amounts of reagents, including concentrated acids, and have to be subjected to prolonged high temperature treatments that may be a source of sample contamination.[1,15]

Apart from the above, a number of disadvantages have been recognized in regard to the application of those techniques, including bulky and complex instrumentation, high power and gas consumption, and high purchasing and operating costs.

To overcome those inconveniences, the attention of many researchers has been attracted to the development of novel miniaturized excitation sources of simplified design used for OES measurements which would assure similar or better (to the currently applied large-scale ICP instrumentation) analytical

Wroclaw University of Science and Technology, Faculty of Chemistry, Division of Analytical Chemistry and Chemical Metallurgy, Wybrzeze Stanislawa Wyspianskiego 27, 50-370 Wroclaw, Poland. E-mail: monika.gorska@pwr.edu.pl

† Electronic supplementary information (ESI) available. See DOI: 10.1039/d1ja00127b

characteristics at low costs, reduced power, and reduced/no gas consumption.[19–21] Discharges generated in contact with liquids enjoy a special interest and a number of such techniques has been proposed for the time being, *e.g.*, electrolyte jet cathode glow discharge (EJC GD),[22] discharge on boiling in a channel (DBC),[23] liquid electrode plasma (LEP),[24] electrolyte cathode discharge (ELCAD),[25] solution cathode glow discharge (SCGD),[26] flowing liquid cathode-atmospheric pressure glow discharge (FLC APGD),[27] liquid sampling-atmospheric pressure glow discharge (LS APGD),[28] solution anode glow discharge (SAGD),[29] flowing liquid anode-atmospheric pressure glow discharge (FLA APGD),[30] liquid drop anode-atmospheric pressure glow discharge (LDA APGD),[31] and hanging drop electrode-atmospheric pressure glow discharge (HDE APGD).[32] From all the aforesaid methods, FLC APGD and FLA APGD seem to be the most promising ones. FLA APGD offers detection limits (DLs) that are incomparably better than the ones reported for the other methods, nonetheless the FLA APGD technique suffers from significant matrix effects coming from concomitant ions, present in the FLA solution, which restricts the real sample analysis.[30,33–36] Moreover, the application of the FLA APGD method is restricted to the determination of only 8 elements (namely Ag, Bi, Cd, In, Hg, Pb, Tl, and Zn) which are known to be transported to this excitation source in the form of volatile species.[30,33,37] On the other hand, although the DLs achievable in the FLC APGD method are up to a few orders of magnitude higher and of a similar level to those obtained for the ICP OES method, this method is quite resistant to matrix effects.[30,38–41] Therefore, the latter method could be successfully applied in the elemental analysis of different environmental and food samples, including aquatic plants,[42] blood,[40] coal fly ashes,[43] human hair,[44] ores,[45] soils,[46] stream sediments,[44] tuna fish,[42] and wastewater,[47] after their digestion or extraction. Moreover, ground,[43] mineral,[48] natural,[49] pond,[46] river,[50] and tap[49] waters as well as brines[51] and honeys[52] were directly analyzed, proving high sensitivity, precision and accuracy of the developed systems.

Hence, the suitability of the APGD microsource generated between a small-sized FLC solution and a pin-type tungsten anode for the determination of Ca, K, Mg, and Na in different juice samples with a simplified sample preparation procedure, involving only their dilution and acidification, was examined. To the best of our knowledge, such analysis for juices using either the FLC APGD method or any other microplasma source has never been performed. To achieve that goal, the crucial operating parameters of the discharge were optimized at first. Subsequently, the DLs of the analytes were assessed in the optimized conditions. Furthermore, the impact of the dilution factor on the analytes signal intensities was studied to verify both the impact of the organic matrix on the analytes signals as well as the plasma resistance on this matrix. The proposed method was then applied for an analysis of 8 commercial fruit juices for the content of Ca, K, Mg, and Na. The results obtained for FLC APGD measurements were compared to those provided by a reference method (ICP OES with wet digestion) and discussed.

2. Experimental

2.1. Instrumentation

A schematic drawing of the studied FLC APGD system is displayed in Fig. 1. The discharge was sustained in an open-to-air chamber between a tungsten nozzle (OD/ID 3/1 mm, length 50 mm) and a vertically oriented tungsten rod (OD 2 mm, length 170 mm). The sample solutions acidified with HNO_3 to its concentration up to 0.1 mol L^{-1}, which served as the cathode, were pumped through the tungsten nozzle by means of a 3-channel REGLO ICC peristaltic pump (Ismatec, USA) at different flow rates being set in the 1.0–4.0 mL min^{-1} range. As the solution reached the tungsten tube's top it flowed down to a PTFE reservoir, from which it was pumped out with the aid of the previously mentioned peristaltic pump. The distance between the solution surface and the anode rod (so-called discharge gap) was set to approximately 1.5 mm. The electrical contact was provided directly to the tungsten rod and with the aid of a platinum spiral wrapped around the tungsten nozzle. The voltage being in the 800–1200 V range was applied to both electrodes by a HV dc power supply (model DP50H-024PH, DSC-Electronics, Germany). Its exact value was depended on the applied sample flow rate and the discharge current. To stabilize the discharge, a 6.9 kΩ ballast resistor was connected into the circuit.

The radiation emitted by APGD was imaged (1 : 1) on the entrance slit (10 μm) of a Shamrock 500i imaging spectrometer (Andor, UK), using an achromatic quartz lens (f = 80). The spectrometer was equipped with a holographic grating (1800 lines mm^{-1}) and a Newton DU-920P-OE UV-Vis CCD camera (Andor, UK). The integration time was 10 s during all experiments and intensities of atomic emission lines of the studied elements were background corrected. The following wavelengths of the analytes were traced during all experiments: Ca (422.7 nm), K (766.5 nm), Mg (285.2 nm), and Na (589.0 nm).

An Agilent 5110 synchronous vertical dual view (SVDV) ICP OES instrument was used to measure total concentrations of studied elements in digested fruit juices *versus* simple standards solutions. The ICP OES spectrometer was equipped with an easy-fit quartz torch with a standard 1.8 mm injector and a sample introduction system consisted of a Seaspray nebulizer and a double-pass glass cyclonic spray chamber. The instrument was run under operating conditions given in Table SI-1,† combining axial and radial acquisition of radiation emitted by the vertical plasma over the entire wavelength range and in a single measurement.

2.2. Reagents and sample preparation

Deionized water (18.2 MΩ cm) from a Polwater water purification system (Labopol-Polwater, Poland) was used throughout the study. All chemicals were at least of analytical grade. Stock standard solutions of Ca, K, Mg, and Na (1000 mg L^{-1}), obtained from Sigma-Aldrich (Germany), were utilized to prepare all working standard solutions. To acidify the FLC solutions, an ACS grade concentrated HNO_3 (65% m/m) solution (Merck, Germany) was employed. The same concentrated HNO_3 along

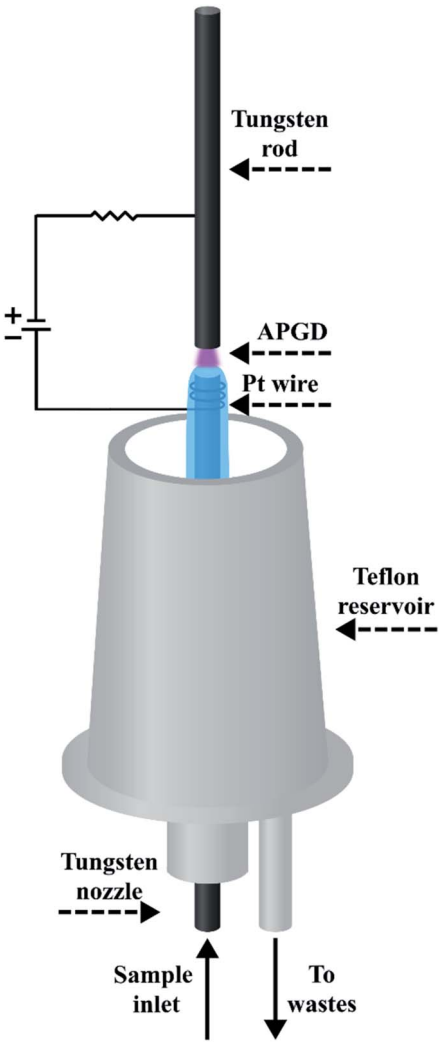

Fig. 1 A schematic drawing of the developed FLC APGD systems.

with a solution of 30% H_2O_2 (Merck, Germany) were applied for samples digestion before their analysis with the aid of ICP OES.

Samples of 8 fruit juices were purchased at local stores. They were produced by 6 different manufacturers, which were encoded with the first letters of their names, *i.e.*, E, F, H, X, K, and T, and included apple (A), banana (B), blackcurrant (C), lemon (L), lime (M), pomegranate (P), quince (Q), and tomato (T) juices.

Prior to FLC APGD OES measurements, the samples of banana and tomato juices were initially centrifuged at 15 000 rpm for 10 min to remove any dissolved particles. Followingly, appropriate aliquots of each of the analyzed juices were transferred into a twist-cup container and acidified with concentrated HNO_3 to its concentration of 0.1 mol L^{-1}. Finally, all samples were filled with deionized water to reach the final dilution of the juices of 1000-fold (on the weight basis). Such prepared samples were analyzed in regard to the external calibration curves with simple standards solutions.

All juice samples were also analyzed using the standard addition method for calibration. In this case, all the above mentioned steps of sample preparation were repeated, however, after the acidification, each sample was divided into four separate parts, and the standard addition was performed on the last three of them, using a mixed solution of Ca and Mg (10 mg L^{-1}). Subsequently, all samples were filled with deionized water to reach the final dilution of the juices of 1000-fold (on the weight basis).

As regards ICP OES measurements, the aforesaid juice samples were wet-digested in order to destroy the organic matrix. For this purpose, samples of 5.0 g of each juice and concentrated HNO_3 (5.0 mL) were transferred into a DigiPrep tube and heated for 180 min at 120 °C. After cooling, 5.0 mL of H_2O_2 (30%) was added and the samples were further heated for 60 min. Followingly, such prepared samples were filled with deionized water to 50.0 g. After that, appropriate amounts of digested solutions were transferred into a twist-cup container and filled with deionized water up to 30.0 g. Two dilutions of each juice sample were prepared, *i.e.*, 12-fold and 750-fold (on the weight basis).

All the above mentioned samples were prepared in triplicates, besides, appropriate procedural blanks were prepared and considered in the final results. The determination of Ca, K, Mg, and Na was performed, for all samples, in regard to the external calibration curves with simple standards solutions.

3. Results and discussion

3.1. Optimization of working parameters

In order to successfully apply the proposed FLC APGD method for the elemental analysis of juices and considering especially the elements of poorer sensitivity and present at lower concentrations, *i.e.*, Ca and Mg, the optimization of operating parameters was performed. The sample flow rate (1.0–4.0 mL min^{-1}) along with the discharge current (30–60 mA) were identified to have a significant impact on the analytes signal intensities. The acid concentration was omitted during the optimization step as it was repeatedly shown that the most optimal acid concentration is 0.1 mol L^{-1} (or similar). Therefore, all studied samples were acidified with HNO_3 to the concentration of 0.1 mol L^{-1}. The optimization was carried out using a mixed standard solutions of Ca, K, Mg and Na at their concentrations of 0.1 (K, Na) or 0.5 mg L^{-1} (Ca, Mg). Based on our previous experience,[33,35] it was to be expected that those parameters would be dependent on each other, therefore, there were optimized together. The results are presented in Fig. 2.

As it can be seen from the figure, the discharge could be stably maintained over the whole range of sample flow rates, but only for the discharge current of 30 mA. At higher amperages, the discharge was unstable when lower flow rates were applied. That being so, for the highest studied discharge current, *i.e.*, 60 mA, the discharge could be maintained only for the samples flow rates of 3.5 and 4.0 mL min^{-1}, however its visual stability was still slightly impaired. The reason for the observed lack of the stability was likely an insufficient electrical conductivity of the solution at lower samples flow rates.

As for the relationship between the applied discharge current and the received signal-to-background ratios (SBRs), it was revealed that SBRs of all studied elements increased with

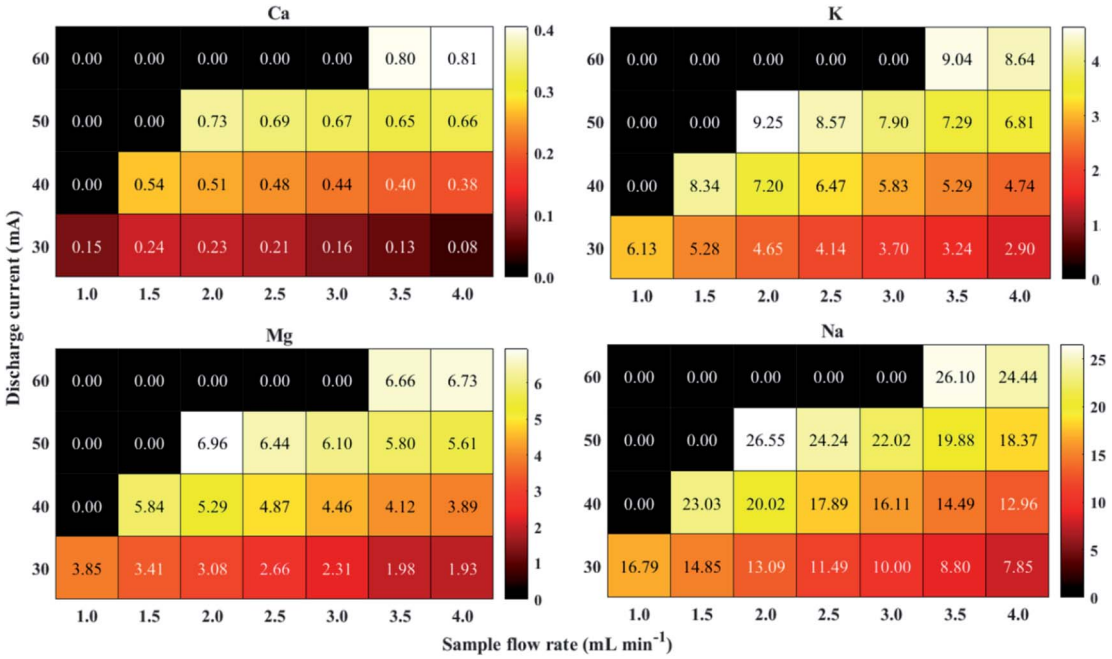

Fig. 2 The effect of the sample flow rate and the discharge current on the signal to background ratio (SBR) of the analytical lines of Ca, K Mg, and Na. "0.00" indicates the parameters combination at which the discharge was unstable and the measurement could not be taken.

Table 1 The analytical performance of the studied FLC APGD OES system[a]

Element	DL (μg L^{-1})	ULR (mg L^{-1})	R^2	Sensitivity (a.u. per mg per L)	RSD (%)
Ca	5.69	10	0.9998	2.32×10^4	1.02
K	0.14	10	0.9999	3.01×10^6	1.12
Mg	0.63	10	0.9992	7.67×10^5	0.73
Na	0.02	5	1.0000	1.02×10^7	0.89

[a] DL – detection limit. ULR – upper linearity range.

a growing discharge current. These results are consistent with what had previously been reported.[53,54] The most probable explanation for the increase of the SBRs values along with the increase of the discharge current is higher electron density in the discharge. This in turn leads to better excitation conditions.

The results reported previously regarding the impact of the sample flow rate on the signal intensity/SBR are ambiguous. Usually, as the sample flow rate is growing, the response from the analytes is found to either increase or decrease up to a certain limit and increase afterward.[39,45,55,56] However, a decreasing tendency of the response from the analytes over the whole range of the sample flow rates was noted as well.[35,57] Herein, the SBR values generally declined for all analytes with the increasing sample flow rate, regardless of the discharge current applied. The root of the aforesaid results is unclear and a more in-depth study is needed to provide a reliable clarification, however, this was not the aim of this work.

It is noteworthy that the increasing tendency of the SBR values observed at higher discharge currents was compensated by the decreasing tendency coming from higher solution flow rates, as the discharge could not be maintained at the lower ones in these conditions. This made the evaluation of the optimal operating parameters not to be so obvious. The highest SBR for Ca was received for the discharge current of 60 mA and the solution flow rate of 4.0 mL min^{-1}, while slightly higher SBR for the other analytes was obtained when the discharge current of 50 mA and the sample flow rate of 2.0 mL min^{-1} were applied. As an attempt of performing long-time analyses was made, the plasma stability was taken into consideration and the visual discharge stability was noted to be better at the discharge current of 50 mA and the sample flow rate of 2.0 mL min^{-1}. Therefore, those parameters were established to be optimal for multi-element analysis, hence they were applied in all subsequent experiments.

3.2. Analytical characteristics

To have a better insight into the appropriate juice samples dilution for their analysis on the content of Ca, K, Mg, and Na in the further part of this study, the analytical performance of the developed FLC APGD system was determined under the optimized conditions. For that purpose, the DLs, the upper linearity ranges (ULRs) as well as the precision were determined for all studied elements (see Table 1). Instrumental DLs were calculated as $3s/a$, where "$3s$" stands for 3 times the standard deviation of 10 consecutive measurements of an appropriate blank solution, and "a" stands for the sensitivity of a corresponding calibration curve. The upper linearity range was examined using 9 standard solutions in the concentration range of 0.01–10 mg L^{-1}. The precision was expressed as the relative standard deviation (RSD) for 10 consecutive measurements of the standard solutions, containing Ca, K, Mg, and Na at the

Table 2 The upper linearity ranges (ULR), expressed as the highest percentage juice concentrations (corresponding to the possible lowest dilutions) at which the curves of the signal intensity of the analytical line *versus* these concentrations are still linear, the slopes of the received curves along with their R^2, and the range of relative standard deviation (RSD) values, received for different dilutions of analyzed juices, for Ca, K, Mg and Na during the FLC APGD OES analysis

Element	Parameter	AT	BX	CF	LE	ME	PH	QK	TT
Ca	ULR (%)	10 (10-fold)	10 (10-fold)	10 (10-fold)	2 (50-fold)	2 (50-fold)	2 (50-fold)	2 (50-fold)	2 (50-fold)
	Slope	6.94×10^3	3.60×10^3	1.49×10^4	2.83×10^4	2.51×10^4	1.46×10^4	2.51×10^4	1.22×10^4
	R^2	0.9952	0.9992	0.9962	0.9932	0.9976	0.9958	0.9976	0.9965
	RSD (%)[a]	0.36–8.15	0.87–8.41	0.27–4.58	0.60–3.90	0.41–3.26	0.36–4.73	0.10–2.89	0.42–2.97
K	ULR (%)	2 (50-fold)	2 (50-fold)	2 (50-fold)	1 (100-fold)	1 (100-fold)	1 (100-fold)	1 (100-fold)	1 (100-fold)
	Slope	2.40×10^7	2.37×10^7	1.45×10^7	4.27×10^7	4.65×10^7	5.67×10^7	3.97×10^7	5.45×10^7
	R^2	0.9996	0.9994	0.9964	0.9993	0.9989	0.9997	0.9997	0.9984
	RSD (%)[a]	0.19–0.64	0.12–0.39	0.07–0.62	0.20–0.25	0.03–0.34	0.03–0.54	0.21–0.56	0.14–0.37
Mg	ULR (%)	10 (10-fold)	10 (10-fold)	10 (10-fold)	10 (10-fold)	10 (10-fold)	10 (10-fold)	10 (10-fold)	10 (10-fold)
	Slope	1.73×10^5	2.58×10^5	1.17×10^5	3.14×10^5	3.20×10^5	2.85×10^5	3.82×10^5	2.08×10^5
	R^2	0.9969	0.9993	0.9978	0.9945	0.9945	0.9925	0.9931	0.9596
	RSD (%)[a]	0.29–0.96	0.19–1.16	0.20–1.42	0.26–1.61	0.06–1.91	0.43–2.13	0.71–1.52	0.65–2.62
Na	ULR (%)	10 (10-fold)	10 (10-fold)	10 (10-fold)	2 (50-fold)	2 (50-fold)	2 (50-fold)	2 (50-fold)	0.2 (500-fold)
	Slope	1.34×10^6	6.71×10^5	3.32×10^6	6.06×10^6	5.65×10^6	2.00×10^7	1.03×10^7	2.08×10^8
	R^2	0.9952	0.9990	0.9999	0.9997	0.9998	0.9995	0.9998	0.9999
	RSD (%)[a]	0.11–1.71	0.15–0.96	0.16–0.89	0.07–0.53	0.53–0.71	0.08–0.67	0.39–2.11	0.40–0.59

[a] Expressed as the RSD range for all dilutions measurements.

concentrations of 200, 10, 100 and 10 μg L^{-1}, respectively. The RSD was measured 3 times and the averaged results were given. When comparing the received DLs with those reported over the last five years for similar FLC APGD systems,[58] they were similar (in the case of K) or significantly improved (in the case of all analytes), *i.e.*, 2–81 times for Ca, 0.9–2785 times for K, 3–540 times for Mg, and 2–2400 times for Na. The DLs presented herein are also similar or better to those achieved for other spectrometric techniques, such as FAAS,[59–62] or ICP OES.[60,63,64] In such a case, it was expected the obtained low DLs of Ca, K, Mg

Table 3 The content of K and Na determined in the analyzed juice samples, *i.e.*, apple (AT), banana (BX), blackcurrant (CF), lemon (LE), lime (ME), pomegranate (PH), quince (QK), and tomato (TT) juices, using simple standard solutions for calibration[a]

		K		Na	
Juice	Method	Mean ± CI	RSD (%)	Mean ± CI	RSD (%)
AP	ICP OES	931.18 ± 5.09	0.22	11.54 ± 0.15	0.54
	FLC APGD	1014.6 ± 24.69	0.98	11.94 ± 0.52	1.77
	Recovery (%)	109		103	
BX	ICP OES	897.56 ± 21.64	0.97	6.21 ± 0.17	1.06
	FLC APGD	966.48 ± 17.76	0.74	6.65 ± 0.37	2.19
	Recovery (%)	108		107	
CF	ICP OES	482.67 ± 23.38	1.95	30.72 ± 0.07	0.10
	FLC APGD	492.38 ± 17.74	1.45	34.08 ± 0.84	0.99
	Recovery (%)	102		111	
LE	ICP OES	1610.92 ± 58.43	1.46	53.11 ± 6.31	4.78
	FLC APGD	1745.16 ± 44.67	1.03	56.8 ± 3.06	2.16
	Recovery (%)	108		107	
ME	ICP OES	1766.92 ± 22.38	0.51	52.16 ± 0.32	0.24
	FLC APGD	1893.04 ± 31.50	0.67	55.03 ± 0.99	0.72
	Recovery (%)	107		106	
PH	ICP OES	2157.64 ± 43.43	0.81	183.07 ± 7.45	1.64
	FLC APGD	2241.24 ± 47.33	0.85	177.43 ± 10.48	2.38
	Recovery (%)	104		96.9	
QK	ICP OES	1438.33 ± 13.22	0.37	89.27 ± 1.14	0.51
	FLC APGD	1536.04 ± 38.93	1.02	92.31 ± 3.13	1.37
	Recovery (%)	107		103	
TT	ICP OES	2261.23 ± 10.68	0.19	2250.12 ± 16.77	0.3
	FLC APGD	2326.93 ± 24.87	0.43	2263.95 ± 37.12	0.66
	Recovery (%)	103		101	

[a] CI – confidence interval (for 95% confidence level).

Table 4 The content of Ca and Mg determined in the analyzed juice samples, *i.e.*, apple (AT), banana (BX), blackcurrant (CF), lemon (LE), lime (ME), pomegranate (PH), quince (QK), and tomato (TT) juices, using standard addition method for calibration[a]

		Ca		Mg	
Juice	Method	Mean ± CI	RSD (%)	Mean ± CI	RSD (%)
AP	ICP OES	43.11 ± 0.67	0.62	45.17 ± 0.12	0.10
	FLC APGD	43.89 ± 1.91	1.76	49.39 ± 0.72	0.58
	Recovery (%)	102		109	
BX	ICP OES	18.41 ± 2.58	5.67	70.35 ± 0.67	0.39
	FLC APGD	19.28 ± 0.32	0.68	67.61 ± 1.17	0.69
	Recovery (%)	105		96.1	
CF	ICP OES	106.38 ± 0.97	0.37	30.55 ± 0.10	0.14
	FLC APGD	110.31 ± 4.02	1.47	30.27 ± 0.17	0.22
	Recovery (%)	104		99.1	
LE	ICP OES	196.25 ± 41.93	8.60	125.15 ± 0.89	0.29
	FLC APGD	201.68 ± 5.37	1.07	128.73 ± 4.55	1.42
	Recovery (%)	103		103	
ME	ICP OES	217.34 ± 3.23	0.60	107.25 ± 1.69	0.63
	FLC APGD	232.3 ± 10.33	1.79	109.34 ± 5.04	1.86
	Recovery (%)	107		102	
PH	ICP OES	96.42 ± 1.09	0.46	78.33 ± 0.84	0.43
	FLC APGD	90.83 ± 12.17	5.40	77.14 ± 0.30	0.15
	Recovery (%)	94.2		98.5	
QK	ICP OES	258.67 ± 10.53	1.64	113.35 ± 1.04	0.37
	FLC APGD	260.30 ± 34.98	5.41	109.84 ± 9.49	3.48
	Recovery (%)	101		96.9	
TT	ICP OES	106.63 ± 1.37	0.52	105.26 ± 2.14	0.82
	FLC APGD	108.38 ± 5.59	2.08	96.74 ± 1.02	0.41
	Recovery (%)	102		91.9	

[a] CI – confidence interval (for 95% confidence level).

and Na would allow to apply higher dilutions of the analyzed juices, in order to avoid matrix effects coming from organic and inorganic constituents of the samples.

The calibration curves were linear ($R^2 > 0.999$) over the whole studied concentration range, *i.e.*, up to 10 mg L^{-1}. As for Na, its calibration curve was linear ($R^2 = 1$) only up to the Na concentration of 5 mg L^{-1} due to its high sensitivity which led to the saturation of the CCD detector above this concentration. Such dynamic linearity ranges are suitable for multi-element analysis, therefore it was expected that it would be possible to analyze all studied elements preparing only one dilution of the analyzed samples.

Regarding the measurements precision, it was found that the developed FLC APGD OES method assured excellent precision, changing in the range of 0.73–1.12% for relatively low analytes concentrations.

3.3. Plasma stability and matrix effects

To assess the suitability of the developed FLC APGD method for determining the content of Ca, K, Mg, and Na in various fruit juices, only diluted in water (without any digestion) and acidified with HNO_3 to 0.1 mol L^{-1}, two aspects had to be considered at the beginning. The first one was the plasma robustness in reference to the juice matrix and the second one were the matrix effects, *i.e.*, the impact of both organic and inorganic constituents of juices on the analytes signal intensities. Due to high variety of different elements as well as organic compounds, and their concentrations, present in different types of juice,[65–68] the results obtained based on a solution containing a juice-like organic matrix would not be of great credibility. Therefore, both those factors were determined by measuring the analytes signal intensities in five different dilutions (namely 10-, 50-, 100, 500-, and 1000-fold) of each analyzed juice, corresponding to its concentration in a prepared sample solution of 10, 2, 1, 0.2 and 0.1%. To reliably assess the impact of each juice matrix on the analytes signal intensities, they were depicted on a graph presenting the relationship between the analyte signal intensity and the juice dilution (expressed as the abovementioned percentage concentration) and the linearity of the received relationships was investigated to evaluate the concentration ranges at which the curve is linear, meaning, supposedly there are no matrix effects. For better visibility, the data obtained from those graphs was shown in Table 2, which presents the upper linearity ranges, expressed as the highest percentage concentrations (corresponding to the possible lowest dilutions) at which the curves were still linear, the slopes of the received curves along with their R^2, and the range of the RSD values, received for different dilutions of a given juice, for all analytes.

As it can be seen from that table, the upper linearity ranges differed between elements and the type of juices. Only the signal of Mg increased linearly over the whole range of the studied dilutions, regardless of the juice type. For Ca and Na, the highest possible concentration giving the linear response differed between juices, however, it was the same for a given

juice. Exemplary, the upper linearity range for Ca in quince (QK) and tomato (TT) juices are equal to 10 and 2% (10- and 50-fold dilution), respectively and the same upper linearity range is observed for Na in those (and any others) juices. It is also noteworthy that the mentioned upper linearity ranges for Ca and Na correlated well with the sensitivity of the received curves (the poorer sensitivity, the higher upper linearity range). The only exception from that rule is tomato (TT) juice, for which the dilutions above 500-fold (0.2%) could not be measured at all due to the saturation of the CCD detector, suggesting a very high concentration of this element in this juice. This was also the case for other juices (namely lemon (LE), lime (ME), pomegranate (PH), and quince (QK) juices) for Na but only when the juice concentration exceeded 2% (which corresponds to the dilutions being lower than 50-fold). Thus, it can be stated that the curves of Na were linear in the whole range which could be actually measured. However, there was no saturation of the CCD camera observed when Ca was measured, therefore, apparently, some matrix effects occur when a given juice contains higher content of Ca. As for K, its content in each of the analyzed juices was too high to be able to measure the whole dilution ranges and, similarly to Na, the obtained curves were linear in the whole possible-to-study range, *i.e.*, 1 (lemon (LE), lime (ME), pomegranate (PH), quince (QK), and tomato (TT) juices) or 2% (apple (AT), banana (BX), and blackcurrant (CF) juices). The aforesaid results may suggest that there are no matrix effects for the majority of the analytes (with exception of Ca at 10% samples of some juices), regardless of the juice type and its dilution. Nevertheless, the possibility of measuring the signal intensities of K and Na should be taken into account when considering higher dilutions of juices samples.

The plasma stability was evaluated based on the RSD of 10 consecutive measurements of each analytical line as well as visual observations for all studied sample dilutions. It was established that the RSD of the signal intensities of K and Na was below 1% in all (K) or in the vast majority (Na) of cases, indicating excellent precision, regardless of the juice type and applied dilution. For Mg, the RSD values were slightly higher, however they still did not exceed 3% for any juice at any dilution. Nevertheless, relatively high RSD values (4.5–8.5%) were obtained for Ca but only for the dilution factor of 1000 and only for a few juice types. It was also noted that the RSD values of this element (in 1000-fold diluted samples) correlated well with the sensitivity of the obtained curves (the poorer sensitivity, the worse RSD), meaning that the observed impaired signal stability was due to a relatively low Ca concentration in some juice samples, leading quite low analyte signal intensity after their 1000-fold dilution. Visually, lower stability was observed only when a 10-fold diluted solution was introduced into the FLC APGD system, however, considering the abovementioned precision, it was concluded that it was stable enough to perform the analysis.

3.4. Determination of selected elements in juice samples

Concentrations of Ca, K, Mg, and Na were measured in 8 different fruit juices with the aid of the FLC APGD OES method. The analyzed samples were diluted 1000-fold and acidified with HNO_3 to 0.1 mol L^{-1}. It was expected that applying a high dilution factor, the sample matrix would not influence neither the background intensity nor the analytes sensitivity, which then would not deteriorate the method DLs of Ca, K, Mg and Na in regard to the instrumental DLs presented above.

At first, simple standard solutions were used for calibration. To assess the reliability of the proposed method, all the abovementioned juices were also analyzed by ICP OES, however in this case, the samples needed to be wet-digested before the analysis. The obtained results are displayed in Tables 3 and 4.

Tables 3 and SI-2† present the content of Ca, K, Mg, and Na in the analyzed juices obtained from ICP OES measurements along with the corresponding results received from the FLC APGD OES measurements (using simple standard solutions for calibration), and the precision for all those results. The measured concentrations of Ca, K, Mg, and Na corresponded well to those reported for other juices of the same kind.[1,11,12,69,70] Apparently, K was the most abundant mineral in all analyzed juices. Its concentration varied in the range of 0.5–2 g L^{-1}, depending on the juice type. The content of Mg was roughly similar in the analyzed juices and changed in the 30–125 mg L^{-1} range. The concentrations of Ca and Na were the most diversified as they ranged within 18–259 and 6–2250 mg L^{-1}, respectively. Nevertheless, in the analyzed juices of different types, a very favorable K-to-Na concentration ratio was observed, ranging from 13 to 145. The exception was tomato (TT) juice, for which these concentrations were similar, which indicates that the juice is salted. Also, the Ca-to-Na concentration ratio was similar and ranged from 2.6 to 4.2 with the exception of tomato (TT), pomegranate (PH), and quince (QK) juices.

As regards the results received for the FLC APGD OES measurements, the concentrations of K and Na were consistent with the results obtained from ICP OES. The recoveries of those elements varied in the 96–111% range, confirming quite good accuracy of the developed FLC APGD method. Unfortunately, the results received for Ca and Mg were lesser. In the case of Ca, good accuracy (91–109%) was obtained for half of the analyzed juices, *i.e.*, apple (AP), blackcurrant (CF), lemon (LE), and quince (QK). However, for the other juices, the recoveries either changed in the 70–79% range (lime (ME), pomegranate (PH), and tomato (TT)) or was equal to 157% (banana (BX)). Even worse results were obtained for Mg, which recoveries changed in the range of 48–57% for all analyzed juices. These results were quite unexpected, bearing in mind high sample dilution and the apparent lack of matrix effects described above. Nevertheless, the obtained recovery values for Ca and (especially) Mg may be explained assuming that in all those juices there are organic compounds present, *i.e.*, carboxylic acids, at high concentrations, that forms complexes with those metals. In such a case, the relationship between the signal intensity of their analytical lines and the juice percentage concentration would be still linear as the dilution does not change the analyte to interfering compounds concentrations ratio. Due to high variety of organic compounds existing in juices in very high abundances,[68,71,72] it is difficult to designate a particular compound being responsible for the signal intensity decline,

unambiguously. Considering the recovery values for Ca and Mg, it can be stated, however, that these compounds form stronger complexes rather with Mg than Ca.

Nevertheless, due to the unsatisfactory recovery values obtained for Ca and – especially – Mg, the determination of those two metals was repeated using the standard addition method for calibration. The results are presented in Table 4. The recoveries received for the standard addition method were fallen in the range of 91–109% and confirmed very good accuracy of the applied method.

Regarding the precision of results obtained from those two calibration methods for FLC APGD OES measurements, expressed as the RSD from 3 independently repeated analyses, it can be seen that it was very good as usually did not exceeded 5%. The RSD values ranged within 0.10–2.97% for Ca, 0.43–1.45% for K, 0.78–4.48% for Mg, and 0.66–2.38% for Na (the calibration curve with simple standard solutions method) as well as 0.68–5.41% for Ca and 0.22–3.48% for Mg (the calibration with the standard addition method). Higher RSD values (*i.e.*, 5.40 and 5.41%) were obtained only for Ca and only in juices containing relatively small (in regard to the sensitivity of its analytical line) amounts of Ca after 1000-dilution, which resulted in quite small signals. It is also noteworthy that even worse RSD values (*i.e.*, 5.67 and 8.60%) were obtained for some of the ICP OES measurements, likely owing to the digestion step which was required for this method to obtain reliable results.

4. Conclusions

It was demonstrated that the proposed FLC APGD OES method provides reliable results for the determination of Ca, K, Na, and Mg in different kinds of juices. The precision of the obtained results was comparable to the one obtained from the ICP OES measurements. The presented simplified method requires only sample dilution and acidification, completely omitting the wet digesting, which is time-consuming process and requires the use of concentrated acids (HNO_3, HCl, HF, $HClO_4$) as well as H_2O_2, a high amount of energy, and it usually takes a couple of hours. There is also the possibility of sample contamination, during this step. Moreover, the use of the proposed FLC APGD OES method is associated with all advantages regarding techniques being premised on microplasma excitation sources. As opposed to the commercially applied spectrometric techniques, the FLC APGD OES method offers the advantages of small size, no requirement of the use of noble gases, and stable operation at low electric current power consumption, which is particularly important and useful for routine analyses of juices with very different chemical matrices. All of this translates to significantly reduced operating costs. Taking all of this into account, it may be concluded that the proposed method is a reliable alternative for commercially applied bulky instrumentation, *e.g.*, AAS or ICP OES. The only disadvantage of the developed method is the necessity of the standard addition method for calibration for the determination of Mg and Ca, due to the matrix effects, which cannot be overcome by the sample dilution. We believe, this finding is relevant as it will be true also for the juices determination by other spectrometric methods, *e.g.*, ICP-OES, ICP-MS, AAS, AFS. Nevertheless, the standard addition method is still less time-consuming than performing wet digestion. Moreover, due to simple design and miniaturization of the proposed FLC-APGD system, it might be automated by coupling it with a diluter and/or a mixer (for the standard addition method), making the analysis even simpler and faster.

Conflicts of interest

There are no conflicts to declare.

Acknowledgements

Monika Gorska and Pawel Pohl acknowledge the financial support from Polish National Science Center (2019/33/B/ST4/00356).

References

1 A. Szymczycha-Madeja, M. Welna, D. Jedryczko and P. Pohl, Developments and strategies in the spectrochemical elemental analysis of fruit juices, *Trends Anal. Chem.*, 2014, **55**, 68–80.
2 F. Demir, A. Seyhun Kipcak, O. Dere Ozdemir and E. Moroydor Derun, Determination of essential and non-essential element concentrations and health risk assessment of some commercial fruit juices in Turkey, *J. Food Sci. Technol.*, 2020, **57**, 4432–4442.
3 P. Pohl, A revisited FAAS method for very simple and fast determination of total concentrations of Cu, Fe, Mn and Zn in grape juices with sample preparation developed by modeling experimental design and optimization, *Microchem. J.*, 2020, **157**, 104998.
4 N. Jalbani, F. Ahmed, T. Gul Kazi, U. Rashid, A. Bano Munshi and A. Kandhro, Determination of essential elements (Cu, Fe and Zn) in juices of commercially available in Pakistan, *Food Chem. Toxicol.*, 2010, **48**, 2737–2740.
5 I. Maia Toaldo, F. Alves Cruz, T. de Lima Alves, J. Santos de Gois, D. L. G. Borges, H. Pamplona Cunha, E. Luiz Da Silva and M. T. Bordignon-Luiz, Bioactive potential of *Vitis labrusca* L. grape juices from the Southern Region of Brazil: phenolic and elemental composition and effect on lipid peroxidation in healthy subjects, *Food Chem.*, 2015, **173**, 527–535.
6 B. K. Tiwari and G. Rajauria, *Fruit Juices*, Academic Press, London, 2018.
7 M. M. Ghuniem, M. A. Korshed and E. R. Souaya, Optimization and Validation of an Analytical Method for the Determination of Some Trace and Toxic Elements in Canned Fruit Juices Using Quadrupole Inductively Coupled Plasma Mass Spectrometer, *J. AOAC Int.*, 2018, 262–270.
8 M. Conceicao Prudencio Da Dutra, L. Leonice Rodrigues, D. de Oliveira, G. Elias Pereira and M. Dos Santos Lima, Integrated analyses of phenolic compounds and minerals of Brazilian organic and conventional grape juices and wines: validation of a method for determination of Cu, Fe and Mn, *Food Chem.*, 2018, **269**, 157–165.

9 V. Luiz Cordoba Braganca, P. Melnikov and L. Z. Zanoni, Trace elements in fruit juices, *Biol. Trace Elem. Res.*, 2012, **146**, 256–261.
10 A. Paiva Oliveira, J. Anchieta Gomes Neto, J. Araujo Nobrega, P. Rogerio Miranda Correia and P. Vitoriano Oliveira, Determination of selenium in nutritionally relevant foods by graphite furnace atomic absorption spectrometry using arsenic as internal standard, *Food Chem.*, 2005, **93**, 355–360.
11 I. Juranovic Cindric, M. Zeiner, M. Kroppl and G. Stingeder, Comparison of sample preparation methods for the ICP-AES determination of minor and major elements in clarified apple juices, *Microchem. J.*, 2011, **99**, 364–369.
12 A. Szymczycha-Madeja and M. Welna, Evaluation of a simple and fast method for the multi-elemental analysis in commercial fruit juice samples using atomic emission spectrometry, *Food Chem.*, 2013, **141**, 3466–3472.
13 I. Cristina Da Silva Haas, I. Maia Toaldo, T. Margarida Gomes, A. S. Luna, J. Santos de Gois and M. T. Bordignon-Luiz, Polyphenolic profile, macro- and microelements in bioaccessible fractions of grape juice sediment using in vitro gastrointestinal simulation, *Food Biosci.*, 2019, **27**, 66–74.
14 A. Cristina Silva de Lima, D. Josino Soares, L. Morais Ribeiro Da Silva, R. Wilane de Figueiredo, P. Henrique Machado de Sousa and E. de Abreu Menezes, In vitro bioaccessibility of copper, iron, zinc and antioxidant compounds of whole cashew apple juice and cashew apple fibre (*Anacardium occidentale* L.) following simulated gastro-intestinal digestion, *Food Chem.*, 2014, **161**, 142–147.
15 L. Tormen, D. Placido Torres, I. Maria Dittert, R. G. O. Araujo, V. L. A. Frescura and A. Jose Curtius, Rapid assessment of metal contamination in commercial fruit juices by inductively coupled mass spectrometry after a simple dilution, *J. Food Compos. Anal.*, 2011, **24**, 95–102.
16 G. Cristea, A. Dehelean, C. Voica, I. Feher, R. Puscas and D. Alina Magdas, Isotopic and Elemental Analysis of Apple and Orange Juice by Isotope Ratio Mass Spectrometry (IRMS) and Inductively Coupled Plasma-Mass Spectrometry (ICP-MS), *Anal. Lett.*, 2020, 1–15.
17 S. Millour, L. Noel, A. Kadar, R. Chekri, C. Vastel and T. Guerin, Simultaneous analysis of 21 elements in foodstuffs by ICP-MS after closed-vessel microwave digestion: method validation, *J. Food Compos. Anal.*, 2011, **24**, 111–120.
18 W. A. Simpkins, H. Louie, M. Wu, M. Harrison and D. Goldberg, Trace elements in Australian orange juice and other products, *Food Chem.*, 2000, **71**, 423–433.
19 P. Pohl, P. Jamroz, K. Swiderski, A. Dzimitrowicz and A. Lesniewicz, Critical evaluation of recent achievements in low power glow discharge generated at atmospheric pressure between a flowing liquid cathode and a metallic anode for element analysis by optical emission spectrometry, *Trends Anal. Chem.*, 2017, **88**, 119–133.
20 X. Peng and Z. Wang, Ultrasensitive Determination of Selenium and Arsenic by Modified Helium Atmospheric Pressure Glow Discharge Optical Emission Spectrometry Coupled with Hydride Generation, *Anal. Chem.*, 2019, **91**, 10073–10080.
21 M. Gorska, K. Greda and P. Pohl, On the coupling of hydride generation (HG) with flowing liquid anode atmospheric pressure glow discharge (FLA-APGD) for determination of traces of As, Bi, Hg, Sb and Se by optical emission spectrometry (OES), *Talanta*, 2021, **222**, 121510.
22 V. V. Yagov, M. L. Getsina and B. K. Zuev, Use of Electrolyte Jet Cathode Glow Discharges as Sources of Emission Spectra for Atomic Emission Detectors in Flow-Injection Analysis, *J. Anal. Chem.*, 2004, **59**, 1037–1041.
23 B. K. Zuev, V. V. Yagov, M. L. Getsina and B. A. Rudenko, Discharge on Boiling in a Channel as a New Atomization and Excitation Source for the Flow Determination of Metals by Atomic Emission Spectrometry, *J. Anal. Chem.*, 2002, **57**, 907–911.
24 A. Kitano, A. Iiduka, T. Yamamoto, Y. Ukita, E. Tamiya and Y. Takamura, Highly sensitive elemental analysis for Cd and Pb by liquid electrode plasma atomic emission spectrometry with quartz glass chip and sample flow, *Anal. Chem.*, 2011, **83**, 9424–9430.
25 T. Cserfalvi, P. Mezei and P. Apai, Emission studies on a glow discharge in atmospheric pressure air using water as a cathode, *J. Phys. D: Appl. Phys.*, 1993, **26**, 2184–2188.
26 M. R. Webb, F. J. Andrade, G. Gamez, R. McCrindle and G. M. Hieftje, Spectroscopic and electrical studies of a solution-cathode glow discharge, *J. Anal. At. Spectrom.*, 2005, **20**, 1218–1225.
27 P. Jamroz and W. Zyrnicki, Spectroscopic Characterization of Miniaturized Atmospheric-Pressure dc Glow Discharge Generated in Contact with Flowing Small Size Liquid Cathode, *Plasma Chem. Plasma Process.*, 2011, **31**, 681–696.
28 H. W. Paing, K. A. Hall and R. Kenneth Marcus, Sheathing of the liquid sampling – atmospheric pressure glow discharge microplasma from ambient atmosphere and its implications for optical emission spectroscopy, *Spectrochim. Acta, Part B*, 2019, **155**, 99–106.
29 X. Liu, Z. Zhu, D. He, H. Zheng, Y. Gan, N. Stanley Belshaw, S. Hu and Y. Wang, Highly sensitive elemental analysis of Cd and Zn by solution anode glow discharge atomic emission spectrometry, *J. Anal. At. Spectrom.*, 2016, **31**, 1089–1096.
30 K. Greda, K. Swiderski, P. Jamroz and P. Pohl, Flowing Liquid Anode Atmospheric Pressure Glow Discharge as an Excitation Source for Optical Emission Spectrometry with the Improved Detectability of Ag, Cd, Hg, Pb, Tl, and Zn, *Anal. Chem.*, 2016, **88**, 8812–8820.
31 P. Jamroz, K. Greda, A. Dzimitrowicz, K. Swiderski and P. Pohl, Sensitive Determination of Cd in Small-Volume Samples by Miniaturized Liquid Drop Anode Atmospheric Pressure Glow Discharge Optical Emission Spectrometry, *Anal. Chem.*, 2017, **89**, 5729–5733.
32 K. Swiderski, P. Pohl and P. Jamroz, A miniaturized atmospheric pressure glow microdischarge system generated in contact with a hanging drop electrode – a new approach to spectrochemical analysis of liquid microsamples, *J. Anal. At. Spectrom.*, 2019, **34**, 1287–1293.

33 K. Greda, M. Gorska, M. Welna, P. Jamroz and P. Pohl, In-situ generation of Ag, Cd, Hg, In, Pb, Tl and Zn volatile species by flowing liquid anode atmospheric pressure glow discharge operated in gaseous jet mode – evaluation of excitation processes and analytical performance, *Talanta*, 2019, **199**, 107–115.

34 K. Greda, A. Szymczycha-Madeja and P. Pohl, Study and reduction of matrix effects in flowing liquid anode – atmospheric pressure glow discharge – optical emission spectrometry, *Anal. Chim. Acta*, 2020, **1123**, 81–90.

35 M. Gorska, K. Greda and P. Pohl, Determination of bismuth by optical emission spectrometry with liquid anode/cathode atmospheric pressure glow discharge, *J. Anal. At. Spectrom.*, 2021, **36**, 165–177.

36 X. Liu, Z. Liu, Z. Zhu, D. He, S. Yao, H. Zheng and S. Hu, Generation of Volatile Cadmium and Zinc Species Based on Solution Anode Glow Discharge Induced Plasma Electrochemical Processes, *Anal. Chem.*, 2017, **89**, 3739–3746.

37 M. Yuan, X. Peng, F. Ge, Q. Li, K. Wang, D.-G. Yu and Z. Wang, Simplified design for solution anode glow discharge atomic emission spectrometry device for highly sensitive detection of Ag, Bi, Cd, Hg, Pb, Tl, and Zn, *Microchem. J.*, 2020, **155**, 104785.

38 J. Yu, L. Yin, Q. Lu, F. Feng, Y. Kang and H. Luo, Highly sensitive determination of mercury by improved liquid cathode glow discharge with the addition of chemical modifiers, *Anal. Chim. Acta*, 2020, **1131**, 25–34.

39 Q. Lu, F. Feng, J. Yu, L. Yin, Y. Kang, H. Luo, D. Sun and W. Yang, Determination of trace cadmium in zinc concentrate by liquid cathode glow discharge with a modified sampling system and addition of chemical modifiers for improved sensitivity, *Microchem. J.*, 2020, **152**, 104308.

40 J. Yu, X. Zhang, Q. Lu, X. Wang, D. Sun, Y. Wang and W. Yang, Determination of calcium and zinc in gluconates oral solution and blood samples by liquid cathode glow discharge-atomic emission spectrometry, *Talanta*, 2017, **175**, 150–157.

41 W. Zu, Y. Yang, Y. Wang, X. Yang, C. Liu and M. Ren, Rapid determination of indium in water samples using a portable solution cathode glow discharge-atomic emission spectrometer, *Microchem. J.*, 2018, **137**, 266–271.

42 R. Shekhar, Improvement of sensitivity of electrolyte cathode discharge atomic emission spectrometry (ELCAD-AES) for mercury using acetic acid medium, *Talanta*, 2012, **93**, 32–36.

43 R. Shekhar, K. Madhavi, N. N. Meeravali and S. Jai Kumar, Determination of thallium at trace levels by electrolyte cathode discharge atomic emission spectrometry with improved sensitivity, *Anal. Methods*, 2014, **6**, 732–740.

44 Z. Zhang, Z. Wang, Q. Li, H. Zou and Y. Shi, Determination of trace heavy metals in environmental and biological samples by solution cathode glow discharge-atomic emission spectrometry and addition of ionic surfactants for improved sensitivity, *Talanta*, 2014, **119**, 613–619.

45 J. Yu, S. Yang, Q. Lu, D. Sun, J. Zheng, X. Zhang, X. Wang and W. Yang, Evaluation of liquid cathode glow discharge-atomic emission spectrometry for determination of copper and lead in ores samples, *Talanta*, 2017, **164**, 216–221.

46 K. Greda, P. Jamroz and P. Pohl, The improvement of the analytical performance of direct current atmospheric pressure glow discharge generated in contact with the small-sized liquid cathode after the addition of non-ionic surfactants to electrolyte solutions, *Talanta*, 2013, **108**, 74–82.

47 C. Huang, Q. Li, J. Mo and Z. Wang, Ultratrace Determination of Tin, Germanium, and Selenium by Hydride Generation Coupled with a Novel Solution-Cathode Glow Discharge-Atomic Emission Spectrometry Method, *Anal. Chem.*, 2016, **88**, 11559–11567.

48 P. Jamroz, P. Pohl and W. Zyrnicki, An analytical performance of atmospheric pressure glow discharge generated in contact with flowing small size liquid cathode, *J. Anal. At. Spectrom.*, 2012, **27**, 1032–1037.

49 Q. Xiao, Z. Zhu, H. Zheng, H. He, C. Huang and S. Hu, Significant sensitivity improvement of alternating current driven-liquid discharge by using formic acid medium for optical determination of elements, *Talanta*, 2013, **106**, 144–149.

50 J. Mo, L. Zhou, X. Li, Q. Li, L. Wang and Z. Wang, On-line separation and pre-concentration on a mesoporous silica-grafted graphene oxide adsorbent coupled with solution cathode glow discharge-atomic emission spectrometry for the determination of lead, *Microchem. J.*, 2017, **130**, 353–359.

51 C. Yang, L. Wang, Z. Zhu, L. Jin, H. Zheng, N. Stanley Belshaw and S. Hu, Evaluation of flow injection-solution cathode glow discharge-atomic emission spectrometry for the determination of major elements in brines, *Talanta*, 2016, **155**, 314–320.

52 K. Greda, P. Jamroz, A. Dzimitrowicz and P. Pohl, Direct elemental analysis of honeys by atmospheric pressure glow discharge generated in contact with a flowing liquid cathode, *J. Anal. At. Spectrom.*, 2015, **30**, 154–161.

53 J. Wang, P. Tang, P. Zheng and X. Zhai, Analysis of metal elements by solution cathode glow discharge-atomic emission spectrometry with a modified pulsation damper, *J. Anal. At. Spectrom.*, 2017, **32**, 1925–1931.

54 P. Zheng, X. Zhai, J. Wang and P. Tang, Analytical Characterization of a Solution Cathode Glow Discharge with an Interference Filter Wheel for Spectral Discrimination, *Anal. Lett.*, 2018, **51**, 2304–2315.

55 H. Yuan, D.-Z. Yang, X. Li, L. Zhang, X.-F. Zhou, W.-C. Wang and Y. Xu, A pulsed electrolyte cathode discharge used for metal element analysis by atomic emission spectrometry, *Phys. Plasmas*, 2019, **26**, 53505.

56 P. Zheng, Y. Gong, J. Wang and X. Zeng, Elemental Analysis of Mineral Water by Solution-Cathode Glow Discharge–Atomic Emission Spectrometry, *Anal. Lett.*, 2017, **50**, 1512–1520.

57 P. Zheng, Y. Chen, J. Wang and S. Xue, A pulsed atmospheric-pressure discharge generated in contact with flowing electrolyte solutions for metal element analysis by optical emission spectrometry, *J. Anal. At. Spectrom.*, 2016, **31**, 2037–2044.

58 P. Pohl, P. Jamroz, K. Greda, M. Gorska, A. Dzimitrowicz, M. Welna and A. Szymczycha-Madeja, Five years of innovations in development of glow discharges generated in contact with liquids for spectrochemical elemental analysis by optical emission spectrometry, *Anal. Chim. Acta*, 2021, 338399.

59 P. Pohl, H. Stecka and P. Jamroz, Solid phase extraction with flame atomic absorption spectrometry for determination of traces of Ca, K, Mg and Na in quality control of white sugar, *Food Chem.*, 2012, **130**, 441–446.

60 A. Szymczycha-Madeja, M. Welna and P. Pohl, Determination of essential and non-essential elements in green and black teas by FAAS and ICP OES simplified – multivariate classification of different tea products, *Microchem. J.*, 2015, **121**, 122–129.

61 P. Pohl, M. Kalinka and M. Pieprz, Development of a very simple and fast analytical methodology for FAAS/FAES measurements of Ca, K, Mg and Na in red beetroot juices along with chemical fractionation of Ca and Mg by solid phase extraction, *Microchem. J.*, 2019, **147**, 538–544.

62 S. Ruella de Oliveira, J. Luiz Raposo and J. Anchieta Gomes Neto, Fast sequential multi-element determination of Ca, Mg, K, Cu, Fe, Mn and Zn for foliar diagnosis using high-resolution continuum source flame atomic absorption spectrometry: Feasibility of secondary lines, side pixel registration and least-squares background correction, *Spectrochim. Acta, Part B*, 2009, **64**, 593–596.

63 R. Martins de Souza, L. Gustavo Leocadio and C. L. P. Da Silveira, ICP OES Simultaneous Determination of Ca, Cu, Fe, Mg, Mn, Na, and P in Biodiesel by Axial and Radial Inductively Coupled Plasma-Optical Emission Spectrometry, *Anal. Lett.*, 2008, **41**, 1615–1622.

64 H. M. Santos, J. P. Coutinho, F. A. C. Amorim, I. P. Lobo, L. S. Moreira, M. M. Nascimento and R. M. de Jesus, Microwave-assisted digestion using diluted HNO_3 and H_2O_2 for macro and microelements determination in guarana samples by ICP OES, *Food Chem.*, 2019, **273**, 159–165.

65 A. Vallverdu-Queralt, A. Medina-Remon, I. Casals-Ribes and R. M. Lamuela-Raventos, Is there any difference between the phenolic content of organic and conventional tomato juices?, *Food Chem.*, 2012, **130**, 222–227.

66 G. R. Schmutzer, A. Dehelean, D. Alina Magdas, G. Cristea and C. Voica, Determination of Stable Isotopes, Minerals, and Volatile Organic Compounds in Romanian Orange Juice, *Anal. Lett.*, 2016, **49**, 2644–2658.

67 S. Medina, R. Perestrelo, R. Santos, R. Pereira and J. S. Camara, Differential volatile organic compounds signatures of apple juices from Madeira Island according to variety and geographical origin, *Microchem. J.*, 2019, **150**, 104094.

68 M. Dos Santos Lima, I. de Souza Veras Silani, I. Maia Toaldo, L. Claudio Correa, A. Camarao Telles Biasoto, G. Elias Pereira, M. T. Bordignon-Luiz and J. Luiz Ninow, Phenolic compounds, organic acids and antioxidant activity of grape juices produced from new Brazilian varieties planted in the Northeast Region of Brazil, *Food Chem.*, 2014, **161**, 94–103.

69 P. Pohl, A. Dzimitrowicz, P. Jamroz and K. Greda, Development and optimization of simplified method of fast sequential HR-CS-FAAS analysis of apple juices on the content of Ca, Fe, K, Mg, Mn and Na with the aid of response surface methodology, *Talanta*, 2018, **189**, 182–189.

70 M. Dzugan, M. Wesolowska, G. Zagula and C. Puchalski, The comparison of the physicochemical parameters and antioxidant activity of homemade and commercial pomegranate juices, *Acta Sci. Pol., Technol. Aliment.*, 2018, **17**, 59–68.

71 J. Li, C. Zhang, H. Liu, J. Liu and Z. Jiao, Profiles of Sugar and Organic Acid of Fruit Juices: A Comparative Study and Implication for Authentication, *J. Food Qual.*, 2020, **2020**, 1–11.

72 C. Dani, L. S. Oliboni, R. Vanderlinde, D. Bonatto, M. Salvador and J. A. P. Henriques, Phenolic content and antioxidant activities of white and purple juices manufactured with organically- or conventionally-produced grapes, *Food Chem. Toxicol.*, 2007, **45**, 2574–2580.

Supporting Information

Simplified and rapid determination of Ca, K, Mg, and Na in fruit juices by flowing liquid cathode atmospheric glow discharge optical emission spectrometry

Monika Gorska*, Pawel Pohl

Wroclaw University of Science and Technology, Faculty of Chemistry, Division of Analytical Chemistry and Chemical Metallurgy, Wybrzeze Stanislawa Wyspianskiego 27, 50-370 Wroclaw, Poland
* Corresponding author. E-mail address: monika.gorska@pwr.edu.pl (Monika Gorska)

Table SI-1. Agilent 5110 SVDV ICP OES operating parameters.

RF power (kW)	1.50
Plasma Ar flow rate (L min^{-1})	12.0
Nebulizing Ar flow rate (L min^{-1})	0.7
Auxiliary Ar flow rate (L min^{-1})	1.0
Uptake delay time (s)	10
Read time (s)	5
Number of replicates	3
Stabilization time (s)	15
Viewing mode	SVDS
Viewing height (mm)	8
Pump speed (rpm)	12
Background correction	Off-peak, fitted, 2 pixels
Analytical line (nm)	280.3 (Mg), 422.7 (Ca), 589.6 (Na), 766.5 (K)

Table SI-2. The content of Ca and Mg determined in the analyzed juice samples, *i.e.*, apple (AT), banana (BX), blackcurrant (CF), lemon (LE), lime (ME), pomegranate (PH), quince (QK), and tomato (TT) juices, using simple standard solutions for calibration.

Juice	Method	Ca		Mg	
		Mean±CI	**RSD (%)**	**Mean±CI**	**RSD (%)**
AP	ICP OES	43.11±0.67	0.62	45.17±0.12	0.10
	FLC APGD	47.04±0.94	0.81	24.03±1.07	1.79
	Recovery (%)	109		53.2	
BX	ICP OES	18.41±2.58	5.67	70.35±0.67	0.39
	FLC APGD	28.94±1.29	1.80	37.87±3.40	3.62
	Recovery (%)	157		53.8	
CF	ICP OES	106.38±0.97	0.37	30.55±0.10	0.14
	FLC APGD	103.67±0.25	0.10	16.78±0.32	0.78
	Recovery (%)	97.5		54.9	
LE	ICP OES	196.25±41.93	8.60	125.15±0.89	0.29
	FLC APGD	204.79±10.63	2.09	61.06±3.40	2.24
	Recovery (%)	104		48.8	
ME	ICP OES	217.34±3.23	0.60	107.25±1.69	0.63
	FLC APGD	172.65±9.02	2.10	60.9±2.61	1.72
	Recovery (%)	79.4		56.8	
PH	ICP OES	96.42±1.09	0.46	78.33±0.84	0.43
	FLC APGD	70.58±2.01	1.15	42.65±4.74	4.48
	Recovery (%)	73.2		54.5	
QK	ICP OES	258.67±10.53	1.64	113.35±1.04	0.37
	FLC APGD	235.41±8.37	1.43	57.35±1.89	1.32
	Recovery (%)	91.0		50.6	
TT	ICP OES	106.63±1.37	0.52	105.26±2.14	0.82
	FLC APGD	77.22±5.69	2.97	54.79±1.19	0.87
	Recovery (%)	72.4		52.0	

CI – confidence interval (for 95% confidence level).

Analytical Methods

ROYAL SOCIETY OF CHEMISTRY

PAPER

View Article Online
View Journal | View Issue

Cite this: *Anal. Methods*, 2023, **15**, 1775

Fast and simple analysis of the content of Zn, Mg, Ca, Na, and K in selected beverages widely consumed by athletes by flowing liquid cathode atmospheric pressure glow discharge optical emission spectrometry†

Monika Gorska, * Joanna Weiss and Pawel Pohl

An atmospheric pressure glow discharge (APGD) system, generated between a flowing liquid cathode (FLC) and a gas (He) jet anode, was applied for the determination of Zn, Mg, Ca, Na, and K in selected beverages commonly chosen by athletes (namely Coca-Cola Zero, energy and vitamin drinks, pre-workout, branched-chain amino acids, almond drink, and whey protein) by optical emission spectrometry (OES). In some cases (*i.e.*, Coca-Cola, energy drink, and almond drink), sugared and sugar-free versions of the beverages were analyzed with the purpose of establishing the impact of added sugar on the analyte signal intensities. The analysis was performed after a simplified sample preparation procedure, which involved only their dilution and acidification with HNO_3 to a concentration of 0.2 mol L^{-1}. To determine the most suitable conditions for performing the analysis, optimization of the crucial operating parameters and sample dilution was carried out. Under the compromise conditions, the instrumental detection limits (DLs) were established and found to be 21, 0.91, 20, 0.062, and 0.14 μg L^{-1} for Zn, Mg, Ca, Na, and K, respectively. Due to the relatively low detection limits, the analyte content could be determined for a fairly high dilution, being concurrently the same for all analytes, which further simplified the whole procedure. It was found that the vast majority of samples could be determined using external calibration with simple standard solutions. The standard addition technique used for calibration was only required for the determination of Mg in three samples. The analysis results were consistent (in the majority of cases the recovery values were in the range of 88–111%) with the values obtained for the reference method (inductively coupled plasma optical emission spectrometry, ICP-OES), which proved the reliability of the results obtained from the developed FLC-APGD-OES system.

Received 17th January 2023
Accepted 13th March 2023

DOI: 10.1039/d3ay00092c

rsc.li/methods

1. Introduction

Over the last few years, an increasing number of various types of supplements that are supposed to enhance the training performance of participants or have a beneficial impact on overall health has been observed in the fitness industry.[1,2] Nowadays, the number of supplements that are available in this market is very high. They include whey, casein, and vegan protein powders, branched-chain amino acids (BCAAs), beta-alanine, glutamine, arginine, different chemical forms of creatine, citrulline malate, turkesterone, dehydroepiandrosterone (DHEA), ashwagandha, pre-workouts, and multivitamins. However, according to the data available in the related literature, they are generally either not needed or the scientific consensus is ambiguous, and thus, more research is needed to confirm or refute their usefulness to athletes. For instance, BCAA supplements contain three of the essential amino acids (EAAs), namely leucine, isoleucine, and valine. Given that the EAAs cannot be synthesized by humans at a fast enough rate, they have to come from an appropriately balanced diet. Concurrently, these three amino acids, particularly leucine, are key components for the synthesis of muscle protein, which is obviously important for body-builders.[3] However, not all dietary proteins contain all these amino acids, and it has also been shown that all EAAs are needed for effective muscle protein stimulation.[3–5] Therefore, supplementation with BCAAs makes sense only when ingested with a meal that contains a proper amount of other EAAs, and even then it is still less effective than the case of an equal amount of a high-quality dietary protein source.[6,7] Another group of supplements that are readily used by athletes are pre-workouts. They are meant to be taken prior to exercise and usually contain a blend of different ingredients,

Wroclaw University of Science and Technology, Faculty of Chemistry, Division of Analytical Chemistry and Chemical Metallurgy, Wybrzeze Stanislawa Wyspianskiego 27, 50-370 Wroclaw, Poland. E-mail: monika.gorska@pwr.edu.pl

† Electronic supplementary information (ESI) available. See DOI: https://doi.org/10.1039/d3ay00092c

e.g., amino acids, beta-alanine, caffeine, carbohydrates, creatine, and others, which as a whole are supposed to boost the exercise performance and subsequent recovery.[2,8] However, there are a few issues related to this particular group of supplements. Firstly, many of the ingredients are found in real food, *e.g.*, amino acids and carbohydrates. Secondly, unlike the pre-workout itself, some of its ingredients, such as amino acids and creatine, are intended to be taken daily to observe significant effects.[9] Moreover, the actual composition of several pre-workout supplements are often not clear due to the common habit of displaying "proprietary blend" on the supplement facts label.[2,10,11] Additionally, many of the actual ingredients of pre-workouts are underdosed.[10] Another type of widely consumed supplements is multivitamins, which not only contain vitamins but a wide variety of minerals and are expected to prevent and treat vitamin and mineral deficiencies from their insufficient intake from real food.[11] However, given that the manufacturers of minerals and vitamins are not obligated to submit the thorough documentation regarding their safety and effectiveness, their intake is related to many potential harmful effects, usually resulting from overdosing. Moreover, they can be contaminated with doping substances.[11–13] Accordingly, the only supplements that seem to be worthwhile are protein powder and creatine, which are usually the only supplements recommended by coaches, especially for beginners. Nevertheless, protein powder is still not needed in the majority of cases if enough protein is consumed with a well-balanced diet. Moreover, some of these supplements may contain heavy metals, such as Cd, Hg, and Pb.[14,15]

Unfortunately, there are very few papers regarding the mineral content in these supplements and when they appear, they focus on heavy metals.[14–16] Generally, to assess the elemental content of selected metals in the above-mentioned supplements, graphite furnace atomic absorption spectrometry (GF-AAS), inductively coupled plasma optical emission spectrometry (ICP-OES) and inductively coupled plasma mass spectrometry (ICP-MS) are applied.[14] Nevertheless, the analysis performed using the above-mentioned instruments may be challenging due to certain issues related to their practical application. Firstly, the necessity of performing the time-consuming digestion of samples that contain significant amounts of organic matrix, high viscosity or dissolved solid particles given that all these factors negatively impact (decrease) the signal intensity of the analyte. Moreover, the presence of solid particles in the analyzed solutions may clog the solution delivery capillaries in the instruments. Thus, the digestion procedure is performed with relatively high amounts of concentrated reagents (mostly acids), high temperature, and sometimes decreased pressure. Another disadvantage is the complex and bulky setup required to perform the analyses. Moreover, the costs associated with the use of the apparatus is very high due to its high power and gas consumption. All of this translates to high purchasing and operating costs related to the practical application of these instruments.

Thus, to address this issue, many researchers have devoted their efforts to developing alternative instruments that can performing the analysis with equal reliability, similar or better DLs of elements, and high accuracy and precision of measurements but at significantly reduced costs of both developing the necessary setup and applying it for the analysis of real samples. Currently, instruments in which a discharge is generated upon contact with liquids are being widely developed. Furthermore, various excitation sources have been proposed, including electrolyte jet cathode glow discharge (EJC-GD),[17] liquid electrode plasma (LEP),[18] discharge on boiling in a channel (DBC),[19] electrolyte cathode discharge (ELCAD),[20] liquid sampling-atmospheric pressure glow discharge (LS-APGD),[21] flowing liquid cathode-atmospheric pressure glow discharge (FLC-APGD),[21] solution cathode glow discharge (SCGD),[22] hanging drop electrode-atmospheric pressure glow discharge (HDE-APGD),[23] flowing liquid anode-atmospheric pressure glow discharge (FLA-APGD),[24] solution anode glow discharge (SAGD),[25] and liquid drop anode-atmospheric pressure glow discharge (LDA-APGD).[26] Among them, FLC-APGD seems to be one of the most promising sources. This is due to several factors, which are mentioned below, that make the FLC-APGD system suitable for real samples analysis. Although the DLs of elements obtained with this system are not the highest (the FLA-APGD system offers significantly lower DLs but for a limited group of elements, *i.e.*, Ag, Bi, Cd, Hg, In, Pb, Tl, and Zn), they are still comparable to or better than that offered by atomic absorption spectrometry (AAS) and ICP-OES.[27–29] Alternatively, in the FLA-APGD-OES method, matrix effects are not often observed and even if they are present, their extent is acceptably low.[30,31] Moreover, similar to ICP-OES, FLC-APGD-OES enables the analysis of the content of many different elements in samples.[32–35] Owing to all these advantages, the FLC-APGD-OES method has been successfully applied for the analysis of different samples with complex matrices, such as blood,[36] honey,[37] human hair,[38] fruit juices,[28] soils,[33] and wines[29] as well as samples with simpler matrices such as different types of water.[39–45]

The costs involved in the application of large-scale commercial instrumentation such as ICP-OES vary depending on several factors, including the specific instrument being used, the cost of consumables (*e.g.*, plasma gas, nebulizer, and pump tubing), and the cost of electricity. Additionally, maintenance and repair costs should be considered. Due to the complexity of these instruments, the overall purchasing costs are very high, whereas the developed microplasma systems are comprised of cheap elements, such as graphite tubes and PTFE reservoirs. Also, many of the large-scale setup elements need to be replaced every few months. Routine maintenance, such as cleaning and calibration, can cost several hundred dollars a year. Repairs can cost several thousand dollars, depending on the extent of the damage. Regarding the operating costs, compared to the currently developed microplasma sources, the plasma gas (argon) usage is typically several dozen higher for ICP-OES. However, many microplasma systems can be operated without the use of any gas. Moreover, the microplasma sources do not require any nebulizer for transporting the analytes into the plasma. Also, the power consumption is several dozen times lower in the case of microplasma excitation sources. All these facts translate to a significant reduction in operating costs when

applying microplasma sources instead of the currently used large-scale instrumentation.

Therefore, the aim of this work was to show the suitability of the miniaturized FLC-APGD excitation source for the OES determination of different elements in various types of beverages commonly chosen by athletes. This was done using a simplified sample preparation procedure that completely avoided any type of sample pre-digestion and included only sample dilution and acidification. To the best of our knowledge, the analysis of such samples is rarely done using conventional instrumentation and has never been carried out with the aid of any type of microplasma source. The selected matrices, with particular emphasis on the protein matrix, have never been analyzed thus far, using the above-mentioned APGD sources. Additionally, compared to our previous works,[28] the design of the studied FLC-APGD system was modified by replacing the tungsten rod with a tungsten tube, which improved the discharge stability by using an He jet anode and cooling the tube with the He gas flux. To achieve the goal of this work, the optimization of the most crucial operating parameters was performed initially, followed by the optimization of the sample dilutions to find the most suitable one. Subsequently, the DLs of the analytes (Zn, Mg, Ca, Na, and K) were established under the compromise conditions. Finally, the developed method was applied for the analysis of 13 different beverages for their content of Zn, Mg, Ca, Na, and K. The obtained results were compared with that obtained from ICP-OES measurements of the analyzed samples, after their wet-digestion, and discussed.

2. Experimental

2.1. Instrumentation

A schematic image of the studied FLC-APGD system is shown in Fig. 1. The discharge was generated in an open-to-air chamber between two tungsten tubes (OD/ID 3/2 mm, length 50 mm), serving as the solution and He delivery tubes. This is the difference to our previous FLC-APGD setup,[28] which was intended to enhance the stability of the measurements of samples comprised of highly complex matrix components. The distance between the tubes (so-called the discharge gap) was constant throughout the experiments and set to approximately 1 mm. The liquid cathode solutions acidified with HNO_3 were introduced in the bottom tungsten tube with the aid of a 3-channel REGLO ICC peristaltic pump (Ismatec, USA) at various flow rates in the range of 2.0–4.0 mL min^{-1}. As the solution flowed down to a PTFE reservoir, it was pumped out from it by means of the previously mentioned peristaltic pump. The He gas was introduced through the upper tube at various flow rates in the range of 50–350 mL min^{-1}. The electrical contact was provided directly in the case of the upper gas delivery tungsten tube and with a platinum spiral wrapped around the bottom solution delivery tube. The voltage was applied to both tubes by means of an HV dc power supply (model DP50H-024PH, DSC-Electronics, Germany) and its value changed in the range of 800–1200 V, depending on the applied discharge current, acid concentration and the gas and sample flow rates. A 6.9 kΩ ballast resistor was connected to the electrical circuit to achieve the discharge stabilization.

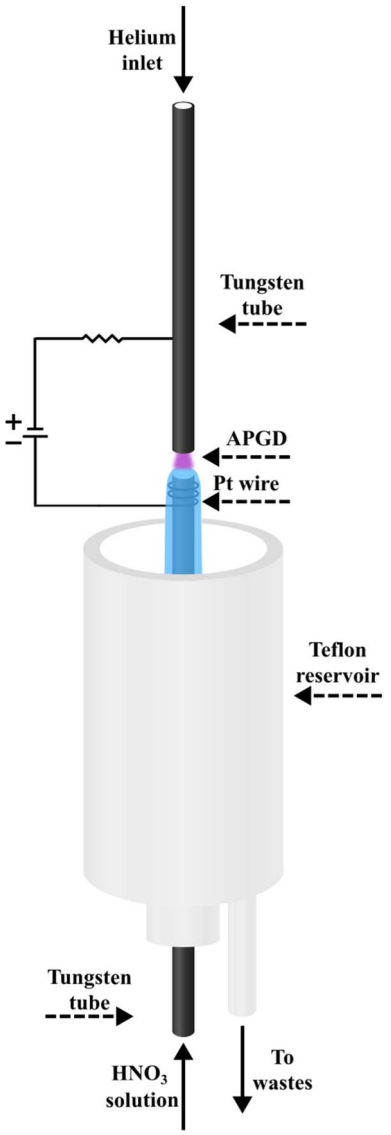

Fig. 1 Schematic drawing of the developed FLC-APGD system.

The radiation emitted by the discharge was imaged (1 : 1) on the entrance slit (10 μm) of a Shamrock 500i imaging spectrometer (Andor, UK), using an achromatic quartz lens ($f = 80$). The spectrometer setup consisted of a holographic grating (1800 lines per mm) and a Newton DU-920P-OE UV-Vis CCD camera (Andor, UK). The integration time was 10 s for all experiments and the traced emission lines of the studied elements were as follows: Zn (213.9 nm), Mg (285.2 nm), Ca (422.7 nm), Na (589.0 nm), and K (766.5 nm). Unless stated otherwise, each spectrum was recorded three times and the average results were given.

To obtain the reference values of the concentration of Zn, Mg, Ca, Na, and K in the analyzed samples, the samples were wet-digested and subjected to analysis by means of ICP-OES using an Agilent 5110 Synchronous Vertical Dual View (SVDV)

instrument. The spectrometer was equipped with an easy-to-fit quartz torch with a standard 1.8 mm injector and a sample introduction system, which consisted of a Seaspray nebulizer and a double-pass glass cyclonic spray chamber. The operating conditions used to for the ICP-OES instrument are presented in Table SI1.†

2.2. Reagents and sample preparation

Deionized water (18.2 MΩ cm) was obtained from an Polwater water purification system (Labopol-Polwater, Poland) and was used during the whole study. High-purity He (99.999%) was provided by Air Products (Poland). The purity of all chemicals was at least of analytical grade. Stock standard solutions of Zn, Mg, Ca, Na, and K (1000 mg L^{-1}) were supplied by Sigma-Aldrich (Germany) and used to prepare all working standard solutions. For the acidification of the FLC solutions, a Suprapur® grade concentrated HNO_3 (65% m m^{-1}) solution from Merck (Germany) was applied. A Suprapur® 30% H_2O_2 solution (Merck, Germany) along with the mentioned concentrated HNO_3 solution were employed for the sample digestion before the ICP-OES analysis.

Various products willingly chosen by athletes were employed to perform this study, including Coca-Cola Zero, energy drinks, pre-workout, BCAAs, almond drink, and protein powders. For comparison, sugared and sugar-free versions of Coca-Cola, black energy drink, and almond drink were studied. All the mentioned samples were purchased at local stores, with the exception of the protein powders, which were purchased from an online shop. Henceforth, the following abbreviations will be used for the simplification: CCZ (Coca-Cola Zero), CCO (Coca-Cola Original, sugared), VMg (multi-vitamin energy drink with added Mg), VZn (multi-vitamin energy drink with added Zn), BSF (Black, Sugar-Free), BS (Black, Sugared), PW (pre-workout), BCAA-1, BCAA-2 (two different samples of BCAAs varying only in taste), ADSF (almond drink, sugar-free), ADS (almond drink, sugared), WPC (whey protein, chocolate flavor), and WPS (whey protein, strawberry flavor). At this point, it is worth briefly mentioning that almond drink is better known as almond milk, however, the term "milk" should be avoided given that according to the European Court of Justice statement, this term means only the natural secretion of mammals, not plants.[46] Therefore, the term "drink" will be used herein.

The almond drink and whey protein samples had to be filtered prior to both FLC-APGD-OES and ICP-OES analysis. To achieve this, they were filtered through 0.45 μm syringe filters, given that the formation of protein precipitates occurred after the addition of HNO_3. To prepare the sample solutions for the FLC-APGD-OES measurements, appropriate amounts of each of the studied samples were transferred to twist-cup containers and acidified with concentrated HNO_3 to the final concentration of 0.2 mol L^{-1}. Subsequently, the solutions were filled with deionized water to reach final dilutions that were 50-, 100-, 500-, or 5000-fold (depending on the sample). The prepared solutions were analyzed in regard to the external calibration curves with simple standards solutions, and – if needed – using the standard addition technique. In the latter case, all the mentioned sample preparation steps were repeated but after the sample acidification, each sample was divided into three separate parts and two standard additions of Mg were added to reach the concentration of 50 and 100 μg L^{-1}, respectively. Subsequently, all the samples were filled with deionized water to reach the final dilution of 100- or 500-fold.

For the ICP-OES analysis, all the studied samples had to be wet-digested prior to the actual analysis, with the purpose of destroying any type of organic matrix present in them. To achieve this, aliquots of 5.0 g of each studied sample (or filtrates of almond drink and whey protein) along with 5.0 mL of concentrated HNO_3 were transferred to a DigiPrep tube and heated in a DigiPrep block digestion system for 180 min at 120 °C. Subsequently, the resulting sample digests were cooled and 5.0 mL of H_2O_2 (30%) was added. Then, the digested samples were further heated for 60 min. After cooling, the final digested samples were filled with deionized water to the mass of 50.0 g. Subsequently, appropriate amounts of digested samples were transferred to twist-cup containers and filled with deionized water up to 30.0 g. The final dilutions (on the weight basis) of the samples were 10- (CCZ and CCO), 100- (VMg, VZn, BSF, BS, PW, BCAA-1, BCAA-2, ADSF, and ADS) or 1000-fold (WPC and WPS).

All the analyzed samples were prepared in triplicate along with the appropriate procedural blanks that were considered in the final results. The analytes were determined in regard to the external calibration curves with simple standards solutions.

3. Results and discussion

3.1. Optimization of discharge operating conditions

Initially, to establish which elements were actually present in the studied samples, a preliminary study was carried out. To achieve this, samples of different dilutions varying in the 10–100-fold range were introduced in the FLC-APGD discharge and the emission spectra in the range of 200–900 nm were recorded for each of them. The analytical lines of Mg, Ca, Na, and K were detected in each of the samples. Additionally, a relatively high signal of Zn was detected in the VZn sample. Besides these elements, no other elements were found in any of these samples, indicating that they were likely present at concentrations lower than the respective detection limits (DLs) achievable with FLC-APGD-OES. It was noted that the signals of the analytes differed between the samples in terms of their intensity, which was obviously expected. Nevertheless, in the case of the WPC and WPS samples, the analyte signal intensities were significantly higher (compared to the other samples) in the 100-fold diluted samples. Thus, it was decided to apply higher dilutions of these two samples for each subsequent research step. Consequently, unless stated otherwise, the samples dilutions applied in this study were 10- (CCZ and CCO), 20- (VMg, VZn, BSF, BS, PW, BCAA-1, BCAA-2, ADSF, and ADS) or 1000-fold (WPC and WPS) and the operating conditions were as follows: acid concentration of 0.1 mol L^{-1}, discharge current of 40 mA, He gas flow rate of 200 mL min^{-1}, and sample flow rate of 3.0 mL min^{-1}.

Initially, to successfully apply the developed FLC-APGD system for the determination of Zn, Mg, Ca, Na, and K in the studied samples, optimization of the most crucial operating parameters was carried out. The following parameters were found to have a significant impact on the analyte signals and were included in the optimization step: the acid concentration (0.01–0.20 mol L^{-1}) used for the acidification of the sample solutions, the discharge current (20–60 mA), the gas flow rate (50–350 mL min^{-1}) in the case of the He jet anode, and the sample flow rate (2.0–4.0 mL min^{-1}) in the case of the FLC solution. The measured response of the analytes was the signal-to-background ratio (SBR) of their analytical lines.

Initially, the optimization was performed on a solution containing only the studied analytes and acidified with HNO_3. The analyte concentrations were 200, 200, 600, 100, and 100 μg L^{-1} for Zn, Mg, Ca, Na, and K, respectively. The results are shown in Fig. 2, which indicated that the SBRs for the atomic emission lines of the studied analytes increased with an increase in the acid concentration and discharge current, but decreased with an increase in the He gas flow rate and sample flow rate. These results are consistent with the related literature data[26,47,48] for similar systems. Although the analyte response was similar for each investigated parameter, some differences for the impact of these parameters between themselves on the analyte signals were noted. For example, an increase of HNO_3 concentration had a greater impact on the enhancement of the SBR values than an increase of the discharge current, while an increase of the He gas flow rate caused a more noticeable drop in the SBRs than an increase of the sample flow rate. Considering that the discharge stability was impaired for some values of the studied parameters (*e.g.*, the discharge current of 60 mA or the sample flow rate of 2.0 mL min^{-1}), this observation was important for choosing the compromise operating conditions.

The reasons for the observed impact of each of the investigated parameters on the SBR values are not fully clear, however, some assumptions have been made on this matter in the previous studies. Regarding the acid concentration, the growing tendency of the analytical signals, as a result of its increasing values, are usually explained by higher solution conductivity and lower water evaporation observed for higher acid concentrations.[27] For the discharge current, its increasing values caused improved atomization and excitation conditions due to the higher population of high-energy electrons present in the discharge.[27,28,45] The decreasing tendency of the analyte signals for the increasing He gas flow rate in the FLC-APGD system with the He jet as the anode is likely due to a narrowed diffusion of the analyte atoms in the discharge zone as a result of the stronger gas flux.[45,49] Finally, the impact of the sample flow rate on the intensity of the atomic lines is not as straightforward as expected. Intuitively, it was assumed that the analyte signals would increase with an increase of the sample flow rate due to the higher amounts of analyte atoms being released into the discharge per unit time, which was actually observed in many previous works.[25,50,51] Alternatively, at higher sample flow rates, higher amounts of water are also present in the interfacial zone as a result of the higher water evaporation per unit time. This

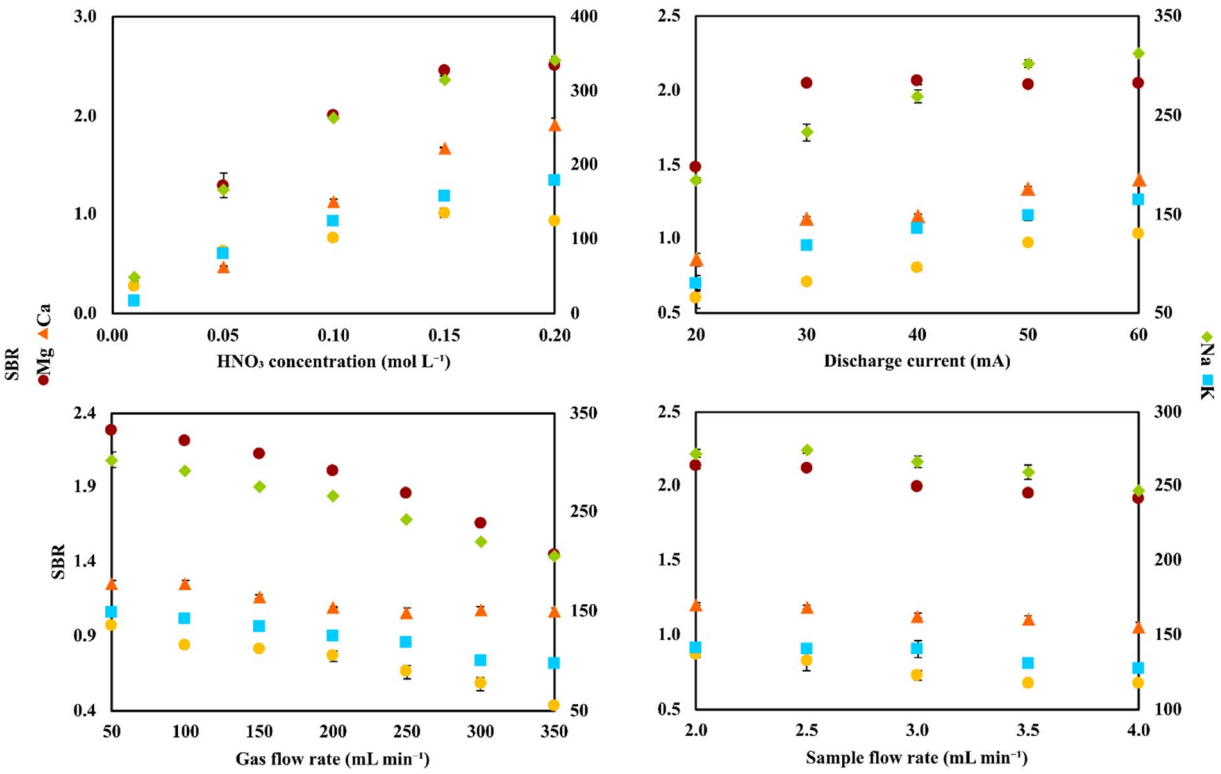

Fig. 2 The impact of HNO_3 concentration, discharge current, gas flow rate, and sample flow rate on the SBR values of the analytical lines of the studied elements for a solution containing only the analytes.

can cause impaired atomization and excitation conditions in the discharge, yielding decreased analyte signals. This was also the case in many related papers.[47,52,53] Therefore, it can be concluded that the obtained intensity or SBR values for the analytical lines of Zn, Mg, Ca, Na, and K are the result of these two effects taking place simultaneously. However, it should be noted that different results obtained by various research groups are likely related to the different system setups used and varying operating conditions, which can co-influence the sputtering efficiency and water evaporation of the system.

Nevertheless, for the elemental analysis of real samples, the impact of the sample matrix on the overall signal behavior should be considered. Thus, in this part of the study, the optimization was repeated for the studied samples to observe any possible differences in the signal behavior between samples with and without the matrix. Consequently, not only the optimal conditions for the actual samples could be established but some insight into the potential matrix effects could be gained. Therefore, the studied samples were diluted 10- (CCZ and CCO), 20- (VMg, VZn, BSF, BS, PW, BCAA-1, BCAA-2, ADSF, and ADS) or 1000-fold (WPC and WPS) and the optimization of these samples was performed. The obtained results are shown in Fig. SI1–SI7.† As it can be seen, the general tendencies in terms of the impact of a given parameter on the SBRs of the analytical lines were similar to that obtained for the sample solutions without any matrix (just standard). This finding suggests that the behavior of the analyte signals was indeed dependent on the atomization and excitation conditions in the discharge, as mentioned previously, and the sample matrices had nothing to do with these tendencies. Therefore, it can be assumed at this stage that either there were no matrix effects observed under these conditions or their contribution was minor. Although the latter conclusion cannot be stated with absolute certainty, it would be expected that the presence of some matrix effects would impact the signal sensitivity and give different results regarding the impact of these parameters on the SBR values. This is because the sample matrix can impact the atomization and excitation conditions in the discharge, leading to different signal behaviors under the same conditions. Alternatively, the matrix of real samples certainly influenced the stability of the atomic signals, which was noted while performing the measurements and it was elucidated on the figures by the error bars. This led to the conclusion that the sample dilution should be further decreased for the actual analysis.

Nevertheless, it can be concluded that the most favorable conditions in terms of the SBR values of the analytical lines of Zn, Mg, Ca, Na, and K were acid concentration of 0.2 mol L^{-1}, discharge current of 60 mA, He gas flow rate of 50 mL min^{-1}, and sample flow rate of 2.0 mL min^{-1}. However, based on our previous experience,[28,54] it was expected that the combination of all these parameters would result in significant instability of the discharge operation. This assumption is supported by the observations made herein, indicating lower discharge stability for the combination of just one of the above-mentioned parameter values with the other ones, being in the middle of the studied ranges. Thus, we decided to choose the most favorable conditions only in the case of the parameters that influenced the analyte signals the most and less suitable conditions for the rest of them. Moreover, the impact of each of the studied parameters on the discharge stability was also considered. For example, both the discharge current and sample flow rate influenced the SBRs of the analytical lines to a lower extent (than the other studied parameters), but higher discharge current values caused a lower discharge stability than lower sample flow rates. Consequently, the compromise conditions applied for all further experiments were as follows: acid concentration of 0.2 mol L^{-1}, discharge current of 40 mA, He gas flow rate of 50 mL min^{-1}, and sample flow rate of 2.5 mL min^{-1}.

3.2. Analytical performance

To establish the most suitable dilutions of the studied samples for their analysis by FLC-APGD-OES for the content of Zn, Mg, Ca, Na, and K, the analytical characteristics of the developed method were determined under the compromise conditions. For this purpose, the DLs of Zn, Mg, Ca, Na, and K, and the upper linearity ranges (ULRs) of the respective calibration curves were determined. The precision (expressed as RSD) was omitted in this study given that it was assumed that this parameter would strongly depend on both the sample dilution as well the sample composition with particular emphasis on the organic matrix. Therefore, the measured RSD values for the solutions containing only the analytes would not probably elucidate well the actual precision in the real samples. The DL values were calculated as $3\sigma/a$, with "σ" representing 3 times the standard deviation of 10 consecutive measurements of an acidified blank solution and "a" the sensitivity of a corresponding calibration curve. The upper linearity range was determined using 8 standard solutions in varying concentration ranges for different elements including 0.2–2 mg L^{-1} for Zn and Ca, 0.1–1 mg L^{-1} for Mg, and 0.05–0.5 mg L^{-1} for Na and K. The obtained results are shown in Table SI2.†

The DLs of the elements in this study for the developed FLC-APGD-OES method were 21, 0.91, 20, 0.062, and 0.14 μg L^{-1} for Zn, Mg, Ca, Na, and K, respectively. These values are similar or slightly worse compared to that obtained by our group in previous studies.[28,29] The small differences between the DLs obtained in these three works likely resulted from the slightly different operating conditions (which affected not only the signal intensities but also the background level in the vicinity of the analytical lines) as well as tubes of different diameters applied in this work, which we know from our expercience to slightly affect the signal intensities. Comparing the obtained DLs of Zn, Mg, Ca, Na, and K with the values reported by other researchers for similar FLC-APGD systems (see Table 1), it can be noticed that the DLs of the elements obtained herein are on average 1 order of magnitude better than those published in the majority of recently published papers. In this case, it can be expected that these low DLs of Zn, Mg, Ca, Na and K will enable the determination of the studied analytes in relatively highly diluted samples.

Regarding the calibration curves, they were found to be linear ($R^2 > 0.999$) over the whole investigated concentration range. This was especially beneficial given that we attempted to determine all

Table 1 Comparison between the analytical performance of different FLC-APGD systems combined with OES detection

Element	System	DL ($\mu g\ L^{-1}$)	Reference
Zn	FLC-APGD[a]	21	This work
	LCGD	50	48
	HA-SCGD	201	47
	HDE-APGD	6	24
Mg	FLC-APGD[a]	0.91	This work
	LCGD	40	48
	HA-SCGD	21.6	47
	FIA-SCGD	5.5	41
	SCGD	54.9	40
	LCGD	10	55
Ca	FLC-APGD[a]	20	This work
	LCGD	190	48
	HA-SCGD	240	47
	FIA-SCGD	11	41
	SCGD	131	40
	LCGD	10	55
Na	FLC-APGD[a]	0.062	This work
	LCGD	40	48
	HA-SCGD	0.22	47
	FIA-SCGD	0.14	41
	SCGD	1.51	40
	LCGD	20	55
K	FLC-APGD[a]	0.14	This work
	LCGD	20	48
	HA-SCGD	1.33	47
	FIA-SCGD	0.49	41
	SCGD	4.13	40
	LCGD	200	55

[a] Compared to the listed excitation sources, an He gaseous jet anode was used in the place of a pin metallic anode. FLC-APGD – flowing liquid cathode atmospheric pressure glow discharge, LCGD – liquid cathode glow discharge, HA-SCGD – hollow anode solution cathode glow discharge, HDE-APGD – hanging drop electrode atmospheric pressure glow discharge, FIA-SCGD – flow injection analysis solution cathode glow discharge.

the analytes at one dilution of each sample. This is because the intensities of the Na and K emission lines were significantly higher compared to that of the Zn, Mg, and Ca emission lines, which would require a dynamic linearity range to be able to determine the concentration of these elements simultaneously.

3.3. Optimization of sample dilution

To perform the real sample analysis after dilution and acidification, two aspects were initially considered. One was the FLC-APGD stability during its operation, given that it is known that this discharge can be successfully operated only up to a certain threshold of the FLC solution conductivity.[28,29,54] This was particularly the case herein, given that the chosen acid concentration was 0.2 mol L^{-1}, which is higher than the concentration commonly used in the majority of works focusing on FLC-APGD or similar discharge systems. Thus, it was expected that the discharge stability would be impaired for lower dilutions of certain samples, which was actually observed during the previous optimization step. The second aspect was the interference effects coming from both the organic and inorganic matrix, which are usually expected to occur in the case of lower sample dilutions. In this case, the inorganic matrix was not expected to be an issue since, firstly, the studied samples did not contain much of it, and secondly the FLC-APGD system was repeatedly proven to be relatively resistant to it.[30,31,50,54,55] However, the samples analyzed in this study contained more of the organic matrix (depending on the sample), which differed between them. Considering all these facts, it was established optimization of the sample dilution is needed to evaluate its impact on both the discharge stability and the linearity of the analyte signal response. Therefore, different dilutions of each studied sample, in the range of 10–100 (CCZ, CCO, VMg, VZn, BSF, BS, PW, BCAA-1, and BCAA-2), 10–1000 (ADSF and ADS) or 100–10 000 (WPC and WPS), were tested. For a better overview of the linearity of the analyte signal response, the results were presented as a function of the percent sample concentration (in the final sample solution), which corresponded to 1–10% for CCZ, CCO, VMg, VZn, BSF, BS, PW, BCAA-1, and BCAA-2, 0.1–10% for ADSF and ADS, and 0.01–1% for WPC and WPS. The measured response was the SBR value and the results are shown in Fig. 3 and 4.

As it can be seen, the intensity of the atomic emission lines of Mg and Ca changed linearly in the whole studied range for all the samples, whereas the response of the atomic emission lines of Na and K varied, depending on the sample. For some of them (*e.g.*, WPS), this response for both analytes was still linear, for others (*e.g.*, CCO, BS, BCAA-2, and ADSF) only one of the elements gave a linear response, whereas for the majority, both analytes presented some deviation from linearity starting from a given dilution. This observation can be easily clarified if considering the intensity of the signals. For the majority of samples, the SBRs of Mg and Ca did not exceed 3.0, whereas the SBRs of Na and K were at least a couple of hundred. Thus, it was to be expected that the signals of Na and K would be over the upper linearity range, causing them to decrease starting from a given dilution. This finding suggests that the cause of the decline in signal intensity for the lower sample dilutions was not the matrix effects but the limited upper linearity ranges. Balancing this finding against the linear response from Mg and Ca, it led to the further assumption of the matrix effects not being the case for all samples at the studied dilution ranges. However, it is worth noting that in some cases the drop in the Na emission line was observed at a given SBR value, whereas for other samples this drop was not observed even though the SBR values were similar or even higher, *e.g.*, BSF and BS. Therefore, it seems like the matrix effects could have some impact on the linearity range shifts. In the case of Zn, it was present only in the VZn sample; however, the behavior of its emission line in this particular sample was observed to be similar to the Mg and Ca lines in the other samples.

In terms of the discharge stability, it was established based on visual observations of its behavior during the measurements of the optimized sample dilutions. As expected, it was found that the lower the dilution, the worse the robustness of the discharge. Particularly, this was the case for the samples that were both measured up to the 10-fold dilution and contained a relatively rich organic matrix, *e.g.*, the samples of BCAAs and

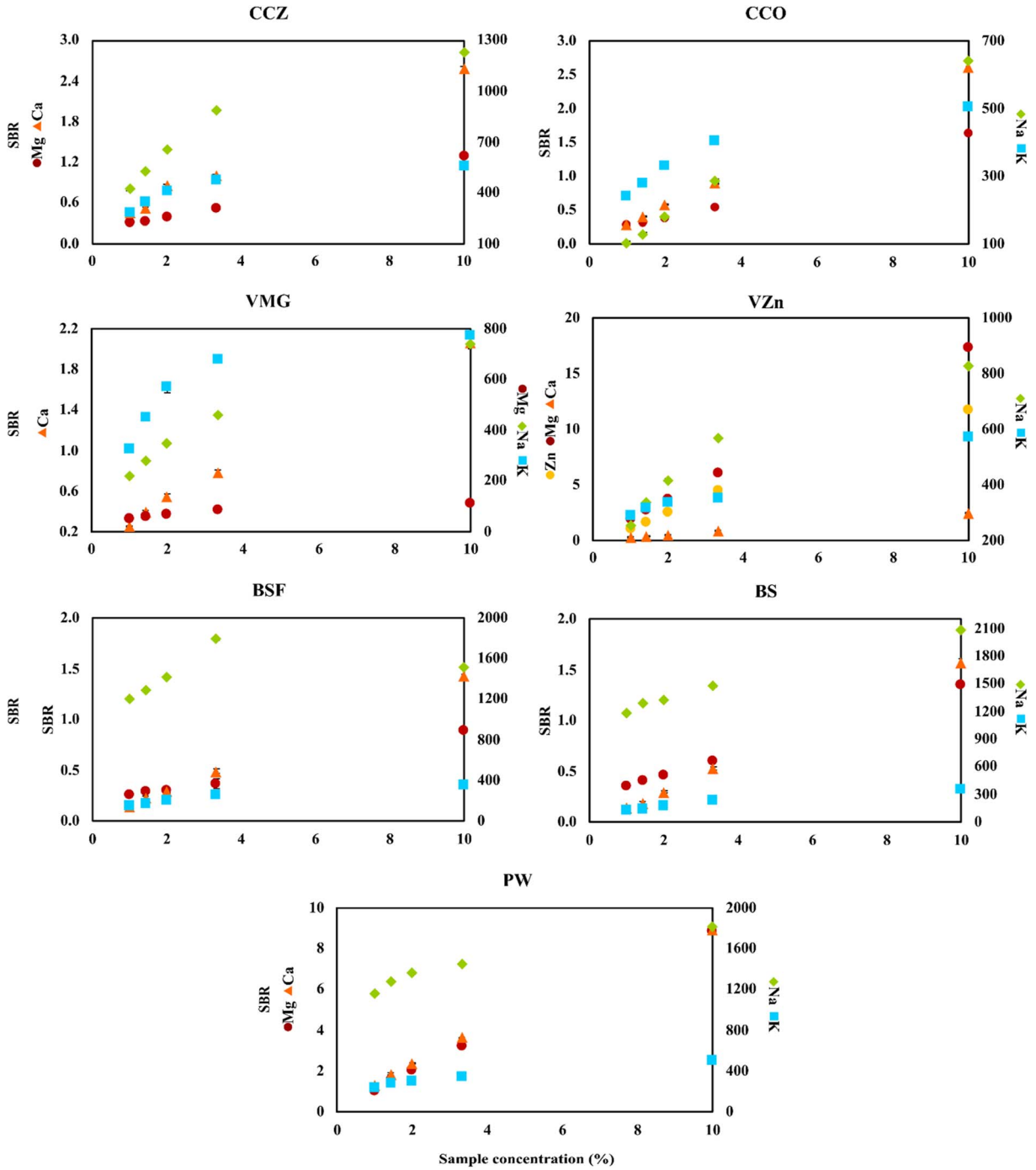

Fig. 3 Impact of the sample dilutions (expressed as percent sample concentration) on the SBR values of the analytical lines of the studied elements for the samples of CCZ, CCO, VMg, VZn, BSF, BS, and PW.

almond drink. Alternatively, relatively good discharge stability was noted for WPC and WPS in the whole measured range of the sample dilutions. This was due to lower samples dilutions in this case as well as the filtering process carried out before the measurements of these samples. Accordingly, much better discharge stability was observed for the samples containing less organic matrix, *e.g.*, the cola and black soda samples.

Considering all the above-mentioned findings, it can be concluded that almost any studied dilution factor can be applied in this work, as long as the discharge can be stably operated, given that the matrix effects were not an issue herein. Nevertheless, higher samples dilutions seemed to be favorable for the determination of Na and K because they exceeded the upper linearity range observed for these elements at lower sample dilutions. Hence, considering the relatively low DLs of the elements in this study and to prove the ability of the investigated system to determine these elements present in the samples at both low (Mg and Ca) and high (Zn, Na, and K) concentration

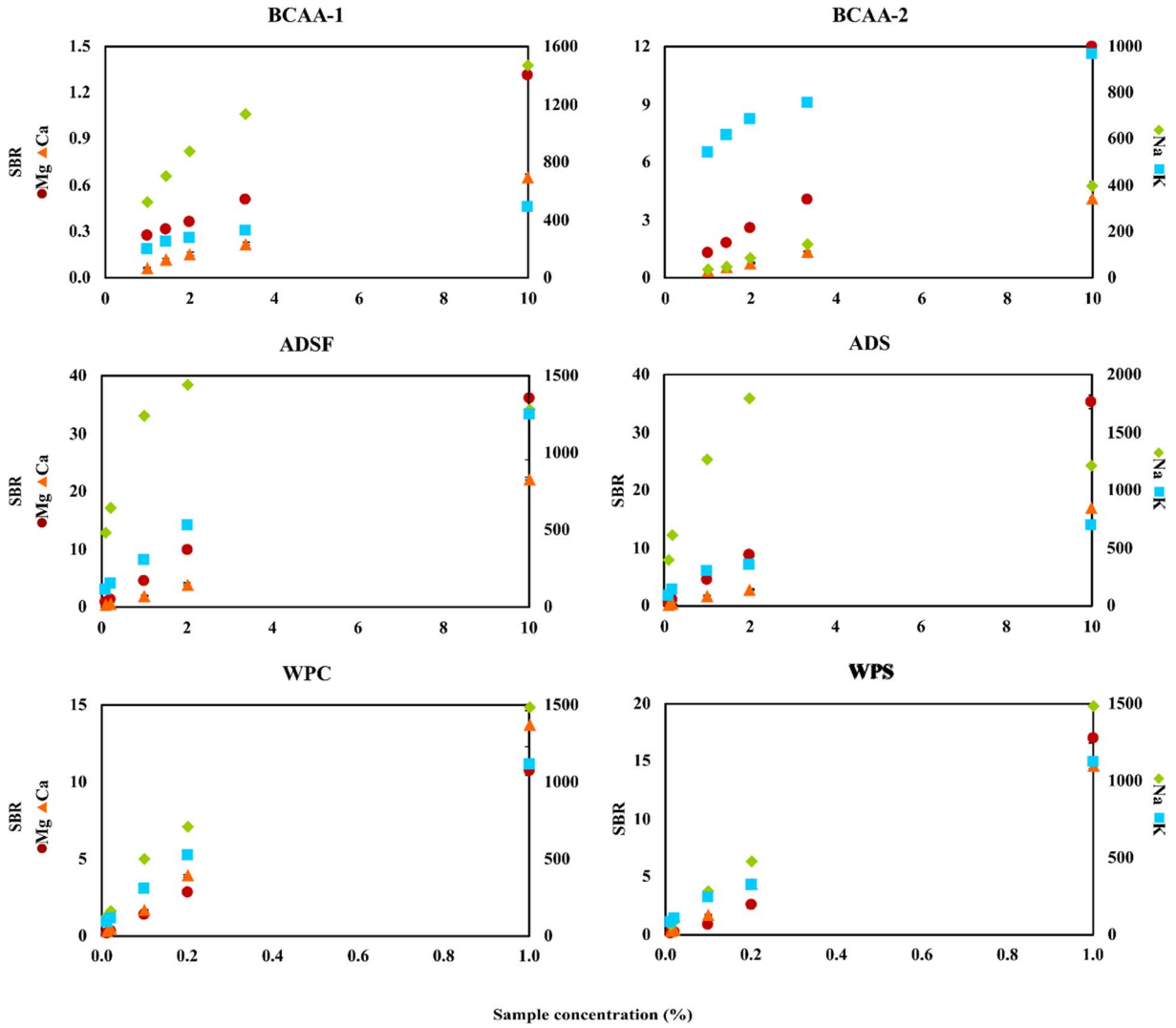

Fig. 4 Impact of the sample dilutions (expressed as percent sample concentration) on the SBR values of the analytical lines of the studied elements for the samples of BCAA-1, BCAA-2, ADSF, ADS, WPC, and WPS.

ranges, we decided to choose the following dilutions of the analyzed samples for their analysis: 50-fold for CCZ, CCO, BBC, BZC, PW, BCAA-1, and BCAA-2, 100-fold for VMg and VZn, 500-fold for ADSF and ADS, and 5000-fold for WPC and WPS.

3.4. Sample analysis

To show the credibility of the developed method to analyze real samples, the content of Zn, Mg, Ca, Na, and K was determined in all the studied samples and compared with the results obtained for the ICP-OES measurements. Obviously, all the analyzed samples needed to be wet-digested before the ICP-OES analysis. After performing the wet-digestion procedure, the samples were diluted 10- (CCZ and CCO), 100- (VMg, VZn, BSF, BS, PW, BCAA-1, BCAA-2, ADSF, and ADS) or 10 000-fold (WPC and WPS) and the resultant sample acidification was ~1.4 mol L^{-1}. The measurements were performed using the external calibration curves. In the case of the FLC-APGD-OES system, the samples were only diluted to the appropriate factors (being the same in most cases, except the WPC and WPS samples, which were highly diluted, *i.e.*, 5000-fold) and acidified with HNO_3 up to 0.2 mol L^{-1}. The samples of ADSF and ADS were also filtered after their preparation using syringe filters. In the case of the WPC and WPS samples, we attempted to determine the analyte content in these samples without the filtration process. According to our past experience,[28,56] this system is resistant to the presence of some suspensions or even precipitates, as long as their abundance in the sample is fairly low. Thus, given that the dilution of the WPC and WPS samples was as high as 5000-fold, it was assumed the protein precipitates that formed after the acidification would neither deteriorate the analyte signals nor the discharge stability to a significant extent.

Initially, the external calibration curve (in the concentration range of 0.1–10 mg L^{-1}) was used for the determination of Zn, Mg, Ca, Na, and K in the prepared solutions by FLC-APGD-OES. The results are presented in Table 2, which clearly show that almost all the analytes could be successfully determined with the aid of external calibration curves with simple standards

Table 2 The content of Zn, Mg, Ca, Na, and K in the analyzed samples

		Concentration (mg L^{-1})			
Element	Sample	ICP-OES (RSD, %)	FLC-APGD-OES (RSD, %)	Recovery (%)	RDA[a] (%)
Zn	VZn	31.15 ± 0.17 (0.55)	29.23 ± 1.01 (3.46)	93.8	62.6
Mg	CCZ	1.10 ± 0.01 (0.91)	1.14 ± 0.07 (6.14)	103.6	0.1
	CCO	0.98 ± 0.01 (1.02)	0.97 ± 0.03 (3.09)	99.0	0.1
	VMg	641.66 ± 1.67 (0.26)	370.35 ± 3.11 (0.84)	57.7	57.6
			671.63 ± 3.61[b] (0.54)	104.7	
	VZn	15.49 ± 0.12 (0.77)	15.89 ± 1.32 (8.31)	102.6	1.4
	BSF	0.70 ± 0.01 (1.43)	0.62 ± 0.04 (6.45)	88.6	0.1
	BS	0.60 ± 0.01 (1.67)	0.55 ± 0.04 (7.27)	91.7	0.1
	PW	6.57 ± 0.01 (0.15)	6.44 ± 0.07 (1.09)	98.0	0.2
	BCAA-1	1.07 ± 0.01 (0.93)	1.06 ± 0.02 (1.89)	99.1	0.1
	BCAA-2	10.87 ± 0.20 (1.84)	9.63 ± 0.04 (0.42)	88.6	0.8
	ADSF	64.75 ± 0.21 (0.32)	42.66 ± 0.01 (0.02)	65.9	5.3
			61.82 ± 3.44[b] (5.56)	95.5	
	ADS	64.04 ± 0.51 (0.80)	48.33 ± 2.22 (4.59)	75.5	5.6
			65.60 ± 3.42[b] (5.21)	102.4	
	WPC	181.25 ± 1.76 (0.97)	170.01 ± 4.26 (2.51)	93.8	9.7
	WPS	98.78 ± 4.22 (4.27)	91.28 ± 2.22 (2.43)	92.4	5.2
Ca	CCZ	8.06 ± 0.15 (1.86)	7.68 ± 0.41 (5.34)	95.3	0.3
	CCO	7.38 ± 0.02 (0.27)	7.29 ± 0.39 (5.35)	98.8	0.2
	VMg	9.93 ± 0.36 (3.63)	9.26 ± 0.22 (2.38)	93.3	0.3
	VZn	8.18 ± 0.22 (2.69)	9.13 ± 0.13 (1.42)	111.6	0.3
	BSF	5.73 ± 0.02 (0.35)	5.37 ± 0.13 (2.42)	93.7	0.2
	BS	5.67 ± 0.06 (1.06)	5.57 ± 0.16 (2.87)	98.2	0.2
	PW	41.59 ± 0.15 (0.36)	40.06 ± 0.81 (2.02)	96.3	0.4
	BCAA-1	3.18 ± 0.09 (2.83)	3.37 ± 0.19 (5.64)	106.0	0.1
	BCAA-2	15.85 ± 0.24 (1.51)	15.07 ± 0.15 (1.00)	95.1	0.5
	ADSF	96.27 ± 0.55 (0.57)	101.52 ± 2.79 (2.75)	105.5	3.4
	ADS	103.48 ± 0.95 (0.92)	96.90 ± 5.30 (5.47)	93.6	3.2
	WPC	695.09 ± 3.46 (0.50)	771.98 ± 20.47 (2.65)	111.1	17.2
	WPS	715.65 ± 29.80 (4.16)	785.92 ± 22.30 (2.84)	109.8	17.5
Na	CCZ	69.75 ± 0.44 (0.63)	63.71 ± 2.20 (3.45)	91.3	3.3
	CCO	6.69 ± 0.03 (0.45)	6.13 ± 0.28 (4.57)	91.6	0.3
	VMg	25.52 ± 0.21 (0.82)	26.38 ± 0.75 (2.84)	103.4	1.4
	VZn	25.88 ± 0.13 (0.50)	25.75 ± 0.18 (0.70)	99.5	1.3
	BSF	711.21 ± 1.89 (0.27)	672.29 ± 10.80 (1.61)	94.5	34.0
			652.47 ± 4.57[c] (0.70)	91.7	
	BS	715.73 ± 2.39 (0.33)	672.09 ± 9.98 (1.48)	93.9	35.4
			678.30 ± 19.41[c] (2.86)	94.8	
	PW	367.64 ± 1.05 (0.29)	365.26 ± 2.07 (0.57)	99.4	5.1
	BCAA-1	99.28 ± 1.00 (1.01)	90.53 ± 2.34 (2.58)	91.2	4.7
	BCAA-2	4.16 ± 0.09 (2.16)	4.48 ± 0.20 (4.46)	107.7	0.2
	ADSF	495.94 ± 1.06 (0.21)	493.95 ± 38.66 (7.83)	99.6	25.8
	ADS	496.52 ± 2.01 (0.40)	446.21 ± 20.63 (4.62)	89.9	23.3
	WPC	431.25 ± 8.31 (1.93)	388.60 ± 8.65 (2.23)	90.1	13.5
	WPS	274.35 ± 12.55 (4.57)	272.43 ± 8.94 (3.28)	99.3	9.5
K	CCZ	57.33 ± 0.29 (0.51)	57.82 ± 1.75 (3.03)	100.9	0.5
	CCO	33.18 ± 0.25 (0.75)	36.99 ± 0.87 (2.35)	111.5	0.3
	VMg	231.82 ± 1.60 (0.69)	233.82 ± 4.43 (1.89)	100.9	2.0
	VZn	230.37 ± 0.61 (0.26)	227.72 ± 3.41 (1.50)	98.9	2.0
	BSF	27.37 ± 0.61 (2.23)	27.39 ± 0.80 (2.92)	100.1	0.2
	BS	13.39 ± 0.17 (1.27)	14.31 ± 0.64 (4.47)	106.9	0.1
	PW	55.19 ± 0.59 (1.07)	58.59 ± 1.20 (2.05)	106.2	0.1
	BCAA-1	79.47 ± 0.44 (0.55)	75.86 ± 3.55 (4.68)	95.5	0.7
	BCAA-2	221.66 ± 0.10 (0.05)	213.86 ± 2.63 (1.23)	96.5	1.8
	ADSF	123.93 ± 1.26 (1.02)	132.86 ± 4.23 (3.18)	107.2	1.1
	ADS	124.68 ± 0.59 (0.47)	134.21 ± 6.40 (4.77)	107.6	1.2
	WPC	1150.07 ± 3.92 (0.34)	1048.36 ± 25.46 (2.43)	91.2	6.0
	WPS	606.82 ± 52.19 (8.60)	564.51 ± 4.14 (0.73)	93.0	3.2

[a] Per portion, meaning 300 mL for CCZ, CCO, VMg, VZn, BSF, BS, BCAA-1, BCAA-2, ADSF, and ADS; 80 mL (one shot) for PW, and 30 g (one scoop) for WPC and WPC. [b] Using the standard addition technique. [c] For the dilution factor of 500.

solutions. The recovery values (calculated as the percent value of measured with FLC-APGD-OES with reference to ICP-OES) in the majority of cases were in the range of 88–111%, further confirming the lack of the matrix effects. Only the results obtained for the determination of Mg in VMg, ADSF, and ADS led to the recoveries being significantly lower, *i.e.*, around 57%, 66%, and 75%, respectively. This was likely due to the presence of certain compounds in these samples that formed complexes and/or sediments with Mg, which could not be fully atomized in the discharge. Some additional reactions taking place between Mg and other samples compounds with the aid of the discharge constituents could also occur. In this case, the concentration of Mg in these samples was determined once more, this time using the standard addition technique, which resulted in the recovery values being the range of 95–105%. Moreover, the determination of BSF and BS was challenging due to high amounts of Na present in these samples. Due to the relatively low concentrations of the other elements (particularly Mg and Ca), BSF and BS could not be further diluted; however, in this case, the intensity of the Na atomic emission lines exceeded the measured range of the linearity of this element. Nevertheless, the recoveries of Na in these samples was around 94%, suggesting that the actual upper linearity range was not exceeded. Therefore, to be certain, the analysis of these samples for the content of Na was repeated in a more diluted sample (namely 500-fold) and the obtained results agreed well with that obtained for a 50-fold diluted sample. It is also worth noting that there were no differences between the results obtained for the sugared and sugar-free samples of the same type. This was interesting considering previous studies reporting the observed matrix effects coming from the presence of sugar in a similar system.[36] Nevertheless, the lack of matrix effects observed in this study was most likely due to the relatively low sugar amounts (around a few grams per 100 mL), which apparently was not high enough to cause any serious matrix effects. Regarding the measurement precision (expressed as RSD), it varied in the range of 0.05–8.60% range for ICP-OES and 0.02–8.31% for the FLC-APGD-OES method. The average RSD values were 1.28% and 3.12% for ICP- and FLC-APGD-OES, respectively. This indicated that the measurement precision was slightly worse for the FLC-APGD-OES method; nevertheless, most of the results still fitted below the acceptable level of 5%. Moreover, given that almost all the RSD values obtained for whey protein fell in the range of 0.50–4.57%, it was proven that at this high dilution the samples could be reliably analyzed even without the filtration process.

Therefore, in summary, based on the results obtained at this stage of research, it can be stated that the developed FLC-APGD-OES method gave reliable results and can be effectively applied for the determination of this type of sample. Additionally, in contrast to the application of ICP-OES, the samples did not need to be digested. FLC-APGD-OES also requires a significantly lower acid concentration and has the advantage of being resistant to the presence of suspensions or sediments, which allowed the filtration step to be omitted once the sample was significantly diluted. This, together with the fairly low DLs of the studied elements make this method a very promising alternative for the currently applied methods with the bulky instrumentation such as FAAS, ICP-OES or ICP-MS.

3.5. Evaluation of nutritional quality

To evaluate the nutritional quality of the studied beverages, the concentrations of the determined elements were correlated with the percent of the recommended daily allowance (RDA), which is 14, 350, 900, 575, and 3500 mg day^{-1}, for Zn, Mg, Ca, Na, and K, respectively[57] (see Table 2). The percent of RDA was calculated from the concentrations obtained for the FLC-APGD-OES analysis and with reference to one portion. Given that most of the drinks were of portions of around 300 mL, this value was considered to be a portion for the majority of the samples (including almond drink, which was supposed to be used for comparison purposes). The only exceptions were PW given that it was sold as one shot (80 mL) and the whey protein samples, in which the manufacturer recommended one scoop (around 30 g) per a portion. As can be seen from the table, Zn was only present in one sample (VZn); however, one portion of this beverage covered over 60% of its RDA. In the case of Mg, most of the analyzed drinks (except VMg, ADSF, ADS, WPC, and WPS) turned out to be a very poor source of this element given that the RDA was only in the range of 0.05–1.36%. Even worse results were obtained for Ca given that almost all the studied samples (except ADSF, ADS, WPC, and WPS) contained this element at concentrations equal to or below 0.5% of its RDA. Much better outcomes were observed for Na given that many of the analyzed samples (namely BSF, BS, ADSF, ADS, WPC, and WPS) contained Na at concentrations covering over 9% of its RDA and the percentage of the RDA varied for the other samples in the range of 0.23–5.08%. This was most likely due to the presence of Na-based salts, which are commonly used as preservatives. Regarding the K content, it was rather low and varied in the range of 0.12–6.00% of its RDA, depending on the sample.

A fairly high coverage of the RDAs for the studied elements was observed for the almond drink and whey protein samples. Nevertheless, it is worth mentioning that the concentration of Mg, Ca, and K in the almond drink was still noticeably lower than that in the animal-based milk, whereas the concentration of Na was similar.[58] Nevertheless, given that the concentration differences in Mg, Ca, and Na between the animal-based milk and almond drink were not very high, it can be stated that almond drink is still an acceptably good source of these elements. The highest coverage of all determined elements (except Zn) was found in the whey protein samples, which means that whey protein is not only a very good source of high-quality protein but also significantly supplements the studied elements. Therefore, compared to the BCAA samples, it can be concluded that whey protein is superior not only in terms of its amino acid profile but also in terms of the mineral content. When comparing energy drinks to the pre-workout sample (which are used for similar purposes), it can be noticed that even though none of these samples were a good source of the analyzed minerals, pre-workout contained significantly higher amounts of Mg, Ca, and K, which makes it a superior supplement. Nevertheless, it should be noted that the content of these

elements (with particular emphasis on Mg, Ca, and K) is noticeably higher in regular coffee (assuming preparing the coffee beverage from 10 g of dry coffee).[59–61] Thus, according to all the above-mentioned observations, it can be stated that most of the studied samples are not a decent source of minerals and should be replaced with regular food that contains not only the necessary elements but in most cases, also high amounts of antioxidants. Alternatively, almond drink seems to be an interesting alternative for vegetarians as well as a part of a low-calorie diet, whereas whey protein is a fair supplement for athletes struggling with meeting their daily protein intake. However, it should be considered that the mineral bioavailability from plant-based beverages, including almond drink, is usually quite poor.[62]

4. Conclusions

The FLC-APGD system along with an He jet anode was applied to determine the content of certain elements (namely Zn, Mg, Ca, Na, and K) in samples of selected drinks commonly chosen by athletes, using OES detection. To achieve this, optimization of the crucial operating parameters and different samples solution was carried out. It was found that higher acid concentrations and discharge currents as well as lower He gas and sample flow rates favored better analyte detectability (in terms of the signal intensities of the analytes). It was established that the most suitable operating conditions had to be a compromise due to the discharge stability issues. Therefore, the conditions that resulted in the highest signal intensity enhancement (namely the acid concentration and sample flow rate) were set to the most suitable values, whereas the values of the other parameters (the discharge current and the He gas flow rate) were lowered to the value that ensured good discharge stability. Regarding the sample dilutions, it was found that even for the highest studied dilution, the signals of all the elements could be detected. Moreover, the investigation of the sample dilution showed an almost linear response for the analytes signals. The only exceptions were the signals of Na and K, which due to their high sensitivity likely exceeded the upper linearity range. This finding suggested the lack of matrix effects, which could affect the sample analysis. This assumption was further confirmed during the actual analysis, given that for the majority of cases the obtained results agreed well with that obtained previously for the ICP-OES measurements. Only the content of Mg in certain samples (namely VMg, ADSF, and ADS) could not be determined using the external calibration curve. Nevertheless, the standard addition technique solved this issue.

Considering all the above-mentioned results, it was concluded that the developed FLC-APGD-OES method can be a reliable alternative to the ICP-OES method, as well as other methods that use commercially available bulky instrumentation such as FAAS or AFS. The proposed method not only assured similar DLs of Zn, Mg, Ca, Na, and K but also allowed the sample analysis to be performed without any sample predigestion, which was not the case for ICP-OES. It was also shown that for higher dilutions even the filtering process could be omitted given that the FLC-APGD system was fairly resistant to the presence of some suspensions and sediments in the sample. Notably, this enabled us to simplify the sample preparation procedure, reducing the cost because we avoided the use of concentrated reagents and a heating block or another digestion unit. Moreover, it was found that in almost all cases, the analyte content could be determined using only the external calibration with simple standard solutions. Additionally, the developed FLC-APGD-OES method had the advantages of small size, which is promising for the future miniaturization of the whole system, requiring significantly lower acid concentration and gas flow rate (as compared to ICP-OES), and thus noticeably reducing the time and cost of the performed analysis. Therefore, the added value of the present work is the simplicity of the measurement system and extremely low costs associated with its construction, operation and sample preparation.

Conflicts of interest

The authors declare that they have no known competing financial interests or personal relationships that could have appeared to influence the work reported in this paper.

References

1 R. Crowley and L. Harvey FitzGerald, The impact of cGMP compliance on consumer confidence in dietary supplement products, *Toxicology*, 2006, **221**, 9–16.
2 P. S. Harty, H. A. Zabriskie, J. L. Erickson, P. E. Molling, C. M. Kerksick and A. R. Jagim, Multi-ingredient pre-workout supplements, safety implications, and performance outcomes: a brief review, *J. Int. Soc. Sports Nutr.*, 2018, **15**, 41–69.
3 R. R. Wolfe, Branched-chain amino acids and muscle protein synthesis in humans: myth or reality?, *J. Int. Soc. Sports Nutr.*, 2017, **14**, 30–37.
4 E. Volpi, H. Kobayashi, M. Sheffield-Moore, B. Mittendorfer and R. R. Wolfe, Essential amino acids are primarily responsible for the amino acid stimulation of muscle protein anabolism in healthy elderly adults, *Am. J. Clin. Nutr.*, 2003, **78**, 250–258.
5 S. R. Jackman, O. C. Witard, A. Philp, G. A. Wallis, K. Baar and K. D. Tipton, Branched-Chain Amino Acid Ingestion Stimulates Muscle Myofibrillar Protein Synthesis following Resistance Exercise in Humans, *Front. Physiol.*, 2017, **8**, 390–402.
6 T. A. Churchward-Venne, N. A. Burd, C. J. Mitchell, D. W. D. West, A. Philp, G. R. Marcotte, S. K. Baker, K. Baar and S. M. Phillips, Supplementation of a suboptimal protein dose with leucine or essential amino acids: effects on myofibrillar protein synthesis at rest and following resistance exercise in men, *J. Physiol.*, 2012, **590**, 2751–2765.
7 D. L. Plotkin, K. Delcastillo, D. W. van Every, K. D. Tipton, A. A. Aragon and B. J. Schoenfeld, Isolated Leucine and Branched-Chain Amino Acid Supplementation for Enhancing Muscular Strength and Hypertrophy: A

Narrative Review, *Int. J. Sport Nutr. Exercise Metab.*, 2021, **31**, 292–301.

8 A. William Kedia, J. E. Hofheins, S. M. Habowski, A. A. Ferrando, M. David Gothard and H. L. Lopez, Effects of a pre-workout supplement on lean mass, muscular performance, subjective workout experience and biomarkers of safety, *Int. J. Med. Sci.*, 2014, **11**, 116–126.

9 J. R. Poortmans and M. Francaux, Adverse effects of creatine supplementation: fact or fiction?, *Sports Med.*, 2000, **30**, 155–170.

10 A. R. Jagim, P. S. Harty and C. L. Camic, Common Ingredient Profiles of Multi-Ingredient Pre-Workout Supplements, *Nutrients*, 2019, **11**, 254–262.

11 I. Garthe, Dietary supplements and elite athletes: when nature becomes high risk, *Curr. Opin. Endocr. Metab. Res.*, 2019, **9**, 66–73.

12 H. Geyer, M. Kristina Parr, K. Koehler, U. Mareck, W. Schänzer and M. Thevis, Nutritional supplements cross-contaminated and faked with doping substances, *J. Mass Spectrom.*, 2008, **43**, 892–902.

13 G. Moses, The safety of commonly used vitamins and minerals, *Aust. Prescr.*, 2021, **44**, 119–123.

14 S. M. Elgammal, M. A. Khorshed and E. H. Ismail, Determination of heavy metal content in whey protein samples from markets in Giza, Egypt, using inductively coupled plasma optical emission spectrometry and graphite furnace atomic absorption spectrometry: A probabilistic risk assessment study, *J. Food Compos. Anal.*, 2019, **84**, 103300.

15 S. Moret, A. Prevarin and F. Tubaro, Levels of creatine, organic contaminants and heavy metals in creatine dietary supplements, *Food Chem.*, 2011, **126**, 1232–1238.

16 B. Ruiz Brandao Da Costa, R. Rocha Roiffe and M. Nogueira Silva de La Cruz, Quality Control of Protein Supplements: A Review, *Int. J. Sport Nutr. Exercise Metab.*, 2021, **31**, 369–379.

17 V. V. Yagov, M. L. Getsina and B. K. Zuev, Use of Electrolyte Jet Cathode Glow Discharges as Sources of Emission Spectra for Atomic Emission Detectors in Flow-Injection Analysis, *J. Anal. Chem.*, 2004, **59**, 1037–1041.

18 A. Kitano, A. Iiduka, T. Yamamoto, Y. Ukita, E. Tamiya and Y. Takamura, Highly sensitive elemental analysis for Cd and Pb by liquid electrode plasma atomic emission spectrometry with quartz glass chip and sample flow, *Anal. Chem.*, 2011, **83**, 9424–9430.

19 B. K. Zuev, V. V. Yagov, M. L. Getsina and B. A. Rudenko, Discharge on Boiling in a Channel as a New Atomization and Excitation Source for the Flow Determination of Metals by Atomic Emission Spectrometry, *J. Anal. Chem.*, 2002, **57**, 907–911.

20 T. Cserfalvi, P. Mezei and P. Apai, Emission studies on a glow discharge in atmospheric pressure air using water as a cathode, *J. Phys. D: Appl. Phys.*, 1993, **26**, 2184–2188.

21 P. Jamroz and W. Zyrnicki, Spectroscopic Characterization of Miniaturized Atmospheric-Pressure dc Glow Discharge Generated in Contact with Flowing Small Size Liquid Cathode, *Plasma Chem. Plasma Process.*, 2011, **31**, 681–696.

22 M. R. Webb, F. J. Andrade, G. Gamez, R. McCrindle and G. M. Hieftje, Spectroscopic and electrical studies of a solution-cathode glow discharge, *J. Anal. At. Spectrom.*, 2005, **20**, 1218–1225.

23 K. Swiderski, P. Pohl and P. Jamroz, A miniaturized atmospheric pressure glow microdischarge system generated in contact with a hanging drop electrode – a new approach to spectrochemical analysis of liquid microsamples, *J. Anal. At. Spectrom.*, 2019, **34**, 1287–1293.

24 K. Greda, K. Swiderski, P. Jamroz and P. Pohl, Flowing Liquid Anode Atmospheric Pressure Glow Discharge as an Excitation Source for Optical Emission Spectrometry with the Improved Detectability of Ag, Cd, Hg, Pb, Tl, and Zn, *Anal. Chem.*, 2016, **88**, 8812–8820.

25 X. Liu, Z. Zhu, D. He, H. Zheng, Y. Gan, N. Stanley Belshaw, S. Hu and Y. Wang, Highly sensitive elemental analysis of Cd and Zn by solution anode glow discharge atomic emission spectrometry, *J. Anal. At. Spectrom.*, 2016, **31**, 1089–1096.

26 P. Jamroz, K. Greda, A. Dzimitrowicz, K. Swiderski and P. Pohl, Sensitive Determination of Cd in Small-Volume Samples by Miniaturized Liquid Drop Anode Atmospheric Pressure Glow Discharge Optical Emission Spectrometry, *Anal. Chem.*, 2017, **89**, 5729–5733.

27 P. Pohl, P. Jamroz, K. Greda, M. Gorska, A. Dzimitrowicz, M. Welna and A. Szymczycha-Madeja, Five years of innovations in development of glow discharges generated in contact with liquids for spectrochemical elemental analysis by optical emission spectrometry, *Anal. Chim. Acta*, 2021, **1169**, 338399.

28 M. Gorska and P. Pohl, Simplified and rapid determination of Ca, K, Mg, and Na in fruit juices by flowing liquid cathode atmospheric glow discharge optical emission spectrometry, *J. Anal. At. Spectrom.*, 2021, **36**, 1455–1465.

29 K. Greda and P. Pohl, Direct analysis of wines from the province of Lower Silesia (Poland) by microplasma source optical emission spectrometry, *Food Chem.*, 2022, **371**, 131178.

30 Q. Lu, F. Feng, J. Yu, L. Yin, Y. Kang, H. Luo, D. Sun and W. Yang, Determination of trace cadmium in zinc concentrate by liquid cathode glow discharge with a modified sampling system and addition of chemical modifiers for improved sensitivity, *Microchem. J.*, 2020, **152**, 104308.

31 J. Yu, Y. Kang, Q. Lu, H. Luo, Z. Lu, L. Cui and J. Li, Improvement of analytical performance of liquid cathode glow discharge for the determination of bismuth using formic acid as a matrix modifier, *Microchem. J.*, 2020, **159**, 105507.

32 R. Manjusha, M. A. Reddy, R. Shekhar and S. Jaikumar, Determination of major to trace level elements in Zircaloys by electrolyte cathode discharge atomic emission spectrometry using formic acid, *J. Anal. At. Spectrom.*, 2013, **28**, 1932–1939.

33 K. Greda, P. Jamroz and P. Pohl, The improvement of the analytical performance of direct current atmospheric pressure glow discharge generated in contact with the small-sized liquid cathode after the addition of non-ionic

surfactants to electrolyte solutions, *Talanta*, 2013, **108**, 74–82.

34 L. Bencs, N. Laczai, P. Mezei and T. Cserfalvi, Detection of some industrially relevant elements in water by electrolyte cathode atmospheric glow discharge optical emission spectrometry, *Spectrochim. Acta, Part B*, 2015, **107**, 139–145.

35 M. Gorska and P. Pohl, Application of atmospheric pressure glow discharge generated in contact with liquids for determination of chloride and bromide in water and juice samples by optical emission spectrometry, *Talanta*, 2022, **237**, 122921.

36 J. Yu, X. Zhang, Q. Lu, X. Wang, D. Sun, Y. Wang and W. Yang, Determination of calcium and zinc in gluconates oral solution and blood samples by liquid cathode glow discharge-atomic emission spectrometry, *Talanta*, 2017, **175**, 150–157.

37 K. Greda, P. Jamroz, A. Dzimitrowicz and P. Pohl, Direct elemental analysis of honeys by atmospheric pressure glow discharge generated in contact with a flowing liquid cathode, *J. Anal. At. Spectrom.*, 2015, **30**, 154–161.

38 Z. Zhang, Z. Wang, Q. Li, H. Zou and Y. Shi, Determination of trace heavy metals in environmental and biological samples by solution cathode glow discharge-atomic emission spectrometry and addition of ionic surfactants for improved sensitivity, *Talanta*, 2014, **119**, 613–619.

39 P. Zheng, Y. Gong, J. Wang and X. Zeng, Elemental Analysis of Mineral Water by Solution-Cathode Glow Discharge–Atomic Emission Spectrometry, *Anal. Lett.*, 2017, **50**, 1512–1520.

40 C. Yang, L. Wang, Z. Zhu, L. Jin, H. Zheng, N. Stanley Belshaw and S. Hu, Evaluation of flow injection-solution cathode glow discharge-atomic emission spectrometry for the determination of major elements in brines, *Talanta*, 2016, **155**, 314–320.

41 R. Shekhar, K. Madhavi, N. N. Meeravali and S. Jai Kumar, Determination of thallium at trace levels by electrolyte cathode discharge atomic emission spectrometry with improved sensitivity, *Anal. Methods*, 2014, **6**, 732–740.

42 J. Mo, L. Zhou, X. Li, Q. Li, L. Wang and Z. Wang, On-line separation and pre-concentration on a mesoporous silica-grafted graphene oxide adsorbent coupled with solution cathode glow discharge-atomic emission spectrometry for the determination of lead, *Microchem. J.*, 2017, **130**, 353–359.

43 C. Huang, Q. Li, J. Mo and Z. Wang, Ultratrace Determination of Tin, Germanium, and Selenium by Hydride Generation Coupled with a Novel Solution-Cathode Glow Discharge-Atomic Emission Spectrometry Method, *Anal. Chem.*, 2016, **88**, 11559–11567.

44 P. Jamroz, P. Pohl and W. Zyrnicki, An analytical performance of atmospheric pressure glow discharge generated in contact with flowing small size liquid cathode, *J. Anal. At. Spectrom.*, 2012, **27**, 1032–1037.

45 M. Gorska, K. Greda and P. Pohl, Determination of bismuth by optical emission spectrometry with liquid anode/cathode atmospheric pressure glow discharge, *J. Anal. At. Spectrom.*, 2021, **36**, 165–177.

46 K. E. Scholz-Ahrens, F. Ahrens and C. A. Barth, Nutritional and health attributes of milk and milk imitations, *Eur. J. Nutr.*, 2020, **59**, 19–34.

47 P. Zheng, W. Li, J. Wang, N. Wang, C. Zhong, Y. Luo, X. Wang, X. Mao and C. Lai, Analytical Performance of Hollow Anode-Solution Cathode Glow Discharge-Atomic Emission Spectrometry, *Anal. Lett.*, 2020, **53**, 693–704.

48 J. Yu, S. Yang, D. Sun, Q. Lu, J. Zheng, X. Zhang and X. Wang, Simultaneously determination of multi metal elements in water samples by liquid cathode glow discharge-atomic emission spectrometry, *Microchem. J.*, 2016, **128**, 325–330.

49 K. Greda, P. Jamroz and P. Pohl, Comparison of the performance of direct current atmospheric pressure glow microdischarges operated between a small sized flowing liquid cathode and miniature argon or helium flow microjets, *J. Anal. At. Spectrom.*, 2013, **28**, 1233–1241.

50 J. Yu, L. Yin, Q. Lu, F. Feng, Y. Kang and H. Luo, Highly sensitive determination of mercury by improved liquid cathode glow discharge with the addition of chemical modifiers, *Anal. Chim. Acta*, 2020, **1131**, 25–34.

51 J. Yu, S. Zhu, Q. Lu, Z. Zhang, D. Sun, X. Zhang, X. Wang and W. Yang, Liquid Cathode Glow Discharge as a Microplasma Excitation Source for Atomic Emission Spectrometry for the Determination of Trace Heavy Metals in Ore Samples, *Anal. Lett.*, 2018, **51**, 2128–2140.

52 P. Zheng, X. Zhai, J. Wang and P. Tang, Analytical Characterization of a Solution Cathode Glow Discharge with an Interference Filter Wheel for Spectral Discrimination, *Anal. Lett.*, 2018, **51**, 2304–2315.

53 P. Zheng, Y. Chen, J. Wang and S. Xue, A pulsed atmospheric-pressure discharge generated in contact with flowing electrolyte solutions for metal element analysis by optical emission spectrometry, *J. Anal. At. Spectrom.*, 2016, **31**, 2037–2044.

54 M. Gorska and P. Pohl, Comparison of the performance of atmospheric pressure glow discharges operated between a flowing liquid cathode and either a pin-type anode or a helium jet anode for the Ga and In determination by the optical emission spectrometry, *Talanta*, 2021, **226**, 122155.

55 J. Yu, X. Zhang, Q. Lu, L. Yin, F. Feng, H. Luo and Y. Kang, Liquid Cathode Glow Discharge as an Excitation Source for the Analysis of Complex Water Samples with Atomic Emission Spectrometry, *ACS Omega*, 2020, **5**, 19541–19547.

56 M. Gorska and P. Pohl, The application of tetramethylammonium hydroxide for generating atmospheric pressure glow discharge in contact with alkalized flowing liquid cathode solutions – evaluation of the analytical performance, *J. Anal. At. Spectrom.*, 2021, **36**, 1768–1781.

57 M. Grembecka, E. Malinowska and P. Szefer, Differentiation of market coffee and its infusions in view of their mineral composition, *Sci. Total Environ.*, 2007, **383**, 59–69.

58 T. J. M. Jeurnink and K. G. de Kruif, Calcium concentration in milk in relation to heat stability and fouling, *Neth. Milk Dairy J.*, 1995, **1995**, 151–165.

59 I. Gogoasa, A. Pirvu, L. M. Alda, A. Velciov, M. Rada, D. M. Bordean, D. Moigradean, A. Simion and I. Gergen,

The Mineral Content of Different Coffee Brands, *Journal of Horticulture, Forestry and Biotechnology*, 2013, **2013**, 68–71.

60 P. Pohl, E. Stelmach, M. Welna and A. Szymczycha-Madeja, Determination of the Elemental Composition of Coffee Using Instrumental Methods, *Food Anal. Methods*, 2013, **6**, 598–613.

61 P. Pohl, M. Welna, A. Szymczycha-Madeja, K. Greda, P. Jamroz and A. Dzimitrowicz, Response surface methodology assisted development of a simplified sample preparation procedure for the multielement (Ba, Ca, Cu, Fe, K, Mg, Mn, Na, Sr and Zn) analysis of different coffee brews by means of inductively coupled plasma optical emission spectrometry, *Talanta*, 2022, **241**, 123215.

62 E. Feyza Aydar, S. Tutuncu and B. Ozcelik, Plant-based milk substitutes: Bioactive compounds, conventional and novel processes, bioavailability studies, and health effects, *J. Funct. Foods*, 2020, **70**, 103975.

Supporting Information

Fast and simple analysis of selected beverages widely consumed by athletes on the content of Zn, Mg, Ca, Na, and K by flowing liquid cathode atmospheric pressure glow discharge optical emission spectrometry

Monika Gorska*, Joanna Weiss, Pawel Pohl

Wroclaw University of Science and Technology, Faculty of Chemistry, Division of Analytical Chemistry and Chemical Metallurgy, Wybrzeze Stanislawa Wyspianskiego 27, 50-370 Wroclaw, Poland

* Corresponding author. E-mail address: monika.gorska@pwr.edu.pl (Monika Gorska)

Table SI1. Agilent 5110 SVDV ICP-OES operating parameters.

RF power (kW)	1.50
Plasma Ar flow rate (L min^{-1})	12.0
Nebulizing Ar flow rate (L min^{-1})	0.7
Auxiliary Ar flow rate (L min^{-1})	1.0
Uptake delay time (s)	10
Read time (s)	5
Number of replicates	3
Stabilization time (s)	15
Viewing mode	SVDS
Viewing height (mm)	8
Pump speed (rpm)	12
Background correction	Off-peak, fitted, 2 pixels
Analytical line (nm)	280.3 (Mg), 422.7 (Ca), 589.6 (Na), 766.5 (K)

Table SI2. Analytical performance of the investigated FLC-APGD system combined with the OES detection.

Element	DL (µg L^{-1})	ULR (mg L^{-1})	a (a.u. per µg L^{-1})
Zn	21	2.00	$1.33 \cdot 10^{1}$
Mg	0.91	1.00	$6.13 \cdot 10^{2}$
Ca	20	2.00	$1.57 \cdot 10^{1}$
Na	0.062	0.50	$5.70 \cdot 10^{3}$
K	0.14	0.50	$1.74 \cdot 10^{3}$

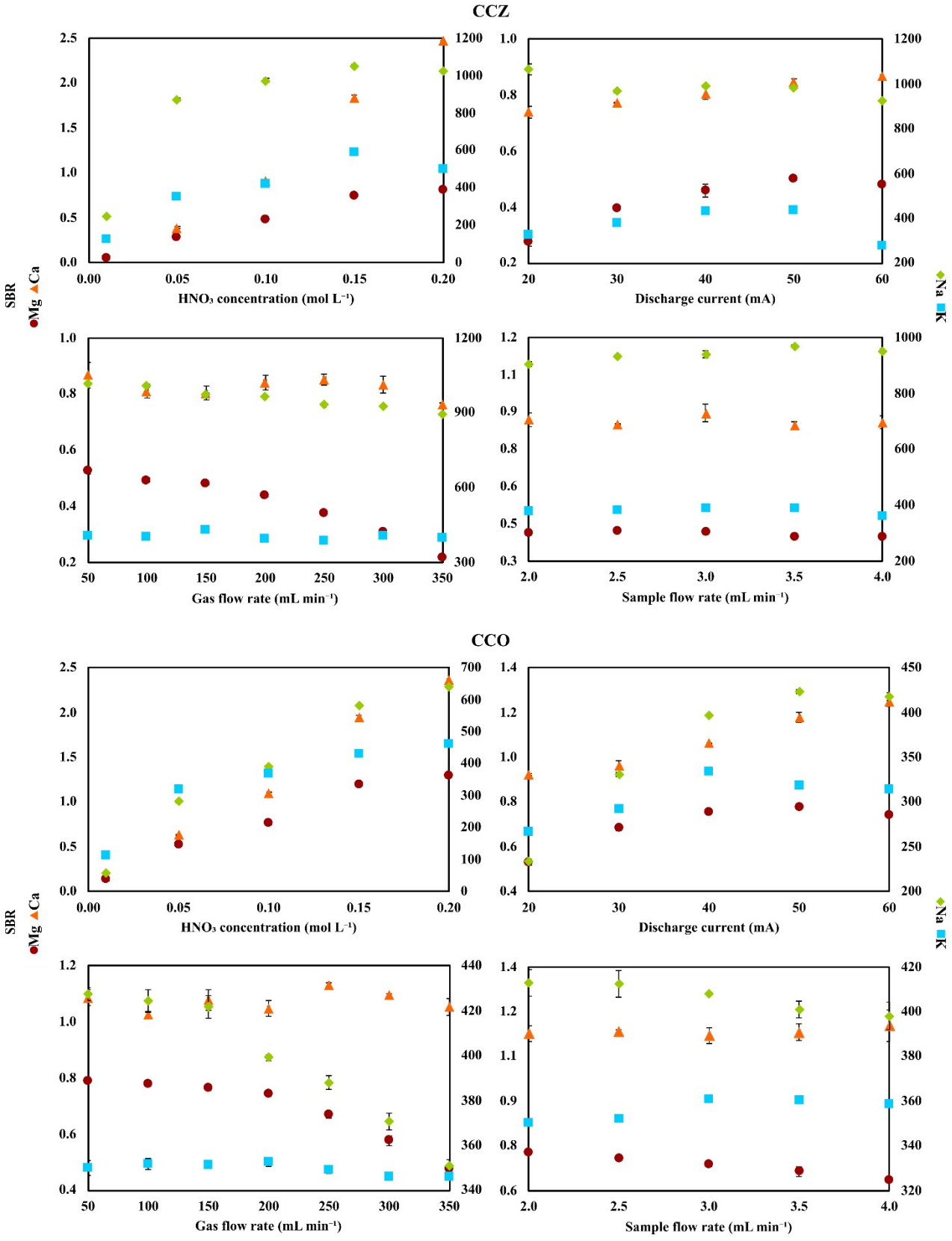

Fig. SI1. The impact of the HNO_3 concentration, the discharge current, the gas flow rate, and the sample flow rate on the SBR values of the analytical lines of the studied elements for the CCZ and CCO samples.

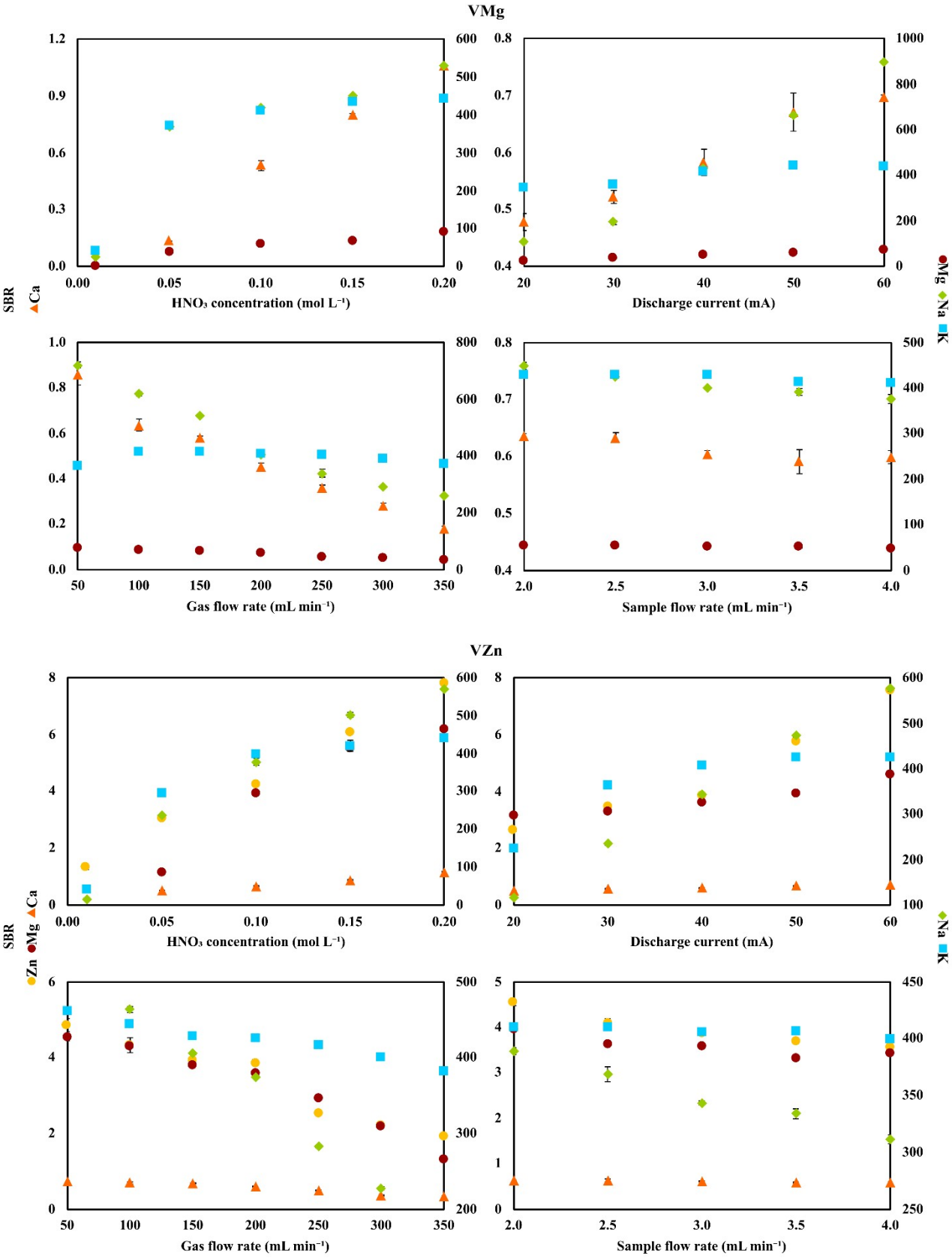

Fig. SI2. The impact of the HNO_3 concentration, the discharge current, the gas flow rate, and the sample flow rate on the SBR values of the analytical lines of the studied elements for the VMg and VZn samples.

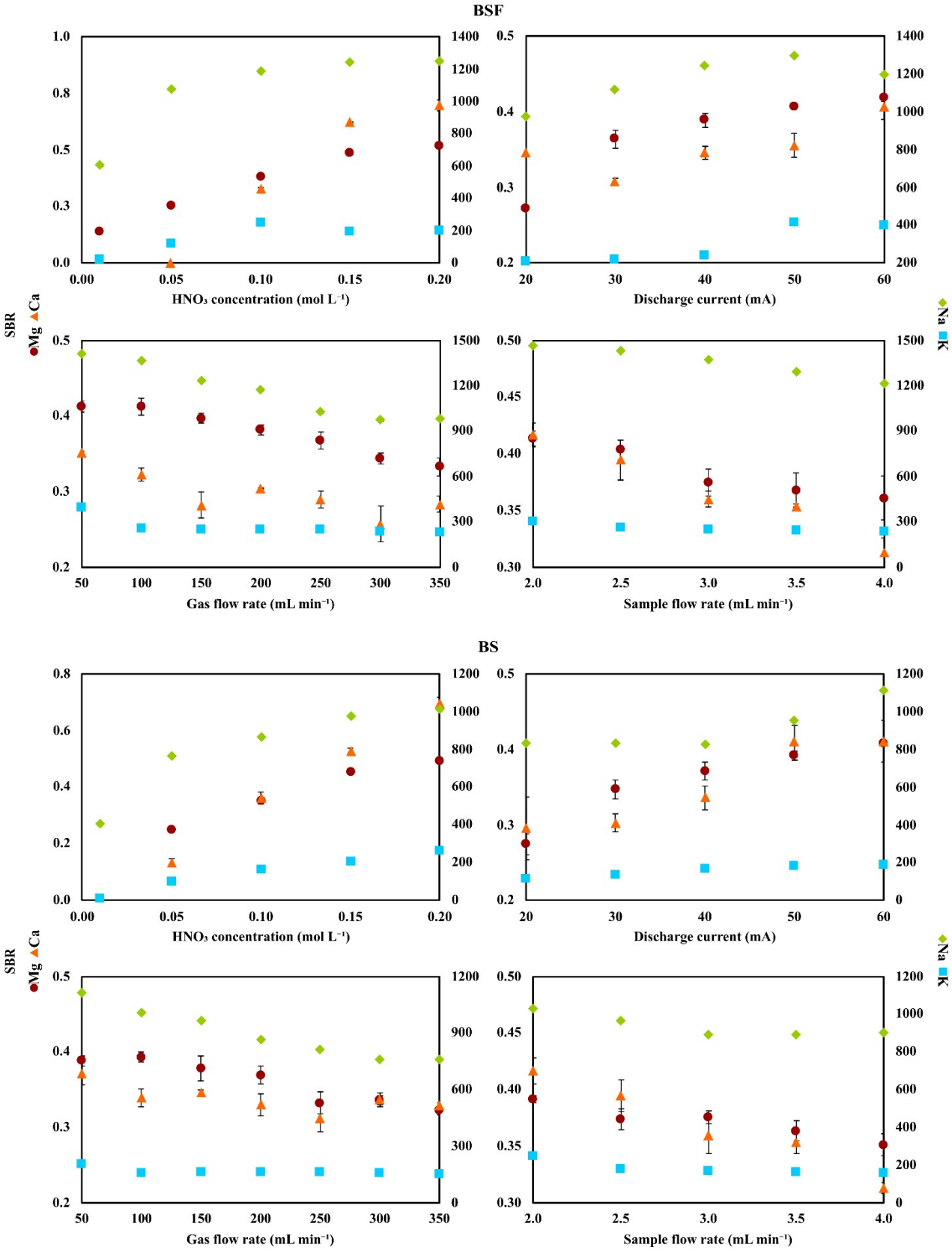

Fig. SI3. The impact of the HNO_3 concentration, the discharge current, the gas flow rate, and the sample flow rate on the SBR values of the analytical lines of the studied elements for the BSF and BS samples.

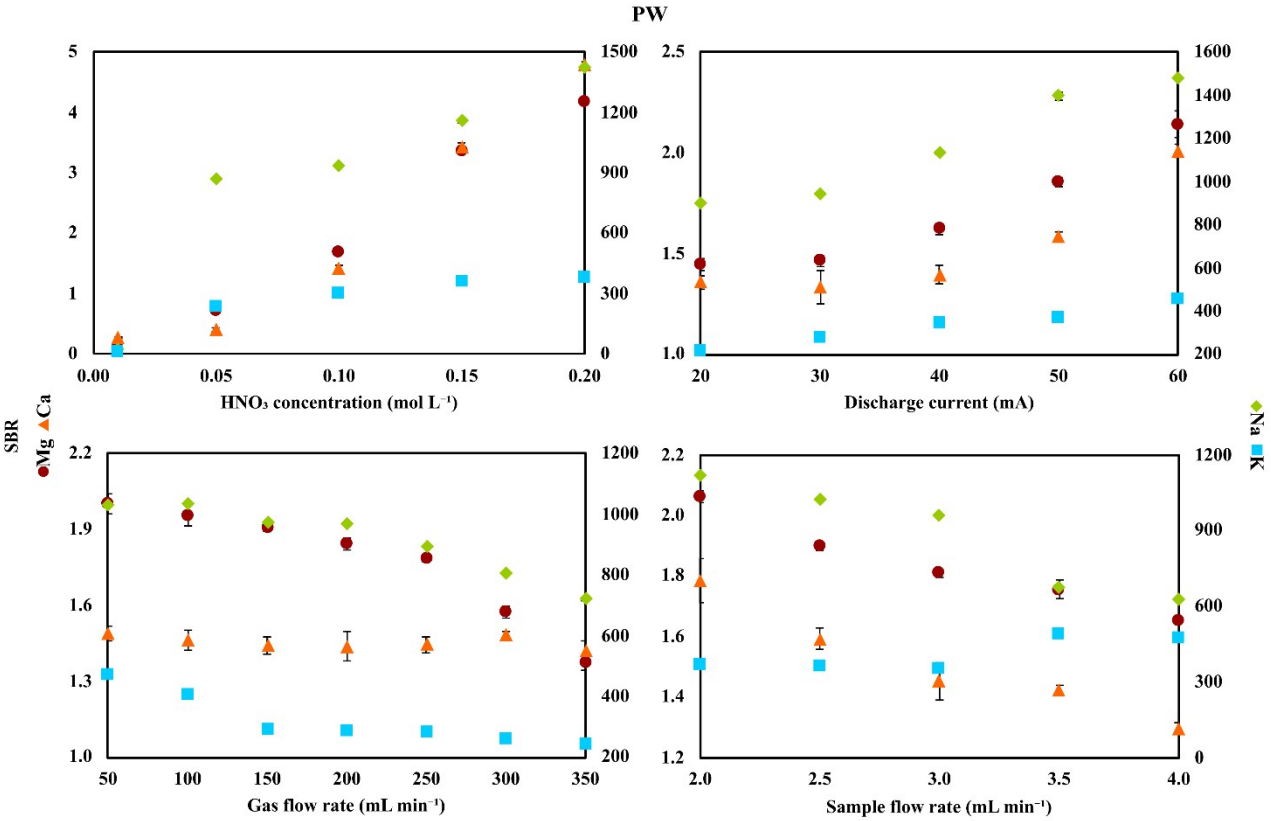

Fig. SI4. The impact of the HNO_3 concentration, the discharge current, the gas flow rate, and the sample flow rate on the SBR values of the analytical lines of the studied elements for the PW sample solution.

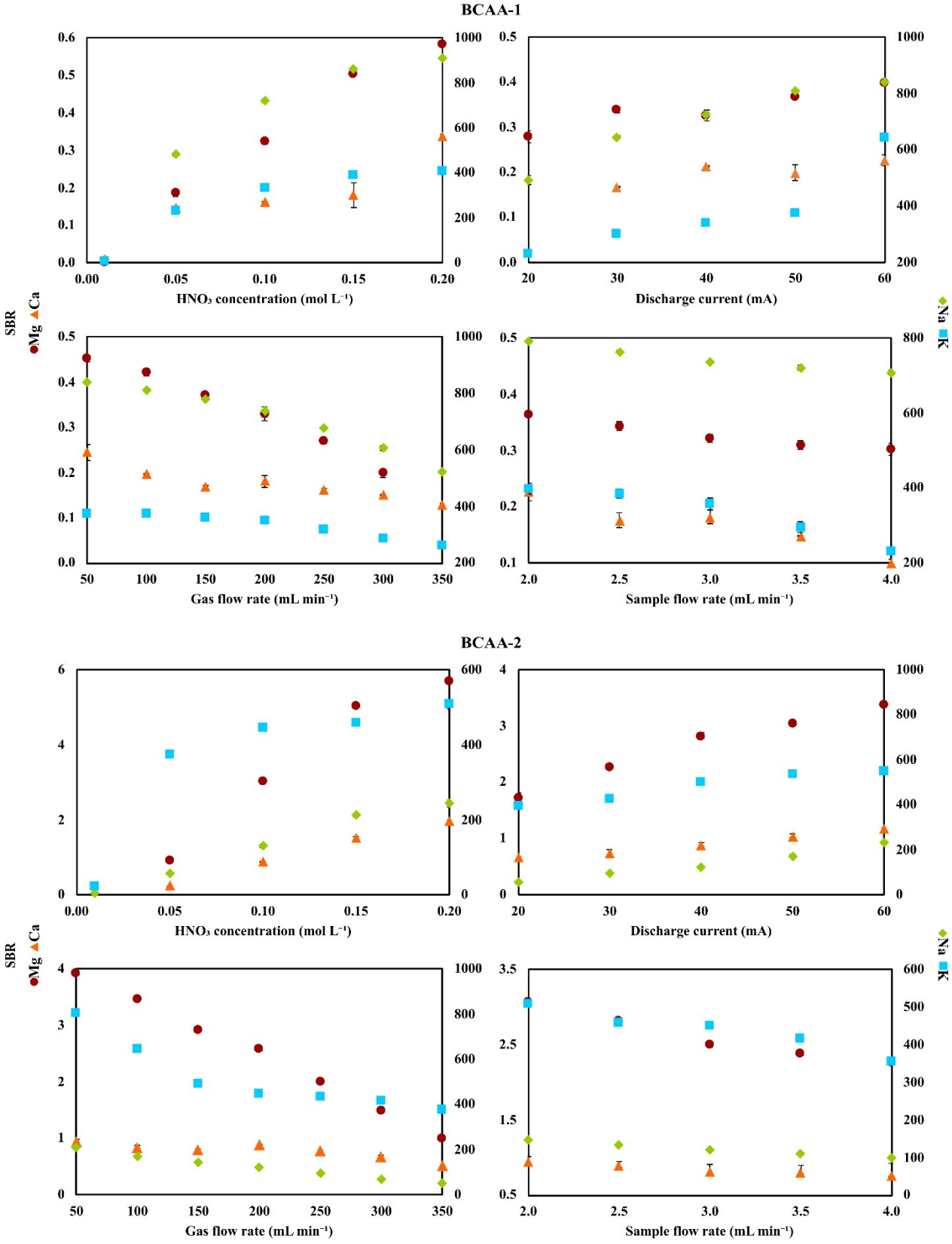

Fig. SI5. The impact of the HNO_3 concentration, the discharge current, the gas flow rate, and the sample flow rate on the SBR values of the analytical lines of the studied elements for the BCAA-1 and BCAA-2 samples.

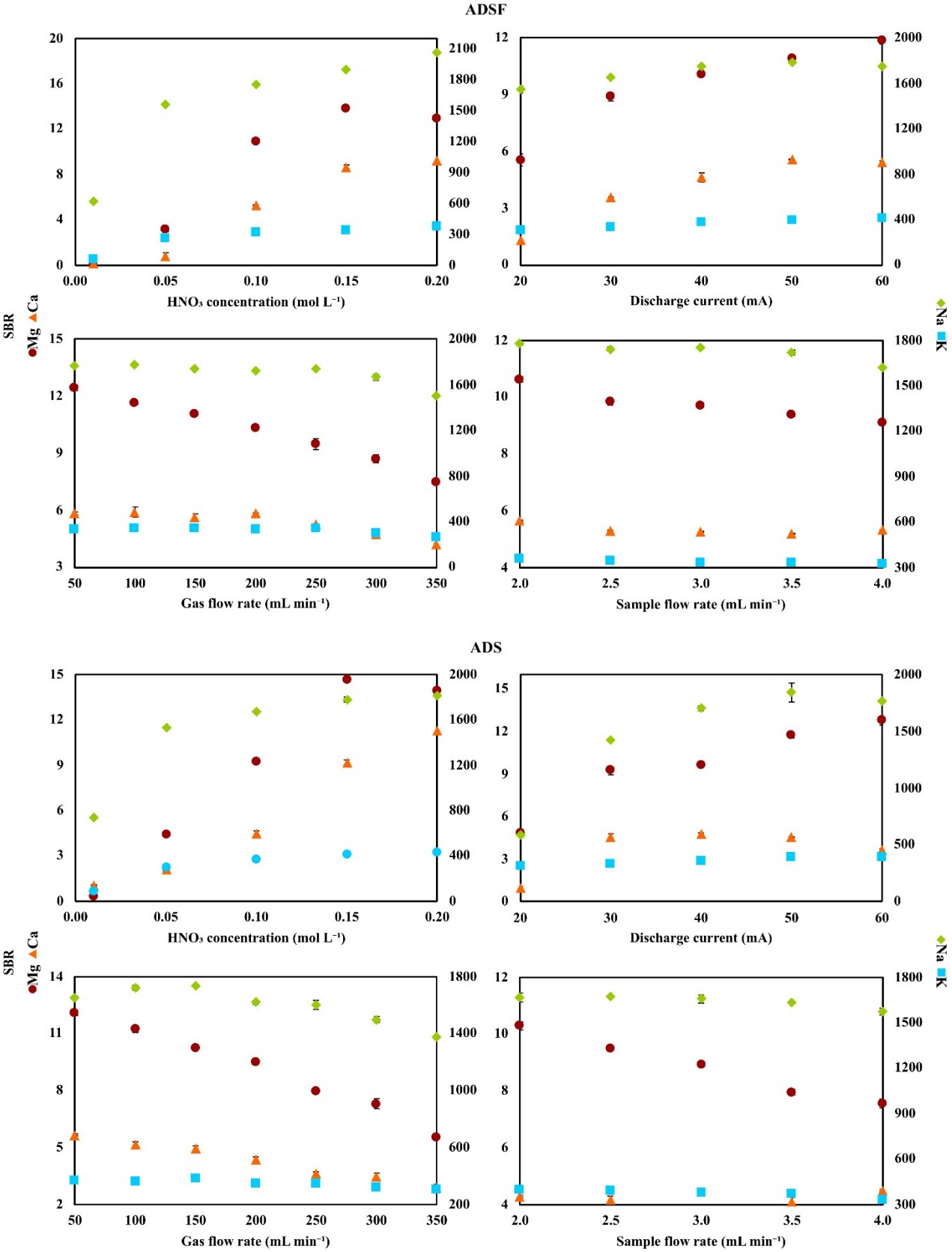

Fig. SI6. The impact of the HNO_3 concentration, the discharge current, the gas flow rate, and the sample flow rate on the SBR values of the analytical lines of the studied elements for the AMSF and AMS samples.

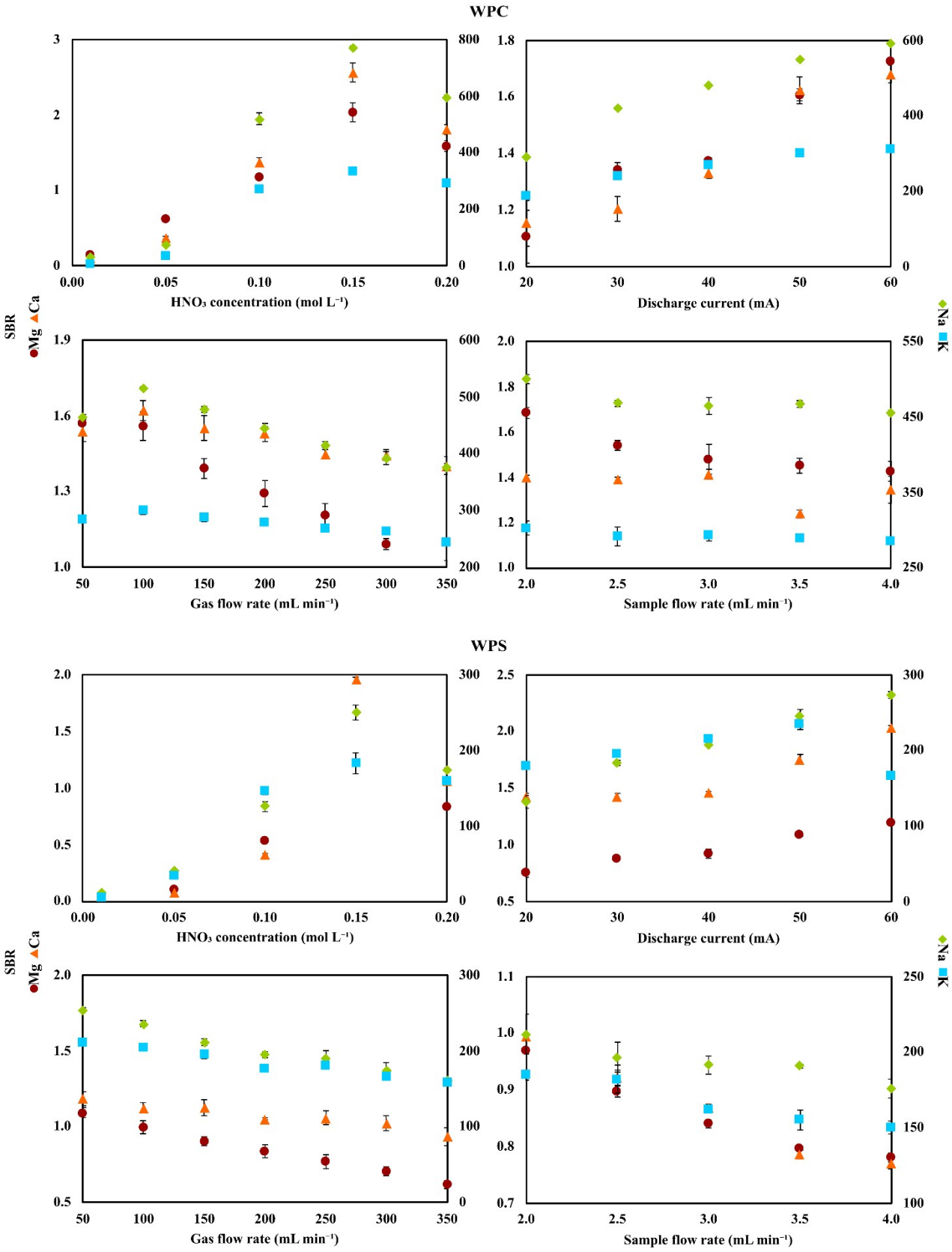

Fig. SI7. The impact of the HNO_3 concentration, the discharge current, the gas flow rate, and the sample flow rate on the SBR values of the analytical lines of the studied elements for the WPC and WPS samples.

Wrocław, dnia 12.07.2023

OŚWIADCZENIE

Oświadczam, że w pracy:

M. Górska, K. Gręda, P. Pohl, Determination of bismuth by optical emission spectrometry with liquid anode/cathode atmospheric pressure glow discharge. Journal of Analytical Atomic Spectrometry 2021, 36, 165-177

mój wkład polegał na współudziale w opracowaniu koncepcji i metodologii badań, przeprowadzeniu eksperymentów i opracowaniu ich wyników, współudziale w interpretacji wyników badań, przygotowaniu pierwszej wersji manuskryptu oraz współudziale w przygotowywaniu finalnej wersji manuskryptu.

...Krzysztof...Gręda...
Dr inż. Krzysztof Gręda

P. Pohl
.....
Prof. dr hab. inż. Paweł Pohl

Wrocław, dnia 12.07.2023

OŚWIADCZENIE

Oświadczam, że w pracy:

M. Górska, P. Pohl, Application of atmospheric pressure glow discharge generated in contact with liquids for determination of chloride and bromide in water and juice samples by optical emission spectrometry. Talanta 2022, 237, 1-11.

mój wkład polegał na współudziale w opracowaniu koncepcji i metodologii badań, przeprowadzeniu eksperymentów i opracowaniu ich wyników, współudziale w interpretacji wyników badań, współudziale w przeprowadzeniu pomiarów ICP OES oraz interpretacji ich wyników, przygotowaniu pierwszej wersji manuskryptu oraz współudziale w przygotowywaniu finalnej wersji manuskryptu.

P. Pohl

.....

Prof. dr hab. inż. Paweł Pohl

Wrocław, dnia 12.07.2023

OŚWIADCZENIE

Oświadczam, że w pracy:

M. Górska, P. Pohl, Coupling of chemical vapor generation with atmospheric pressure glow discharge optical emission spectrometry generated in contact with flowing liquid electrodes for determination of Br in water samples. Microchemical Journal 2022, 178, 1-9.

mój wkład polegał na współudziale w opracowaniu koncepcji i metodologii badań, przeprowadzeniu eksperymentów i opracowaniu ich wyników, interpretacji wyników badań, współudziale w przeprowadzeniu pomiarów ICP OES oraz interpretacji ich wyników, przygotowaniu pierwszej wersji manuskryptu oraz współudziale w przygotowywaniu finalnej wersji manuskryptu.

P. Pohl

.....

Prof. dr hab. inż. Paweł Pohl

Wrocław, dnia 12.07.2023

OŚWIADCZENIE

Oświadczam, że w pracy:

M. Górska, K. Gręda, P. Pohl, On the coupling of hydride generation (HG) with flowing liquid anode atmospheric pressure glow discharge (FLA-APGD) for determination of traces of As, Bi, Hg, Sb and Se by optical emission spectrometry (OES). Talanta 2021, 222, 1-10.

mój wkład polegał na współudziale w opracowaniu koncepcji i metodologii badań, przeprowadzeniu części eksperymentów i współudziale w prowadzeniu pozostałych, współudziale w interpretacji wyników badań, opracowaniu wyników badań, przygotowaniu pierwszej wersji manuskryptu oraz współudziale w przygotowywaniu finalnej wersji manuskryptu.

Krzysztof Gręda
.....
Dr inż. Krzysztof Gręda

P. Pohl
.....
Prof. dr hab. inż. Paweł Pohl

Wrocław, dnia 12.07.2023

OŚWIADCZENIE

Oświadczam, że w pracy:

M. Górska, P. Pohl, Simplified and rapid determination of Ca, K, Mg, and Na in fruit juices by flowing liquid cathode atmospheric glow discharge optical emission spectrometry. Journal of Analytical Atomic Spectrometry 2021, 36, 1455-1465.

mój wkład polegał na współudziale w opracowaniu koncepcji i metodologii badań, przeprowadzeniu eksperymentów i opracowaniu ich wyników, interpretacji wyników badań, współudziale w przeprowadzeniu pomiarów ICP OES oraz interpretacji ich wyników, przygotowaniu pierwszej wersji manuskryptu oraz współudziale w przygotowywaniu finalnej wersji manuskryptu.

P. Pohl

.....

Prof. dr hab. inż. Paweł Pohl

Wrocław, dnia 12.07.2023

OŚWIADCZENIE

Oświadczam, że w pracy:

M. Górska, J. Weiss, P. Pohl, Fast and simple analysis of the content of Zn, Mg, Ca, Na, and K in selected beverages widely consumed by athletes by flowing liquid cathode atmospheric pressure glow discharge optical emission spectrometry. Analytical Methods 2023, 15, 1775-1789.

mój wkład polegał na opracowaniu koncepcji i metodologii badań, współudziale w przeprowadzeniu eksperymentów i opracowaniu ich wyników, interpretacji wyników badań, współudziale w przeprowadzeniu pomiarów ICP OES oraz interpretacji ich wyników, przygotowaniu pierwszej wersji manuskryptu oraz współudziale w przygotowywaniu finalnej wersji manuskryptu.

Joanna Weiss

Joanna Weiss

P. Pohl

Prof. dr hab. inż. Paweł Pohl